Integration of Anaerobic Digestion into a Catalytic Lignocellulosic Biorefinery

G Hurst

PhD 2022

Integration of Anaerobic Digestion into a Catalytic Lignocellulosic Biorefinery

GEORGE HURST

A thesis submitted in partial fulfilment of the requirements of Manchester Metropolitan University for the degree of Doctor of Philosophy

Department of Engineering

Manchester Metropolitan University

2022

Declaration

No part of this project has been submitted in support of an application for any other degree or qualification at this or any other institute of learning. Apart from those parts of the project containing citations to the work of others, this project is my own unaided work. This work has been carried out in accordance with the Manchester Metropolitan University research ethics procedures, and has received ethical approval

Name: 

Date Signed: 21/1/22

Acknowledgements

First of all, I would like to thank my supervisory team. I owe a massive thankyou to my director of studies Dr Silvia Tedesco, for all of her support, patience and expert knowledge. Her constant guidance and reassurance has been utterly essential for my progress which has allowed me to grow as both as a researcher and a person. I would also like to thank Dr Marloes Peeters for her involvement and insightful advice with the project.

I am also very grateful to the technical staff across multiple departments for their invaluable help and advice with all my endeavours. I am most indebted to Mike Green, Stephen Lloyd and John Penfold for tolerating the occasional bad smells that emanated from my equipment and for all their technical help. I would also like to thank Dr Saeed Gulzar for all his advice and patience with regards to the HPLC as well as for occasionally fixing it. I also owe a huge thanks to David McKendry for his technical support and insights.

I would also like to extend my gratitude to Dr Sharon Ruiz-Lopez and Dr Damien Rivett for their graciously helping complete the microbial compositional experiments and analysis. I must also thank Dr Juan Maria González-Carballo and everyone at Drochaid Research for their help synthesising solid acid catalysts used in this thesis, as well as Dr Lubomira Tosheva for her assistance with material characterisation. In addition, I would like to thank Dr Daniel Hayes and everyone at Celignis for his help with the biomass characterisation and inviting me to their lab. I feel obligated to acknowledge the support of the 7th Floor HPLC for its inconsistent but frequent cooperation with my research. Without it's occasional support I could not have finished my PhD and it taught me invaluable lessons.

Finally, I would like to thank my family, friends and the PhD office JDE.033 that kept me sane through my PhD. In particular, Adil, Gemma, Chloe, Ruth, Ola and Laila for the wonderful atmosphere, friendly banter and their constant reassurance. They made this journey so much more enjoyable and I must owe them my many thanks.

Abstract

During the acid catalysed production of platform chemical such as levulinic acid, furfural and 5-hydroxymethylfurfural from lignocellulosic biomass, significant amounts of insoluble carbonaceous solid residue is produced as by-product. The solid residue by-product represents a significant waste stream that contributes to the biorefinery inefficiency which requires characterisation and valorisation for the efficient use of the whole biomass feedstock. The solid residue was composed of a matrix of unreacted biomass, inert biomass fractions, acid catalysed humins from the cross-polymerisation of reactive intermediates and the carbonised chars, that vary in composition and properties due to both catalysts type and reaction conditions. Solid residue produced with homogenous catalysis under aqueous conditions primarily consists of oxygen-rich surface properties due to humin condensation, similar to that of hydrochar formed under hydrothermal carbonisation. While solid residue formed with heterogeneous catalysts showed markedly different properties that were more akin to unreacted biomass, with minimal surface or bulk modification.

Response surface methodology was determined to be sufficient to model solid residue yields alongside high value product yields, most notable levulinic acid. The reaction temperature was found to have the largest effect on both surface properties and yields with lesser effects due to reaction temperature and catalyst concentration. The modelling of the aqueous by-product found that formic acid was consumed during the acid catalysis process and may also contribute to the solid residue condensation products. While the addition of trace hydrochloric acid was found to significantly improve levulinic acid yields with sulphated zirconia suggesting synergistic catalysis could improve a range of heterogeneous catalysts.

The solid residue properties where characterised in depth with the homogenous catalyst related solid residue found to have similar properties to that of hydrochar sufficient to improve anaerobic digestion. During the anaerobic digestion of animal manures, the effects of solid residue was found to reduce ammonium inhibitor concentrations and improve microbial diversity sufficient to increase 14-day methane yields. The application of solid residue from lignocellulosic biorefineries as an anaerobic digestion supplement could provide a low-cost adsorbent material for the improvement of a wide range of nitrogen-rich feedstocks that would otherwise be under-utilised and present environmental concern. Such integration would reduce the carbon emissions from green chemical production while adding increasing the value of the largest waste product.

List of Publications

This thesis is based on:

Hurst G., Brangeli I., Peeters M., Tedesco S., “Solid residue and by-product yields from acid catalysed conversion of poplar wood to levulinic acid”, *Chemical Papers*, **74**:1647-1661 (2019) DOI:10.1007/s11696-019-01013-3

Hurst G., Carballo JM., Tosheva L., Tedesco D., “Synergistic Catalytic Effect of Sulphated Zirconia—HCl System for Levulinic Acid and Solid Residue Production Using Microwave Irradiation”., *Energies*, **14**(6):1582 (2021) DOI: 10.3390/en14061582

Hurst G., Peeters M., Tedesco S. “Integration of Catalytic Biofuel Production and Anaerobic Digestion for Biogas Production”. In: Mporas I., Kourtessis P., Al-Habaibeh A., Asthana A., Vukovic V., Senior J. (eds) *Energy and Sustainable Futures*. Springer Proceedings in Energy. Springer, Cham. (2021) DOI: 10.1007/978-3-030-63916-7_16

Hurst G., Ruiz-Lopez, S., Rivett D., Tedesco S., “Effect of Hydrochar from Acid Hydrolysis on Anaerobic Digestion of Chicken Manure” under review in *Journal for Environmental Chemical Engineering*

Other Publications:

Betlem K, Kaur A, Hudson A, Crapnell R, Hurst G, Singla P, Zubko M, Tedesco S, Banks C, Whitehead K, Peeters M. “Heat-Transfer Method: A Thermal Analysis Technique for the Real-Time Monitoring of Staphylococcus aureus Growth in Buffered Solutions and Digestate Samples.” *ACS Applied Biomaterials,* **2**(9), 3790-3798 (2019) DOI: 10.1021/acsabm.9b00409

Tedesco S., Hurst G., Imtiaz I., Ratova M., Tosheva., Kelly P., “TiO2 supported natural zeolites as biogas enhancers through photocatalytic pretreatment of Miscanthus x giganteous crops.” *Energy*, **205**(21), 117954, (2020) DOI: 10.1016/j.energy.2020.117954

Ahmed A., Hurst G., Peeters M., Tedesco S., “Performance of Brewery Digestate as a Potential Water Substitute in Concrete Applications” Research & Development in Material Science, **14**(1), (2020) DOI: 10.31031/RDMS.2020.14.000830

Tedesco S., Hurst G., Randviir EP., Francavilla M., “A comparative investigation of non-catalysed versus catalysed microwave-assisted hydrolysis of common North and South European seaweeds to produce biochemicals” *Algal Research*, 60, 102489, (2021) DOI: 10.1016/j.algal.2021.102489

Table of Contents

Chapter 3: Methodology

Chapter 8: Conclusions and Recommendations

List of Tables

List of Figures

Nomenclature

ε''	Dielectric loss factor
λ	Microbial lag phase
AD	Anaerobic Digestion
A_{Max}	Maximum Methane Production
ANOVA	ANalysis Of VAriance
BET	Brunauer-Emmett-Teller
BMP	BioMethane Potential
C4	4-Carbon photosynthesis fixation
C5	5-Carbon Sugars
C6	6-Carbon Sugar
CBR	Catalyst to Biomass Ratio
C_{H2SO4}	Molar concentration sulphuric acid
CI	Crystallinity Index
C/N	Atomic Carbon to Nitrogen ratio
CM	Chicken Manure
DIET	Direct Interspecies Electron Transfer
DOE	Design Of Experiments
EDX	Energy Dispersive X-Ray Analysis
FF	Furfural
FTIR	Fourier Transform InfraRed
GC-MS	Gas Chromatography Mass Spectrometry
GHG	GreenHouse Gas
GVL	Gamma-ValerLactone
5-HMF	5- Hydroxymethylfurfural
HPLC	High Perfomance Liquid Chromatography
HTC	Hydrothermal Carbonisation
HHV	Higher Heating Value
ICP	Inductively Coupled Plasma
LA	Levulinic Acid
LHV	Lower Heating Value
M	Molar concentration
MRT	Mean Residence Time
MW	Microwave
NMR	Nuclear Magnetic Resonance
NREL	National Renewable Energy Laboratory
NNFCC	National Non-Food Crops Centre
PFA	Perfluoroalkoxy alkanes
RID	Refractive Index Detector
R_{Max}	Maximum Methane Production rate
RSM	Response Surface Methodology

SEM	Scanning Electron Microscope
SR	Solid Residue
SRC	Short Rotation Coppice
T	Temperature
t	time
TGA	Thermogravimetric analysis
TCD	Thermal Conductivity Detector
TS	Total Solids
VFA	Volatile Fatty Acids
VS	Volatile Solids
XRD	X-Ray Diffraction
XRF	X-Ray Fluorescence
UK	United Kingdom
UV-DAD	Ultraviolet – Diode Array Detctor
ZSM-5	Zeolite Socony Mobil–5

Chapter 1: General Introduction

1.1 Overview

The primary aim of this research was to investigate the integration of anaerobic digestion of solid residues from chemocatalytic conversion of lignocellulosic biomass. The disposal and valorisation of this potential waste products will become an increasingly large part of biorefinery design. At present there is a gap in knowledge regarding solid residue yields from chemocatalytic conversion of lignocellulose, as well as the residues physical properties and possible applications. Part of this research was to quantify and evaluate the by-products yields from acid hydrolysis for minimisation and evaluation of possible applications. Which is critical for the development of low carbon chemicals. In addition, this research sought to evaluate the potential application of solid residue to anaerobic digestion as carbonaceous char as a novel application for the solid residue. The desired advantage of this research is that a biorefinery by-product could be utilised for no direct combustion purposes (associated with CO_2 emissions) and to improve the efficiency of anaerobic digestion across a multitude of industries.

1.2 Background and Motivation

Humanity is facing an existential crisis with the looming threat of climate change that requires the immediate development of new technologies to reduce anthropogenic greenhouse gas emissions. The unfettered use of carbon dioxide producing fuels has already caused a +1 °C rise in global temperatures compared with 1900. Without immediate action the UN estimates that average global warming could reach +3.0 °C, which will cause significant climate and societal disruption [1]. The IPCC estimates that a 49% reduction in greenhouse gas emissions relative to 2017 by 2030 is required [2]. As part of this the UK has committed to being zero net emissions by 2050 and will require the development of a low carbon bioinspired economy [3]. These pressing environmental concerns have recently resulted in the development of clean electricity, battery transportation and reduced energy intensity [4], however all aspects of the society must be considered if these goals are to be achieved. Fossil fuels are also used for the production of a vast range of physical materials including steel, concrete and chemicals. The chemical sector is one of the largest industrial sources of CO_2 emissions for both bulk and fine chemicals such as plastic and solvents [5]. Modern society is heavily reliant on organic compounds for material applications, which are primarily produced from hydrocarbons such as oil and gas. As a result, low-carbon chemical manufacturing from biomass has received significant interest and investment in recent years.

Biomass is among the most abundant renewable energy feedstocks available worldwide [6]. Over the last twenty years, significant commercialisation of first generation biorefineries has enabled the production of bioethanol and biodiesel, using fermentation and transesterification technologies respectively [7]. First generation

biorefineries utilise simple sugars and vegetable oils from various crops including corn and rapeseed that are concentrated in the flower seeds. Though more recently the carbon mitigation and socioeconomic effects of using food grade feedstocks has been questioned [8–10].

First generation biorefineries can only utilise a small group of feedstocks, which are rich in simple sugars such as corn, rapeseed and sugarcane that directly compete with food production. The effects on consumer food prices, coupled with the low yields per hectare and high fertiliser requirements has resulted in their continued production for energy purposes being seen as unsustainable [11,12]. First generation biorefineries primarily utilise the seed related fraction of biomass and are unable to efficiently utilise the more abundant structural cellulose and lignin fractions available in the all above ground plant matter [13]. Therefore, there has been a growing focus on the utilisation of the more ethical and abundant lignocellulosic biomass types, such as wood, straw and grasses [14]. Lignocellulosic biomass can also be grown on marginal lands unsuitable for food, with high yields per hectare and less fertiliser consumption [15]. Biomass and lignocellulose in particular have been recognised as part of the UK's long-term industrial decarbonisation pathway [16,17]. However, the conversion of lignocellulose towards biochemicals is challenging.

Lignocellulosic biomass is an abundant and renewable resource from plants mainly composed of polysaccharides (cellulose and hemicellulose) and aromatic polymers (lignin) [18]. The components form part of the heterogeneous cell wall that are interlinked and can reach lengths of several thousand base units. This differs significantly from first generation biomass such as rapeseed or corn, which are composed of oligomer sugars and oils of no more than 10 units. As the polymer chains form a crystalline

structure, intramolecular bonding occurs between the chains requiring “harsher” processing conditions than fermentation to produce individual sugars [19]. Lignocellulose can be grouped into 4 primary categories: cellulose, hemi-cellulose, lignin and other products (which include extractives). The four principal components are composed of distinct monomeric units that can be individually or collectively converted into high value platform chemicals. The cellulose is the single largest fraction that constitutes between 40 - 60 wt.% of lignocellulose and is the primary valorisation target in biorefinery conversion. The conversion of the cellulose to usable chemical compounds can be achieved using various different biorefinery technologies or concepts.

The use of lignocellulose as a feedstock for the production of biochemicals requires the development of integrated conversion facilities called biorefineries, which convert renewable materials towards low carbon chemicals, analogous to current oil refineries[20]. The wide scale commercialisation of biomass conversion requires the complete and efficient valorisation of all fractions towards high value products. Many different biocatalytic, thermochemical and chemocatalytic methods have been proposed as to convert biomass into value added products with various possible integration pathways [21–23], as shown below.

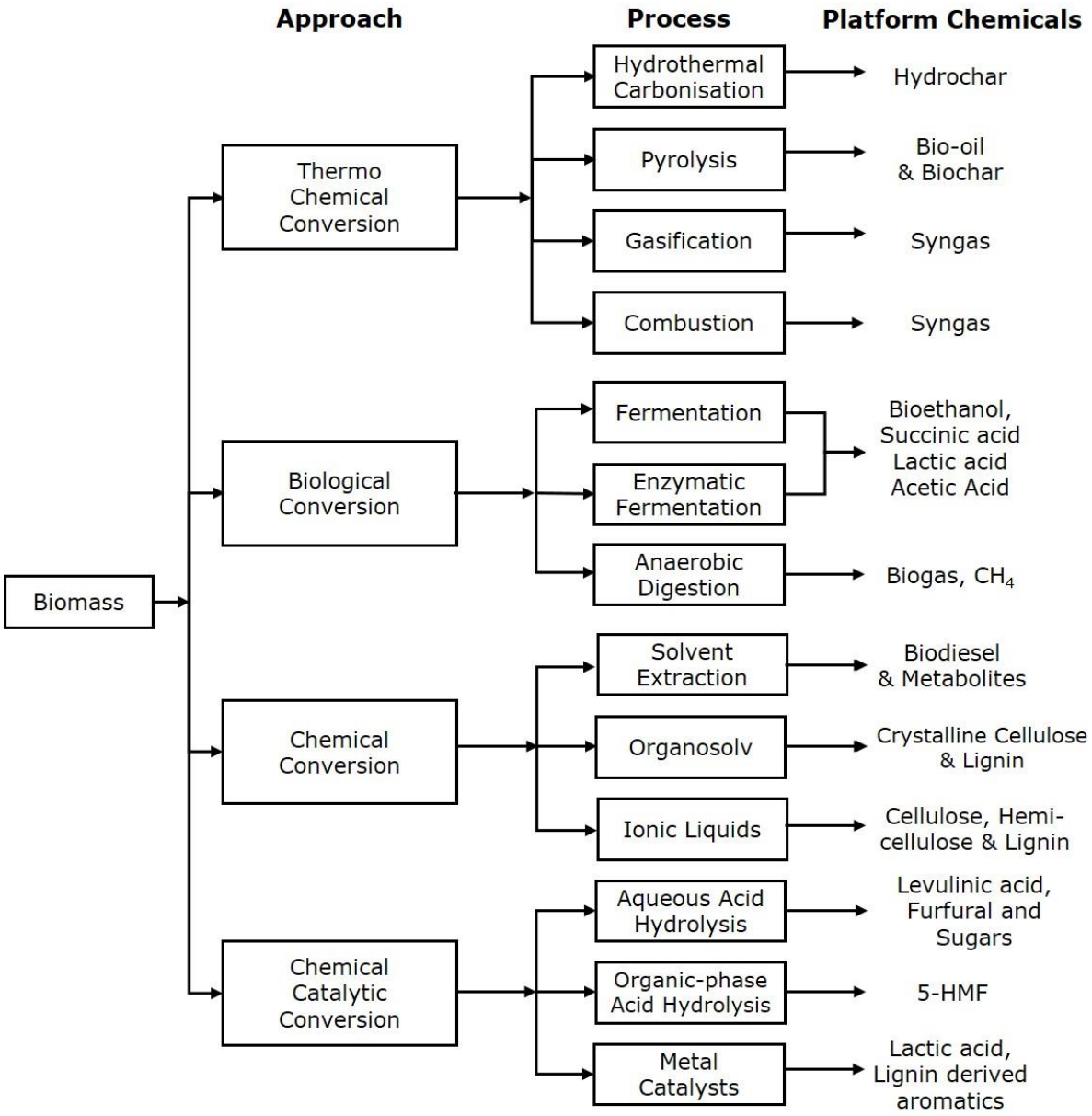

Figure 1.1: Summary of possible biomass conversion pathways

The simplest conversion option for the complete lignocellulosic biomass is by thermochemical techniques. For example, gasification via incomplete combustion seeks to produce H_2 and CO, also called syngas, to be used for the production of alkanes by Fisher-Tropsch synthesis, among other options [21]. Gasification is a near universal conversion for all dry lignocellulosic biomass, operating at temperatures between 700-900 °C; however significant further processing is required to remove impurities, more specifically Fischer-Tropsch catalyst poisons [24]. Pyrolysis is a cheap

alternative to gasification, which utilises incomplete combustion at lower thermal ranges than gasification, such as 400-600 °C, to produce syngas, pyrolysis oil and biochar [22]. The three-product process allows significant integration potential and concentration of impurities in the biochar fraction reduces poisons issues. Despite these advantages, the bio-oil product is compositionally complex and requires extensive separating or upgrading to be suitable for fuel or fine chemicals production[25].

Chemo-catalytic methods such as acid hydrolysis are among the most developed lignocellulose biorefinery technologies [22]. Chemo-catalytic methods achieve higher selectivity towards platform chemicals compared with gasification and pyrolysis. Acid hydrolysis is a sub-process that focuses on the use of mineral acids such as HCl and H_2SO_4 to release monomeric sugars from polysaccharides and the subsequent dehydration to 5-hydroxymethfurfural, levulinic acid furfural [26,27]. These platform chemicals can then be further upgraded to plastics, solvents and fuels to replace equivalent hydrocarbon derived products. Unfortunately, the heterogeneous nature of the biomass does not facilitate the easy one-step conversion of all biomass fractions towards high value products. By-products include degradation products from acid hydrolysis and inert biomass fraction such as Klason lignin [28]. Currently there are limited applications for the biorefinery waste products resulting in significant costs associated with waste disposal. Valorisation of all biorefinery by-products will become an increasingly large part of the overall biorefinery design and will require the investigation of novel waste applications.

The solid residue from acid hydrolysis for the production of levulinic acid has been widely reported as both a catalytic by-product [29–31] and a combination of unreactive

inerts [28,32]. The formation mechanisms of catalytic by-products from acid hydrolysis, also known as humins, have been elucidated by several authors [33–35]. Humins are produced primarily via aldol-condensation of intermediate products, most notably 5-HMF, that results in a furan-rich polymeric structure that can undergo further carbonisation. However, the solid residue formed from real lignocellulosic biomass matrices also includes lignin, pectins and other degradation products, which have not been investigated in great depth. Previous studies have reported a wide variety of solid residue yields of 31-52% with minimal concern to minimisation of solid residues yields [28,36]. Understanding the effects of reaction conditions on by-products yields and properties in conjunction with platform chemical yields is essential for a proper and cost-effective optimisation of the overall process.

The full valorisation of the minimised solid residue is therefore of utmost importance to enable the integrated biorefinery concept. Several integrated biorefinery proposals have suggested the utilisation of the solid residue as a combustion fuel for the generation of low pressure steam to fuel the biorefinery internal demand [37]. However, the solid residue has similar combustion properties to that of coal, which conflicts with the goals of a net-zero carbon economy and therefore the elimination of high carbon sources of energy is required. The transition of biorefineries towards zero-carbon-electricity powered microwave process heating reduces the need of low pressure steam and enabling other valorisation pathways. Several research groups have sought to use solid residue as feedstock for further chemical production via methods such as pyrolysis [28,38,39], although bio-oil yields have been notably lower than expected. Other applications have sought to use solid residue as a recyclable solid acid catalyst or building material with mixed results [39–41]. Another alternative the utilisation of the

microporous structures present, in the solid residues as an inhibitor adsorbent and microbial growth promoter in the context of anaerobic digestion.

Anaerobic digestion is a commonly utilised a biological waste disposal method of organic material that also produce renewable energy in the form of biogas. Complex synergistic microbial communities under controlled anaerobic conditions can degrade wastes such as waste water, animal manures and food waste [42]. However, the degradation of these waste materials is often limited by the presence of microbial inhibitors, most prominently ammonium, which disrupt the degradation process by reducing microbial diversity and populations [43–45]. The addition of carbonaceous residues has received significant attention in recent years to mitigate these issues and improve the anaerobic digestion potential [46–49]. However the production of carbon rich materials such as biochar or hydrochar from pyrolysis and hydrothermal carbonisation respectively, has proven expensive [50]. The solid residues from acid catalysis have shown similar properties to that of hydrochar with proposed similar reaction mechanisms. The utilisation of solid residue in this filed would not only offer a valorisation solution to biorefinery process, but also improve the waste management of difficult materials.

The integration of established technologies into novel lignocellulosic biorefineries could reduce the technical uncertainty of the overall project and hasten the development of the bioeconomy. Despite the carbon emissions are associated with biogas combustion, biogas consumption is essential to the zero-carbon economy, due to high methane emissions associated with natural decomposition of organic waste materials that outweigh the carbon impact of combustion [51]. Moreover, the methane

containing biogas produced during anaerobic digestion is a low-carbon fuel that would act as a secondary income source, in addition to the combustion nature of the process. There is further synergy in that chars used anaerobic digestion have been proposed as a form of carbon sequestration [52]. Therefore, it is essential to investigate the integration of anaerobic digestion into chemocatalytic processes in a detailed and comprehensive manner.

1.3 Research Gap

This thesis explores the gap in research regarding the lack of empirical data characterising the solid residue by-product yields from lignocellulosic catalysis. Specifically, the lack of understanding on the effects of process conditions on solid residue yield and composition. The lack of empirical data regarding solid residue waste by-product compared with detailed modelling of the primary products is due to both of a lack of understanding of the underlying mechanisms and their importance. This gap in knowledge of solid by-product yield limits the optimization of existing processes and inhibits the possible tunability of solid residue properties for different applications.

This also includes the gap in knowledge regarding the differences between solid residue derived from homogenous and heterogeneous catalysts. Very few studies have investigated solid residue properties under different reaction conditions, and even less literature is available on their possible valorisation pathways. The effects of different catalysts on the by-product yields hampers the effective comparison of different catalysts for effective commercialisation. Also, the comparison of solid residues produced with different catalyst would enable better understanding of the underlying solid residue formation mechanisms and their relative importance. By addressing this gap it would not only enable future work for valorisation of the waste solid residue but also reduce process uncertainty regarding the whole biorefinery concept.

Despite the similarities in formation mechanisms and properties between solid residues and hydrochar, the investigation of solid residue applications has been limited, including their role as an anaerobic digestion supplement. There are currently

no studies investigating the application of solid residue as an anaerobic digestion supplement, despite the significant overlap in material properties with hydrochar. This work not only evaluates the solid residue as an anaerobic digestion supplement, but also looks at the underlying microbial promotion mechanisms. By investigating anaerobic digestion inhibitor concentrations, trace metal content and microbial diversity, it is possible to understand the explicit effect of solid residues on anaerobic digestion performance and stability. The unique residue properties will greatly advance the knowledge in this area and add to current literature in the broader carbon-supplemented anaerobic digestion field.

The development of this novel research proposal will fill an important gap in the biorefinery circular economy. Through anaerobic digestion the residual nutrients can be applied to land in the form of digestate in effect recycling nutrients and carbon. This would enable a closed loop approach for lignocellulosic biorefinery design that also facilitates carbon sequestration. The avoidance of combustion of lignite-like solid residue offer a low-carbon application for a difficult waste feedstock that fits into the COP26 framework.

1.4 Aims and Objectives

The aim of this thesis is to investigate the integration of anaerobic digestion into catalytic lignocellulosic biorefineries. In order to achieve this, the key objectives are:

1. To identify and characterise possible lignocellulosic biomass materials suitable for further study;
2. Study the effects of operating parameters on the by-product yields of a catalytic biorefinery process for possible minimisation and optimisation with homogenous catalyst;
3. Characterise the solid residue from the homogenous and heterogeneous catalysis of biomass as a potential inhibitor adsorbing material for anaerobic digestion supplementation;
4. To investigate the solid residue from levulinic acid production for anaerobic digestion for the improvement of methane yields, ammonium adsorption and microbial diversity;

1.5 Structure of Thesis

This thesis starts with a literature review in **Chapter 2**, exploring the biorefinery concept, by-products from acid hydrolysis and solid residue characteristics. This chapter also includes a detailed description of the anaerobic digestion process, the effects of hydrochar on anaerobic digestion and benefits of hydrochar application.

Chapter 3 describes the methodologies used in this thesis, in addition to the characterisation of different lignocellulosic feedstocks available in the UK suitable for chemocatalytic conversion.

Chapter 4 survey and evaluate different lignocellulosic biomass feedstocks

Chapter 5 investigates the effects of reaction conditions on by-product yields from the sulphuric acid catalysed production on levulinic acid from poplar wood

Chapter 6 presents the results of synergistic heterogeneous catalysis for the production of levulinic, with detailed characterisation of the solid residue and catalysts recyclability

Chapter 7 reports the in-depth characterisation of several solid residues and their application as a supplement for the 14-day anaerobic digestion of chicken manure

Chapter 8 evaluates the overall process using techno-economic and socio-economic models

Chapter 9 concludes the thesis results with general comments and future work

1.6 References

1. IPCC. Global warming of 1.5°C. An IPCC Special Report on the impacts of global warming of 1.5°C above pre-industrial levels and related global greenhouse gas emission pathways, in the context of strengthening the global response to the threat of climate change,. Ipcc - Sr15 2, 17–20 (2018).
2. IPCC. Climate Change 2021: The Physical Science Basis. Contribution of Working Group I to the Sixth Assessment Report of the Intergovernmental Panel on Climate Change [Masson-Delmotte, V., P. Zhai, A. Pirani, S. L. Connors, C. Péan, S. Berger, N. Caud, Y. Chen,. Cambridge Univ. Press 3949 (2021).
3. Committee on Climate Change. Net Zero: The UK's contribution to stopping global warming. Comm. Clim. Chang. 275 (2019).
4. Climate Change Committee. Progress in reducing emissions: 2021 Report to Parliament. (2021).
5. Fischedick, M. & Roy, J. Industry. In: Climate Change 2014: Mitigation of Climate Change. Contribution of Working Group III to the Fifth Assessment Report of the Intergovernmental Panel on Climate Change. (2019). doi:10.7312/beik90104-006
6. Owusu, P. A. & Asumadu-Sarkodie, S. A review of renewable energy sources, sustainability issues and climate change mitigation. Cogent Eng. 3, (2016).
7. Naik, S. N., Goud, V. V, Rout, P. K. & Dalai, A. K. Production of first and second generation biofuels : A comprehensive review. Renewable and Sustainable Energy Review. 14, 578–597 (2010).

8. Gasparatos, A., Stromberg, P. & Takeuchi, K. Sustainability impacts of first-generation biofuels. Animal Frontiers. 3, 12–26 (2013).

9. Matsuda, H. & Takeuchi, K. Approach to Biofuel Issues from the Perspective of Sustainability. Science Studies. (2018). doi:10.1007/978-4-431-54895-9_2

10. Tenebaum, D. J. Food vs Fuel Diversion of Crops Could Cause More Hunger. Environ. Health Perspect. 116, 254–257 (2008).

11. Fridrihsone, A., Romagnoli, F. & Cabulis, U. Environmental life cycle assessment of rapeseed and rapeseed oil produced in Northern Europe: A Latvian case study. Sustainability. 12, 5699 (2020).

12. Sanford, G. R., Oates, L. G., Roley, S. S., Duncan, D. S., Jackson, R. D., Robertson, G. P., Thelen, K. D. Biomass production a stronger driver of cellulosic ethanol yield than biomass quality. Agron. J. 109, 1911–1922 (2017).

13. Padella, M., O'Connell, A. & Prussi, M. What is still limiting the deployment of cellulosic ethanol? Analysis of the current status of the sector. Applied Sciience 9, (2019).

14. Nuffield Council of Bioethics. Biofuels: ethical issues. (2011).

15. Visser, R. G. F., Trindade, L. M. & Breeding, P. The potential of C4 grasses for cellulosic biofuel production. 4, 1–18 (2013).

16. HM Government. Industrial Decarbonisation Strategy. HM Government (2021).

17. Committee on Climate Change. Biomass in a low-carbon economy. 161 (2018).

18. Zoghlami, A. & Paës, G. Lignocellulosic Biomass: Understanding Recalcitrance and Predicting Hydrolysis. Frontiers in Chemistry 7, (2019).

19. Zhao, H. Kwak, J. H., Wang, Y, Franz, J. A., White, J. M., Holladay, J. E., Effects of crystallinity on dilute acid hydrolysis of cellulose by cellulose ball-milling study. Energy and Fuels 20, 807–811 (2006).

20. Jong, E., Higson, A., Walsh, P. & Wellisch, M. Task 42 Biobased Chemicals - Value Added Products from Biorefineries. A Rep. Prep. IEA Bioenergy-Task 36 (2011).

21. Nanda, S., Mohammad, J., Reddy, S. N., Kozinski, J. A. & Dalai, A. K. Pathways of lignocellulosic biomass conversion to renewable fuels. Biomass Convers. Biorefinery 4, 157–191 (2014).

22. Lee, S. Y., Sankaran, R., Chew, K. W., Tan, C. H., Krishnamoorthy, R., Chu, D. T., Show, P. L. Waste to bioenergy: a review on the recent conversion technologies. BMC Energy 1, 1–22 (2019).

23. Fülöp, L. & Ecker, J. An overview of biomass conversion: Exploring new opportunities. PeerJ 8, (2020).

24. Hu, J., Yu, F. & Lu, Y. Application of fischer-tropsch synthesis in biomass to liquid conversion. Catalysts 2, 303–326 (2012).

25. Yang, H., Yao, J., Chen, G., Ma, W., Yan, B., Qi, Y. Overview of upgrading of pyrolysis oil of biomass. Energy Procedia 61, 1306–1309 (2014).

26. Girisuta, B., Janssen, L. P. B. M & Heeres, H. J. Kinetic study on the acid-catalyzed hydrolysis of cellulose to levulinic acid. Ind. Eng. Chem. Res. 46, 1696–1708 (2007).

27. Girisuta, B., Dussan, K., Haverty, D., Leahy, J. J. & Hayes, M. H. B. A kinetic study of acid catalysed hydrolysis of sugar cane bagasse to levulinic acid. Chem. Eng. J. 217, 61–70 (2013).

28. Melligan, F., Dussan, K., Auccaise, R., Novonty, E. H., Leahy, J. J., Hayes, M. H. B., Kwapinski, W. Characterisation of the products from pyrolysis of residues after acid hydrolysis of Miscanthus. Bioresource Technology. 108, 258–263 (2012).

29. van Zandvoort, I., Koers, E. J., Weingarth, M., Bruijnincx, P. C. A., Baldus, M., Weckhuysen, B. M. Structural characterization of 13C-enriched humins and alkali-treated 13C humins by 2D solid-state NMR. Green Chemistry. 17. 4383–4392 (2015). doi:10.1039/c5gc00327j

30. Girisuta, B., Janssen, L. P. B. M. & Heeres, H. J. A kinetic study on the decomposition of 5-hydroxymethylfurfural into levulinic acid. 701–709 (2006). doi:10.1039/b518176c

31. Patil, S. K. R. & Lund, C. R. F. Formation and Growth of Humins via Aldol Addition and Condensation during Acid-Catalyzed Conversion of 5-Hydroxymethylfurfural. 4745–4755 (2011). doi:10.1021/ef2010157

32. Dussan, K., Girisuta, B., Lopes, M., Leahy, J. J. & Hayes, M. H. B. Effects of Soluble Lignin on the Formic Acid-Catalyzed Formation of Furfural: A Case Study for the Upgrading of Hemicellulose. ChemSusChem 9, 492–504 (2016).

33. van Zandvoort, I., Wang, Y., Rasrendra, C. B., van Eck, E. R, Bruijnincx, P. C. A., Heeres, H. J., Weckhuysen, B. M. Formation , Molecular Structure , and Morphology of Humins in Biomass Conversion : Influence of Feedstock and Processing Conditions. 1745–1758 (2013). doi:10.1002/cssc.201300332

34. Patil, S. K. R. R., Heltzel, J. & Lund, C. R. F. F. Comparison of structural features of humins formed catalytically from glucose, fructose, and 5-hydroxymethylfurfuraldehyde. Energy and Fuels 26, 5281–5293 (2012).

35. Dussan, K., Girisuta, B., Haverty, D., Leahy, J. J. & Hayes, M. H. B. Kinetics of levulinic acid and furfural production from Miscanthus×giganteus. Bioresour. Technol. 149, 216–224 (2013).

36. Sweygers, N., Somers, M. H. & Appels, L. Optimization of hydrothermal conversion of bamboo (Phyllostachys aureosulcata) to levulinic acid via response surface methodology. J. Environ. Manage. 219, 95–102 (2018).

37. Giuliano, A., Cerulli, R., Poletto, M., Raiconi, G. & Barletta, D. Process Pathways Optimization for a Lignocellulosic Biorefinery Producing Levulinic Acid, Succinic Acid, and Ethanol. Ind. Eng. Chem. Res. 55, 10699–10717 (2016).

38. Agarwal, S., Es, D. Van, Jan, H., van Es, D. & Heeres, H. J. Catalytic pyrolysis of recalcitrant, insoluble humin byproducts from C6 sugar biorefineries. J. Anal. Appl. Pyrolysis 123, 134–143 (2017).

39. Rasrendra, C. B., Windt, H., Wang, Y., Adisasmito, S., Makertihartha, I. G. B. N., van Eck, E. R., Meier, D., Heeres, H. J. Experimental studies on the pyrolysis of humins from the acid-catalysed dehydration of C6-sugars. J. Anal. Appl. Pyrolysis 104, 299–307 (2013).

40. Mija, A., Waal, J. C. Van Der, Pin, J., Guigo, N. & Jong, E. De. Humins as promising material for producing sustainable carbohydrate-derived building materials. Constr. Build. Mater. 139, 594–601 (2017).

41. Kobayashi, H., Kaiki, H., Shrotri, A., Techikawara, K. & Fukuoka, A. Hydrolysis of woody biomass by a biomass-derived reusable heterogeneous catalyst. Chem. Sci. 7, 692–696 (2016).

42. Van, D. P., Fujiwara, T., Tho, B. L., Toan, P. P. S. & Minh, G. H. A review of anaerobic digestion systems for biodegradable waste: Configurations, operating parameters, and current trends. Environ. Eng. Res. 25, 1–17 (2020).

43. Chen, J. L., Ortiz, R., Steele, T. W. J. J. & Stuckey, D. C. Toxicants inhibiting anaerobic digestion: A review. Biotechnology Advances 32, 1523–1534 (2014).

44. Si, B., Li, J., Zhu, Z., Shen, M., Lu, J., Duan, N., Zhang, Y., Liao, Q., Huang, Y., Liu, Z. Science of the Total Environment Inhibitors degradation and microbial response during continuous anaerobic conversion of hydrothermal liquefaction wastewater. Sci. Total Environ. 630, 1124–1132 (2018).

45. Hou, L., Ji, D. & Zang, L. Inhibition of Anaerobic Biological Treatment: A Review. IOP Conf. Ser. Earth Environ. Sci. 112, (2018).

46. Xu, J., Mustafa, A. M., Lin, H., Choe, U. Y. & Sheng, K. Effect of hydrochar on anaerobic digestion of dead pig carcass after hydrothermal pretreatment. Waste Manag. 78, 849–856 (2018).

47. Masebinu, S. O., Akinlabi, E. T., Muzenda, E. & Aboyade, A. O. A review of biochar properties and their roles in mitigating challenges with anaerobic digestion. Renew. Sustain. Energy Rev. 103, 291–307 (2019).

48. Qiu, L., Deng, Y. F., Wang, F., Davaritouchaee, M. & Yao, Y. Q. A review on biochar-mediated anaerobic digestion with enhanced methane recovery. Renew. Sustain. Energy Rev. 115, 109373 (2019).

49. González, J., Sánchez, M. & Gómez, X. Enhancing Anaerobic Digestion: The Effect of Carbon Conductive Materials. C 4, 59 (2018).

50. Yihunu, E. W., Minale, M., Abebe, S. & Limin, M. Preparation, characterization and cost analysis of activated biochar and hydrochar derived from agricultural waste: a comparative study. SN Appl. Sci. 1, 1–8 (2019).

51. Daniel-Gromke, J., Liebetrau, J., Denysenko, V. & Krebs, C. Digestion of bio-waste - GHG emissions and mitigation potential. Energy. Sustain. Soc. 5, 1–12 (2015).

52. Majumder, S., Neogi, S., Dutta, T., Powel, M. A. & Banik, P. The impact of biochar on soil carbon sequestration: Meta-analytical approach to evaluating

environmental and economic advantages. J. Environ. Manage. 250, 109466 (2019).

Chapter 2: Literature Review

2.1 Introduction

In recent years, integrated biorefineries have received growing interest as to maximise the extractable value from biomass in the form of green platform chemicals in order to support the establishment of a low carbon economy. Research and development in this area has focused on the conversion of lignocellulosic biomass, regarded as second generation feedstocks, into a multitude of biochemicals from numerous different plant-based feedstocks with a wide range of catalytic systems. This chapter will critically review the most significant and pertinent literature with regards to the aims and objectives of the thesis. Areas of particular concern include lignocellulosic biomass, biomass fractionation (including microwave heating), acid catalysis, solid residue formation from acid catalysis and anaerobic digestion. The review will also highlight the gaps in knowledge and synthesise new concepts to bridge these gaps in research. This was most pertinently applied to the solid residue formation and properties, with key links between multiple fields defined for the first time.

2.2 Lignocellulosic biomass

Lignocellulosic biomass is often defined as plant biomass that is composed of interlinked cellulose, hemicellulose and lignin polymers [1]. The polymers are the principal components of plant cell walls as shown in Figure 2.1 [2,3] and are composed of several thousand polymerised sugars or phenols.

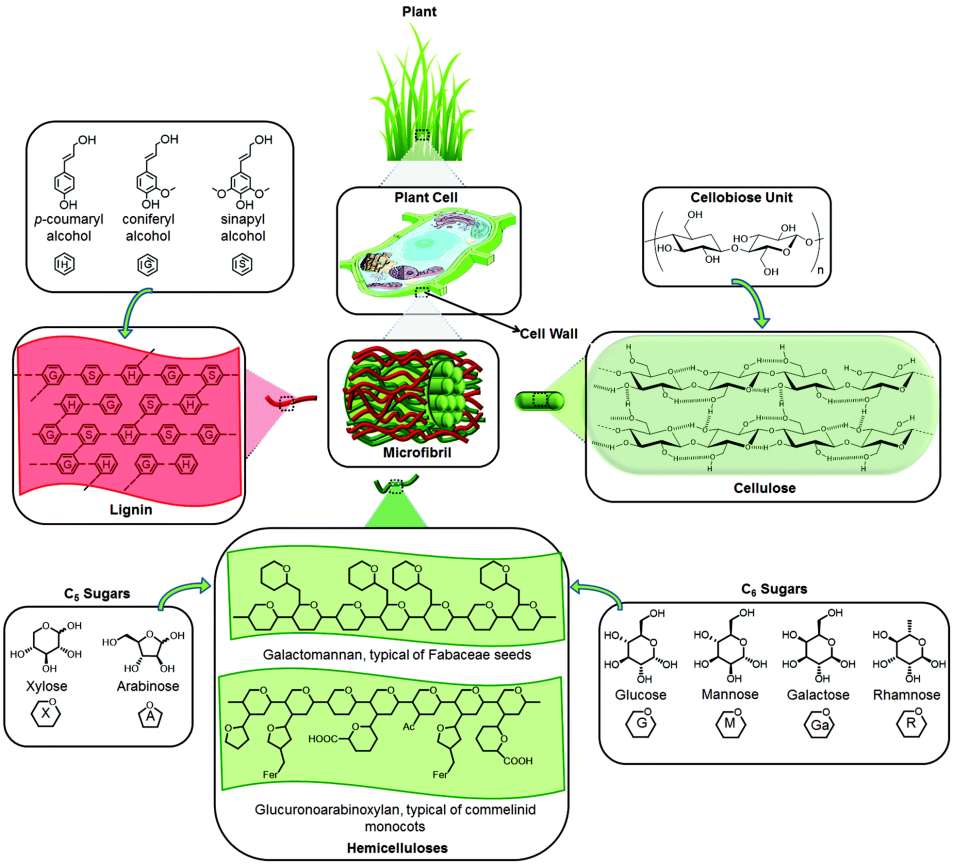

Figure 2.1: The main components and structure of plant cell walls in lignocellulosic biomass. Reproduced from Iskigor *et al*. with permission.[3]

Lignocelluloses differ significantly from first generation biomass such as rapeseed or corn, which are composed of oligomer sugars and oils of no more than 10 units. As the polymer chains form a crystalline structure, intramolecular bonding occurs between the chains requiring “harsher” processing conditions than enzymatic fermentation to produce individual sugars. The heterogeneous nature of lignocellulosic

biomass necessitates the understanding of all constituent fractions to understand the overall conversion process and possible interactions between breakdown products

The largest single constituent of lignocellulosic biomass is cellulose, accounting for up to 50% of the dry weight and it is considered the primary target of lignocellulosic conversion to platform chemicals or biofuels. Cellulose is composed of 15-20 nm wide microfibrils that contain β-1-4-glycosidic bonds linked glucose units that form the plant cell wall [4]. The arrangement of the cellulose microfibrils provides structural strength to the cell wall and plant, by utilising a rigid crystalline structure that causes significant intramolecular hydrogen bonding networks [5]. The crystalline structure is recalcitrant and insoluble under normal conditions, however the linking glycosidic bonds are susceptible to acidic and enzymatic hydrolysis. Transitionary zones of less organised cellulose chains identified as amorphous cellulose, exist between crystalline cellulose microfibrils, as shown in Figure 2.2.

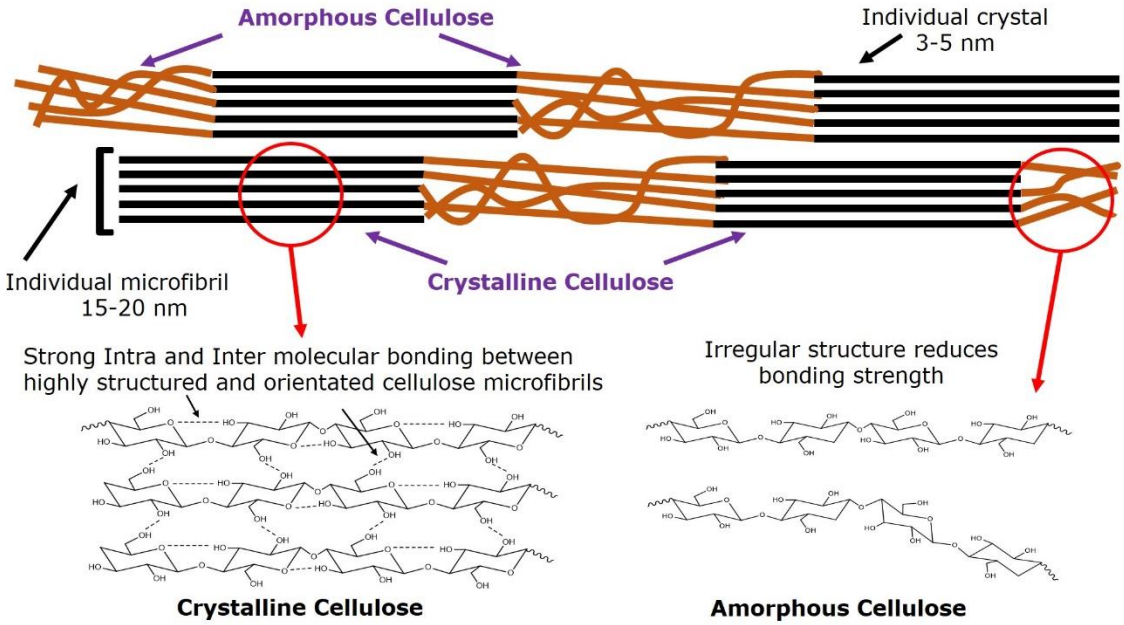

Figure 2.2: Difference between crystalline and amorphous cellulose

The degree of disorder reduces the intermolecular bonding and has been extensively reported to be more readily hydrolysed than crystalline structures [6]. The crystalline

structures can be measured relative to the total cellulose content referred to as the crystallinity index (CI), using X-ray Diffraction (XRD) [7]. The relative CI of biomass increases as the hydrolysis progresses due to amorphous cellulose degrading faster than crystalline cellulose.

Hemicellulose is the next largest component of lignocelluloses, characterised by an amorphous structure, as it is composed primarily of xylose but also includes a variety of other sugars including galactose, glucose, mannose and arabinose, as well as acetic acid [8]. Its primary function in the cell wall is to bind cellulose to lignin and it is inherently amorphous with very few protecting groups to the linking glycosidic bonds. Hemicellulose plant content and sugar composition differs significantly between species, with switch grass showcasing values of nearly 30% compared with woods, which frequently contain less than 10% [9]. The primary constituent (xylose) is a five carbon (C5) sugar, hence it differs from glucose (C6 sugar) and these undergo different reaction pathways during hydrolysis. Currently, the largest application of xylose is for the production of the platform chemical furfural, which can be utilised for the production of solvents, polymers and fuel additives [10,11]. Xylose can be separated from lignocellulosic biomass via sequential hydrolysis or steam explosion [12]. Despite that, due to the relatively small abundance compared with cellulose its valorisation is not prioritised.

Finally, lignin is a three-dimensional polymer of phenylpropanoid units [3]. Its biological purpose is to provide stiffness and strength to the plant material and is primarily composed of a non-repeating structure, primarily derived from p-coumaryl, coniferyl, and sinapyl alcohols [13]. Lignin is most commonly classified in two types by literature as Klason lignin and acid soluble lignin. Klason lignin is defined as the insoluble

material remaining after a 72 wt.% H_2SO_4 hydrolysis of lignin, which can be liberated into is aromatic monomers using oxidative processes (including white fungi, alkaline, oxidation, fast pyrolysis and hydrogenolysis) [14–16]. These aromatic compounds are currently of great commercial interest for use in production of vanillin, biofuels and styrenes [17], but for the most part lignin is mostly recalcitrant to degradation under non-oxidative conditions [18,19]. Several other methods have been developed to increase lignin accessibility, including catalytic, ionic liquids and enzymatic processes [20–22]. However, the aryl bonds in Klason lignin groups are significantly more difficult to break than glycosidic bonds or those present in acid soluble lignin. Nonetheless, β-O-4′ aryl-ether linkages between courmayl units in Klason Lignin can be homolytically cleaved and repolymerised under hydrothermal conditions that can result in the rearrangement of lignin structures [23]. It has also been noted that hydrothermal conditions can induce aromatisation and dehydration of lignin [24].

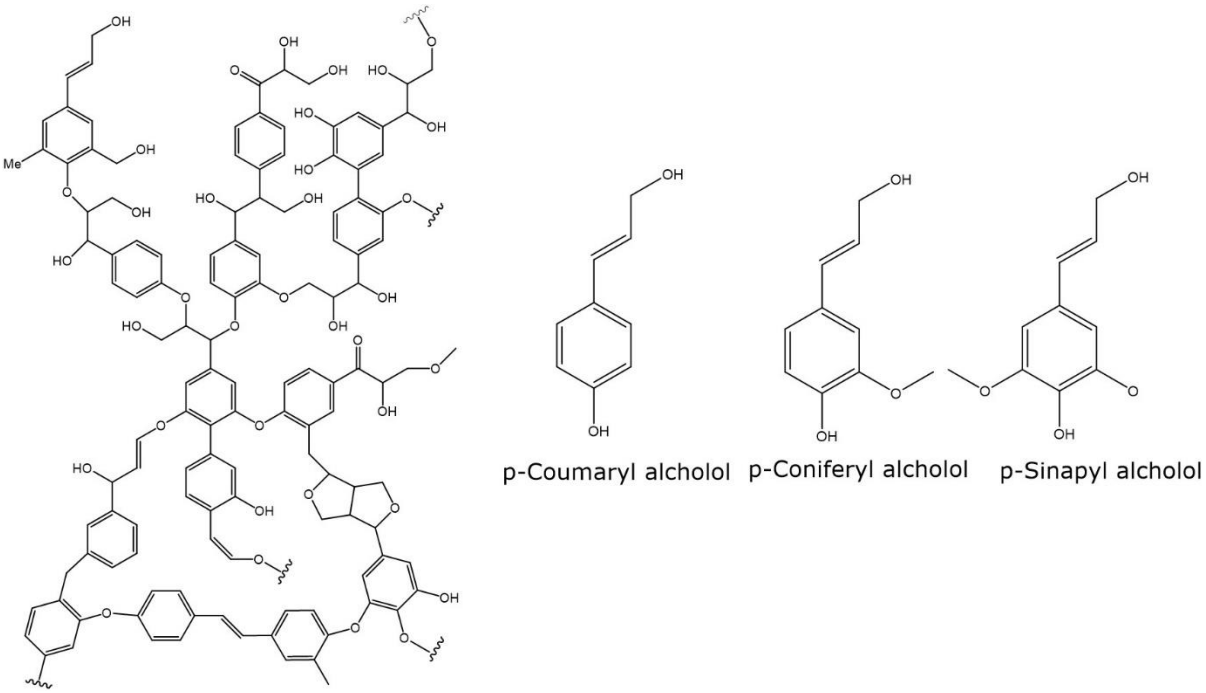

Figure 2.3: A) Example lignin network formed of irregularly organised building blocks, B) structures of three most common lignin monomers

Acid soluble lignin is composed of short-chained hydrophilic phenolic compounds [25,26] and its content in lignocelluloses varies between 3-10% of plant dry matter. Acid soluble lignin has been observed to react with various sugar compounds under hydrothermal and acidic conditions to produce pseudo-lignin [27,28]. Pseudo-lignin is an aromatic material which contributes to Klason lignin content but is not derived thereof. The individual reactions of acid soluble lignin under various operating conditions is not well understood, but can be broadly described as condensation reactions forming insoluble materials akin to Klason lignin.

Alongside these three constituents, there are a range of other simple sugars, proteins, pectin and oils as well a multitude of trace chemicals that make up to 20% of biomass. These other components can either be inert and/or reactive under processing conditions. Determining the relative reactivity of the extractive fraction is possible through experimental methods only, which is one of the reasons why a multitude of feedstocks must be trialled.

2.3 Polysaccharide fractionation

2.3.1 Hydrothermal non-catalysed hydrolysis

Given the complexity and insolubility of the polysaccharide matrix, it is beneficial to degrade the long-chained polymers into individual monomers before further valorisation. This can be achieved using catalyst-free processing methods such as ionic liquids, solvent extraction, hot water extraction and steam explosion [29–31]. Ionic liquids are room temperature molten salts, which have gained increasing prominence for the tuneable ability to degrade cellulose, hemi-cellulose and lignin, with varying degrees of selectivity at low temperatures [32]. However, ionic liquids are currently prohibitively expensive for commercial uses and can easily precipitate with ash impurities in lignocellulosic feedstocks [33]. Alternatives, such as gamma-valerolactone (GVL) and deep euletic solvents, can transform 30-40 wt.% of lignin at temperatures of 140-180 °C to low molecular weight monomers without affecting cellulose structures [34,35]. Delignification is not only a source of monomeric lignin, but it also improves the digestibility of cellulose, although complete solvent removable has proven difficult and was not investigated further in this study.

Cellulose and hemicellulose require the presence of water in order to undergo hydrolysis. Sub-critical water extraction can reduce up to 75% hemicellulose and cellulose 45% to monomeric sugars, respectively at temperatures of 150-200 °C [6,36]. Water extraction uses the solvation properties of water to disrupt the polysaccharide matrixes to increase the biomass surface area, reduce its chlorine content and solubilise easily extractable compounds such as acetic acid, which in turn reduces the water pH. This method can be further supplemented by using steam explosion, which utilises high pressure steam to fully solvate and penetrate the polymer matrix using

capillary action, before rapid decompression that generates shear force to hydrolyse glycosidic bonds [37]. This violent internal expansion force acts as a partially-mechanical pretreatment to increase the biomass surface area and increase enzymatic digestibility by up to 90% [38]. Steam explosion and sub-critical water extraction cannot fully hydrolyse sugar-based polymers without producing significant by-products from hydrothermal decomposition such as levolglucosan, furfural and glycoaldehyde [36] .

2.3.2 Acid Catalysed Hydrolysis

Acid catalysed hydrolysis can selectively hydrolyse β-1-4-glycosidic bonds between repeating sugars at moderate temperatures (120-250 °C) with mineral and organic acids such as hydrochloric, sulphuric, formic and oxalic acid [39]. In the last 20 years, the acid hydrolysis of large variety of materials including crystalline cellulose, bagasse, wood, energy crops, grasses and agricultural wastes, has been extensively investigated for the production of monomeric sugars [40–43]. The acid catalysed hydrolysis of β-1-4-glycosidic bonds is a three step process, which is outlined in Figure 2.4 [44]. The first stage of the reaction is the rapid formation of a conjugate acid on the glycosidic oxygen linking two sugar units before breaking down into a cyclic carbonium ion with C-O cleavage. This is followed by a rapid addition of water to produce a monomeric sugar and a proton. The intermediate carbonium ion appears more frequently at the end of polymer chains and is somewhat sterically limited, due to the glycosidic bond being protected. The process has been extensively modelled using first order kinetic models [45].

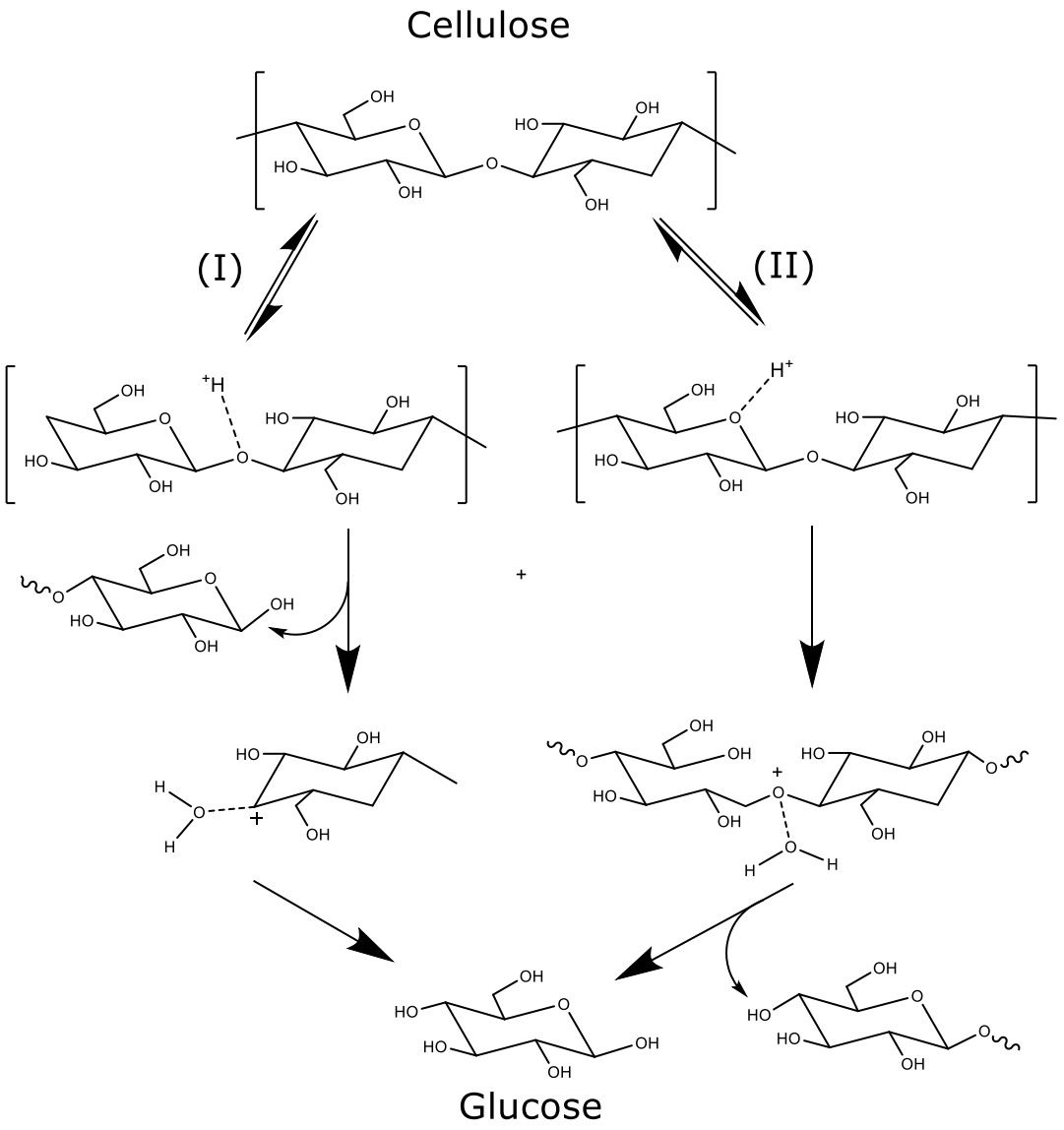

Figure 2.4: Mechanism of acid catalyzed hydrolysis of β-1-4 glucan.

Dilute acid hydrolysis is sufficient to selectively decompose glycosidic bonds in hemicellulose with conversions of up 90% facilitated by acid concentrations of 0.5-2.0 wt.% and temperatures of 70-120 °C [9]. However, the hydrolysis of the crystalline cellulose requires higher reaction temperatures of 180-200 °C [46]. This difference in hydrolysis rates is caused by the differences in the physical properties between the two polysaccharides and can, therefore, be individually hydrolysed in a two-stage temperature ramped process [40,47]. This can be combined with catalysis to completely convert xylose before cellulose hydrolysis starts [48]. In line with this objective, acid

hydrolysis has been used as pre-treatment for other processes, including ethanol and lactic acid fermentation, heterogeneous catalysis and anaerobic digestion [49–51]. The low operating temperatures and small amount of catalyst required, has made it an attractive low cost-pre-treatment method. However, the homogenous acid catalyst requires neutralisation for biological applications and the sugar decomposition limits yields. Under acidic conditions the degradation of sugars commences at ~90 °C [52] and can produce a range of products including 5-hydroxymethylfurfural (5-HMF), phenols, short organic acids such as formic and acetic acid as well as solid products [53]. Solid products are the largest by-product of acid hydrolysis and can be formed via several reaction process, which are discussed in detail in section 2.5. The formation of phenolic and other aromatic compounds in high concentrations can inhibit microbial processes, hence limiting the commercial application of dilute hydrolysis to non-microbial processes[54].

2.3.3 Microwave Assisted Heating

The use of microwave heating has been widely demonstrated as an effective heating system compared with conventional systems for the conversion of biomass. Conventional thermal heating systems require convection and conductive heat transfer mechanisms to distribute heat from the outside of the heating vessel to the interior. This results in a gradient heat profile across the reactor and biomass particle cross-section. Microwave heating utilises electromagnetic waves with the frequency of 2.45 GHz to penetrate substances and heat molecules throughout the cross-section producing a more homogenous heat profile [55], as shown in Figure 2.5.

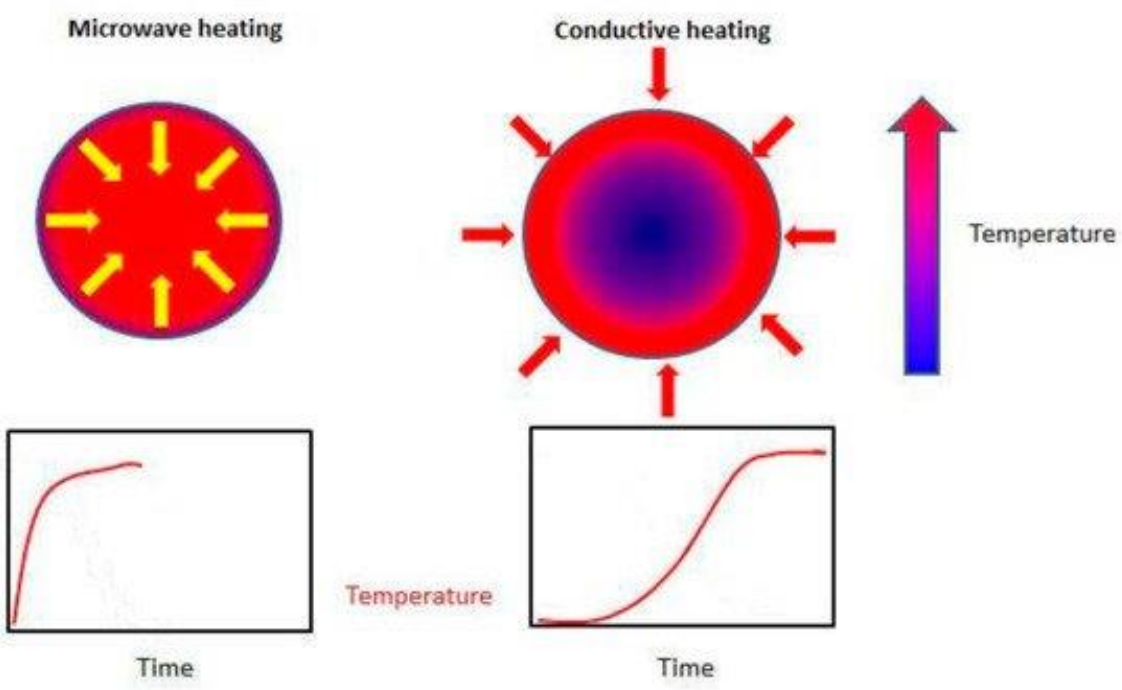

Figure 2.5: Difference between microwave and conductive heating across a biomass particle, reproduced from Palma *et al*. with permission [56]

Under an oscillating microwave field, polar molecules with an electrical dipole, such as water, will rapidly align themselves the electric fields and will rotate. As the field alternates, the molecules reverse direction: the rotating molecules push, pull and collide with one another, resulting in energy loss in the form of thermal energy. The

rapid increase in temperature has been likened to steam explosion as a pre-treatment [57]. Microwave processes have also been found to increase lignocellulose surface area relative to conventional heating, which in turns increases the amount of amorphous cellulose [58], aiding hydrolysis. Zhu *et al*.[59] achieved a 75.3 % carbohydrate yield recovery from *Miscanthus x Giganteus* with 0.2 M H_2SO_4 at 180 °C for 20 minutes, which was 12 times higher than that from conventional heating with similar conditions.

Acid hydrolysis of biomass under conventional and microwave heating has been investigated and compared by Mukhergee *et al*.[60] using kinetic modelling. They proposed that faster heating and cooling rates, associated with microwave heating, lowered the overall reaction temperature of the HCl catalysed process, which decreased the by-product yields. Mukhergee *et al*. also noted a decrease in the apparent activation energy for the conversion of starch to glucose with microwave heating. Similar work with Amberlyst IR-120 catalyst also found a decreased apparent activation energy for the conversion of sucrose to glucose under microwave heating [61], which has also been found by other authors to increase protein peptide hydrolysis and biomass oxidation [62,63]. Faster hydrolysis can therefore lead to process intensification through the thermal effects of the microwave induction on water solvation on biomass. Water is an excellent microwave absorber with a dielectric loss factors ε'' of 78 at 25 °C, which decreases to 56 at 100 °C [64]. The latter values are significantly higher than that of lignocellulosic biomass, which varies between 0.2 - 3.0 [57]. Therefore, the microwave direct heating of biomass can mostly be considered negligible at high water contents. Microwave induced heating of internal cell moisture has been proposed to increase cell rupture and disruption of the cellulose hydrogen bonding network [65]. As such the benefits of microwave heating has been directly linked

with water-to-solids ratio and water diffusion. However, microwave induced hydrothermal carbonisation must be considered at high solids content due to anhydrous decomposition of cellulose [66].

Despite the reported benefits of microwave heating, its wide scale commercial adoption has been limited. Previously, its use has been constrained by high electricity costs, high capital costs and low scalability [67]. More recent developments however have sought to reduce these costs by adopting modular microwave approaches that increase scalability and reduce capital costs via process intensification. While the price of electricity will remain comparatively higher than fossil fuel derived low pressure steam, the development of low-carbon electricity grids can potentially significantly reduce the carbon impact of process heating [68]. The electrification of industrial processes is considered a key challenge in meeting carbon reduction emissions and the use of microwave heating would help meet these goals [69].

2.4 Acid Catalysis

2.4.1 Levulinic Acid and Furfural

The acid catalysed dehydration of xylose to furfural was first reported by Döbereiner in 1832 [70], while the sulphuric acid dehydration of glucose to levulinic acid and formic acid was reported by Mulder in 1840 [71]. Since then, acid catalysed dehydration of sugars has gained increasing attention in recent years as a source of renewable biochemicals. Both levulinic acid and furfural have been considered among the most promising biorefinery platform chemicals for the production of a range of applications. For example, hydrogenation of levulinic acid to valeric acid (pentatonic acid) and subsequent esterification to valerate esters will yield petrol and diesel-grade compunds [72], as shown in Figure 2.6.

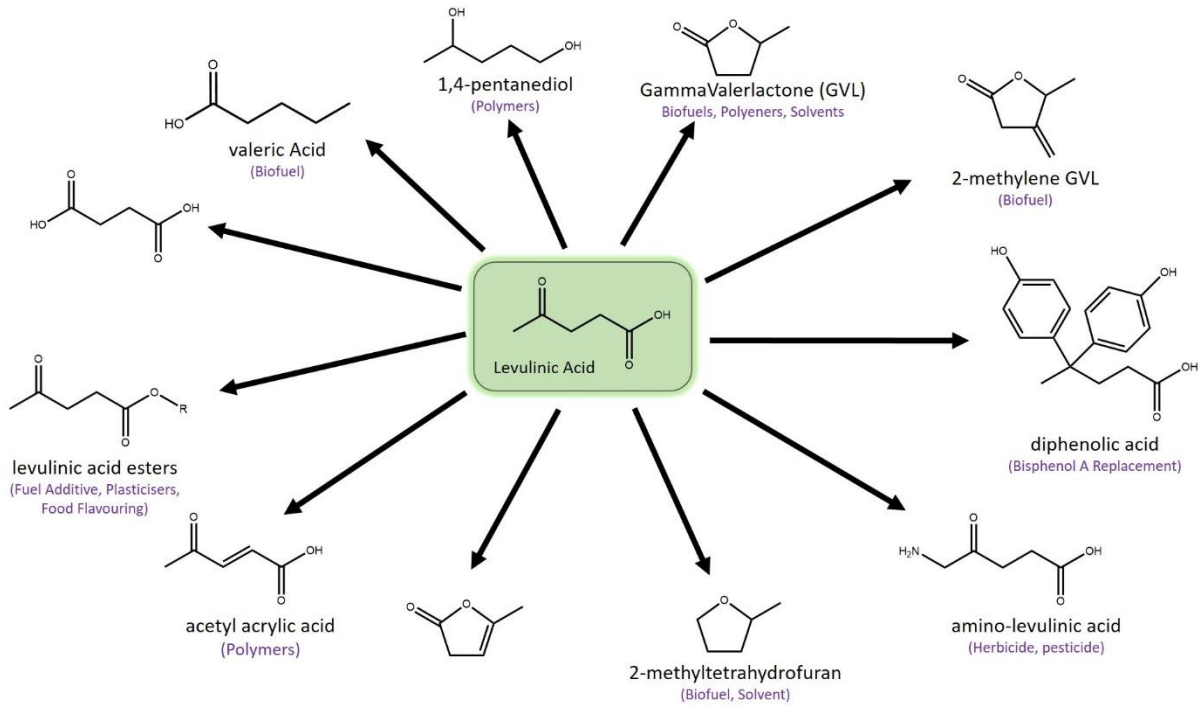

Figure 2.6: Levulinic acid as a platform chemical for multiple applications

Levulinic acid can also be oxidised to succinic acid [73], which is a C4 platform chemical [74],. It can be hydrogenated to gamma-valerlactone (GVL),a useful solvent and polymer

precursor [75], or undergo amination to form the herbicide amino-levulinic acid, among other applications. The commercial attractiveness of levulinic acid as a platform chemical is dependent on its low-cost production capability in order to compete with fossil fuel derived chemicals. Therefore, it is imperative to maximise yields, minimise by-product yields and, where necessary, find potential valorisation applications for all by-products.

Similar to levulinic acid, furfural can be utilised as a platform chemical for a wide range of applications, as shown in Figure 2.7. The largest current application is the hydrogenation of furfural to furfuryl alcohol, which is used for polymer production, wood glues, resins and coatings [76]. Further hydrogenation of furfuryl alcohol yields tetrahydrofurfuryl, which is used as a solvent and biofuel. Furfural can also undergo reductive amination to furfurylamine, oxidation to furoic acid or decarbonylation to 2-methyl furan [77]. This is in addition to the current application for furfural as a biofuel and fuel additive [78]. The co-production of furfural alongside levulinic acid is an essential part of the biomass valorisation process.

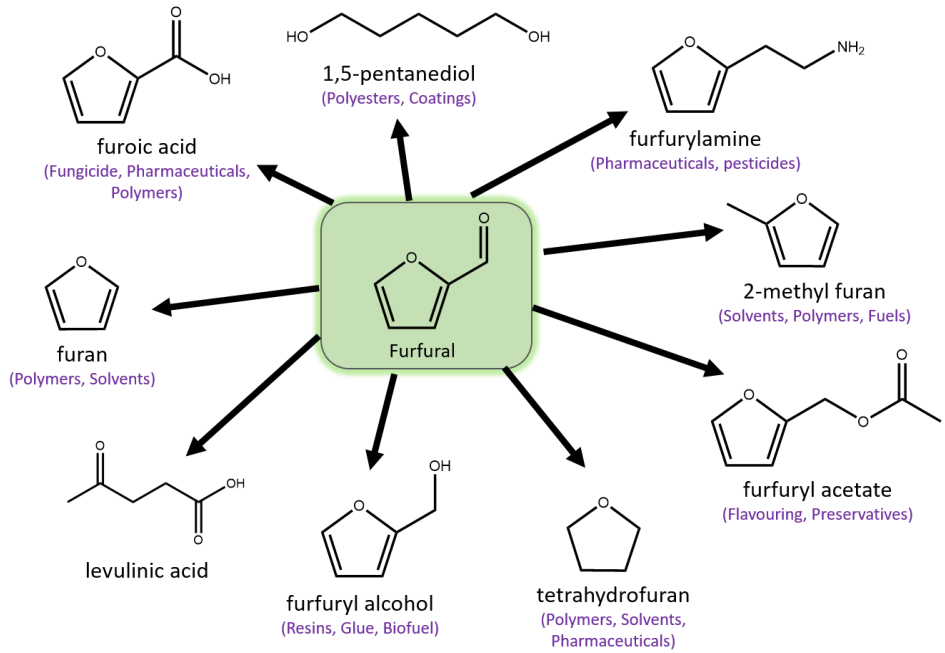

Figure 2.7: Furfural as a platform chemical for multiple applications

Both levulinic acid and furfural are key platform chemicals, which can be used to replace fossil fuels in a broad range of applications for the development of a lo carbon economy. The predominant methods for producing both platform chemicals are via acid catalysed sugar dehydration in aqueous media.

2.4.2 Levulinic Acid Synthesis

The acid catalysed conversion of sugars can be combined with the polysaccharide hydrolysis, resulting a “one-pot” process for the direct production of biochemicals from lignocellulosic biomass. The advantages of aqueous catalysis is the low-energy requirement for pre-treatment other than size reduction, and also the low reaction thermal range (<200 °C) and the relatively low cost of catalyst [79]. Using homogenous and heterogeneous catalysts exhibiting both Brønsted and Lewis acid properties, cellulose can be hydrolysed to glucose, as previously discussed, before transformation into levulinic acid, following the paths shown in Figure 2.8 [80].

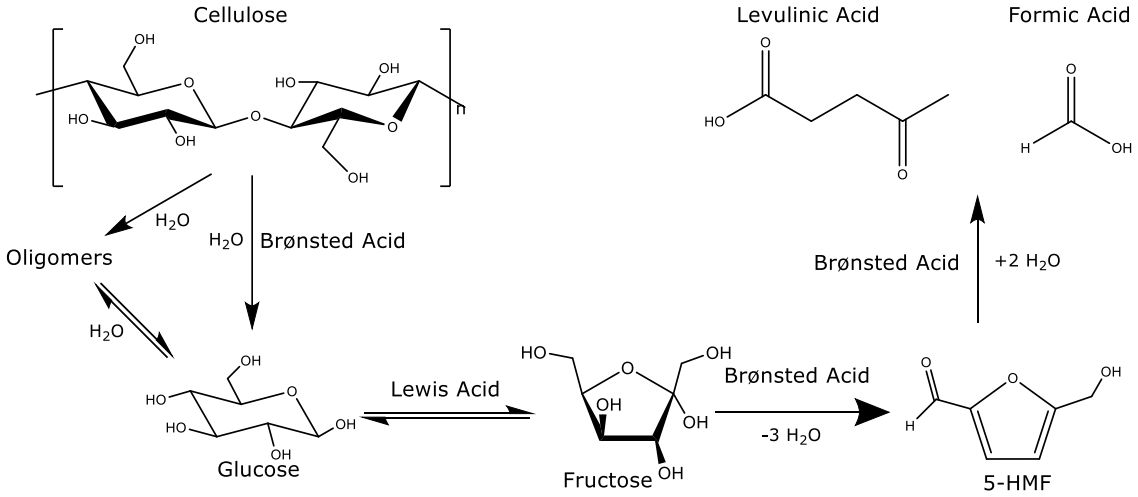

Figure 2.8: Production of levulinic acid from cellulose with intermediate glucose, fructose and 5-HMF

Lewis acids can readily isomerise glucose to fructose, in which the pyranose structure is converted to furanose fructose, which is known to be more unstable [81]. Fructose can

then undergo the acid catalysed triple dehydration to form the intermediate, and highly reactive, 5-HMF [82]. The subsequent double rehydration of 5-HMF produces a stoichiometric equal mixture of levulinic and formic acid. Formic acid is a versatile biochemical that can be utilised in a multitude of processes in a biorefinery context [83] and can easily be separated from levulinic acid using either esterification, phase separation or a combination of both [84].

Homogenous catalysts such as mineral acids, metal salts and organic acids have been used for the conversion of sugars, cellulose and real lignocellulosic biomass, as shown in Table 2.1. Levulinic yields have varied from 30 to 80%, from a variety of feedstocks and reaction conditions. In 2006, Girisuta *et al.* [85] utilised H_2SO_4 (0.05-1.0 M) to achieve levulinic acid yields exceeding 80% using glucose as a feedstock at 140 °C. The accompanying kinetic model identified that the lower operating temperatures (towards 140 °C) improved the selectivity of glucose towards levulinic acid over side reactions. This is in contrast to the higher operating temperatures of 200 °C required for cellulose hydrolysis, requiring careful optimisation of operating conditions specific for each catalyst and feedstock combination. This limitation is not an issue for the conversion of simple sugars such as glucose and fructose, leading to yields of over 70% with catalyst HCl, H_2SO_4 and $AlCl_3$. Several studies report that fructose is nearly 100 times more reactive than glucose [86,87] and that metal ions, such as Al^{3+}, Sn^{2+} and Cr^{3+}, can greatly improve the isomerisation of the glucose to fructose [88]. However, levulinic acid yields from sugars are limited by the formation of by-products, which reduce molar yields to below 80%.

Table 2.1: Summary of levulinic acid yields from a range of feedstocks with homogenous catalysts

Catalyst	Substrate	Substrate Loading (w/w%)	Temperature (°C)	Reaction time (Hours)	Other	Yield (mol. %)	Reference
2M H_2SO_4	Fructose	5.00%	170	8		69%	89
30 w/w% NaCl	Fructose	10%	110	24		75%	90
0.1 M HCl	Glucose	10	160	4		51%	91
0.5 M H_2SO_4	Glucose	0.18%	140	8		80%	85
$SnCl_4$	Glucose	1.90%	190	1.5		45%	92
0.01M $AlCl_3$	Glucose	2.00%	180	2		71%	93
1M H_2SO_4	Cellulose	1.70%	150	-		76%	80
0.75M HCl	Cellulose	2.00%	155	1.6	GVL/H2O Solvent	71%	94
1.37 M HCl	Cellulose	1.00%	200	0.05	MW	43%	95
0.01M $AlCl_3$	Cellulose	2.00%	180	2		24%	93
0.02M $CrCl_3$	Cellulose	5.00%	200	3		67%	93
$[HO_3S\text{-}(CH2)3\text{-}py]Cl\text{-}FeCl_3$	Cellulose	1.67%	180	10		49%	96
0.1M H_2SO_4	Euctalyptus	5.00%	190	1		29%	97
2.5M H_2SO_4	Kernel grain sorghum	10.00%	200	40 mins	MW	33%	98
5% w/w H_2SO_4	Poplar Wood	10.00%	190	50 mins		54%	99
37 w/w% HCl	Poplar Wood	7.2%	200	1	MW	71.3	100
2 M HCl	Corn Starch	1.00%	165	0.25		55%	60
0.37 M HCl	Bamboo	10.00 %	160	3	MW	48%	101
0.6M HCl	Pre- treated Cow-Dung	3.30%	180	2.5		81%	102
$[C_3SO_3Hmim]Cl_2$	Rice straw	-	180	1.5		21%	103
$[BMIMSO_3H]\ HSO_4$	Corn Stover	-	95	1		70%	104
2M Maleic acid + $Al_2(SO_4)_3$	Mandarin Peel	4.30%	180	0.63		86%	105

Cellulose conversion to levulinic acid requires the additional step of the cellulose hydrolysis to sugars, which increases the overall complexity of the system. Using microcrystalline cellulose, it is possible to achieve levulinic acid yields exceeding 60 % with HCl, H_2SO_4 and $CrCl_3$ as shown in Table 2.1. Mineral acids are of greatest interest for this application, due to their availability, low-cost and high yields however, their corrosive properties have been reported to damage vessels and pipeline systems [106]. Transition metal chlorides also received attention in this area, due to the low concentrations required (<0.1 M) to achieve high yields compared with HCl (0.1-1.0 M) and H_2SO_4 (0.5-2M) [93]. It has been hypothesised that the chloride counter ion has an additional positive effect of stabilising intermediate products [107]. More recently, neutral NaCl salts have been reported to achieve yields over 75% from fructose under relatively mild conditions (<150 °C) [90], however chloride ions under neutral conditions have not been reported to fully depolymerise cellulose or isomerise glucose to fructose.

Due to the complexity of lignocellulosic biomass, the screening the of catalysts with glucose and cellulose can be used to estimate the levulinic acid yields but does not estimate the interference of other compounds on catalysis. This is most evident with metal salt catalysts such as $AlCl_3$, which have a tendency to precipitate with counter ions found in real lignocellulosic biomass [108], despite achieving similar yields to that with pure cellulose. Ion precipitation is a considerable expense for ionic liquids conversion of real biomass, due to the low catalyst recyclability [32]. The salt precipitation issue is less significant with mineral acids, primarily HCl and H_2SO_4, due to the wide solubility of their respective salts under aqueous conditions. Antonetti *et al*. [100] achieved levulinic acid yields exceeding 70% with a range of feedstocks

including poplar wood, waste paper and olive tree prunings at 200 °C for 1 hour with microwave heating, with similar yields being achieved with bamboo, cow dung and rice straw by other authors [101,102,109]. Despite the high yields consistently achieved with hydrochloric acid, the high corrosivity of the catalyst requires advanced alloy materials, greatly adding to initial capital costs [110]. Sulphuric acid has therefore been used as the compromise catalyst in several pilot plants in Caserta (Italy) and Minnesota (USA) [111], despite the possible $CaSO_4$ fouling issues with certain feedstocks such as waste paper and tobacco waste [100,112]. Sulphuric acid has achieved yields of 50-70% with poplar wood, bagasse and food wastes [113–115]. The Biofine process reported sulphuric acid recyclability of over 98% with minimal fouling on a large scale [106] which has also been demonstrated on a lab scale [84,89]. As sulphuric acid has been successfully investigated for the production of levulinic acid from an ever-increasing number of lignocellulosic materials, it has become the ubiquitous default homogenous catalyst. Therefore, it is has become imperative to optimise the reaction's operating conditions to minimise by-products formed under the acidic conditions.

The kinetic model of the cascade catalytic process, including by-products, has been investigated in great depth from both cellulose [80,116] and real lignocellulosic biomass [117–119]. Using the reaction kinetics continuous plug-flow reactors (PFR) have been designed for the large scale production of levulinic acid and also implemented in pilot plants [91,111]. One of the advantages of PFR reactors is the minimisation of by-product yields, when using the Biofine process, to ~50 wt.% of the feedstock. Dussan *et al.*[48] proposed two PFRs in series, operating at 185 °C and 180 °C respectively, to achieve overall 72% levulinic acid yield from *Miscanthus x Giganteus,* with 27 % furfural yields

in under 20 minutes. The modelling of the reaction kinetics with multiple feedstocks have found similar reaction rates for the conversion of glucose towards levulinic aid across multiple studies. While the differences in cellulose structure result in widely differing the kinetic data for polysaccharide hydrolysis. The variance in cellulose structure and CI has been attributed as the cause of such difference along with the presence of inert fractions such as lignin and pectin [120]. Nevertheless, this results in each feedstock needing an individual and custom evaluation for this application.

2.4.3 Heterogeneous Catalysts

As a result of the ever-growing trend towards greener processes, the replacement of corrosive and harmful mineral acids with solid catalysts is becoming more attractive. Heterogeneous catalysts containing Lewis and Brønsted acidity can catalyse the conversion of biomasses to levulinic acid. In recent years, a large variety of solid acid catalysts has been investigated for the catalysis of sugars, cellulose and real biomass, as shown in Table 2.2. Such catalysts include insoluble metal oxides, zeolites, acidic ion-exchange resins and functionalised hydrochars. The use of solid catalysts significantly decreases the catalyst separation costs compared with homogenous catalysts, with minimal corrosion concerns [121]. Another key advantage of solid acid catalysts is their high temperature stability as well as the tunability of their surface acidity to improve catalyst selectivity by reducing by-product formation [122]. These properties make heterogeneous catalysts suitable for large scale commercial application in this field, including levulinic acid production.

Table 2.2: Summary of levulinic acid yields from a range of feedstocks with homogenous catalysts

Catalyst	Catalyst to Biomass ratio (w/w%)	Substrate	Substrate Loading (w/w%)	Temperature / (°C)	Reaction time (hours)	Other	Yield (mol. %)	Reference
Amberlyst 15	2.2	Glucose	10.00%	140	8		59	123
ZSM-5	0.75	Glucose	4.00%	180	3		53.2	124
Graphene-SO_3H	0.025	Glucose	15.00%	200	2		78	125
Amberlyst 15	2.2	Glucose	10.00%	140	8		26.7	123
Amberlite IR-105	0.7	Sucrose	10.00%	130	0.05		19	126
Zirconium Phosphate	1	Cellulose	4.00%	220	2		18	127
Amberlyst -70	3	Cellulose	2.00%	160	16		23	128
C-SO_3H-Fe_3O_4	1.6	Cellulose	12%	190	3.5	MW Magnetic	25.3	129
Sulfated TiO_2	1	Cellulose	2.50%	240	0.25		32	130
Zirconium	1	Cellulose	2.00%	180	3			131
Al-$NbOPO_4$	0.8	Cellulose	5.00%	180	24		53	132
Amberlyst 36	1	Paper Towels	5%	150	0.33	MW	30	133
$CrCl_3$/HY	12	Kenaf	1%	145	2.5			134
Amberlyst 36	20 wt%	Sugar Beet Molasses	0.1	140	180		78	135

The first solid acid catalyst for levulinic acid production utilised acidic ion-exchange resin, Amberlite IR-105, to achieve yields of 19 wt.% (28 mol. %) from sucrose at 130 °C in 5-6 minutes under reduced pressures [126]. The use of this solid acid catalyst was able to significantly drop the reaction temperature and time compared with mineral acids. Acidic ion-exchange catalysts are made from functionalised polymers, most commonly sulfonated polystyrene, that can be produced at large scale with highly tuneable surface, porosity and ion exchange capacity. The sulphonic acid group (-SO_3H) is a strong acid that has similar acidic properties to sulphuric acid, without the associated corrosion issues. More recent works with Amberlyst has achieved levulinic acid yields of the 57% with fructose, 27% with glucose and 30% with waste paper sludge [123,127,133]. The limiting factor with ionic polymers is the low isomerisation of glucose to fructose which can be mitigated by active basic catalytic sites [136] or the addition synergistic catalysts with soluble Lewis acids [90].

The cationic metal centres of metal oxides act as Lewis acids that can isomerise glucose to fructose, with high selectivity at low temperatures of <100 °C [121]. Zirconium dioxide has been reported to produce a molar levulinic acid yield of 54% at 180 °C for 3 hours from cellulose [131]. However, the direct conversion of cellulose to levulinic acid with a single metal oxide has mostly proven difficult, due to imbalances in the acid functional sites. This is due to the high catalytic activity of many metals, which can catalyse the formation of formic, acetic acid lactic acid from sugars [137], along with the further conversion of levulinic acid into higher value products such γ-valerlactone [138]. Ding *et al*. [132] suggested that the optimum Brønsted/Lewis acid ratio for the conversion of cellulose to levulinic acid is 1.2:1. Hybrid metal catalysts can easily be tailored to optimise acids sites with catalysts such as Al-Zr, zirconium phosphate and Ru/C for

the conversion of sugars [127,132,139]. Nonetheless, it should be noted the use of metal catalysts has been limited for the production of levulinic acid for many reasons, but primarily for the strong adsorption of LA and degradation products onto the catalysts surface area, which can decrease levulinic acid yields over multiple cycles[140].

Zeolites are aluminosilicate minerals that are widely used by the petrochemical industry as a solid acid catalyst for processes such as catalytic cracking, isomerization and alkylation reactions. Zeolites can form naturally as minerals (e.g. clinoptilolite) however, synthetic zeolites can easily be fabricated at laboratory and industrial scale. The variation of the synthesis conditions can create a wide variety of microporous crystal structures, such as ZSM-5, X/Y, β, and A [141], which can be further modified with metal doping [142]. As early as 1987, Jow *et al*. [143] used LZY zeolite to convert fructose to levulinic acid at 140 °C for 15 hours with a 43.2% yield, with the high selectivity attributed to molecular sieving ability, in addition to Lewis acid sites. Also, H-USY zeolite (Si:Al of 30) has shown remarkable selectivity (>90%) for the isomerisation of glucose to fructose at temperatures as low as 120 °C [144]. Ya'aini *et al.*[134] found that $CrCl_3$/HY catalyst can reach levulinic acid yields of 55.2 and 53.2% from cellulose and kenaf respectively, at 145 °C for 2.5 hours. In this case, the high yields were attributed to pore structure trapping intermediate 5-HMF [134]. In addition, the catalytic activity of zeolites for the conversion of sugars and cellulose has shown remarkable stability of up to 5 recyles [144–146].

However, the recyclability of zeolites for the conversion real lignocellulosic biomass has proven more challenging, with yields decreasing by up to 60% over 3 recycles [147]. Low recyclability was attributed to several phenomena, including coking [148] and acid site leaching [149]. The coking phenomena also include the catalytic formation of

insoluble humins via dehydration of intermediate compounds and also lignocellulosic extractives blocking the catalyst the surface area, which are discussed in more depth in section 2.5.

Metal-organic catalysts utilise organic frameworks to support metal oxides or metal oxide nanoparticles have been investigated for an increased surface area and tuneable pore structure [150]. Yields of nearly 32% levulinic acid have been achieved with a high selectivity (68%) with regards to levulinic acid, although the hydrothermal stability of such catalysts has proven troublesome and metal-organic framework catalysts have not been largely explored for cellulose conversion [96]. A simpler method for the tailoring metal oxides for use in levulinic acid production is the surface modification via sulphation, to increase catalyst acidity. Kobayshi *et al*. [151] developed a recyclable heterogeneous catalyst from the sulphated carbon chars resulting from the production of glucose from eucalyptus. Sulphated titanium dioxide and zirconia catalysts achieved levulinic acid yields of 32% and 59% respectively from cellulose [130,152]. Heterogeneous catalysts surface modification by sulphation has been found to increase the number of overall acid sites as well as allow the tunable modification of the Brønsted/Lewis acid site ratio [153]. The sulphation of zirconia increased the catalysts selectivity for levulinic acid from cellulose from 32% to 53% and showed remarkable stability over 5 recycles with lignocellulose. However, the use of heterogeneous catalysts with lignocellulose has been shown insufficient to achieve high (>60%) levulinic acid yields.

2.4.4 Synergistic Catalysis

Heterogeneous catalysts can be synergistically promoted by the addition of salts or acids in the aqueous phase, as shown in Table 2.3.

Table 2.3: Promotion of heterogeneous catalysts

Catalyst	Feedstock	Yield Without Promoter	Catalyst Promoter	Yield With Promoter	References
DOWEX DR-2030	Glucose	28% Levulinic acid	1:1 Salt to sugar ratio	71% Levulinic Acid	90
Nanofin	Cellulose	14% Levulinic Acid	25 wt% NaCl	72% Levulinic Acid	154
Ru(1.8)/H–USY	Cellulose	1% Sorbitol	1 mM HCl	29% Sorbitol	155
Sulfonated Carbon	Eucalpytus	31% Glucose	13 mM HCl	78% Glucose	151

Previous studies have found that high concentrations of NaCl (20 wt.%) under hydrothermal conditions could partially depolymerise cellulose and, simultaneously, reduce the average molecular weight of cellulose by up to 50% without forming free sugars [156]. In this regard it was proposed that the Cl^- anion could disrupt the cellulose hydrogen bonding network. Other works have proposed that cellulose depolymerisation is enhanced in the order of $CO_3^{2-} > F^- >> Cl^- > NO_3^- > SO_4^{2-}$. Similarly, Pyo *et al*. [90] proposed $Cl^- > CO_3^{2-} > SO_4^{2-}$ for the dehydration of the fructose to levulinic acid. The use of NaCl has been found to drastically increase the yields of levulinic acid with sulphated polymers however, it was shown to require high salt concentrations, exceeding 10 wt.%. Kobayshi *et al*. [151]was able to substitute concentred NaCl with dilute 13 mM HCl for the promotion of glucose formation from real biomass, which increased from 31% to 78%. While Geboers *et al*.[155] was instead able to improve sorbitol production via hydrogenation from cellulose by nearly 27 fold with only 1 mM HCl. These remarkable improvements with trace mineral acids can be

used with a wide range of heterogeneous catalysts, by debottlenecking both the cellulose hydrolysis and 5-HMF hydration stages with Cl^- anions.

Although the use of even trace mineral acids, especially hydrochloric acid, could still result in both reactor and catalysts corrosion. Zirconium dioxide has shown ability to partially avoid this issue, to due zirconia's notable hydrochloric acid resistance. In addition, soluble Zr(IV) has been proposed as cellulose to levulinic acid catalyst [131]. In addition, Kassaye *et al*. [152] previously investigated sulphated zirconia for levulinic acid production, finding limited cellulose depolymerisation capability despite high overall selectivity of the catalyst. Therefore, sulphated zirconia would be a promising catalyst to investigate in conjunction with the addition of trace mineral acids for levulinic acid production.

2.5 Acid Catalysis Derived Solid Residues

Alongside the high value products, such as levulinic acid, from the acid hydrolysis of lignocellulosic biomass, significant quantities of by-products are formed. By-products include inert biomass fractions and acid catalysed dehydration products that primarily consist of organic acids and insoluble solid residues. Optimised levulinic acid production systems using lignocellulosic biomass result in solid residue yields between 40-50 wt.%, despite high levulinic acid yields of 60-70 mol% [101,106,157,158]. The solid residue is an unavoidable by-product, due to inert solid lignocellulosic biomass fractions and from degradation production. Among the most studied of the by-products is the formation of "humin" from the acid catalysed polymerisation of 5-HMF. Humin formation from pure sugars has been studied in depth by multiple authors [82,159–162] and has been linked closely with hydrothermal carbonisation. Hydrothermal carbonisation

(HTC) is aqueous carbonisation occurring under elevated temperatures of 180-400 °C, forming primarily via dehydration mechanisms, which constitute the majority of the solid residue from levulinic acid production, although other routes such as the condensation of acid soluble lignin and other extractives cannot be ignored. Due to the overall complexity of the sources of slid residue yields, they should be examined individually.

2.5.1 Humin Formation

Humins are formed during hydrothermal treatment of sugars under acidic conditions. Multiple kinetic studies investigating the formation of levulinic acid have included the formation of humin by-products from both glucose and 5-HMF [48,80,114,116,163]. Humin formation has been considered an almost first-order reaction with regard to acid concentration [82] and Lund *et al.*[160] showed that levulinic acid selectivity could be increased over that of humins using high acid concentrations. In addition, both Girisuta and Dussan [48,80] estimated the activation of energy for the formation of humins is much higher than all other activation energies during the acid catalysed dehydration, showing that lower reaction temperatures can limit humin formation. In particular, the kinetic modelling studies of the acid catalysed process have suggested humin yields can be minimised with lower reaction temperatures, low residence times and high catalyst concentration.

Several mechanisms of humin formation have been proposed by Lund and Patil [160], Huber *et al*. [91], Zandvoort *et al*.[157] and Heeres *et al.* [80] among others. These models have consistently proposed humin formation as an overall dehydration process via aldol condensation. Baugh *et al*. [164] found in 1985 that different C6 sugar isomers and processing conditions altered the elemental composition of humin formation, 56-61

wt.% C. The variation of humin's elemental composition with reaction conditions was further investigated by the Heeres group, 60-65 wt.% C, which suggested that the humins may be the result of multiple different reactions [165,166]. However, Zandvoort *et al*. [157] demonstrated such differences in elemental composition can be explained as different degrees of dehydration of the overall structure. While Sumerskii *et al*. [167] estimated the humin structural composition consisted of ~60 wt.% furan rings weight and ~20 wt.% linking aliphatic linkers. Furthermore, using C13 NMR, GC-MS and IR, it was estimated that humins consisted of polymers chains varying in chain length with a similar composition of functional groups. IR spectra specifically suggested the presence of a significant number of oxygen functional groups, as well as furanic surface structures with acidic properties [159,161,168].

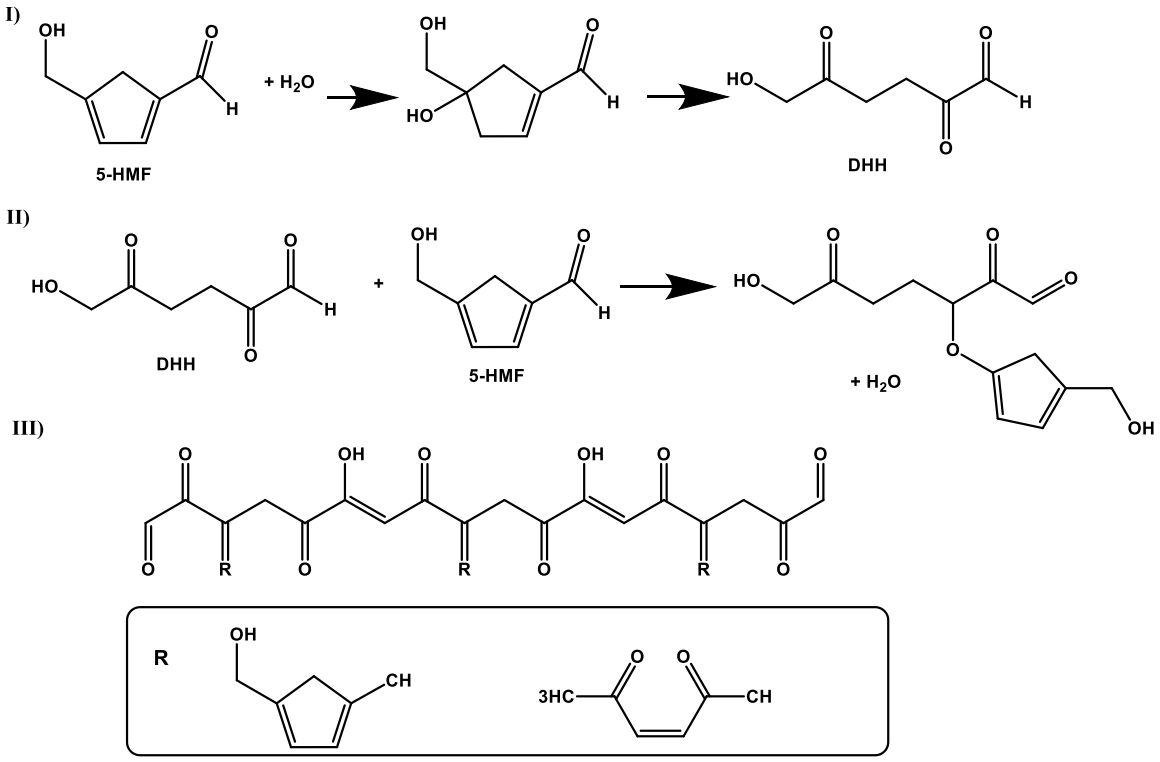

Figure 2.9: I) Hydration of 5-HMF to form 2,5-dioxo-6-hdrydoxyhexanal (DHH) by II) First condensation step of 5-HMF with DHH. III) Proposed structure of humins formed via aldol condensation reactions of 5-HMF with DHH according to Lund *et al*., adapted with permission[160]

Patil and Lund [160] proposed a humin formation mechanism from 5-HMF explaining their findings on structural investigations, as shown in Figure 2.9. The proposed mechanism involved 2,5-dioxo-6-hydroxyhexanal (DHH) formed by rehydration of 5-HMF as an intermediate product for further polymerisation. Specifically, polymerisation occurred between the carbonyl group of 5-HMF and DHH enolate group, with the subsequent product maintaining the enolate group for chain reaction aldol condensation. The solid residue from acid hydrolysis of sugars using ionic liquids, suggested that the primary humin formation rapidly occurred between soluble compounds, with slower solid-liquid and solid-solid interactions [169]. The particle size of the humins structures was found to increase with reaction time and could include levulinic acid fragments as part of the structure. Morphological SEM analysis suggested that the humins formed in the shape of spherical units [157,170]. Thus, the sugar-derived humins structures can be described as an oxygenated, time-dependant polymer with furanic cross-branching.

Humin substance formed when using real lignocellulosic biomass is even more structurally complex, due to the incorporation of unconverted biomass fragments. Chars formed from the Biofine process, for the production of levulinic acid from wheat straw, showed (via TGA analysis) that the char included cellulose and hemicellulose, in addition to lignin [111]. Furthermore, C13 analysis indicates possible cross-linking between the humins and unreacted biomass fractions, as well as symmetric peak patterns that are indicative of fused polyaromatic rings. Similar results were found by Agarwal *et al*.[166], which studied the acid catalysed solid residue from pinewood, contained cross-linking cellulose and hemicellulose fragments. While Runge and Zhang [99] reported “tar-like” substances on-top of unreacted lignocellulosic biomass during acid hydrolysis, which limited lignocellulose conversion. That study proposed

that fast-forming furfural could undergo decomposition and polymerisation to form humin-like materials [162,171]. Zandvoort *et al.* [172] found that xylose derived humins were chemically and thermally more recalcitrant than glucose derived humins possibly due to their more conjugated structures. It is therefore imperative to minimise initial humin formation in order to maximise hydrolysis of unconverted cellulose.

It should be noted that there is remarkable similarity between the humins and the soil organic material humus, after which humins are named [172]. Soil humus is formed from the decay of animal and plant material with a complex aromatic structure, predominantly composed of furanic polymers with oxygen and nitrogen functionalities. Fulvic and humic acids found in soil have been found to have similar structures to catalytically derived humins, but also incorporate fatty acids, amino acids and lignin [173]. Soil humus is an essential fraction of healthy soil and has been proposed to improve soil fertility. Effective humus has additionally been proposed to provide a source of nutrients and organic matter for the soil microbiome, as well improving the bulk soil water retention [174]. The similarities between humins and soil humus indicate potential cross application of humin materials, more specifically as a form of carbon sequestration or microbial promotion.

2.5.2 Hydrothermal Carbonisation

Hydrothermal carbonisation is a thermochemical process for the conversion of organic compounds to structured carbons. Under aqueous conditions, elevated temperatures (180 – 250 °C) at autogenous pressure, biomass that reduces both the oxygen and hydrogen content of the feedstock through dehydration and decarboxylation [175]. Hydrothermal carbonisation has been investigated for the production of both bio-oil and solid hydrochar fuels [176–179]. Among the many advantages, the process can utilise

a wide range of wet biomass feedstocks, eliminating the requirement for costly drying, and has been of notable interest for the disposal of difficult waste feedstocks, such as wastewater sludge [179]. In which, subcritical water acts as a catalyst for the conversion of biomass, with diffusive solvation properties for both polar and non-polar compounds. The hydrothermal carbonisation process has been proposed to include dehydration, decarboxylation, polysaccharide hydrolysis, retro-aldol cleavage and condensation as well as aromatisation [175]. These reactions are predominantly controlled by reaction temperature and, to lesser degrees, by reaction time and pH. Hydrothermal carbonisation has been found to occur during aqueous acid catalysis and affects polysaccharides, lignin and humin fractions, altering the solid residue composition and structure.

Hydrothermal conditions below 250 °C have reported negligible bio-oil yields with hydrochar as the primary product (>60 w.t.%) [180]. At temperatures of <250 °C, negligible direct aromatization of cellulose occurs, with the predominant hydrochar formation mechanisms being polysaccharide hydrolysis, followed by condensation of aqueous and furanic compounds [176]. Sevilla *et al.* [181] proposed that low temperature hydrochars from sugars formed as carbon rich spheres, with an oxygen-rich outer shell and carbon-rich core, as shown in Figure 2.10. Where, aqueous compounds condense via aldol condensation on the surface structure, followed by subsequent aromatization. Shi *et al*.[177] suggested that humins are an intermediate product of hydrochar formation, in agreement with the 'shell and core' model, where aromatization of the furanic polymer network occurs via a combination of acetal-cyclisation, 1,2-hydride shift, intramolecular aldol condensation, and dehydration to form a polycyclic and phenolic rich polymer core.

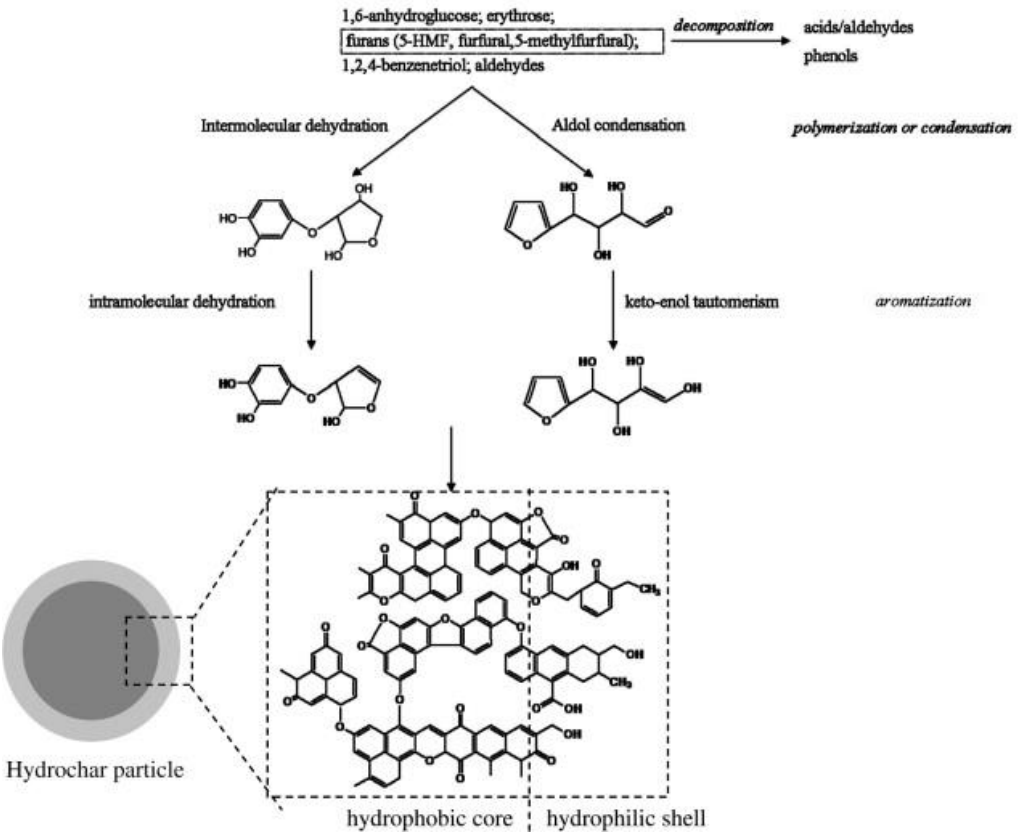

Figure 2.10: Molecular structure of hydrochar from sugars as proposed by Sevilla *et al*. Adapted with permission[181].

The proposed aromatisation of furanic humin structures towards poly-aromatic hydrochar, has similarities to that of humin formation, discussed in section 2.5.2. The similarities in formation mechanisms result in minimal differences between the two independently studied materials. However, the small differences in structures may affect the possible applications of the two solid products. In fact, hydrochars have been reported to have higher Higher Heating Values (HHV) than that of humins [182]. The more abundant polycyclic compounds found in hydrochars (primarily due to higher reaction temperature) have been reported to increase cation exchange capacity of the material, at the expense of increased microbial inhibition [183]. While, the aromatic structure of hydrochar has also been proposed to increase fixed carbon, soil stability and nutrient availability [175,184]. As humins could be best described, as an intermediate

product of hydrochar formation, it can be hypothesised that they will exhibit similar material properties but needs further validation.

The rate of hydrochar formation can be controlled through manipulation of operating conditions such as reaction time, temperature, pressure, solids loading, with reaction temperature representing the most critical factor for the HTC process [175]. Temperatures of <300 °C have proved insufficient to cause decarboxylation of cellulose [185] however, they are sufficient for aldol condensation and aromatization, with higher aromatization having a higher activation energy [186]. Interestingly, acidic HTC processes have been found to decrease hydrochar yields, due to in the increase polysaccharide hydrolysis, resulting in higher water soluble organic yields [187]. Hydochar yields have also found to increase with longer reaction times, similar to humin yields. Yields have additionally been positively correlated to increasing solids loading (due to a bottleneck with polysaccharide hydrolysis and sugar dehydration, which can be alleviated with the addition of acids) as well as longer reaction times (due to condensation reactions, again similar to humin yields). Because of the similar effects on yields, the formation of hydrochar relative to humins cannot be easily controlled with reaction time or solids loading. Therefore, reaction temperature and acid concentration are more appropriate parameters modifying the humin:hydrochar ratio.

2.5.3 Aqueous By-products

It should be noted that aqueous by-products are also formed along with the formation of the solid residue by-products during acid hydrolysis. Most notably, organic acids such as formic and acetic acid, acid soluble lignin and aliphatic hydrocarbons. The

interaction of acid soluble lignin with humin and hydrochar formation was discussed in detail in earlier sections, although also the interactions of organic acids with solid residue formation must be considered.

Formic acid is formed in equimolar ratio to levulinic acid and is also a degradation product of multiple biomass products. The presence of formic acid is often reported after acid hydrolysis, however the quantification of formic acid concentrations has infrequently been reported. Formic acid has been found to be stable during the mineral acid hydrolysis [188,189] However, Świątek *et al.* [46] identified that formic acid degraded under dilute hydrolysis of sugars, suggesting its consumption to be linked to the nature of the lignocellulose feedstock. In fact, formic acid reacts with acid soluble lignin and formylation of solid residues from acid hydrolysis could be possible [190,191].

Acetic acid is also naturally present in biomass in the form of acetylated hemicellulose. The acetate content of biomass varies up to 2 wt.% in certain woods, and is considered easily hydrolysable [192]. The effects of concentrated acetic acid (10 wt.%) on hydrothermal carbonisation has been found to increase hydrochar carbon content and HHV [193], which suggests acetic acid becomes incorporated into the hydrochar structures. However, the effects of dilute acetic acid (~1 wt.%) were found to have minimal effect on hydrochar properties [187]. Moreover, the effects of acetic acid on solid residue under acid catalysis have not been investigated and may be of great interest.

It should also be mentioned that acid-soluble lignin can represent a large fraction of the initial biomass, which will be solubilised during acid catalysis. Acid soluble lignin has been reported to actively react with xylose under acidic conditions [25]. In support of this, Dussan *et al*. [28] found that soluble lignin could decrease furfural yields by up

24%, with the formation of an insoluble pseudo-lignin residue by-product. It was also proposed that acid-soluble lignin could react with itself to form pseudo-lignin in significant quantities under acidic conditions [194]. Another study by Aarum *et al*. [195] reports pseudo-lignin was incorporated into the humic structures on the particle surface and, as such, is difficult characterise pseud-lignin in detail. Nitrogen containing compounds were also found by Leng *et al.* [196]incorporated into pseudo-lignin structures. The rate of the pseudo-lignin incorporation into humin structures is unknown to date and difficult to quantify, due to complexity of measuring acid soluble lignin.

2.5.4 Acid Hydrolysis Solid Residues

The solid residue from acid hydrolysis of biomass is inherently complex, due to the heterogonous nature of the feedstock, as the solid residue not only contains degradation products including humins, hydrochar and pseudo-lignin, but also unreacted biomass and unreacted lignocellulosic structures. Most notably, Klason-lignin has been found to be inert under sub 300 ˚C acidic reaction conditions [24], and will form a significant fraction of the solid residue. However, Klason Lignin does not contribute to the solid residue surface properties, due to the presence of unreacted cellulose on top of the lignin structures. Unreacted cellulose will contribute a decreasing fraction to the bulk and surface properties of the solid residue, as the acid hydrolysis process progresses, but will dominate the surface properties under mild reaction conditions. Later in the acid catalysis process, solid condensation products come to dominate the surface properties of the residue. Initially, humin formation enriches the surface area with oxygen-rich functional groups that increases the

surface hydrophilicity. Higher reaction temperatures however, will increase the rate hydrochar formation, surface hydrophobicity and surface area. The carbon sphere condensation product also includes pseudo-lignin and nitrogen containing compounds, which are considered to exert minor effects on the solid residue surface area. These interacting condensation reactions will result in an overall dehydration process of the solid residue with significant surface and bulk property differences related to reaction conditions.

2.5.5 Humins and Hydrochar Applications

Several studies have looked at the application of humins and solid residues for the valorisation of waste products from levulinic acid production. Most commonly, the solid residue has been proposed as a solid combustion fuel, for the production of steam, to be utilised for the heating of the acid hydrolysis process as well as the separation of levulinic acid via distillation [106,197,] . Techno-economic analysis results the aforentioned studies suggest that solid residue as fuel is sufficient to provide the heat required by the levulinic acid production process. However, due to its carbon content exceeding 60 wt.%, the solid residue combustion resembles that of coal with regards to CO_2 emissions [198]. This would significantly increase the carbon emissions associated to the manufacture of levulinic acid. As previously discussed, the use of the microwave heating not only improves cellulose hydrolysis but could also eliminate the requirement of combustion derived steam. Therefore, enabling the investigation of alternative non-combustion applications for the solid by-product.

Sugar-derived humins were investigated by Rasrendra *et al.* [165] as a feedstock for pyrolysis. The primary reaction product was biochar (70-72 wt.%), with bio-oil and

syngas yields of 8-10 wt.% and 17-22 wt.%, which was lower than that from lignin under similar conditions. Agarwal *et al.*[166] utilised catalytic pyrolysis to increase the bio-oil to 14 wt.% with HZSM-5. Using catalytic fluidised bed reactors, Sumbharaju *et al.* [199] managed to increase bio-oil yields to nearly 20 wt.% with the same catalyst. However, the low bio-oil yields are not sufficient to justify the high processing temperature of nearly 600 °C. Melligan *et al.* [158] as part of the Carbolea research group, was able to achieve bio-oil yields of 12-20 wt.% from the pyrolysis of solid residue from the acid *Miscanthus x Giganteus* without any catalyst. The higher bio-oil yields with real biomass may be attributable to the higher lignin content of solid residue though, biochar remained the primary pyrolysis product. These results indicate that significant further work is necessary for the successful valorisation of solid residues via pyrolysis.

Alternatively, novel applications of humins has gained increasing attention in recent years, which are related to their material properties. For example, humin-impregnated resins have been found as a promising substitute of plywood boards[200]. Humin-based solid foams exhibited remarkable insulation capacity with applications for the building sector [168] . Solid residue from bamboo hydrolysis can be activated with sulphuric acid to from a low cost catalyst for further acid hydrolysis [151], while the residues from the acid hydrolysis of textile waste was found to be a promising electrode material [201]. Also, ionic liquid derived humins from sugars were shown to remove heavy metals from wastewater due to the high surface O/C ratio [169]. In which, the highly functionalised surface areas were able to selectively remove trace elements, due to their high cation exchange capacity. Therefore, the use of solid residues for applications other than combustion, reveals to be an interesting and promising approach to their valorisation as bio-based materials. Non-thermal applications of solid

residue from acid catalysis would also facilitate the storage of carbon, acting as a form of carbon sequestration, thus reducing the CO_2 emissions of the resulting levulinic acid product.

Hydrochar applications are similar to those of humins, with a primary focus in this case, on use as a solid fuel however, in the literature they also found applications as an electrode material, soil amendment and heavy metal removers for soil remediation [179]. Among the novel and growing applications of hydrochar is its use as additive for the promotion of anaerobic digestion. Hydrochar has been found to increase methane yields during anaerobic digestion by improving buffering capacity, providing a source of trace metals, adsorbing inhibitors (such as ammonium and fatty acids) as well promoting microbial activity via direct interspecies electron transfer and acting as a microbial support material [202]. The promotion of anaerobic digestion is most critical for disposal of organic waste materials [203]. Fermentation of organic waste materials, such as nitrogen rich animal manures and food waste, can be easily inhibited my toxic quantities of ammonium, e.g. from the degradation of proteins, that prevent or slow down further microbial activity. Hydrochars have been found to increase the methane yields and degradation of pig waste, fish waste and food waste by +90%, +127% and +80% respectively [204–206]. However, the energy consumption, and subsequent costs of carbonaceous material production, has been so far a limiting factor [207]. Lower cost hydrochar (or analogous materials) have been sought for the supplementation of anaerobic digestion [208]. Solid residue from lignocellulose catalysis, more specifically levulinic acid production, may be chemically and morphologically close enough to hydrochar to provide analogous properties.

2.6 Anaerobic Digestion

2.6.1 Anaerobic Digestion Process

Anaerobic digestion (AD) is a well-established waste disposal process and source of bioenergy in the form of biogas. The UK's AD plant was built in Exeter in 1895 for the treatment of wastewater and to generate street lamp fuel [209]. AD operations have been commercialised with a wide variety feedstocks, with over 2,000 biogas plants of all types operating in the UK alone [210]. Recently, AD-derived biogas has received increasing attention as a low-carbon fuel, as carbon dioxide is removed from the atmosphere during plant cultivation of substrates based on carbon neutrality principles, and is considered a vital part of the transition to a low carbon economy[211].

AD is a biological process that involves microorganisms breaking down organic materials into carbon dioxide and methane in the absence of oxygen [212]. Organic materials such as cellulose, wastewater and animal manures can be broken down by a complex synergistic microbial community of bacteria and archaea. Organic matter is simultaneously degraded in four sequential steps: hydrolysis, acidogenesis, acetogenesis and methanogenesis, as seen in Figure 2.11 [213].

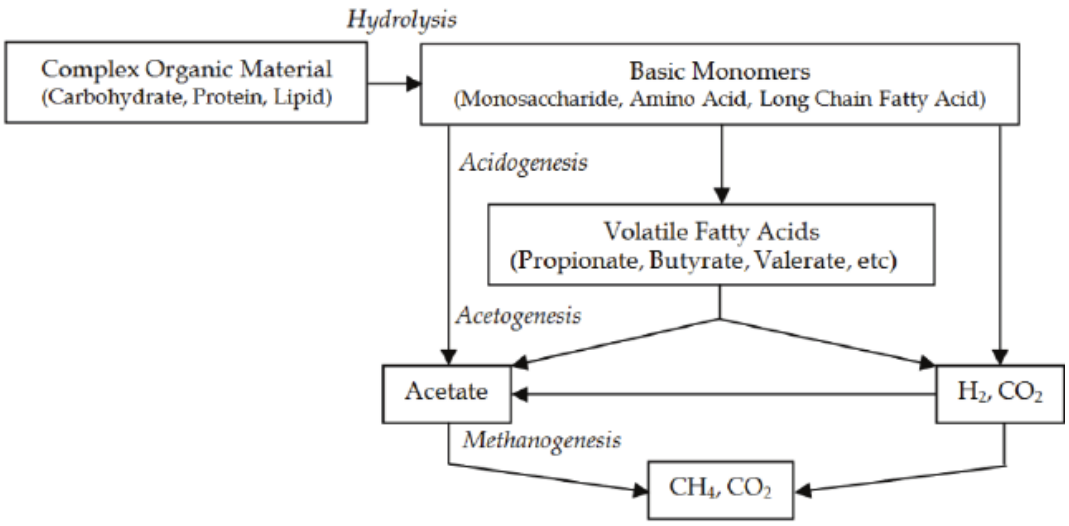

Figure 2.11: Schematic of the major processes for the degradation of organic material under anaerobic digestion. Reproduced from Ersahin *et al*. with permission[213].

During hydrolysis, carbohydrates, proteins and lipids are converted into monomeric compounds, such as sugars, amino acids and fatty acids mostly by hydrolytic bacteria [212]. These monomeric intermediate products are converted to volatile fatty acids (VFA), lactic acid, H_2, CO_2, NH_4^+ and H_2S in the acidogenesis stage. Subsequently, the acidogenesis products are degraded to acetate, formate, H_2 and CO_2 in the acetogenesis. Finally, methanogenic archaea reduce the CO_2 + H_2 and cleave the acetate molecule to produce methane and CO_2. Each of the four sequential stages include several different metabolic pathways that can be facilitated at a range of operating conditions [214]. The operating conditions, however, must be carefully controlled to prevent accumulation of any toxic intermediate products in order to reduce operating instability and microbial collapse[215].

The resulting biogas product is primarily composed of CH_4 (50-75%) and CO_2 (25-50%) with trace quantities of H_2S and NH_3. The HHV of CH_4 as pure gas is 37.78 MJ/m_n^3, therefore, raw biogas has an HHV energy content between 19 and 28 MJ/m_n^3 [216]. Biogas has successfully been used for electricity production and combined heat and power generation with efficiencies of up 80% [217]. The presence of CO_2 and H_2O reduces the LHV of biogas in practice, which can be reduced through biogas upgrading. Impurities can include CO_2, H_2O, NH_3 and $H2_S$, which can be removed using consolidated methods such as water scrubbing, membrane separation, pressure swing adsorption, hydrogen upgrading and inorganic scrubbing, among others, to produce pure methane (known as bio-methane) [218]. While, untreated biogas has also received increasing attention as a feedstock for fuel cells, although catalyst contamination issues have proven troublesome [219].

The AD process in addition to biogas produces a waste product, more often than not consisting of a fibrous solids suspension in aqueous medium, called digestate. Digestate is a nutrient-rich substance composed of indigestible organic material, dead and alive microorganisms and inorganic compounds, such as ammonium and phosphate salts [220]. Digestate is primarily used a soil conditioner and fertiliser that further degrades aerobically in soil, with positive effects on soil fertility [221]. The land application of digestate has been found to increase organic soil carbon, and, thus, improve soil microbiome diversity and resistance to plant diseases [222,223]. Land application of AD digestate reduces the requirements for inorganic or synthetic fertilisers with subsequently reduced greenhouse gases of up to 40% [224]. Barłóg *et al*. [222] found that digestate is also a source of bioavailable trace nutrients including P, K, S, Mg and Cu. In addition, the carbon sequestration of the digestate has received growing interest in recent years, due to the bacterial mineralization of organic matter during AD. Digestate supplemented fields have been reported to exhibit increased organic carbon content for at least 7 years after spreading [225]. Béghin-Tanneau *et al*. [226] found that 60 wt.% of digestate carbon is stable after 6 months, however further work is required to fully quantify this carbon sequestration potential. It should be noted that the improper application of digestate on land can lead to water contamination and secondary biogenic (N_2O) emissions. This said, the valorisation of digestate via land application is essential to maximise the greenhouse gas (GHG) savings of AD as well as for the commercial viability of AD plants.

2.6.2 Anaerobic Digestion Operating Parameters

The process parameters affecting the yield and energy content of biogas include feedstock composition, operating temperature, operating pH, biomass load rate and retention time [227]. The theoretical methane yields of a feedstock can be estimated stoichiometrically by the modified Buswell equation [228], *Equation 2.1*. This is only based on the substrate's empiric formula, thus does not account for microbial inefficiencies. Increased microbial inefficiencies, due to inhibition, can significantly reduce the methane yields and normally higher carbon dioxide production. Microbial inefficiencies can be minimised by operating the AD process at the optimum pH of 6.5-8.0, or more specifically 7.0-7.2 [229]. However, microbial system results in a highly buffered system, primarily consisting of NH_4^+ and CO_3^-, which can maintain stable pH operation, reducing the effects of the system disturbances on pH.

$$C_cH_hO_oN_nS_s + \left(c - \frac{h}{4} - \frac{o}{2} + \frac{3n}{4} + \frac{s}{2}\right)H_2O \rightarrow \left(\frac{c}{2} + \frac{h}{8} - \frac{o}{4} - \frac{3n}{8} - \frac{s}{4}\right)CH_4 + \left(\frac{c}{2} - \frac{h}{8} + \frac{o}{4} + \frac{3n}{8} + \frac{s}{4}\right)CO_2 + nNH_3 + sH_2S$$

Equation 2.1

The AD processes can be further influenced by the operating conditions and reactor design, for example mesophilic (30-40˚C) versus and thermophilic (40-60˚C) or batch versus continuous reactors respectively. Thermophilic operating conditions favour fast degradation of substrates, in the order of 1.5X faster than mesophilic, which is due to higher enzymatic activity. However, higher operating temperatures can cause microbial process imbalances and the accumulation of intermediaries to toxic concentrations, primarily volatile fatty acids (VFAs), which can cause chain reaction acidification. Higher reaction temperatures also reduce the CO_3^- buffering capacity and

shift the NH_4^+/NH_3 towards toxic quantities of free ammonia. Also, pH instability has been found to decrease methane yields at the expense of higher carbon dioxide production associated to microbial stress. The accumulation of toxic inhibitors can be alleviated by using multi-stage or upflow reactors, which enable more flexible balancing of the microbial process [230,231]. For this project only the evaluation of AD potential and maximisation will be investigated. Therefore, simple batch reactors will be used.

The AD process during a batch process with a fixed starting bacteria inoculum and feed materials can be modelled using the modified Gompertz model for AD, as shown in *Equation 2.2* [232]*.* The modified Gompertz models are sigmoid biological growth models that can be utilised to model microbial cell growth, tumour growth and the survival rate of cancer patients that can be fitted using simple regression tools [233].

$$V_{CH4}(t) = A_{max}\exp\left[-\exp\left(\frac{R_{max}*e}{A_{max}}(\lambda - t) + 1\right)\right] \qquad \textit{Equation 2.2}$$

The modified Gompertz model has been successfully applied to predict biogas yields during AD by multiple studies [112,234–238]. Where in $V_{CH4}(t)$, is the predicted cumulative methane production (mL/g VS) at any time t (day), A_{max} is the measured cumulative methane yield (mL/g VS), R_{max} is the maximum methane production rate (mL/g VS·d), e is the mathematical constant 2.718282, and λ is the lag phase delay (day). As such, the model cannot not only predictably model the AD process over a given time period but also allow the comparison of different stages of the AD process between trials. Most notably the lag phase (λ) can indicate microbial inhibition and R_{max} is of great interest for the design of continuous of AD processes. The use of the modified

Gompertz model in this way therefore enables the greater understanding of the AD process through daily gas recordings.

The growth of microbial communities during AD requires a mixture of macronutrients, primarily nitrogen, alongside trace elements including S, P, Co, Mo, Ni, Mn and Fe [239]. The nutrient content of an AD reactor is typically defined by its feedstock C/N ratio, with nitrogen crucial component for protein and nucleic acid synthesis. Despite nitrogen's key role, the biological degradation of excess organic nitrogenous material (C/N <10) increases the ammonium and free nitrogen concentrations of the digester, which can cause inhibition. In nitrogen-rich media, NH_3 can diffuse across the cytoplasmic membrane of microbes in large quantities compared with the active transport of NH_4^+, leading to intracellular ammonium accumulation [240]. This has been found to disrupt the cell potassium pump, deactivation of enzymes and cause nutrient deficiencies [241]. This subsequently leads to reduced methane yields and, in extreme cases, methanogens collapse. In contrast, substrates carrying higher C/N ratios have insufficient nitrogen necessary for microbial growth, resulting in decreased biogas production associated with low utilisation of the carbon source. The optimum C/N ratio for maximum methane yields has been identified as between 20-30 [242].

The C/N ratio of the AD system is therefore of utmost importance and it can be balanced by the co-digestion of multiple feedstocks to achieve the optimum ratio. Feedstocks characterized by higher C/N ratios (>50), such as rice and wheat straws, corn stalks, seaweed and microalgae, can be co-digested with the feedstocks of lower C/N ratios, such as chicken manure, dairy manure and food wastes, which will ensure a suitable nutrient balance for the optimum biogas production [243]. AD is primarily utilised for the valorisation of waste products however, more often than not, these

waste materials exhibit high C/N properties, therefore requiring balancing via co-digestion of nitrogen rich feedstocks. A such, the growth of plant matter solely for the AD stabilisation of nitrogen-rich feedstocks, such as grass silage, has taken place extensively, although this practice has recently been considered unsustainable and the UK government as encouraged AD of nitrogen-rich waste materials without dedicated stabilisation crops [211].

2.6.3 Anaerobic Digestion of Waste Materials

Animal manures are among the largest sources of the organic waste in the UK with over 80 million metric tons produced in 2016 [244]. Over 80% of animal manure slurry is spread directly on land as a natural nitrogen and phosphorous containing fertiliser. However, the direct land application of animal manure can lead to biogenic emissions of significant quantities of CH_4 and N_2O greenhouse gases [245]. Land application of AD digestate has been found to reduce GHG atmosphere emissions from animal manure by over 50% CO_2 eq. compared with direct land application [246]. However, animal manures such as dairy, pig and chicken manures have reported C/N ratios of 15, 11 and 8 respectively [215,247]. The low C/N ratio without co-digestion has proven difficult, due to ammonium inhibition decreasing the process stability and thus the financial viability of the process.

Animal manures can contain between 0.5-4.1 wt.% nitrogen[248], which can cause ammonium concentrations of up to 9 g/L [243]. Under mesophilic conditions (<38 °C), ammonium concentrations of 1.7-1.8 g/L were found to lead to a complete reactor intoxication and failure however, acclimation of the microbial community has been shown to increase tolerance to high ammonium concentrations up to 5.0 g/L [242].

Microbial acclimation has been concluded to reduce ammonium inhibition through the natural selection of microorganisms. In particular, the Angelidaki group found that high ammonium concentrations (>7 g/L) shifted the methanogensis stage away from acetate conversion towards H_2/CO_2, with major changes in microbiome composition for all of the AD stages [249] . However, Morozova *et al*. [250] found that despite the acclimation, a decrease in AD efficiency still occurred along with reactor instability, due to reduced buffering capacity. The reduction in digestion efficiency towards methane formation has a drastic effect on the economic viability of the process, hence AD deployment has so far not been viable without significant government subsidies.

2.6.4 Effect of Hydrochar on AD Methane Yields

In recent years, the use of carbon conductive materials was introduced for improving AD of difficult feedstocks and its success has gained increasing attention[251]. Carbonaceous materials, such as hydrochar and biochar, have been found in particular to increase methane yields by up to +100% from multiple difficult feedstocks, spanning from food waste, to pig carcass and manures [204,252,253]. Several mechanisms have been proposed to explain the increased methane yields, including direct interspecies electron transfer (DIET), micronutrient availability, microbial support and inhibitor adsorption.

In 2004, Gregory *et al.* [254] first found graphite electrodes act as a direct electron donor for AD. The *Geobacter* microbial family was found to oxidise acetate and nitrate to H_2+CO_2 and nitrite respectively on the anode. Summers *et al.* [255] introduced the concept of interspecies electron transfer, by which multiple species transfer electrons from different metabolic pathways via the carbon anode. Morita *et al*. and Zhao *et al*.

found that the electrically conductive AD sludges resulted in higher methane yields, due to DIET [256,257]. An increase in overall conductivity has been positively correlated to improved synergistic metabolic pathways that would not otherwise occur. These increase of microbial efficiency regards most notably methanogens, as DIET has been proposed to increase the number of mechanistically feasible metabolic pathways during the AD of inhibitor-rich substances, even under high microbial stress [258,259]. Oxygen-containing functional groups on hydrochar's surface were also found to increase methane yields by up to 37% from the metabolism of glucose through DIET, by the conversion of H^+, e^-, and CO^2 to CH_4 [260]. Interestingly, a positive, direct correlation between hydrochar surface O/C ratio and higher methane yields was found[260]. The high surface O/C ratio of humins may have similar DIET facilitating properties to that of hydrochar during AD.

Other works have reported that toxics adsorbing materials act through surface adsorption, lowering the inhibitory burden on microorganisms [261]. Traditional zeolite adsorbents, such as bentonite for example, transfer Na^+, Ca^{2+} and Mg^{2+} with excess ammonium NH_4^+ [262], as well adsorb long-chain fatty acids and aromatics [263]. However, due to high zeolite costs, alternative renewable carbonaceous adsorbents were also investigated by scientists. In this respect, biochar formed at 700 °C was found adsorb up to 0.96 gNH_4^+/g by amine, amide and nitrile functional group adsorption [264]. The Ross group found instead a 0.146 and 0.128 gNH_4^+/g adsorption with hydrochar and biochar respectively [265]. Interestingly, the same group found that the effect of surface area was found to be minimal on adsorption capacity, with surface functionality having a greater effect. Two different ammonium adsorption mechanisms have so been proposed: 1) acidic oxygen-containing functional group adsorption and 2) metal-ion

exchange from carbon-rich structures [261,266]. The adsorption of ammonium by hydrochars has been attributed to increases in methane yields from the AD of pig carcass by +90% with 4 g-hydrochar/L [204], +127% methane from the AD of fish waste with 8 g-hydrochar/L [205] and +80% methane from the AD of spent brewers grain at 2 g-hydrochar/L [206]. The aforementioned studies all reported that higher hydrochar concentrations caused minor microbial inhibition, most likely due to the presence of aromatic compounds, though hydrochar has been found to be an adequate adsorbent for volatile organic compounds [267].

Hydrochars have also been proposed to promote microbial biofilm growth and offer bioavailable nutrients during AD [268]. Functionalised porous structures have proven attractive for providing a large surface of interaction for the immobilisation and protection of cells and biofilm formation [269]. Biofilm formation has been linked with increased micro-nutrient bioavailability, though this may be limited to cation exchange capacity of soluble alkali metals [265], which are normally in excess with animal manures. Biofilm promotion, due to organic material degradation in hydrochars, has also been hypothesized however, Berge *et al*. [270] found no correlation between organic material and AD promotion effects. Biofilm formation has been proposed to increase microbial diversity [271], however the difference between DIET and biofilm effects on microbial diversity during AD have not been proven. The intrinsic complexity of the microbial system makes quantitative evaluation of each mechanism on CH_4 yields inconclusive, and thus it is regarded as the result of a combination of the aforementioned processes.

2.6.5 Hydrochar Supplementation of Anaerobic Digestion

Despite the recent interest in the supplementation of AD with hydrochar, commercial applications exploiting this concept are yet to be deployed. Saba *et al.* [272] estimated that *Miscanthus x Giganteus* derived hydrochar would cost $117 per ton with the largest costs associated with feedstock purchasing and process heating at $38 and $46 per ton respectively. Furthermore, despite the improved methane yields from the AD of chicken manure through char additives has an estimated upper value of $60 per ton char, based on work by Pan *et al*.[237] The high feedstock and energy production costs of hydrochar for does not appear economic viable for this application. However, during acid catalysis these costs are spread across both the aqueous high value chemical fractions as well as the solid residue which would reduce the overall cost of the adsorbent material relative to the single product HTC process. While the upscaling of solid residue from a fuel to a higher value adsorbent material would also increase the viability of acid catalysis in a biorefinery concept. Therefore, the initial investigation of a low-cost adsorbent from acid catalysis could replace hydrochar as an anaerobic digestion supplement.

In addition, the potential economic benefits from the land application of hydrochar-enriched digestate has gained recent attention as a form of carbon sequestration [183,273,274]. With the growing market for carbon credits and negative emissions process, mixing hydrochar and digestate would act as an effective short-term carbon sink. Hydrochar stability in soils have been estimated to have Mean Residence Times (MRT) of 4-19 years using two-pool decay models [184,275]. Two-pool methods have been deemed necessary, due to the priming effect of hydrochar decreasing pre-existing organic content. The priming effect is due to the interaction of chars and

organic matter stimulating microbial mineralization of pre-existing soil carbon. The priming effect of biochar was found to be higher at lower process temperatures and low soil carbon content increases soil mineralization [276]. However, hydrothermal decomposition products, namely humins, have been suggested to be more recalcitrant to microbial decomposition due to lack of naturally occurring enzymes [277]. Which is supported by Schulze *et al*. [278] The study found longer hydrochar residence times increased MRT from 4-14 to 11-15 years. The stability of solid residue from acid catalysis requires further investigation, but it can be assumed that a 10 year MRT would sufficiently increase the carbon sequestration potential of the process.

2.7 Conclusions

Renewable low-carbon biochemicals, namely levulinic acid, can be produced from a large variety of lignocellulosic biomass using a range of catalysts. Both homogeneous and heterogeneous catalysts can be employed (with varying degrees of success) for the conversion of lignocellulose towards levulinic acid. To catalyse the chemical reaction, mineral acids such as sulphuric acid or sulphated metal oxides (including sulphated zirconia) are among the most promising catalysts. The conversion of lignocellulose can be assisted by the use of microwave heating to improve cellulose hydrolysis and heterogeneous catalyst may also be promoted using trace acid modifiers. The production of levulinic acid has not yet reached its full potential due to several issues, most notably by-product formation such as solid residues and, to a lesser extent, organic acids.

The thorough review of existing literature suggests that the solid residue will be composed of a matrix of unreacted biomass, humins, pseudo-lignin, carbonised material and possibly other unknown condensation products. However, as discussed in this review chapter, the formation of solid-residue by-product during acid analysis depends significantly on the lignocellulose feedstock, catalyst type and operating conditions. It is most likely that the solid residue will exhibit properties from all the matrix components, although the surface properties are most likely dominated by humin formation. Upon detailed investigation, the similarities between humin and hydrochar formation mechanisms lead to the hypothesis that they will exhibit similar properties.

Anaerobic digestion supplementation with hydrochar is a promising field for the disposal of animal wastes in conjunction with increased methane yields. The digestion of animal manures is most commonly limited by the C/N ratio and the use of carbonaceous adsorbents has been shown my multiple authors to not only reduce ammonium concentrations but also improve microbial diversity. Analogies between the surface composition of hydrochar and catalytically derived solid residue is most likely due to similar humin formation mechanisms. This strongly suggests that the similar surface properties could enable the application of solid residue for the improvement of animal manure digestion and result in increased methane yields. The utilisation of solid residue from catalytic biorefineries as an AD supplement would then reduce the carbon emissions from the typical residue combustion application while also improving the disposal of difficult waste manure materials. The integration of these two processes is therefore of vital interest for the development of integrated biorefineries.

2.8 References

1. Kumar, J. & Reetu, S. Lignocellulosic agriculture wastes as biomass feedstocks for second-generation bioethanol production : concepts and recent developments. Biotech 3, 337–353 (2015).

2. Kang, Q., Appels, L., Tan, T. & Dewil, R. Bioethanol from Lignocellulosic Biomass : Current Findings Determine Research Priorities. Sceintific World J. (2014). doi:10.1155/2014/298153

3. Isikgor, F. H. & C. Remzi Becer. Lignocellulosic Biomass: a sustainable platform for production of bio-based chemicals and polymers. Polym. Chem. 6, 4497–4559 (2015).

4. Song, B., Zhao, S., Shen, W., Collings, C. & Ding, S. Y. Direct Measurement of Plant Cellulose Microfibril and Bundles in Native Cell Walls. Front. Plant Sci. 11, 1–11 (2020).

5. Isikgor, F. H. & Becer, C. R. Polymer Chemistry the production of bio-based chemicals and polymers. 4497–4559 (2015). doi:10.1039/c5py00263j

6. Li, M., Cao, S., Meng, Z., Struder, M., Wyman, C. E., Ragauskas, A. J., Pu, Y. The effect of liquid hot water pretreatment on the chemical-structural alteration and the reduced recalcitrance in poplar. Biotechnol. Biofuels 10, 1–13 (2017).

7. Rongpipi, S., Ye, D., Gomez, E. D. & Gomez, E. W. Progress and opportunities in the characterization of cellulose – an important regulator of cell wall growth and mechanics. Front. Plant Sci. 9, 1–28 (2019).

8. Sluiter, J. B., Ruiz, R. O., Scarlata, C. J., Sluiter, A. D. & Templeton, D. W. Compositional analysis of lignocellulosic feedstocks. 1. Review and description of methods. J. Agric. Food Chem. 58, 9043–9053 (2010).

9. Loow, Y. L., Wu, T. Y., Jahim, J. M., Mohammad, A. W. & Teoh, W. H. Typical conversion of lignocellulosic biomass into reducing sugars using dilute acid hydrolysis and alkaline pretreatment. Cellulose 23, 1491–1520 (2016).

10. Mukherjee, A., Dumont, M. J. & Raghavan, V. Review: Sustainable production of hydroxymethylfurfural and levulinic acid: Challenges and opportunities. Biomass and Bioenergy 72, 143–183 (2015).

11. Xiong, X., Yu, I. K. M., Tsang, D. C. W., Bolan, N. S., Ok, Y. S., Igalvithana, A., Kirkham, M. B., Kim, K., Vibrant, K. Value-added chemicals from food supply chain wastes: State-of-the-art review and future prospects. Chem. Eng. J. 375, 121983 (2019).

12. Delbecq, F., Wang, Y., Muralidhara, A., Ouardi, K. E., Marlair, G., Len, C. Hydrolysis of hemicellulose and derivatives-a review of recent advances in the production of furfural. Front. Chem. 6, (2018).

13. Cesarino, I., Araújo, P., Pereira, A., Júnior, D. & Mazzafera, P. An overview of lignin metabolism and its effect on biomass recalcitrance. 35, 303–311 (2012).

14. Jeffries, T. W. Biodegradation of lignin and hemicelluloses. in Biochemistry of microbial degradation 233–277 (1994). doi:10.1007/978-94-011-1687-9_8

15. Tarabanko, V. E. & Tarabanko, N. Catalytic oxidation of lignins into the aromatic aldehydes: General process trends and development prospects. Int. J. Mol. Sci. 18, (2017).

16. Welker, C. M., Balasubramanian, V. K., Petti, C., Rai, K. M., DeBolt, S., Mendu, V. Engineering plant biomass lignin content and composition for biofuels and bioproducts. Energies 8, 7654–7676 (2015).

17. Wendisch, V. F., Kim, Y. & Lee, J. H. Chemicals from lignin: Recent depolymerization techniques and upgrading extended pathways. Curr. Opin. Green Sustain. Chem. 14, 33–39 (2018).

18. Victor, P. A., Belém, S. & Fabricio, G. Styrene / Lignin-Based Polymeric Composites Obtained Through a Sequential Mass-Suspension Polymerization Process. J. Polym. Environ. 0, 0 (2017).

19. Li, X. Chen, W., Zhao, Y., Xinag, Y., Jiang, h., Zhu, S., Cheng, B. Downregulation of caffeoyl-CoA O-methyltransferase (CCoAOMT) by RNA interference leads to reduced lignin production in maize straw. Genetics and Molecular Biology 36, 540–546 (2013).

20. Rollin, J. A., Zhu, Z., Sathitsuksanoh, N. & Zhang, Y. P. Increasing Cellulose Accessibility Is More Important Than Removing Lignin : A Comparison of Cellulose Solvent-Based Lignocellulose Fractionation and Soaking in Aqueous Ammonia. Biotechnology and Bioengineering 108, 22–30 (2011).

21. De Azevedo Rocha, E. G., Da Costa, A. C. & Aznar, M. Use of protic ionic liquids as biomass pretreatment for lignocellulosic ethanol production. Chem. Eng. Trans. 37, 397–402 (2014).

22. Da Silva, A. S. A., Espinheir, R. P., Teixeira, R. P. S., de Souza, M. F., Ferreira-Leitão, V., Bon, E. Constraints and advances in high-solids enzymatic hydrolysis of lignocellulosic biomass: A critical review. Biotechnol. Biofuels 13, 1–28 (2020).

23. Auxenfans, T., Crônier, D., Chabbert, B. & Paës, G. Understanding the structural and chemical changes of plant biomass following steam explosion pretreatment. Biotechnol. Biofuels 10, 0–16 (2017).

24. Atta-Obeng, E., Dawson-Andoh, B., Seehra, M. S., Geddam, U., Poston, J., Leisen, J. Physico-chemical characterization of carbons produced from technical lignin by sub-critical hydrothermal carbonization. Biomass and Bioenergy 107, 172–181 (2017).

25. Matsushita, Y., Kakehi, A., Miyawaki, S. & Yasuda, S. Formation and chemical structures of acid-soluble lignin II: Reaction of aromatic nuclei model compounds with xylan in the presence of a counterpart for condensation, and behavior of lignin model compounds with guaiacyl and syringyl nuclei in 72% sulfuric. J. Wood Sci. 50, 136–141 (2004).

26. Brumano, G. C., Colodette, J. L., Fernandes, S. A., Barbosa, B. M. & Gomes, J. B. Investigation of eucalypt and pine wood acid-soluble lignin by Py-GC-MS. Wood Res. Technol. 74, 2018–2019 (2019).

27. Yasuda, S., Fukushima, K. & Kakehi, A. Formation and chemical structures of acid-soluble lignin I: Sulfuric acid treatment time and acid-soluble lignin content of hardwood. J. Wood Sci. 47, 69–72 (2001).

28. Dussan, K., Girisuta, B., Lopes, M., Leahy, J. J. & Hayes, M. H. B. Effects of Soluble Lignin on the Formic Acid-Catalyzed Formation of Furfural: A Case Study for the Upgrading of Hemicellulose. ChemSusChem 9, 492–504 (2016).

29. da Costa Lopes, A. M., João, K. G., Morais, A. R. C., Bogel-Łukasik, E. & Bogel-Łukasik, R. Ionic liquids as a tool for lignocellulosic biomass fractionation. Sustain. Chem. Process. 1, (2013).

30. Song, B., Yu, Y. & Wu, H. Solvent effect of gamma-valerolactone (GVL) on cellulose and biomass hydrolysis in hot-compressed GVL/water mixtures. Fuel 232, 317–322 (2018).

31. Wojtasz-Mucha, J., Hasani, M. & Theliander, H. Dissolution of wood components during hot water extraction of birch. Wood Sci. Technol. 55, 811–835 (2021).

32. Hasanov, I., Raud, M. & Kikas, T. The role of ionic liquids in the lignin separation from lignocellulosic biomass. Energies 13, 1–24 (2020).

33. Dibble, D. C. et al. A facile method for the recovery of ionic liquid and lignin from biomass pretreatment. Green Chem. 13, 3255–3264 (2011).

34. Ahmed, M. A., Lee, J. H., Raja, A. A. & Choi, J. W. Effects of gamma-valerolactone assisted fractionation of ball-milled pine wood on lignin extraction and its characterization aswell as its corresponding cellulose digestion. Appl. Sci. 10, (2020).

35. Alvarez-Vasco, C. Ma, R., Quinteo, M., Guo, M., Gelenyse, S., Ramasamy, K. K., Wolcott, M., Zhang, X. Unique low-molecular-weight lignin with high purity

extracted from wood by deep eutectic solvents (DES): A source of lignin for valorization. Green Chem. 18, 5133–5141 (2016).

36. Mohan, M., Timung, R., Deshaveth, N. N., Banerjee, T., Goud, V. V., Dasu, V. V. Optimization and hydrolysis of cellulose under subcritical water treatment for the production of total reducing sugars. RSC Adv. 5, 103265–103275 (2015).

37. Brugnago, R. J., Satyanarayana, K. G., Wypych, F. & Ramos, L. P. The effect of steam explosion on the production of sugarcane bagasse/polyester composites. Compos. Part A Appl. Sci. Manuf. 42, 364–370 (2011).

38. Pielhop, T., Amgarten, J., Von Rohr, P. R. & Studer, M. H. Steam explosion pretreatment of softwood: The effect of the explosive decompression on enzymatic digestibility. Biotechnol. Biofuels 9, 1–13 (2016).

39. Baruah, J. Nath, B. K., Sharma, R., Kumar, S., Deka, R. C., Baruah, D. C., Kalita, E. Recent trends in the pretreatment of lignocellulosic biomass for value-added products. Front. Energy Res. 6, 1–19 (2018).

40. Dussán, K. J., Silva, D. D. V., Moraes, E. J. C., Arruda, P. V. & Felipe, M. G. A. Dilute-acid hydrolysis of cellulose to glucose from sugarcane bagasse. Chem. Eng. Trans. 38, 433–438 (2014).

41. Wang, K., Xie, X., Si, Z., Jiang, J. & Wang, J. Microwave assisted hydrolysis of holocellulose catalyzed with sulfonated char derived from lignin-rich residue. Adv. Mater. Sci. Eng. 2015, 1–6 (2015).

42. Lenihan, P., Orozco, A., O'Niell, E., Ahmad, M.N.M., Rooney, D. W., Walker, G. M. Dilute acid hydrolysis of lignocellulosic biomass. Chem. Eng. J. 156, 395–403 (2010).

43. Zhao, H. Kwak, J. H., Wang, Y, Franz, J. A., White, J. M., Holladay, J. E., Effects of crystallinity on dilute acid hydrolysis of cellulose by cellulose ball-milling study. Energy and Fuels 20, 807–811 (2006).

44. Ehrman, T. et al. Chemical Analysis and Testing Laboratory Analytical Procedures. NREL-Protocols (l. 1-18) 1–186 (1998).

45. Xiang, Q., Lee, Y. Y. & Torget, R. W. Kinetics of Glucose Decomposition During Dilute-Acid Hydrolysis of Lignocellulosic Biomass. Renewable, Natl. 113, 1127–1138 (2004).

46. Świątek, K. Gaag, S., Klier, A., Kruse, A., Sauer, J., Steinbach, D. Acid hydrolysis of lignocellulosic biomass: Sugars and furfurals formation. Catalysts 10, 1–18 (2020).

47. Broduer, G., Telotte, J., Stickel, J.J., Ramakrishnan, S. Two-Stage Dilute-Acid and Organic-Solvent Lignocellulosic Pretreatment for Enhanced Bioprocessing. Bioresource Technology 220, 621-628 (2016)

S.48. Dussan, K., Girisuta, B., Haverty, D., Leahy, J. J. & Hayes, M. H. B. Kinetics of levulinic acid and furfural production from Miscanthus×giganteus. Bioresour. Technol. 149, 216–224 (2013).

49. Dimos, K., Paschos, T., Louloudi, A., Kalogiannis, K. G., Lappas, A. A., Papyannakos, N., Kekos, D., Mamma, D. Effect of various pretreatment methods on bioethanol production from cotton stalks. Fermentation 5, 1–12 (2019).

50. Van Der Pol, E. C., Eggink, G. & Weusthuis, R. A. Production of L(+)-lactic acid from acid pretreated sugarcane bagasse using Bacillus coagulans DSM2314 in a simultaneous saccharification and fermentation strategy. Biotechnol. Biofuels 9, 1–12 (2016).

51. Devlin, D. C., Esteves, S. R. R., Dinsdale, R. M. & Guwy, A. J. The effect of acid pretreatment on the anaerobic digestion and dewatering of waste activated sludge. Bioresour. Technol. 102, 4076–4082 (2011).

52. Megawati, M., Damayanti, A., Putri, R. D. A., Widiyaningsih, D. & Budiarto, R. Optimization based on kinetic of dilute-acid hydrolysis of sugar cane bagasse in bio-ethanol production. AIP Conf. Proc. 2197, (2020).

53. Woo, K. S., Kim, H. Y., Hwang, I. G., Lee, S. H. & Jeong, H. S. Characteristics of the thermal degradation of glucose and maltose solutions. Prev. Nutr. Food Sci. 20, 102–109 (2015).

54. Jönsson, L. J., Alriksson, B. & Nilvebrant, N.-O. Bioconversion of lignocellulose: inhibitors and detoxification. 2Biotechnology for Biofuels 6, (2013).

55. Falciglia, P. P., Roccaro, P., Bonanno, L., De Guidi, G., Vagliasindi, F., Romano, S. A review on the microwave heating as a sustainable technique for environmental remediation/detoxification applications. Renew. Sustain. Energy Rev. 95, 147–170 (2018).

56. Palma, V. Barba, D., Cortese, M., Martino, M., Renda, S., Meloni, E. Microwaves and heterogeneous catalysis: A review on selected catalytic processes. Catalysts 10, (2020).

57. Aguilar-Reynosa, A., Romani, A., Rodríguez-Jasso, R. M., Aguilar, C. N., Garrotte, G., Ruiz, H. A. Microwave heating processing as alternative of pretreatment in second- generation biorefinery : An overview. Energy Convers. Manag. 136, 50–65 (2017).

58. Fan, J. The Microwave Activation of Cellulose. (2013).

59. Zhu, Z., Simister, R., Bird, S., McQueen-Mason, S. J., Gomez, L. D., Macquarrie, D. J. Microwave assisted acid and alkali pretreatment of Miscanthus biomass for biorefineries. AIMS Bioeng. 2, 449–468 (2015).

60. Mukherjee, A., Dumont, M. J. Levulinic Acid Production from Starch Using Microwave and Oil Bath Heating : A Kinetic Modeling Approach. Industrial and Engineering Chemistry Research 55, 8941-8949 (2016).

61. Adnadjevic, B. K. & Jovanovic, J. D. A comparative kinetics study on the isothermal heterogeneous acid-catalyzed hydrolysis of sucrose under conventional and microwave heating. J. Mol. Catal. A Chem. 356, 70–77 (2012).

62. Marconi, E., Panfili, G., Bruschi, L., Vivanti, V. & Pizzoferrato, L. Comparative study on microwave and conventional methods for protein hydrolysis in food. Amino Acids 8, 201–208 (1995).

63. Bizzi, C. A., Flores, E. M. M., Barin, J. S., Garcia, E. E. & Nóbrega, J. A. Understanding the process of microwave-assisted digestion combining diluted nitric acid and oxygen as auxiliary reagent. Microchem. J. 99, 193–196 (2011).

64. Malmberg, C. G. & Maryott, A. A. Dielectric constant of water from 0 to 100 C. J. Res. Natl. Bur. Stand. (1934). 56, 1 (1956).

65. Taqi, A., Farcot, E., Robinson, J. P. & Binner, E. R. Understanding microwave heating in biomass-solvent systems. Chem. Eng. J. 393, 124741 (2020).

66. Afolabi, O. O. D., Sohail, M. & Thomas, C. P. L. Microwave Hydrothermal Carbonization of Human Biowastes. Waste and Biomass Valorization 6, 147–157 (2015).

67. Dąbrowska, S., Chudoba, T., Wojnarowicz, J. & Łojkowski, W. Current Trends in the Development of Microwave Reactors for the Synthesis of Nanomaterials in Laboratories and Industries: A Review. Crystals 8, 379 (2018).

68. Friedmann, S. J., Fan, Z. & Tang, K. Low-Carbon heat solutions for heavy industry: sources, options, and costs today. Columbia Cent. Glob. Energy Policy 44–49 (2019).

69. Element Energy & Jacobs. Industrial Fuel Switching Market Engagement Study. (2018).

70. Döbereiner, J. W. Ueber die medicinische und chemische Anwendung und die vortheilhafte Darstellung der Ameisensäure. Ann. der Pharm. 3, 141–146 (1832).

71. Mulder, G. J. Untersuchungen über die Humussubstanzen. J. für Prakt. Chemie 21, 203–240 (1840).

72. Lange, J. P., Price, R., Ayoub, P., Perus, L., Clarke, L., Gosselink, H. Valeric biofuels: A platform of cellulosic transportation fuels. Cellulosic Biofuels 49, 4479–4483 (2010).

73. Carnevali, D., Rigamonti, M. G., Tabanelli, T., Patience, G. S. & Cavani, F. Levulinic acid upgrade to succinic acid with hydrogen peroxide. Appl. Catal. A Gen. 563, 98–104 (2018).

74. Delhomme, C., Weuster-Botz, D. & Kuhn, F. E. Succinic acid from renewable resources as a C4 building-block chemical—a review of the catalytic possibilities in aqueous media. Green Chem. 11, 13–26 (2009).

75. Genuino, H. C. et al. Catalytic Hydrogenation of Renewable Levulinic Acid to γ-Valerolactone: Insights into the Influence of Feed Impurities on Catalyst Performance in Batch and Flow Reactors. ACS Sustain. Chem. Eng. 8, 5903–5919 (2020).

76. Chen, S., Wojcieszak, R., Dumeignil, F., Marceau, E. & Royer, S. How Catalysts and Experimental Conditions Determine the Selective Hydroconversion of Furfural and 5-Hydroxymethylfurfural. Chem. Rev. 118, 11023–11117 (2018).

77. Kabbour, M. & Luque, R. Furfural as a platform chemical: From production to applications. Biomass, Biofuels, Biochemicals: Recent Advances in Development of Platform Chemicals (2019).

78. Natsir, T. A. & Shimazu, S. Fuels and fuel additives from furfural derivatives via etherification and formation of methylfurans. Fuel Process. Technol. 200, 106308 (2020).

79. Caratzoulas, S., Davis, M., Gorte, R., Gounder, R., Lobo, R., Nikolakis, V., Sandler, S., Snyder, M., Tsapatsis, M., Vlachos, D. Challenges of and Insights into Acid-Catalyzed Transformations of Sugars. J. Phys. Chem. C 118, 22815–22833 (2014).

80. Girisuta, B., Janssen, L. P. B. M. B. M. & Heeres, H. J. Kinetic study on the acid-catalyzed hydrolysis of cellulose to levulinic acid. Ind. Eng. Chem. Res. 46, 1696–1708 (2007).

81. Li, S., Josephson, T., Vlachos, D. G. & Caratzoulas, S. The origin of selectivity in the conversion of glucose to fructose and mannose in Sn-BEA and Na-exchanged Sn-BEA zeolites. J. Catal. 355, 11–16 (2017).

82. Girisuta, B., Janssen, L. P. B. M. & Heeres, H. J. A kinetic study on the decomposition of 5-hydroxymethylfurfural into levulinic acid. Green Chemistry 8, 701–709 (2006). doi:10.1039/b518176c

83. Liu, X., Li, S., Liu, Y. & Cao, Y. Formic acid: A versatile renewable reagent for green and sustainable chemical synthesis. Chinese J. Catal. 36, 1461–1475 (2015).

84. Brouwer, T., Blahusiak, M., Babic, K. & Schuur, B. Reactive extraction and recovery of levulinic acid , formic acid and furfural from aqueous solutions containing sulphuric acid. Sep. Purif. Technol. 185, 186–195 (2017).

85. Girisuta, B., Janssen, L. P. B. M. & Heeres, H. J. A Kinetic Study on the Conversion of Glucose to Levulinic Acid. Chemical Engineering Research and Design 84, 339-349 (2006). doi:10.1205/cherd05038

86. Toftgaard Pedersen, A., Ringborg, R., Grotkjær, T., Pedersen, S. & Woodley, J. M. Synthesis of 5-hydroxymethylfurfural (HMF) by acid catalyzed dehydration of glucose-fructose mixtures. Chem. Eng. J. 273, 455–464 (2015).

87. Tan-Soetedjo, J. N. M., van de Bovenkamp, H. H., Abdilla, R. M., Rasrendra, C. B., Van Ginkel, J., Heeres, H. J. Experimental and Kinetic Modeling Studies on the Conversion of Sucrose to Levulinic Acid and 5-Hydroxymethylfurfural Using Sulfuric Acid in Water. Ind. Eng. Chem. Res. 56, 13228–13239 (2017).

88. Tang, J., Guo, X., Zhu, L. & Hu, C. Mechanistic Study of Glucose-to-Fructose Isomerization in Water Catalyzed by [Al(OH)2(aq)]+. ACS Catal. 5, 5097–5103 (2015).

89. Havasi, D., Pátzay, G., Stelén, G., Tukacs, J. M. & Mika, L. T. Recycling of Sulfuric Acid in the Valorization of Biomass Residues. Periodica Polytechnica Chemical Engineering 61, 283-287 (2017).

90. Pyo, S. H., Glaser, S. J., Rehnberg, N. & Hatti-Kaul, R. Clean Production of Levulinic Acid from Fructose and Glucose in Salt Water by Heterogeneous Catalytic Dehydration. ACS Omega 5, 14275–14282 (2020).

91. Weingarten, R., Cho, J., Xing, W. R., Curtis, C. & Huber, G. W. Kinetics and reaction engineering of levulinic acid production from aqueous glucose solutions. ChemSusChem2 5, 1280–1290 (2012).

92. Asep Bayu, Akihiro Yoshida, a, b Surachai Karnjanakom, Katsuki Kusakabe, Xiaogang Hao, Tirto Prakoso, A. A. Catalytic Conversion of Biomass Derivatives to Lactic Acid with Increased Selectivity in Aqueous Tin(II) Chloride/Choline Chloride System Asep. Green Chemsitry (2018). doi:10.1039/C8GC01022F

93. Peng, L., Lin, L., Zhang, J., Zhuang, J., Zhang, B., Gong, Y. Catalytic Conversion of Cellulose to Levulinic Acid by Metal Chlorides. Molecules 15, 5258–5272 (2010). doi:10.3390/molecules15085258

94. Wettstein, S. G., Alonso, D. M., Chong, Y. & Sumesic, J. A. Production of levulinic acid and gamma-valerolactone (GVL) from cellulose using GVL as a solvent in biphasic systems Stephanie. Energy Environ. Sci. 5, 8199–8203 (2012).

95. Sweygers, N., Dewil, R. & Appels, L. Production of Levulinic Acid and Furfural by Microwave-Assisted Hydrolysis from Model Compounds : Effect of Temperature , Acid Concentration and Reaction Time. Waste and Biomass Valorization 9, 343–355 (2018).

96. Wang, K., Liu, Y., Wu, W., Chen, Y., Li, W., Ji, H. Production of Levulinic Acid via Cellulose Conversion Over Metal Oxide-Loaded MOF Catalysts in Aqueous Medium. Catal. Letters 150, 322–331 (2020).

97. Rivas, S., Maria, A., Galletti, R., Antonetti, C. & Carlos, J. Hemicellulose-Free Eucalyptus Globulus Wood : Production of Concentrated Levulinic Acid Solutions for γ -Valerolactone Sustainable Preparation. Catlysts,8:169 (2018) doi:10.3390/catal8040169

98. Fang, Q. & Hanna, M. A. Experimental studies for levulinic acid production from whole kernel grain sorghum. Bioresource Technology 81, 187–192 (2002).

99. Runge, T. & Zhang, C. Two-Stage Acid-Catalyzed Conversion of Carbohydrates into Levulinic Acid. Industrial and Engineering Chemistry Research 51, 3265-3270 (2012). doi:10.1021/ie2021619

100. Galletti, A. M. R., Antonetti, C., De Luise, V., Licursi, D. & Di Nasso, N. N. O. Levulinic acid production from waste biomass. BioResources 7, 1824–1834 (2012).

101. Sweygers, N., Somers, M. H. & Appels, L. Optimization of hydrothermal conversion of bamboo (Phyllostachys aureosulcata) to levulinic acid via response surface methodology. J. Environ. Manage. 219, 95–102 (2018).

102. Su, J., Shen, F., Qiu, M., Qi, X. High-yield production of levulinic acid from pretreated cow dung in dilute acid aqueous solution. Molecules 22, (2017).

103. Liu, L., Li, Z., Hou, W. & Shen, H. Direct conversion of lignocellulose to levulinic acid catalyzed by ionic liquid. Carbohydr. Polym. 181, 778–784 (2018).

104. Alipour, S. & Omidvarborna, H. High concentration levulinic acid production from corn stover. RSC Adv. 6, 111616–111621 (2016).

105. Aliko, K., Doudin, K., Ostiashtiani, A., Wang, J., GTophamn, P. D., Theodosiou, E. Microwave-assisted synthesis of levulinic acid from low-cost, sustainable feedstocks using organic acids as green catalysts. J. Chem. Technol. Biotechnol. 95, 2110–2119 (2020).

106. Fitzpatrick, S. W. Final technical report: Commercialization of the Biofine technology for levulinic acid production from paper sludge. Other Inf. PBD 23 Apr 2002; PBD 23 Apr 2002 Medium: P; Size: vp. (2002).

107. Shaveta, S., Bansal, N. & Singh, P. F-/Cl- mediated microwave assisted breakdown of cellulose to glucose. Tetrahedron Lett. 55, 2467–2470 (2014).

108. Xiao, S., Liu, B., Wang, Y., Fang, Z. & Zhang, Z. Efficient conversion of cellulose into biofuel precursor 5-hydroxymethylfurfural in dimethyl sulfoxide-ionic liquid mixtures. Bioresour. Technol. 151, 361–366 (2014).

109. Pulidindi, I. N., Kim, T. H. Conversion of Levulinic Acid from Various Herbaceous Biomass Species Using Hydrochloric Acid and Effects of Particle Size and Delignification. Energies 18, (2018). doi:10.3390/en11030621

110. Chen, R., Zhu, S., Chen, C., Cheng, B., Chen, J., Wu, Y. Reviving the acid hydrolysis process of lignocellulosic material in biorefinery. BioResources 9, 1824–1827 (2014).

111. Hayes, D. J., Steve, F., Hayes, M. H. B. & Ross, J. The biofine process - production of levulinic acid, furfural, and formic acid from lignocellulosic feedstocks. Biorefineries-inductrial processes and products: status quo and future directions. (Wiley-VCH Verlag GmbH Weinheim, 2008).

112. Steffen, F., Janzon, R., Wenig, F. & Saake, B. Valorization of waste streams from deinked pulp mills through anaerobic digestion of deinking sludge. BioResources 12, 4547–4566 (2017).

113. Kłosowski, G., Mikulski, D. & Menka, A. Microwave-Assisted One-Step Conversion of Wood Wastes into Levulinic Acid. Catalysts 9, 753 (2019).

114. Girisuta, B., Dussan, K., Haverty, D., Leahy, J. J. & Hayes, M. H. B. A kinetic study of acid catalysed hydrolysis of sugar cane bagasse to levulinic acid. Chem. Eng. J. 217, 61–70 (2013).

115. Lappalainen, K., Volger, N., Kärkkäinen, J., Dong, Y., Rusanen, A., Ruotsalainen, A., Wäli, P., Markkola, A., Lassi, U. Microwave-assisted conversion of novel biomass materials into levulinic acid. Biomass Convers. Biorefinery 8, 965–970 (2018).

116. CHANG, C., MA, X. & CEN, P. Kinetics of Levulinic Acid Formation from Glucose Decomposition at High. Chinese J. Chem. Eng. 14, 708–712 (2006).

117. Girisuta, B., Danon, B., Manurung, R., Janssen, L. P. B. M. & Heeres, H. J. Experimental and kinetic modelling studies on the acid-catalysed hydrolysis of the water hyacinth plant to levulinic acid. Bioresour. Technol. 99, 8367–8375 (2008).

118. Zheng, X., Zhi, Z., Gu, X., Li, X., Zhang, R., Lu, X. Kinetic study of levulinic acid production from corn stalk at mild temperature using FeCl3 as catalyst. Fuel 187, 261–267 (2017).

119. Gozan, M., Panjaitan, J. R. H., Tristantini, D., Alamsyah, R. & Yoo, Y. J. Evaluation of Separate and Simultaneous Kinetic Parameters for Levulinic Acid and Furfural Production from Pretreated Palm Oil Empty Fruit Bunches. Int. J. Chem. Eng. 2018, (2018).

120. Kanchanalai, P., Temani, G., Kawajiri, Y. & Realff, M. J. Reaction Kinetics of Concentrated-Acid Hydrolysis for Cellulose and Hemicellulose and Effect of Crystallinity. BioResources 11, 1672–1689 (2016).

121. Huang, Y. B. & Fu, Y. Hydrolysis of cellulose to glucose by solid acid catalysts. Green Chem. 15, 1095–1111 (2013).

122. Licursi, D., Antonetti, C., Fulignati, S., Giannoni, M. & Raspolli Galletti, A. M. Cascade strategy for the tunable catalytic valorization of levulinic acid and γ-valerolactone to 2-methyltetrahydrofuran and alcohols. Catalysts 8, (2018).

123. Acharjee, T. C. & Lee, Y. Y. Production of levulinic acid from glucose by dual solid-acid catalysts. Environ. Prog. Sustain. Energy 37, 471–480 (2018).

124. Liu, Y., Lin, L., Sui, X., Zhuang, J. & Pang, C. Conversion of Glucose to Levulinic Acid Catalyzed by ZSM-5 Loading SO_4^{2-}/ ZrO_2. Applied Mechanics and Materials 291, 249–252 (2013).

125. Upare, P. P., Yoon, J. W., Kim, M., Kang, H. Y., Hwang, D., Hwang, Y. K., Kung, H., Chang, J. S. Chemical conversion of biomass-derived hexose sugars to levulinic acid over sulfonic acid-functionalized graphene oxide catalysts. Green Chem. 13, 2935–2943 (2013).

126. Redmon, B. C. PROCESS FOR THE PRODUCTION OF LEVULINIC ACID. (1952).

127. Weingarten, R., Conner, W. C. & Huber, G. W. Production of levulinic acid from cellulose by hydrothermal decomposition combined with aqueous phase dehydration with a solid acid catalyst. Energy Environ. Sci. 5, 7559–7574 (2012).

128. Alonso, D. M., Gallo, J. M. R., Mellmer, M. A., Wettstein, S. G. & Dumesic, J. A. Direct conversion of cellulose to levulinic acid and gamma-valerolactone using solid acid catalysts. Catal. Sci. Technol. 3, 927–931 (2013).

129. Liu, B. & Zhang, Z. Catalytic conversion of biomass into chemicals and fuels over magnetic catalysts. ACS Catalysis, 326-338 (2016). doi:10.1021/acscatal.5b02094

130. Wang, P., Zhan, S. & Yu, H. Production of Levulinic Acid from Cellulose Catalyzed by Environmental-Friendly Catalyst. 96, 183–187 (2010).

131. Joshi, S. S., Zodge, A. D., Pandare, K. V. & Kulkarni, B. D. Efficient conversion of cellulose to levulinic acid by hydrothermal treatment using zirconium dioxide as a recyclable solid acid catalyst. Ind. Eng. Chem. Res. 53, 18796–18805 (2014).

132. Ding, D., Wang, J., Xi, J., Liu, X., Lu, G., Wang, Y. High-yield production of levulinic acid from cellulose and its upgrading to γ-valerolactone. Green Chem. 16, 3846–3853 (2014).

133. Chen, S. S., Wang, L., Yu, I. K. M., Tsang, D. C. W., Hunt, A. J., Jérôme, F., Zhang, S., Ok, Y. S., Poon, C. S. Valorization of lignocellulosic fibres of paper waste into levulinic acid using solid and aqueous BrØnsted acid. Bioresour. Technol. 247, 387–394 (2018).

134. Ya'aini, N., Amin, N. A. S. & Asmadi, M. Optimization of levulinic acid from lignocellulosic biomass using a new hybrid catalyst. Bioresour. Technol. 116, 58–65 (2012).

135. Kang, S. & Yu, J. Maintenance of a Highly Active Solid Acid Catalyst in Sugar Beet Molasses for Levulinic Acid Production. Sugar Tech 20, 182–193 (2018).

136. Delidovich, I. & Palkovits, R. Catalytic Isomerization of Biomass-Derived Aldoses: A Review. ChemSusChem 9, 547–561 (2016).

137. Wang, Y., Li, S., Deng, W., Wang, S., Wang, P., An, D., Li, Y., Zhang, Q. Catalytic transformation of cellulose and its derivatives into functionalized organic acids. ChemSusChem 11, 1995–2028 (2018).

138. Xue, Z., Liu, Q., Wang, J. & Mu, T. Valorization of levulinic acid over non-noble metal catalysts: Challenges and opportunities. Green Chem. 20, 4391–4408 (2018).

139. Zeng, W., Cheng, D. G., Chen, F. & Zhan, X. Catalytic conversion of glucose on Al-Zr mixed oxides in hot compressed water. Catal. Letters 133, 221–226 (2009).

140. Antonetti, C., Licursi, D., Fulignati, S., Valentini, G., Galletti, A. M. R. New Frontiers in the Catalytic Synthesis of Levulinic Acid : From Sugars to Raw and Waste Biomass as Starting Feedstock. 1–29 (2016). doi:10.3390/catal6120196

141. Doyle, A. M., Albayati, M. T., Abbas, A. S., Alismaeel, Z. T. Biodiesel production by esterification of oleic acid over zeolite Y prepared from kaolin. Renew. Energy 97, 19–23 (2016).

142. Ya'Aini, N., Amin, N. A. S. & Endud, S. Characterization and performance of hybrid catalysts for levulinic acid production from glucose. Microporous Mesoporous Mater. 171, 14–23 (2013).

143. Jow, J., Rorrer, G. L., Hawley, M. C. & Lamport, D. T. A. Dehydration of d-fructose to levulinic acid over LZY zeolite catalyst. Biomass 14, 185–194 (1987).

144. Saravanamurugan, S., Paniagua, M., Melero, J. A. & Riisager, A. Efficient isomerization of glucose to fructose over zeolites in consecutive reactions in alcohol and aqueous media. J. Am. Chem. Soc. 135, 5246–5249 (2013).

145. Xiang, M., Liu, J., Fu, W., Tang, T. & Wu, D. Improved Activity for Cellulose Conversion to Levulinic Acid through Hierarchization of ETS-10 Zeolite. ACS Sustainable Chemistry and Engineering 5, 5800-5809 (2017).

146. Marianou, A. A. et al. Glucose to Fructose Isomerization in Aqueous Media over Homogeneous and Heterogeneous Catalysts. ChemCatChem 8, 1100–1110 (2016).

147. Kramarenko, A., Etit, D., Laudadio, G. & D'Angelo, F. N. β-Zeolite-Assisted Lignin-First Fractionation in a Flow-Through Reactor. ChemSusChem 14, 3838–3849 (2021).

148. Ennaert, T., van Aelst, J., Dijkmans, J., de Clercq, R., Schutysre, W., Dusselier, M., Verboekend, D., Sesl, B. F. Potential and challenges of zeolite chemistry in the catalytic conversion of biomass. Chem. Soc. Rev. 45, 584–611 (2016).

149. Hartono, C. D., Marlie, K. J., Putro, J. N., Soetardjo, F. E, Ju, Y., Sirodj, D., Ismadji, S. Levulinic acid from corncob by subcritical water process. Int. J. Ind. Chem. 7, 401–409 (2016).

150. Bavykina, A., Koblov, N., Khan, I. S., Bau, J.A., Ramirez, A., Gascon, J. Metal-Organic Frameworks in Heterogeneous Catalysis: Recent Progress, New Trends, and Future Perspectives. Chem. Rev. 120, 8468–8535 (2020).

151. Kobayashi, H., Kaiki, H., Shrotri, A., Techikawara, K. & Fukuoka, A. Hydrolysis of woody biomass by a biomass-derived reusable heterogeneous catalyst. Chem. Sci. 7, 692–696 (2016).

152. Kassaye, S., Pagar, C., Pant, K. K., Jain, S. & Gupta, R. Depolymerization of microcrystalline cellulose to value added chemicals using sulfate ion promoted zirconia catalyst. Bioresour. Technol. 220, 394–400 (2016).

153. Osatiashtiani, A. et al. Hydrothermally Stable, Conformal, Sulfated Zirconia Monolayer Catalysts for Glucose Conversion to 5-HMF. ACS Catal. 5, 4345–4352 (2015).

154. Potvin, J., Sorlien, E., Hegner, J., DeBoef, B. & Lucht, B. L. Effect of NaCl on the conversion of cellulose to glucose and levulinic acid via solid supported acid catalysis. Tetrahedron Lett. 52, 5891–5893 (2011).

155. Geboers, J., Van de Vyver, S., Carpentier, K., Jacobs, P. & Sels, B. Efficient hydrolytic hydrogenation of cellulose in the presence of Ru-loaded zeolites and trace amounts of mineral acid. Chem. Commun. 47, 5590–5592 (2011).

156. Jiang, Z., Yi, J., Li, J., He, T. & Hu, C. Promoting effect of sodium chloride on the solubilization and depolymerization of cellulose from raw biomass materials in water. ChemSusChem 8, 1901–1907 (2015).

157. van Zandvoort, I., Wang, Y., Rasrendra, C. B., van Eck, E. R. H., Bruijincx, P. C. A., Heeres, H. J., Weckhusen, B. M. Formation , Molecular Structure , and Morphology of Humins in Biomass Conversion : Influence of Feedstock and Processing Conditions. Chem. Sus. Chem. 6 1745–1758 (2013).

158. Melligan, F., Dussan, K., Auccaise, R., Novonty, E. H., Leahy, J. J., Hayes, M. H. B., Kwapinski, W. Characterisation of the products from pyrolysis of residues after acid hydrolysis of Miscanthus. Bioresource Technology. 108, 258–263 (2012).

159. Patil, S. K. R. R., Heltzel, J. & Lund, C. R. F. F. Comparison of structural features of humins formed catalytically from glucose, fructose, and 5-hydroxymethylfurfuraldehyde. Energy and Fuels 26, 5281–5293 (2012).

160. Patil, S. K. R. & Lund, C. R. F. Formation and Growth of Humins via Aldol Addition and Condensation during Acid-Catalyzed Conversion of 5-Hydroxymethylfurfural. 4745–4755 (2011). doi:10.1021/ef2010157

161. van Zandvoort, I., Koers, E. J., Weingarth, M., Bruijnincx, P. C. A., Baldus, M., Weckhuysen, B. M. Structural characterization of 13C-enriched humins and alkali-treated 13C humins by 2D solid-state NMR. Green Chemistry. 17. 4383–4392 (2015). doi:10.1039/c5gc00327j

162. Shi, N., Liu, Q., Cen, H., Ju, R., He, X., Ma, L. Formation of humins during degradation of carbohydrates and furfural derivatives in various solvents. Biomass Convers. Biorefinery 10, 277–287 (2020).

163. Shen, J. & Wyman, C. E. Hydrochloric Acid-Catalyzed Levulinic Acid Formation from Cellulose: Data and Kinetic Model to Maximize Yields. AIChE J. 58, 236–246 (2012).

164. Baugh, K. D. & McCarty, P. L. Thermochemical pretreatment of lignocellulose to enhance methane fermentation: I. Monosaccharide and furfurals hydrothermal decomposition and product formation rates. Biotechnol. Bioeng. 31, 50–61 (1988).

165. Rasrendra, C. B., Windt, H., Wang, Y., Adisasmito, S., Makertihartha, I. G. B. N., van Eck, E. R., Meier, D., Heeres, H. J. Experimental studies on the pyrolysis of humins from the acid-catalysed dehydration of C6-sugars. J. Anal. Appl. Pyrolysis 104, 299–307 (2013).

166. Agarwal, S., Es, D. Van, Jan, H., van Es, D. & Heeres, H. J. Catalytic pyrolysis of recalcitrant, insoluble humin byproducts from C6 sugar biorefineries. J. Anal. Appl. Pyrolysis 123, 134–143 (2017).

167. Sumerskii, I. V., Krutov, S. M. & Zarubin, M. Y. Humin-Like substances formed under the conditions of industrial hydrolysis of wood. Russ. J. Appl. Chem. 83, 320–327 (2010).

168. Tosi, P., van Klink, G., Hurel, C., Lomenech, C., Celzard, A., Fierro, V., Delgado-Sanchez, C., Mija, A. Investigating the properties of humins foams, the porous carbonaceous materials derived from biorefinery by-products. Appl. Mater. Today 20, 100622 (2020).

169. Al Ghatta, A., Zhou, X., Casarano, G., Wilton-Ely, J. D. E. T. & Hallett, J. P. Characterization and Valorization of Humins Produced by HMF Degradation in Ionic Liquids: A Valuable Carbonaceous Material for Antimony Removal. ACS Sustain. Chem. Eng. 9, 2212–2223 (2021).

170. Tsilomelekis, G., Orella, M. J., Lin, Z., Cheng, Z., Zheng, W., Nikolakis, V., Vlachos, D. Molecular structure, morphology and growth mechanisms and rates of 5-hydroxymethyl furfural (HMF) derived humins. Green Chem. 18, 1983–1993 (2016).

171. Xu, Q. et al. Cross-polymerisation between furfural and the phenolics of varied molecular structure in bio-oil. Bioresour. Technol. Reports 8, 100324 (2019).

172. Zandvvort, I. Towards the Valorization of Humin By-products : Characterization , Solubilization and Catalysis Ilona van Zandvoort. (2015).

173. Baveye, P. C. & Wander, M. The (bio)chemistry of soil humus and humic substances: Why is the ‘new view’ still considered novel after more than 80 years? Front. Environ. Sci. 7, 1–6 (2019).

174. Shindo, H., Hirahara, O., Yoshida, M. & Yamamoto, A. Effect of continuous compost application on humus composition and nitrogen fertility of soils in a field subjected to double cropping. Biol. Fertil. Soils 42, 437–442 (2006).

175. Wang, T., Zhai, Y., Zhu, Y., Li, C. & Zeng, G. A review of the hydrothermal carbonization of biomass waste for hydrochar formation: Process conditions, fundamentals, and physicochemical properties. Renew. Sustain. Energy Rev. 90, 223–247 (2018).

176. Liu, C., Huang, X. & Kong, L. Efficient low temperature hydrothermal carbonization of Chinese reed for biochar with high energy density. Energies 10, (2017).

177. Shi, N., Liu, Q., He, X., Wang, G., Chen, N., Peng, J., Ma, L. Molecular Structure and Formation Mechanism of Hydrochar from Hydrothermal Carbonization of Carbohydrates. Energy and Fuels 33, 9904–9915 (2019).

178. Cai, J., Li, B., Chen, C., Wang, J., Zhao, M., Zhang, K. Hydrothermal carbonization of tobacco stalk for fuel application. Bioresour. Technol. 220, 305–311 (2016).

179. Fang, J., Zhan, L., Ok, Y. S. & Gao, B. Minireview of potential applications of hydrochar derived from hydrothermal carbonization of biomass. J. Ind. Eng. Chem. 57, 15–21 (2018).

180. Yin, S., Dolan, R., Harris, M. & Tan, Z. Subcritical hydrothermal liquefaction of cattle manure to bio-oil: Effects of conversion parameters on bio-oil yield and characterization of bio-oil. Bioresour. Technol. 101, 3657–3664 (2010).

181. Sevilla, M. & Fuertes, A. B. Chemical and structural properties of carbonaceous products obtained by hydrothermal carbonization of saccharides. Chem. - A Eur. J. 15, 4195–4203 (2009).

182. Kang, S., Li, X., Fan, J. & Chang, J. Characterization of Hydrochars Produced by Hydrothermal Carbonization of Lignin , Cellulose , D -Xylose , and Wood Meal. (2012).

183. Khosravi, A., Zheng, H., Liu, Q., Hashemi, M., Tang, Y., Xing, B. Production and characterization of hydrochars and their application in soil improvement and environmental remediation. Chem. Eng. J. 133142 (2021). doi:10.1016/j.cej.2021.133142

184. Gronwald, M., Vos, C., Helfrich, M. & Don, A. Stability of pyrochar and hydrochar in agricultural soil - a new field incubation method. Geoderma 284, 85–92 (2016).

185. Saha, N., McGaughy, K. & Reza, M. T. Elucidating hydrochar morphology and oxygen functionality change with hydrothermal treatment temperature ranging from subcritical to supercritical conditions. J. Anal. Appl. Pyrolysis 152, 104965 (2020).

186. Lucian, M. & Fiori, L. Hydrothermal carbonization of waste biomass: Process design, modeling, energy efficiency and cost analysis. Energies 10, (2017).

187. Wang, T., Zhai, Y., Zhu, Y., Peng, C., Xu, B., Wang, T., Li, C., Zeng, G. Acetic Acid and Sodium Hydroxide-Aided Hydrothermal Carbonization of Woody Biomass for Enhanced Pelletization and Fuel Properties. Energy and Fuels 31, 12200–12208 (2017).

188. Qi, Y., Song, B. & Qi, Y. The roles of formic acid and levulinic acid on the formation and growth of carbonaceous spheres by hydrothermal carbonization. RSC Adv. 6, 102428–102435 (2016).

189. Flannelly, T., Lopes, M., Kupiainen, L., Dooley, S. & Leahy, J. J. Non-stoichiometric formation of formic and levulinic acids from the hydrolysis of biomass derived hexose carbohydrates. RSC Advances 6, 5797–5804 (2016). doi:10.1039/c5ra25172a

190. Yoon, S. Y., Han, S. H. & Shin, S. J. The effect of hemicelluloses and lignin on acid hydrolysis of cellulose. Energy 77, 19–24 (2014).

191. Wang, Y., Delbecq, F., Varma, R. S. & Len, C. Comprehensive study on expeditious conversion of pre-hydrolyzed alginic acid to furfural in Cu (II) biphasic systems using microwaves. Mol. Catal. 445, 73–79 (2018).

192. Johnson, A. M., Kim, H., Ralph, J. & Mansfield, S. D. Natural acetylation impacts carbohydrate recovery during deconstruction of Populus trichocarpa wood. Biotechnol. Biofuels 10, 1–12 (2017).

193. Koottatep, T., Fakkaew, K., Tajai, N., Pradeep, S. V. & Polprasert, C. Sludge stabilization and energy recovery by hydrothermal carbonization process. Renew. Energy 99, 978–985 (2016).

194. de Carvalho, D. M. & Colodette, J. L. Comparative study of acid hydrolysis of lignin and polysaccharides in biomasses. BioResources 12, 6907–6923 (2017).

195. Aarum, I., Devle, H., Ekeberg, D., Horn, S. J. & Stenstrøm, Y. Characterization of Pseudo-Lignin from Steam Exploded Birch. ACS Omega 3, 4924–4931 (2018).

196. Leng, L., Yang, L., Leng, S., Zhang, W., Zhou, Y., Peng, H., Li, H., Hu, Y., Jiang, S., Li, H. A review on nitrogen transformation in hydrochar during hydrothermal carbonization of biomass containing nitrogen. Sci. Total Environ. 756, 143679 (2021).

197. Leal Silva, J. F., Grekin, R., Mariano, A. P. & Maciel Filho, R. Making Levulinic Acid and Ethyl Levulinate Economically Viable: A Worldwide Technoeconomic and Environmental Assessment of Possible Routes. Energy Technol. 6, 613–639 (2018).

198. Lopes, E. S., Leal-Silva, J .F., Rivera, E. C., Gomes, A. P., Lopes, M. S., Filho, R., Tovar, L. P. Challenges to Levulinic Acid and Humins Valuation in the Sugarcane Bagasse Biorefinery Concept. Bioenergy Res. (2020). doi:10.1007/s12155-020-10124-9

199. Sumbharaju, R., Wild, P. J. de, Laan, R. R. van der & Meyer, D. F. Two-Stage Thermochemical Valorisation of Sugar-Derived. 6–20 (2016).

200. Mija, A., Waal, J. C. Van Der, Pin, J., Guigo, N. & Jong, E. De. Humins as promising material for producing sustainable carbohydrate-derived building materials. Constr. Build. Mater. 139, 594–601 (2017).

201. Randviir, E. P., Kanou, O., Liauw, C., Miller, G. J., Andrews, H., Smith, G. The physicochemical investigation of hydrothermally reduced textile waste and application within carbon-based electrodes. RSC Adv. 9, 11239–11252 (2019).

202. Qiu, L., Deng, Y. F., Wang, F., Davaritouchaee, M. & Yao, Y. Q. A review on biochar-mediated anaerobic digestion with enhanced methane recovery. Renew. Sustain. Energy Rev. 115, 109373 (2019).

203. Khan, U. M. & Ahring, K. B. Improving the biogas yield of manure: Effect of pretreatment on anaerobic digestion of the recalcitrant fraction of manure. Bioresour. Technol. 321, 124427 (2021).

204. Xu, J., Mustafa, A. M., Lin, H., Choe, U. Y. & Sheng, K. Effect of hydrochar on anaerobic digestion of dead pig carcass after hydrothermal pretreatment. Waste Manag. 78, 849–856 (2018).

205. Choe, U., Mustafa, A. M., Lin, H., Xu, J. & Sheng, K. Effect of bamboo hydrochar on anaerobic digestion of fish processing waste for biogas production. Bioresour. Technol. 283, 340–349 (2019).

206. Dudek, M., Świechowski, K., Manczarski, P., Koziel, J. A. & Białowiec, A. The effect of biochar addition on the biogas production kinetics from the anaerobic digestion of brewers' spent grain. Energies 12, 1–22 (2019).

207. Kumar, M. et al. A critical review on biochar for enhancing biogas production from anaerobic digestion of food waste and sludge. J. Clean. Prod. 305, 127143 (2021).

208. Weidemann, E., Niinipuu, M., Fick, J. & Jansson, S. Using carbonized low-cost materials for removal of chemicals of environmental concern from water. Environ. Sci. Pollut. Res. 25, 15793–15801 (2018).

209. McCabe, J. & Eckenfelder, W. Biological Treatment of Sewage and Industrial Wastes. (Renbold Publishing, 1957).

210. Torrijos, M. State of Development of Biogas Production in Europe. Procedia Environ. Sci. 35, 881–889 (2016).

211. Defra. Anaerobic digestion strategy and action plan. Department of Energy & Climate Change (2011).

212. Bajpai, P. Basics of Anaerobic Digestion Process. SpringerBriefs Appl. Sci. Technol. 7–13 (2017). doi:10.1007/978-981-10-4130-3

213. Ersahin, M. E. & Ozgun, H. Anaerobic Treatment of Industrial Effluents : An Overview of Applications. (2013).

214. Hemme, C. L. et al. Metagenomic insights into evolution of a heavy metal-contaminated groundwater microbial community. ISME J. 4, 660–672 (2010).

215. Wang, X., Lu, X., Li, F. & Yang, G. Effects of temperature and Carbon-Nitrogen (C/N) ratio on the performance of anaerobic co-digestion of dairy manure, chicken manure and rice straw: Focusing on ammonia inhibition. PLoS One 9, 1–7 (2014).

216. Solarte-Toro, J. C., Chacón-Pérez, Y. & Cardona-Alzate, C. A. Evaluation of biogas and syngas as energy vectors for heat and power generation using lignocellulosic biomass as raw material. Electron. J. Biotechnol. 33, 52–62 (2018).

217. Kozak T & Majchrzycka A. Application of biogas for combined heat and power production in the rural region. Fac. Math. Nat. Sci. 184–189 (2009).

218. Angelidaki, I., Xie, L., Luo, G., Zhang, Y., Oechsner, H., Lemmer, A., Munoz, R., Kougias. Biogas upgrading: Current and emerging technologies. Biomass, Biofuels, Biochemicals: Biofuels: Alternative Feedstocks and Conversion

Processes for the Production of Liquid and Gaseous Biofuels (2019). doi:10.1016/B978-0-12-816856-1.00033-6

219. Saadabadi, S. A., Thatti, A. T., Fan, L., Lindeboom, R., Spanjers, H., Aravind, P. V. Solid Oxide Fuel Cells fuelled with biogas: Potential and constraints. Renew. Energy 134, 194–214 (2019).

220. Cesaro, A. & Belgiorno, V. Combined biogas and bioethanol production: Opportunities and challenges for industrial application. Energies 8, 8121–8144 (2015). doi:10.3390/en8088121

221. Paolini, V., Petracchini, F., Segreto, M., Tomassetti, L., Naja, N., Ceccinato, A. Environmental impact of biogas: A short review of current knowledge. J. Environ. Sci. Heal. - Part A Toxic/Hazardous Subst. Environ. Eng. 53, 899–906 (2018).

222. Przemysław, B., Hlisnikovský, L. & Eva, K. Effect of Digestate on Soil Organic Carbon and Plant-Available Nutrient Content Compared to Cattle. Agronomy 10, Article no.379, 1-16 (2020).

223. Lim, J. W., Park, T., Tong, Y. W. & Yu, Z. The microbiome driving anaerobic digestion and microbial analysis. Adv. Bioenergy 5, 1–61 (2020).

224. Timonen, K., Sinkko, T., Luostarinen, S., Tampio, E. & Joensuu, K. LCA of anaerobic digestion: Emission allocation for energy and digestate. J. Clean. Prod. 235, 1567–1579 (2019).

225. Bezzi, G., Maggioni, L., Pieroni, C. BIOGASDONERIGHT® MODEL: SOIL CARBON SEQUESTRATION AND EFFICIENCY IN AGRICULTURE (2016). doi:10.5071/24thEUBCE2016-4DO.2.3

226. Béghin-Tanneau, R., Guérin, F., Guiresse, M., Kleiber, D. & Scheiner, J. D. Carbon sequestration in soil amended with anaerobic digested matter. Soil Tillage Res. 192, 87–94 (2019).

227. Meegoda, J. N., Li, B., Patel, K. & Wang, L. B. A review of the processes, parameters, and optimization of anaerobic digestion. Int. J. Environ. Res. Public Health 15, (2018).

228. Buswell, A. M. & Boruff, C. . The relation between the chemical composition of organic matter and the quality and quantity of gas produced during sludge digestion. Sewage Work. J. 454–460 (1932).

229. Rabii, A., Aldin, S., Dahman, Y. & Elbeshbishy, E. A review on anaerobic co-digestion with a focus on the microbial populations and the effect of multi-stage digester configuration. Energies 12, (2019).

230. Zhang, J., Loh, K. C., Lee, J., Wang, C. W., Dai, Y., Tong, Y. W., Three-stage anaerobic co-digestion of food waste and horse manure. Sci. Rep. 7, 1–10 (2017). doi:10.1038/s41598-017-01408-w

231. Haugen, F., Bakke, R., Lie, B., Hovland, J. & Vasdal, K. Optimal design and operation of a UASB reactor for dairy cattle manure. Comput. Electron. Agric. 111, 203–213 (2015).

232. Gibson, A. M., Bratchell, N. & Roberts, T. A. The effect of sodium chloride and temperature on the rate and extent of growth of Clostridium botulinum type A in pasteurized pork slurry. J. Appl. Bacteriol. 62, 479–490 (1987).

233. Tjørve, K. M. C. & Tjørve, E. The use of Gompertz models in growth analyses, and new Gompertz-model approach: An addition to the Unified-Richards family. PLoS One 12, 1–17 (2017).

234. Kafle, G. K. & Chen, L. Comparison on batch anaerobic digestion of five different livestock manures and prediction of biochemical methane potential (BMP) using different statistical models. Waste Manag. 48, 492–502 (2016).

235. Etuwe, C. N., Momoh, Y. O. L. & Iyagba, E. T. Development of Mathematical Models and Application of the Modified Gompertz Model for Designing Batch Biogas Reactors. Waste and Biomass Valorization 7, 543–550 (2016).

236. Arreola-Vargas, J., Flores-larios, A., M, H. O. & Corona-Gonzalez, R. I. Single and two-stage anaerobic digestion for hydrogen and methane production from acid and enzymatic hydrolysates of Agave tequilana bagasse. International Journal of Hydrogen Energy 41, 897-904 (2016).

237. Pan, J., Ma, J., Liu, X., Zhai, L., Ouyang, X., Liu, H. Effects of different types of biochar on the anaerobic digestion of chicken manure. Bioresour. Technol. 275, 258–265 (2019).

238. Huo, Z., Fang, Y., Yao, G., Zeng, X., Ren, D., Jin, F. Improved two-step hydrothermal process for acetic acid production from carbohydrate biomass. J. Energy Chem. 24, 207–212 (2015).

239. Zhang, L., Ouyang, W. & Lia, A. Essential Role of Trace Elements in Continuous Anaerobic Digestion of Food Waste. Procedia Environ. Sci. 16, 102–111 (2012).

240. Müller, T., Walter, B., Wirtz, A. & Burkovski, A. Ammonium Toxicity in Bacteria Ammonium Toxicity in Bacteria. (2006). doi:10.1007/s00284-005-0370-x

241. Jiang, Y., McAdam, E., Zhang, Y., Heaven, S. Ammonia inhibition and toxicity in anaerobic digestion: A critical review. J. Water Process Eng. 32, 1–34 (2019).

242. Yenigün, O. & Demirel, B. Ammonia inhibition in anaerobic digestion: A review. Process Biochem. 48, 901–911 (2013).

243. Sun, C., Cao, W., Banks, C. J., Heaven, S. & Liu, R. Biogas production from undiluted chicken manure and maize silage: A study of ammonia inhibition in high solids anaerobic digestion. Bioresour. Technol. 218, 1215–1223 (2016).

244. Smith, K. A. & Williams, A. G. Production and management of cattle manure in the UK and implications for land application practice. Soil Use Manag. 32, 73–82 (2016).

245. Petersen, S. O., Blanchard, M., Chadwick, D., Prad, A. D., Eduoard, N., Mosquera, J., Sommer, S. G. Manure management for greenhouse gas mitigation. Animal 7, 266–282 (2013).

246. Scott, A. & Blanchard, R. The Role of Anaerobic Digestion in Reducing Dairy Farm Greenhouse Gas Emissions. (2021).

247. Zhou, J. M. The Effect of Different C/N Ratios on the Composting of Pig Manure and Edible Fungus Residue with Rice Bran. Compost Sci. Util. 25, 120–129 (2017).

248. Seaman, A. Production Guide for Organic Cole Crops. New York State IPM Publication (2012).

249. Yan, M., Fotidis, I. A., Tian, H., Khoshnevisana, B., Treu, L., Tsapekos, P., Angelidaki, I. Acclimatization contributes to stable anaerobic digestion of organic fraction of municipal solid waste under extreme ammonia levels: Focusing on microbial community dynamics. Bioresour. Technol. 286, 121376 (2019).

250. Morozova, I., Nikulina, N., Oechsner, H., Krümpel, J. & Lemmer, A. Effects of Increasing Nitrogen Content on Process Anaerobic Digestion. Energies 13, 1139 (2020).

251. González, J., Sánchez, M. & Gómez, X. Enhancing Anaerobic Digestion: The Effect of Carbon Conductive Materials. Journal of Carbon Research 4, 59 (2018).

252. Cruz Viggi, C., Simonetti, S., Palma, E., Pagliaccia, P., Braguglia, C., Faz, S., Baronti, S., Navrarra, M., Pettiti, I., Koch, C., Harnish, F., Aulenta, F. Enhancing methane production from food waste fermentate using biochar: The added value of electrochemical testing in pre-selecting the most effective type of biochar. Biotechnol. Biofuels 10, 1–13 (2017).

253. Jin, H., Sun, E., Xu, Y., Guo, R., Zheng, M., Huang, H., Zhang, S. Hydrochar derived from anaerobic solid digestates of swine manure and rice straw: A potential recyclable material. BioResources 13, 1019–1034 (2018).

254. Gregory, K. B., Bond, D. R. & Lovley, D. R. Graphite electrodes as electron donors for anaerobic respiration. Environ. Microbiol. 6, 596–604 (2004).

255. Summers, Z. M., Fogarty, H. E., Leang, C., Franks, A. E., Malvankar, N. S., Lovely, D.R. Direct exchange of electrons within aggregates of an evolved syntrophic coculture of anaerobic bacteria. Science 330, 1413–1415 (2010).

256. Morita, M., Malvankar, N., Franks, A., Summers, Z., Giloteaux, L., Rotaru, A., Rotaru, C., Lovely, D. Potential for Direct Interspecies Electron Transfer in Methanogenic. MBio 2, 5–7 (2011).

257. Zhao, Z., Zhang, Y., Wang, L. & Quan, X. Potential for direct interspecies electron transfer in an electric-anaerobic system to increase methane production from sludge digestion. Sci. Rep. 5, 1–12 (2015).

258. Wu, B., Yang, Q., Yao, F., Chen, S., He, L., Hou, K., Pi, Z., Yin, H., Fu, J., Wang, D., Li, X. Evaluating the effect of biochar on mesophilic anaerobic digestion of waste activated sludge and microbial diversity. Bioresour. Technol. 294, (2019).

259. Zhang, M., Li, J., Wang, Y. & Yang, C. Impacts of different biochar types on the anaerobic digestion of sewage sludge. RSC Adv. 9, 42375–42386 (2019).

260. Ren, S. et al. Hydrochar-Facilitated Anaerobic Digestion: Evidence for Direct Interspecies Electron Transfer Mediated through Surface Oxygen-Containing Functional Groups. Environ. Sci. Technol. 54, 5755–5766 (2020).

261. Yu, Q., Usman, M., Tsang, C.W., O'thong, S., Angelidaki, I., Zhu, X., Zhang, S., Luo, G. Effectiveness and mechanisms of ammonium adsorption on biochars derived from biogas residues. RSC Adv. 6, 88373–88381 (2016).

262. Montalvo, S., Guerrero, L., Borja, R., Sanchez, E., Milan, Z., Cortes, I., de la Rubia, M. A. Application of natural zeolites in anaerobic digestion processes: A review. Appl. Clay Sci. 58, 125–133 (2012).

263. Angelidaki, I., Petersen, S. P. & Ahring, B. K. Effects of lipids on thermophilic anaerobic digestion and reduction of lipid inhibition upon addition of bentonite. Appl. Microbiol. Biotechnol. 33, 469–472 (1990).

264. Begum, S. A., Golam Hyder, A. H. M., Hicklen, Q., Crocker, T. & Oni, B. Adsorption characteristics of ammonium onto biochar from an aqueous solution. J. Water Supply Res. Technol. - AQUA 70, 113–122 (2021).

265. Takaya, C. A., Fletcher, L. A., Singh, S., Anyikude, K. U. & Ross, A. B. Phosphate and ammonium sorption capacity of biochar and hydrochar from different wastes. Chemosphere 145, 518–527 (2016).

266. Li, N., Ma, X., Zha, Q., Kim, K., Chen, Y., Song, C. Maximizing the number of oxygen-containing functional groups on activated carbon by using ammonium persulfate and improving the temperature-programmed desorption characterization of carbon surface chemistry. Carbon N. Y. 49, 5002–5013 (2011).

267. Zhang, X., Gao, B., Fang, J., Zou, W., Dong, L., Cao, C., Zhang, J., Li, Y., Wang, H. Chemically activated hydrochar as an effective adsorbent for volatile organic compounds (VOCs). Chemosphere 218, 680–686 (2019).

268. Mumme, J., Srocke, F., Heeg, K. & Werner, M. Bioresource Technology Use of biochars in anaerobic digestion. Bioresour. Technol. 164, 189–197 (2014).

269. Ramírez-Montoya, L. A., Hernández-Montoya, V., Montes-Morán, M. A. & Cervantes, F. J. Correlation between mesopore volume of carbon supports and the immobilization of laccase from Trametes versicolor for the decolorization of Acid Orange 7. J. Environ. Manage. 162, 206–214 (2015).

270. Berge, N. D., Li, L., Flora, J. R. V. & Ro, K. S. Assessing the environmental impact of energy production from hydrochar generated via hydrothermal carbonization of food wastes. Waste Manag. 43, 203–217 (2015).

271. Coyte, K. Z., Tabuteau, H., Gaffney, E. A., Fostera, K. R. & Durham, W. M. Microbial competition in porous environments can select against rapid biofilm growth. Proc. Natl. Acad. Sci. U. S. A. 114, E161–E170 (2017).

272. Saba, A., McGaughy, K. & Toufiq Reza, M. Techno-economic assessment of co-hydrothermal carbonization of a coal-Miscanthus blend. Energies 12, 1–17 (2019).

273. Masoumi, S., Borugadda, V. B., Nanda, S. & Dalai, A. K. Hydrochar: A review on its production technologies and applications. Catalysts 11, (2021).

274. Owsianiak, M., Brooks, J., Renz, M. & Laurent, A. Evaluating climate change mitigation potential of hydrochars: compounding insights from three different indicators. GCB Bioenergy 10, 230–245 (2018).

275. Malghani, S. et al. Carbon sequestration potential of hydrothermal carbonization char (hydrochar) in two contrasting soils; results of a 1-year field study. Biol. Fertil. Soils 51, 123–134 (2015).

276. Hoffmann, V., Jung, D., Zimmermann, J., Correa, C., Elluech, A., Halouani, K., Kruse, A. Conductive carbon materials from the hydrothermal carbonization of vineyard residues for the application in electrochemical double-layer capacitors (EDLCs) and direct carbon fuel cells (DCFCs). Materials 12, (2019).

277. Błońska, E., Lasota, J. & Gruba, P. Enzymatic activity and stabilization of organic matter in soil with different detritus inputs. Soil Sci. Plant Nutr. 63, 242–247 (2017).

278. Schulze, M., Mumme, J., Funke, A. & Kern, J. Effects of selected process conditions on the stability of hydrochar in low-carbon sandy soil. Geoderma 267, 137–145 (2016).

Chapter 3: Methodology & Material Characterisation

Abstract

The objective of this research is to evaluate the solid residue from biorefinery catalysis for the promotion of anaerobic digestion as well as the quantification and characterisation of solid residue under different catalysis regimes. This research is primarily quantitative, utilising a variety of standard methodologies and developed methodologies. This includes sample preparation, catalysis process conditions, data collection and data analysis used in this thesis. The methodologies are used to investigate homogenous and heterogeneous catalysis of multiple lignocellulosic biomass types under microwave heating with detailed quantitative liquid analysis with HPLC. Post-catalysis solid residues are characterised with a range of techniques including but limited to EDX, SEM, TGA, XRF and FTIR. The application of solid residue as an anaerobic digestion adsorptive supplement is described in detail in accordance with standard methods. All data collected in this thesis followed the ethical approval process as per MMU guidance.

3.1 Introduction

The previous chapter discussed the theoretical and empirical literature relevant to this thesis with regards to solid residues from lignocellulosic catalysis with homogenous and heterogeneous catalysis for their application as a supplement for the promotion of anaerobic digestion. In this chapter, the methodologies used for biomass characterisation, biomass catalysis, analytical methods, solid residue characterisation, statistical methods and anaerobic digestion have been explained in detail, including materials and equipment used. The methodology consists of a mixture of standard operating procedures and modified methods developed specifically for this project. Therefore, were appropriate design choices have been specified and justified.

3.2 Chemicals

Sulphuric acid (Acros 96%), hydrochloric acid (Primar Plus Trace Analysis ~37%) and nitric acid (Primar Plus Trace Analysis ~67%) were acquired from Fischer Scientific. Analytical standards of celliobiose (98.0% +), glucose (99.5% +), fructose (99.0% +), xylose (99.0% +), formic acid (99.5% +), acetic acid (99.5% +), levulinic acid (98.0% +), 5-HMF (99.0% +) and furfural (99.0% +) were purchased from Sigma-Aldrich. Ethylenediaminetetra-acetic acid (EDTA) elemental standard was sourced from Elementar. HPLC standards were prepared with Grade 1 deionised water and Grade 2 deionised water was used for all catalysis reactions. Lignocellulosic biomass samples of poplar wood, SRC willow, hemp husk, wheat straw, barley straw and three varieties of *Miscanthus x Giganteus* were collected from UK suppliers and discussed in Chapter 4. Sulphated zirconium catalyst was kindly provided by Drochaid Research Limited.

3.3 Biomass Characterisation

3.3.1 Biomass Sample Preparation and Moisture Content

It was critical to prepare the lignocellulosic feedstocks for both characterisation and catalysis while also maintain sample stability over a long-time frame. The biomass samples upon collection were immediately dried at 105 °C overnight to evaluate moisture content as received, which was calculated using *Equation 3.1*.

$$Mositure\ Content\ (wt.\%) = \frac{wet\ weight\ (g) - dry\ weight\ (g)}{wet\ weight\ (g)}\ x\ 100$$

Equation 3.1

After drying the samples were size reduced and homogenised with a Retsch ZM200 ball mill to a fine powder (<1mm). The effect of ball milling has been found to reduce biomass crystallinity by breaking down macroscopic structures, which can significantly improve cellulose hydrolysis [1,2]. Commercial scale biorefineries may not use such fine ball milling procedures and it may affect the post catalysis solid residue properties. However, due to the small scale lab reactors, larger particles sizes would increase the difficulty of suspending the solids in aqueous media which would significantly affect the catalysis set-up. Therefore, a 1 mm grate was used during ball milling, which has been used extensively in other works [3–5]. After size reduction, the biomass samples were stored in airtight containers for long term storage.

3.3.2 Ash Quantification

The total amount of inorganic material in lignocellulosic biomass was conducted in accordance to the US National Renewable Energy Laboratory (NREL) method "Standard Method for Ash in Biomass" [6]. In which the samples were dried overnight at 105 °C in a drying oven to achieve constant weight and remove residual water content. Before, ashing using a carbolite furnace at 550 °C, with marked porcelain crucibles for 6 hours. Biomass samples were conducted in triple replication with a 300 ± 10 mg sample size and the ash content calculated according to *Equation 3.2*. The results were presented as an average of the three replicates and error bars were calculated using the excel function "STDEV.S". The ash content was used to estimate the volatile solids content according to *Equation 3.3.*

$$Ash\ Content\ (wt.\%) = \frac{initail\ weight\ (g) - final\ weight\ (g)}{initial\ weight\ (g)}\ x\ 100$$

Equation 3.2

$$Volatiles\ Solids\ (VS)\ (\%) = 1 - Ash\ content$$

Equation 3.3

3.2.3 Biomass Extractives

It is necessary to remove non-structural material from biomass to reduce interference in later analytical steps for characterisation, therefore the extractable biomass content was quantified in accordance with the NREL method "Determination of Extractives in Biomass" [7]. This involved a twostep process to remove water and ethanol soluble compounds, which can include proteins, non-structural sugars and inorganic material. A Dionex ASE 350 solvent extractor was used with stainless steel flasks in

combination with analytical grade ethanol and deionised water solvents. The analysis was competed in triplicate with 100 ± 10 mg of dried biomass and the results were calculated using *Equation 3.4* on a dry weight basis. The composition of the water and ethanol extractives were not analysed in this study.

$$Extractives\ (wt.\%) = \frac{initail\ weight\ (g) - final\ weight\ (g)}{initial\ weight\ (g)}\ x\ 100$$

Equation 3.4

3.3.4 CHNO Elemental Analysis

The absolute CHNO elemental analysis of biomass was conducted using a VARIO CHNO MACRO cube in accordance with European Standard EN 15104:2011. The elemental analysis utilised the complete combustion of 50 ± 1 mg dried samples at 1100 °C with excess oxygen, combined with gas chromatography using a thermal conductivity detector. The system was calibrated using ethylenediaminetetra-acetic acid (EDTA) analytical standard [1] and adjusted for baseline interference. The carbon, hydrogen and nitrogen fractions were directly quantified while oxygen content was calculated by difference according to *Equation 3.5*.

$$Oxygen\ (wt.\%) = 100 - C\ (wt.\%) - H(wt.\%) - N(wt.\%) - S(wt.\%) - Ash\ (wt.\%)$$

Equation 3.5

[1] 41.09 ± 0.23 wt.% Carbon, 5.51 ± 0.05 wt.% Hydrogen, 9.56 ± 0.14 wt.% Nitrogen

The Higher heating Value (HHV) was estimated using *Equation 3.6*, where C, H, N, O, A represent the weight percentages of carbon, hydrogen, sulphur, oxygen and ash of the sample respectively, according Channiwala and Parikh [8]. The O/C and H/C ratios were calculated on a molar basis.

$$\mathrm{HHV_{predicted}(MJ\ kg^{-1})} = 0.3491\ (\mathrm{C}) + 1.1783(\mathrm{H}) + 0.1005(\mathrm{N}) - 0.1034\ (\mathrm{O}) - 0.0015(\mathrm{A})$$

Equation 3.6

3.3.5 Structural Sugar and Lignin Analysis

The structural polysaccharide matric of cellulose, hemicellulose and lignin was quantitatively evaluated using the NREL method "Determination of Structural Carbohydrates and Lignin in Biomass" [9]. The procedure is suitable for a range of cellulosic feedstocks that do not contain extractives and have ash contents below <10 wt.%. The methodology involved a two-stage acid digestion process. First a digestion was performed at 30 °C for 1 hour with 86 wt.% sulphuric acid conducted using a water bath with frequent stirring, followed by 120 °C autoclave assisted digestion for 1 hour and dilution to 3 wt.% acid, for a near complete hydrolysis of structural sugars to monomeric sugars with minimal sugar degradation. The resulting hydrolysate was measured for celliobiose, fructose, glucose, mannose, galactose, rhamnose, xylose and arabinose using a Dionex ICS-3000 ion-chromatography set-up with a pulsed amperometric detector (PAD). The presence of celliobiose or peaks eluting before celliobiose indicate incomplete hydrolysis and over-hydrolysis respectively. The methodology was completed in triplicate using 300 ± 10 mg of samples.

In addition to structural sugars the acid-soluble and acid insoluble-lignin were also measured. Acid-soluble lignin was measured using UV- absorptivity at 240 nm in

accordance with the recommended NREL absorptivity constants. The acid-insoluble lignin, also known as Klason Lignin, was calculated by the collection of the post hydrolysis residue, drying at 105 °C overnight and subsequent ashing at 550 °C for 6 hours.

3.3.6 Cellulose Crystallinity Index

Crystallographic information about the biomass cellulose crystallinity was obtained using X-Ray Dispersive Diffraction (XRD) with a Panalytical X'pert diffractometer. Operated at 45 kV and 40 mA accelerating voltage and applied current respectively with CuKα1 radiation at 0.154 nm over the range of 20 to 80° 2θ. The cellulose Crystallinity Index (CI) in % of the samples was calculated XRD height method as per *Equation 3.7* by Segal et al [10].

$$CI(\%) = \frac{I_{002} - I_{am}}{I_{002}} x100 \qquad \textit{Equation 3.7}$$

where I_{002} is the intensity of the diffraction at 002 peak position ($2\theta \approx 22.5°$) for cellulose and I_{am} is the peak for the amorphous region at about $2\theta \approx 17.9°$.

3.4 Microwave Catalysis

Microwave catalysis was conducted using two different microwave reactors with different operating procedures in this thesis. An Anton-Parr Monowave 300 microwave reactor was used in Chapter 4 and a CEM MARS 5 Express microwave reactor was used for Chapters 5 & 6.

3.4.1 Anton Parr Monowave 300

The Anton Parr Monowave 300 was used for the sulphuric acid catalysis of poplar wood using 30 borosilicate reactors, shown in Figure 3.1. The system is equipped with an infrared temperature sensor that measured the reaction temperature from outside the reaction vessel. Previous work by Sweygers *et al.* [11] found the microwave reactor model achieved temperatures of 200 °C in less than 2 minutes. The borosilicate vessels are microwave transparent and were operated at a recommended operating volume of 6 ml, which was used in all reaction conditions. The system includes a magnetic stirrer bar placed at the bottom of the reaction vessel with a variable speed which was defined at 600 rpm for all reaction to achieve complete material suspension. The reaction vessels were sealed PEEK caps with Teflon coated silicone seals, which were pressurised with compressed air.

Figure 3.1: A) Anton Paar Monowave 300, B) 30 ml borosilicate reaction vessel

The maximum operating pressure was 30 bar which corresponds with a steam pressure of 230 °C and was the main operating constraint for the system. The microwave reactor included a detailed control panel that was used to set the operating conditions with an air-cooling system that cooled the reaction vessel to < 50 °C in 3-4 minutes.

A typical reaction involved the addition of 0.15g of feedstock to 6 ml of aqueous material to achieve a solids loading of 2.5 wt.%, which was calculated using *Equation 3.8*. The catalysis operating parameters varied were reaction temperature (°C), reaction time (minutes) and catalyst concentration (M).

$$Solids\ loading\ (wt.\%) = \frac{Mass\ of\ feedstock\ (g)}{Volume\ of\ liquid\ (ml)} \qquad \textit{Equation 3.8}$$

3.4.2 CEM MARS 5 Express Reactor

Due to the small size of the Monowave 300 and low production yield of solid residue, the use of a larger microwave reactor was necessary to make sufficient solid residue for more detailed characterisation and applications in anaerobic digesters. The MARS CEM 5 Express, shown in Figure 3.2, consists of a rotating turntable consisting (15 rpm) that can load up to 40 reactions vessels. The system includes 3 infrared temperature sensors to determine the average reaction temperature. The 50 ml reaction vessels are made from microwave transparent PerFluoroAlkoxy (PFA) with a screw lock vessel cap. The vessel cap is specified to 20 bar operating pressure, which corresponds with a steam pressure of ~210 °C, after which the reaction vessel would vent. Before and after the microwave process, each microwave reactor was weighed to evaluate any potential reaction venting.

Figure 3.2: A) CEM MARS 5 Express Reactor, B) 50 ml PFA Reaction vessel

A typical microwave reaction utilised 0.5 g of feedstock in 10 ml of liquid for a solids loading of 5 wt.%, calculated using *Equation 3.8*. With the ability of conducting several reactions simultaneously in a single batch, the MARS CEM 5 was able to produce significantly more solid residue (to be used in subsequent AD fermentative trials) at the expense of detailed temperature control. The catalysis operating parameters varied were reaction temperature (°C), reaction time (minutes) and catalyst concentration. For the heterogeneous catalysis of the lignocellulosic biomass described in Chapter 6, the catalyst to biomass ratio (CBR) was calculated according to *Equation 3.9*.

$$CBR = \frac{Mass\ of\ catalysts\ (g)}{Mass\ of\ biomass\ (g)} \qquad \textit{Equation 3.9}$$

3.4.3 Post Reaction Hydrolysate and Solids Separation

Regardless of the microwave reactor used, the post reaction methodology for hydrolysate and solids separation was conducted as follows. Post reaction, the reaction vessels were allowed to cool to room temperature prior to vacuum filtration.

This used a Buchner funnel configuration, with Fisherbrand 2 µm pre-weighed cellulose filter paper. The liquid fraction was further filtered with a 0.2 µm micro-filter before freezing for later HPLC analysis. All solids were removed from the reaction vessel using deionised water and a minimum of 500 ml of deionised water was used to rinse the filter paper of the homogenous catalysts, following the steps described in Figure 3.3. The solid residue laden filter paper was then oven-dried overnight at 60 °C to minimise filter paper degradation, after which it was weighed and the solid residue yield was calculated using *Equation 3.10*. For the determination of solid residue yields with heterogeneous catalysts, it was assumed that 100% of the catalyst was recovered. The dry solid residue was then stored in airtight containers for further characterisation.

$$Solids\ yield\ (wt.\%) = \frac{Filter\ paper\ with\ solid\ residue\ (g) - dry\ filter\ paper\ (g)}{Mass\ of\ catalysis\ feedstock\ (g)}$$

Equation 3.10

The dry filter paper weights were individually determined through oven-drying over 3-4 days at 60 °C, with daily weight recordings until a constant value was achieved. The dried filter paper was then stored in airtight containers until use. The stable weight of the cellulose filter paper was found to vary by ± 2.0 mg, which introduced a potential source of random error. The latter was minimised by triple replication on all catalysis conditions.

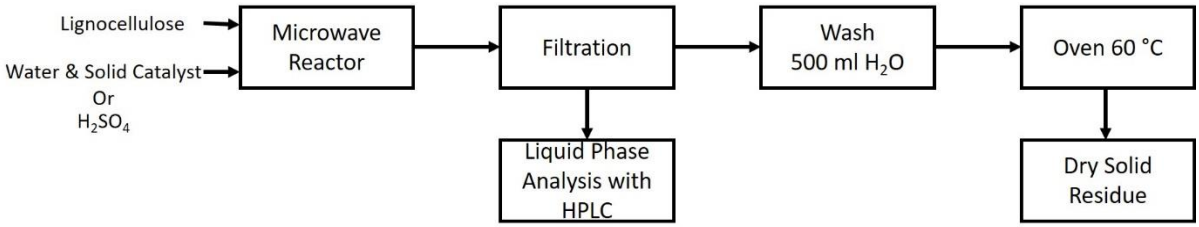

Figure 3.3: Post-catalysis separation and drying process

3.5 HPLC Method

3.5.1 HPLC System

High Performance Liquid Chromatography (HPLC) was used to measure post reaction hydrolysate for organic acids and sugars, using an HP-1100 HPLC with an Agilent 1200 refractive index detector (RID) and HP1100 ultraviolet diode array (UV-DAD). A packed polymer Bio-Rad Aminex HPX-87H column, compromised of sulfonated 8% cross-linked divinyl-styrene hydrogen ionic form was used in all HPLC analysis. The column was used for the separation of various compounds, including celliobiose, glucose, xylose, acetic acid, formic acid, levulinic acid, 5-HMF and furfural in ascending elution times, as shown in Table 3.1. The column and RID temperatures were maintained at 55 ˚C and 5 mM H_2SO_4 eluent was used as the mobile phase with the flowrate maintained at 0.6 ml/min. A polymer de-ashing guard column was attached upstream the main column to reduce ion interference in the separation process.

Table 3.1: HPLC standards and elution Times

Compound	Expected Retention time (min)	Standards Range (mM)
D-(+)- Celliobiose	7.4	1 – 100
D (+) Glucose	8.9	1 – 250
D (+) Fructose	9.6	1 – 100
D (+) Xylose	10.6	1 - 200
Formic Acid	14.1	1 – 100
Acetic Acid	15.4	1 – 100
Levulinic Acid	16.7	1 – 100
5-HMF	136.	1 – 100
Furfural	54.0	1 – 100

In Chapters 5 and 7 only the RID detector¸ which is considered a universal detector, was utilised. While Chapter 6 used exclusively UV-DAD set at the wavelengths of 266 nm for the detection of levulinic acid and 5-HMF, as well as 288 nm for the detection

of furfural [12]. The differences in HPLC methodology used are due RID equipment issues, therefore the UV-DAD was used instead as substitute detector. For both detectors, a series of 5 standards was used to create linear calibration curves to calculate the mM concentration of each compound.

3.5.2 Yield Calculations

Using the given HPLC-derived concentrations the weight percentage yield, Y, of each compound was calculated using *Equation 3.11.*

$$Y_{product} = \frac{Product\ concentration\ (mM)\ x\ volume\ of\ solvent\ (ml)}{dry\ mass\ of\ reactant\ (mg)}\ x\ 1000$$

Equation 3.11

The yield of levulinic acid is more commonly reported as the theoretical molar yield based on the cellulose content according to *Equation 3.12*. Unless stated otherwise % levulinic acid yields are stated as mol.% yields

$$Theoretical\ levulinic\ acid\ yield = \frac{Y_{levulinic\ acid\ (wt\%)}}{cellulose\ content\ (wt.\%) * \frac{Mr\ of\ Levulinic\ ACid}{Mr\ of\ Glucose}}$$

Equation 3.12

For the evaluation of formic acid degradation, the net formic acid yield was calculated by considering, a stoichiometric formation of 1:1 molar levulinic to formic acid yield, with observed formic acid yield. As per *Equation 3.13*

$$Y_{Net\ Formic\ Acid} = Y_{Formic\ Acid} - Y_{Levuulinic\ acid} * 46.06/116.11$$

Equation 3.13

Where; Mr of levulinic acid = 116.11 g/mol and Mr of formic acid = 46.06 g/mol

3.6 Solid Residue Characterisation

3.6.1 Solid Residue Preparation

The labelled solid residue-laden filter papers were stored in airtight containers post reaction until further analysis. Caution was taken to minimise contamination of the solid residue and filter paper when manually separated. Due to the low absolute solids yield, several replicates of the same reaction conditions were mixed to achieve sufficient weight to enable characterisation. To obtain sufficient weight, 5-8 replicates were required using the Monowave 300 reactor and 2-3 with the CEM MARS 5 reactor. Once separated the solid residue was characterised through compositional and structural analysis methods, described in sections 3.6.2 and 3.6.3

The separation of solid residue and heterogeneous catalyst was revealed to be more challenging, due to the differences in particle size between the two components, however it was possible to conduct size separation. The solid residue and heterogeneous catalyst were separated by size using 68 µm and 125 µm mesh screens, using a vibrating sieve shaker, with the <68 µm and >125 µm fractions corresponding with the recycled catalyst and solid residue respectively. This method resulted in two high quality fractions, containing 80%+ of each component and was also validated using XRF to trace the catalyst content.

3.6.2 Compositional Solid Residue Characterisation

The ash content and CHNSO elemental composition were evaluated using the equivalent biomass methods described in sections 3.3.2 and 3.3.4 respectively. The surface elemental composition was measured using energy-dispersive X-ray

spectroscopy (EDX), utilising an AMTEK EDAX TSL. The EDX scanned particle areas of ~0.25 mm^2 and three replications were conducted across each sample to derive a representative average. The bulk heavy metal composition was measured using X-ray Fluorescence spectrometry (XRF) energy conducted using a Rigaku NEX-CG with 1.0 g samples.

3.6.3 Structural Solid Residue Characterisation

The post reaction CI index of the solid residues was calculated using the method described in 3.2.6. The specific surface areas of the samples (catalyst and solid residue) were determined with a Micrometrics ASAP2020 surface area analyser. In detail, samples were degassed for 12 h at 150 °C prior to analysis and surface areas were calculated from nitrogen adsorption data at -196 °C, in the range of relative pressures between 0.05 and 0.3 using the BET model. Total pore volumes were determined from the measurements at p/p_0 of 0.99 using a density conversion factor of 0.001547. External surface areas and micropore areas were determined by the t-lot method. Pore size distributions were calculated based on the Barrett, Joyner, and Halenda (BJH) model from the adsorption branch of the isotherms.

Fourier-Transform-Infrared (FTIR) Spectroscopy was conducted with a Perkin Elmer Spectrum Two, using 16 scans with a resolution of 4 cm^{-1}. For each sample, two spectra were obtained from different subsamples and averaged to give the presented data. Background noise was minimised with background baseline adjustment every 5 minutes. Peak identification was conducted manually using standard reference tables [13]. Surface morphology was evaluated using Scanning Electron Microscopy (SEM) with a Carl Zeiss Supra 40VP-FEG Surface Electron Microscope under a partial

pressure. Thermal Gravimetric Analysis (TGA) was conducted using a TA Instrument SDT Q50 at 10 ˚C /min to 900 ˚C in a nitrogen atmosphere.

3.6.4 Catalyst Characterisation

The catalyst acidity was determined by temperature Programmed Desorption of Ammonia (NH3-TPD) and tests were carried out on a Micromeritics 2920 equipment, which is equipped with a TCD detector and coupled to a Balzers Thermostar quadrupole mass spectrometer. The sample (~80mg) is pretreated under a flow of 50 mL/min argon at 120 °C (5 °C/min) for 30 min and then at 500°C (5°C/min) for 20 min. The sample is then cooled down to 100°C, the argon flow switched to 5% NH_3/H_2 and allowed to interact for 1 hour at 100°C. Subsequently, the system is flushed with helium (before starting the TPD experiment). The sample is then heated up to 500°C (10°C/min) and the effluent gas is monitored by MS and TCD. Acidity is measured based on the TCD detector signal. EDX, SEM, TGA, BET, FTIR and ash content of the catalyst were conducted using the same methods as the solid residue characterisation, as described in Section 3.6.2.

3.7 Statistical Method Design

3.7.1 Response Surface Methodology

The catalysis operating parameters were optimised using Response Surface Methodology (RSM), for its wide ability to simultaneously model multiple parameters that do not adhere to standard reaction kinetics, primarily the solid residue formation mechanisms. As the solid residue yield minimisation was the target objective of the optimisation process and to maintain commonality between by-product and platform chemical production, the RSM method was used to identify and derive all optimised product yields post reaction.

RSM utilises mathematical and statistical techniques for modelling and predicting one or more responses “y” of interest to several input variables “χ” (from level i to j). Ideal reaction conditions can be retrieved from the model by fitting data from each experimental set into a second-order polynomial model as per *Equation 3.14:*

$$Y = \beta_0 + \sum_{i=1}^{n} \beta_i X_i + \sum_{i=1}^{n} \beta_{ii} X_i^2 + \sum_{i}^{n} \sum_{j>1}^{n} \beta_{ij} X_i X_j$$

Equation 3.14

where Y is the predicted response, $ß_0$, $ß_i$, $ß_{ii}$ and $ß_{ij}$ are regression coefficients and n is the number of the experiments conducted. Second order polynomials are sufficient to approximately model chemical reaction processes and physical transformation mechanisms within bounded spaces [3,14,15].

To reduce model overfitting, the sequential F-test, lack-of-fit test and other adequacy measures were used to not only select the best model, but also to reduce unnecessary polynomial variables. This was achieved through analysis of variance (ANOVA) to

evaluate individual terms with an interval of confidence α=0.1 applied to estimate the significance of the model and each of the model terms (Prob. F<p-value). A p-value less than 0.05 was considered statically significant and the p-value are reported accordingly for all variables. The software package Design Expert 11.0 was used to conduct all statistical analysis and generate graphical models.

3.7.2 Design of Experiments

Design of Experiments (DOE) is a powerful data collection and analysis tool that can be used in a variety of experimental situations. In which, the order of variation of experimental parameters are systematically varied to generate an unbiased set of experiments that equally evaluate all parameters within a given range. The use of experimental design reduces the number of experimental points required to generate statistically significant quadratic RSM models compared with a full factorial investigation.

The Box-Behnken experimental design was devised George E.P. Box and Donald Benkhen in 1960 [16] and is a reduced DOE system that has successfully been used to model both platform chemical yields and hydrochar formation [3,14,17]. All variables are encoded as either; -1, 0 or +1 to create three levels for each variable, in which two variables are evaluated simultaneously. Box-Behnken methodology uses a randomised run order and estimates the model variance using 5 replications of the central point. For a given the 3-factor model, this reduces the number of experimental points to 10 in addition to the central point, compared with 18 and 27 for central composite designs or full factorial respectively. The Box-Behnken DOE was created using Design Expert 11.0.

3.8 Anaerobic Digestion

3.8.1 Inoculum Sludge & Characterisation

Anaerobic digestion inoculum was obtained a local brewery's upflow anaerobic sludge bed (UASB) reactor, which was the seed material for all microbial communities. The UASB was operated under mesophilic conditions of 31 ± 1°C and the sludge was collected on the same day of use. As to reduce microbial shock due to temperature change, all anaerobic digestion experiments were conducted at 31 °C, as recommended as part of the German VDI 4630 procedure for AD [18]. All methodologies were in accordance with a 14-day AD procedure. After 14-days the daily CH_4 was less than 1% of the cumulative CH_4 yields validating the experiment length [19].

The anaerobic digestion sludge was characterised using several methods. The Total Solids (TS) content was determined by drying 200 g of sludge in triplicate overnight at 105 °C using *Equation 3.15*. The dried sludge solids were further characterised for ash content and volatile solids as per section 3.2.2 and elemental composition according to section 3.2.4, with a 50 mg sample size and 5 replications. Elemental composition percentages from the ultimate analysis were used to derive the theoretical stoichiometric methane potential (SMP) by means of the well-known stoichiometric Buswell Equation, *Equation 3.16* [20].

$$Total\ Solids\ (wt.\%) = \frac{Dry\ solids\ (g)}{Wet\ sludge\ (g)} \qquad \textit{Equation 3.15}$$

$$C_cH_hO_oN_nS_s + \left(c - \frac{h}{4} - \frac{o}{2} + \frac{3n}{4} + \frac{s}{2}\right)H_2O \rightarrow \left(\frac{c}{2} + \frac{h}{8} - \frac{o}{4} - \frac{3n}{8} - \frac{s}{4}\right)CH_4 + \left(\frac{c}{2} - \frac{h}{8} + \frac{o}{4} + \frac{3n}{8} + \frac{s}{4}\right)CO_2 + nNH_3 + sH_2S$$

Equation 3.16

3.8.2 Anaerobic Digestion Apparatus & Methodology

Anaerobic digestion was conducted in 500 ml Erlenmeyer flasks with ground joint straight joint connectors to minimise gas losses. The flasks were connected using PVC piping to aluminium foil biogas bags through a three-way valve, as shown in Figure 3.4a, to allow sampling gas without affecting the anaerobic conditions. The flasks were maintained at a constant temperature using a water bath, heated using a Thermofisher IsoTemp 2100 circulating heater, Figure 3.4b. The temperature was monitored with an additional two digital thermostats to maintain a constant temperature across the water bath. Measurements of the pH of the samples prior to and at the end of the digestion were taken using a Jenway 3510 pH meter.

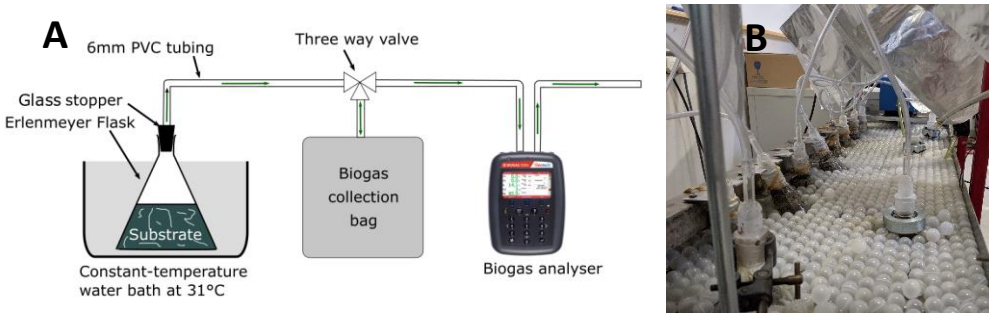

Figure 3.4: A) Schematic of AD system, B) Picture of water bath in operation

A typical anaerobic digestion experiment involved the mixing of 40.0 g of inoculum sludge with 14.0g of chicken manure by the addition of 160.0g of deionised water for a total working volume of approximately 200 ml. The glass vessel was then purged with nitrogen (99 %) for 5 minutes to remove oxygen and then sealed. Each glass vessel was considered an individual bioreactor, with up to 16 reactors operating in parallel or 8 conditions in double replication. The anaerobic digestion was continued for 14-days with daily measurement (excluding weekends) and sampling of the biogas. The volume of biogas contained in each collection bag was determined using an

upturned cylinder and the gas composition was measured using a Geotech Biogas 5000 analyser with a 30 second sample timer. The analyser is equipped with TCD detectors for the vol. % measurement of CH_4, CO_2, H_2S, O_2 and NH_3. All anaerobic digestion experiments were replicated in duplicate. The biodegradability index (BI%) was used to estimate the digestion efficiency and calculated as a % of the SMP yield achieved at the end of the digestion period, refer to *Equation 3.17.*

$$BI\% = \frac{SMP\ (ml\ CH_4) - Actual(ml\ CH_4)}{SMP\ (ml\ CH_4)}\ x100 \qquad \textit{Equation 3.17}$$

3.8.3 Post-Digestion Analytical Methods

At the end of the 14-day digestion the final gas volumes and composition were recorded before freezing the digestate samples. Control reactors composed of only inoculum sludge were conducted in parallel and used to estimate the methane contribution associated with the sludge. The daily methane yield was calculated from the daily methane concentration and total biogas volumes with the cumulative 14-day methane yields referred to as the 14-day bio-methane potential (BMP). The microbial activity was modelled using a modified Gompertz equation by Gibson et al. [21], as shown in *Equation 3.18*.

$$V_{CH4}(t) = A_{max}\exp\left[-\exp\left(\frac{R_{max}*e}{A_{max}}(\lambda - t) + 1\right)\right] \qquad \textit{Equation 3.18}$$

The Gompertz model considers the exponential relationship between the specific growth rate and microbial population density, which was modified to a enzymatic function model that describes cell density in terms of the exponential growth rates and lag phase duration during bacterial growth periods [22]. The cumulative methane yield,

was fitted to *Equation 3.16*, using non-linear regression analysis in Matlab©(2016a) and the statistical fit was evaluated using ANOVA tables. Where, $V_{CH4}(t)$, is the predicted cumulative methane production (mL/g VS) at any time t (day), A_{max} is the measured cumulative methane yield (mL/g VS), R_{max} is the maximum methane production rate (mL/g VS·d), e is the mathematical constant 2.718282, and λ is the lag phase delay (day). The aforementioned parameters enabled the direct comparison of different of conditions at any point over 14 days and better evaluate the effects of solid residue on anaerobic digestion.

After the 14-day digestion the reactor pHs were measured using a Hanna Instruments PH211 calibrated with Fischer Scientific pH 4 and & standards. The ammonium concentration was measured using Ion-Chromatography with a Thermo Scientific ICS5000 using suppressed conductivity detection coupled with a Dionex IonPac CS16 column.

3.8.4 Microbial Analysis Methods

3.8.4.1 Microbial quantification

DNA was extracted from 1 g of sample using the Quick-DNA Fecal/Soil Microbe Miniprep Kit (Zymo Research, Irvine, CA, USA) following the manufacturer's instructions. To determine the abundance of prokaryotic cells in the samples, quantitative PCR (qPCR) was undertaken using SensiFAST Sybr Green Lo-ROX Mix and the MX3000P qPCR System (Agilent Genomics, Headquarters, Santa Clara, CA, United States). The qPCR mix contained universal 16S primers [23] (forward primer and reverse primer both at 25 μM) [23], 2X SensiFAST Sybr Green Lo-ROX Master Mix, molecular grade water and template DNA to a final volume of 12 μl. A standard curve

from known serial dilutions of template DNA (obtained from *Escherichia coli*, NTCT 50167) was constructed and meltcurve analysis corroborated the presence of a single gene-specific peak. The standard curve ranged from 9.4 x 10^3 to 9.4 x 10^8 cells mL^{-1} (5.28x10^{-1} to 5.28x10^{-7} ng DNA mL^{-1}). The cycling conditions consisted of one cycle of denaturation at 94° C for 10 min, followed by 35 three-segment cycles of amplification (94° C for 30 s, 50° C for 30 s and 72° C for 45 s). The baseline adjustment method for the Mx3000 (Agilent) software was used to determine the Ct in each reaction, and the number of cells was obtained by interpolating the Ct value of the unknown samples to the standard curve. Samples were amplified in duplicate, and the mean was used for further analysis. The absolute quantification of the target genes was calculated by the standard-curve (SC) method [24].

3.8.4.2 Microbial composition analysis

Microbial composition was profiled by sequencing the V4 region of the 16S rRNA gene on a MiSeq platform (Illumina, San Diego, CA, United States), using the dual indexing method [25]. The V4 region of the 16S rRNA gene was amplified from each sample using primers 515F and 806R [26] by duplicate by a 2-step PCR. The presence of PCR products was confirmed using 2% (w/v) agarose-TBE gel electrophoresis run for 60 minutes at 90V. Purification of the PCR products was performed using the AMPure XP magnetic beads treatment (Beckman Coulter, Indianapolis, IN, USA) on a ratio of 0.8 and the concentration of PCR purified products was measured using a Qubit 2.0 Fluorometer (ThermoFisher, Scientific). Clean up, normalization, and pooling of the PCR reaction products were performed in one step with SequalPrep Normalization Plates (ThermoFisher Scientific). Raw amplicon sequencing data were processed using the DADA2 pipeline to create amplicon sequence variants (ASVs) present in

each sample [27]. Sequences below 220 bp in length and an average quality score below 30 on a window of 20 bases were discarded. Taxonomy of the ASVs was assigned using a Naive-Bayes approach implemented in the SILVA database [28].

3.8.4.3 Statistical analysis

Experimental bioreactors were run simultaneously in triplicate and values given as means ± 1 standard deviation throughout. All statistical analysis were conducted using parametric tests after visual confirmation that the models conformed to the assumptions, unless otherwise stated in the text. Multivariate models were undertaken using nonmetric multidimensional scaling (NMDS) to separate out microbial communities based on their composition. Differences between the samples were assessed using permutation ANOVA (999 permutations). All diversity metrics (α & β) were calculated, and analysis performed in R (R Core Team, 2017) using the package vegan [30].

3.9 References

1. Jiang, J., Wang, J., Zhang, X. & Wolcott, M. Evaluation of physical structural features on influencing enzymatic hydrolysis efficiency of micronized wood. RSC Adv. 6, 103026–103034 (2016).
2. Yuan, X., Liu, S., Feng, G., Liu, Y., Li, Y., Lu, H., Liang, B. Effects of ball milling on structural changes and hydrolysis of lignocellulosic biomass in liquid hot-water compressed carbon dioxide. Korean J. Chem. Eng. 33, 2134–2141 (2016).
3. Sweygers, N., Somers, M. H. & Appels, L. Optimization of hydrothermal conversion of bamboo (Phyllostachys aureosulcata) to levulinic acid via response surface methodology. J. Environ. Manage. 219, 95–102 (2018).
4. Wang, Y. Y., Eng, W., Wang, B., Zhang, Q., Wan, X., Tang, Z., Wang, Y., Zu, C., Cao, Z., Wang, G., Wan, H. Chemical synthesis of lactic acid from cellulose catalysed by lead(II) ions in water. Nat. Commun. 4, 2141 (2013).
5. Su, J., Shen, F., Qi, X. High-yield production of levulinic acid from pretreated cow dung in dilute acid aqueous solution. Molecules 22, (2017).
6. Sluiter, A. et al. Determination of Ash in Biomass Laboratory Analytical Procedure (LAP) Issue Date : 7 / 17 / 2005 Determination of Ash in Biomass Laboratory Analytical Procedure (LAP). (2008).
7. Sluiter, A. et al. Determination of Extractives in Biomass Laboratory Analytical Procedure (LAP) Issue Date : 7 / 17 / 2005 Determination of Extractives in Biomass Laboratory Analytical Procedure (LAP). (2008).
8. Channiwala, S. A. & Parikh, P. P. A unified correlation for estimating HHV of solid, liquid and gaseous fuels. Fuel 81, 1051–1063 (2002).

9. Sluiter, a. et al. NREL/TP-510-42618 analytical procedure - Determination of structural carbohydrates and lignin in Biomass. Lab. Anal. Proced. 17 (2012). doi:NREL/TP-510-42618

10. Park, S., Baker, J. O., Himmel, M. E., Parilla, P. A. & Johnson, D. K. Cellulose crystallinity index: measurement techniques and their impact on interpreting cellulase performance. Biotechnol. Biofuels 3, 10 (2010).

11. Sweygers, N., Dewil, R. & Appels, L. Production of Levulinic Acid and Furfural by Microwave-Assisted Hydrolysis from Model Compounds : Effect of Temperature , Acid Concentration and Reaction Time. Waste and Biomass Valorization 9, 343–355 (2018).

12. Zhang, J., Li, J., Tang, Y. & Xue, G. Rapid Method for the Determination of 5-Hydroxymethylfurfural and Levulinic Acid Using a Double-Wavelength UV Spectroscopy. 2013, (2013).

13. Aldrich, S. IR Spectrum Table & Chart (2021). Available at: https://www.sigmaaldrich.com/GB/en/technical-documents/technical-article/analytical-chemistry/photometry-and-reflectometry/ir-spectrum-table.

14. Aliko, K., Doudin, K., Ostatiashtiani, A., Wang, J., Topham, P. D., Theodosiou, E. Microwave-assisted synthesis of levulinic acid from low-cost, sustainable feedstocks using organic acids as green catalysts. J. Chem. Technol. Biotechnol. 95, 2110–2119 (2020).

15. Tedesco, S. & Stokes, J. Valorisation to biogas of macroalgal waste streams: A circular approach to bioproducts and bioenergy in Ireland. Chem. Pap. 71, 721–728 (2017).

16. Box, G. & Behnken, D. Some new three level designs for the study of quantitative variables. Technometrics 2, 455–475 (1960).

17. van Zandvoort, I., Wang, Y., Rasrendra, C. B., van Eck, E. R. H., Bruijincx, P. C. A., Heeres, H. J., Weckhusen, B. M. Formation , Molecular Structure , and Morphology of Humins in Biomass Conversion : Influence of Feedstock and Processing Conditions. ChemSusChem 1745–1758 (2013). doi:10.1002/cssc.201300332

18. VDI. VDI 4630: Fermentation of organic materials - Characterisation of the substrate, sampling, collection of material data, fermentation tests. in Handbuch Energietechnik (ed. VDI) 44–59 (Verein Deutscher Ingenieure, 2006).

19. Holliger, C. et al. Towards a standardization of biomethane potential tests. Water Sci. Technol. 74, 2515–2522 (2016).

20. Buswell, A. M. & Boruff, C. The relation between the chemical composition of organic matter and the quality and quantity of gas produced during sludge digestion. Sewage Work. J. 454–460 (1932).

21. Gibson, A. M., Bratchell, N. & Roberts, T. A. The effect of sodium chloride and temperature on the rate and extent of growth of Clostridium botulinum type A in pasteurized pork slurry. J. Appl. Bacteriol. 62, 479–490 (1987).

22. Pan, J., Ma, J., Liu, X., Zhai, L., Ouyang, X., Liu, H. Effects of different types of biochar on the anaerobic digestion of chicken manure. Bioresour. Technol. 275, 258–265 (2019).

23. Nadkarni, M. A., Martin, F. E., Jacques, N. A. & Hunter, N. Determination of bacterial load by real-time PCR using a broad-range (universal) probe and primers set. Microbiology 148, 257–266 (2002).

24. Brankatschk, R., Bodenhausen, N., Zeyer, J. & Burgmann, H. Simple absolute quantification method correcting for quantitative PCR efficiency variations for microbial community samples. Appl. Environ. Microbiol. 78, 4481–4489 (2012).

25. Kozich, J. J., Westcott, S. L., Baxter, N. T., Highlander, S. K. & Schloss, P. D. Development of a dual-index sequencing strategy and curation pipeline for analyzing amplicon sequence data on the miseq illumina sequencing platform. Appl. Environ. Microbiol. 79, 5112–5120 (2013).

26. Caporaso, J. G. et al. Ultra-high-throughput microbial community analysis on the Illumina HiSeq and MiSeq platforms. ISME J. 6, 1621–1624 (2012).

27. Callahan, B. J. et al. DADA2: High resolution sample inference from Illumina amplicon data. Nat. Methods 13, 4–5 (2016).

28. Quast, C. et al. The SILVA ribosomal RNA gene database project: Improved data processing and web-based tools. Nucleic Acids Res. 41, 590–596 (2013).

29. Team R Development Core. A Language and Environment for Statistical Computing. R Found. Stat. Comput. 2, https://www.R-project.org (2017).

30. Oksanen, J. et al. Package ‘vegan’ Title Community Ecology Package. Community Ecol. Packag. 2, 1–297 (2019).

Chapter 4: Biomass Survey & Characterisation

Abstract

One of the most crucial aspects of using of lignocellulosic biomass for the production of high value chemicals using catalysis is the choice of feedstock. Due to the variety of lignocellulosic feedstocks available globally with varying physical properties and compositions, it is not possible to use a universal feedstock. Therefore, this chapter surveys only UK-grown or available feedstocks for large scale commercial applications using semi-empirical methods. From this survey, 8 lignocellulosic feedstocks were chosen for further investigation. The survey considered a range of social, economic and technical challenges of lignocellulose production with regards to the ethical considerations of land use changes. This was followed upon by detailed characterisation of the chosen feedstocks using a range of standard protocols and methods. Data included in this chapter was referred to in later catalysis and results chapters.

4.1 Introduction

The use of real biomass was a key aspect of the earlier identified research gap compared with previous works that utilise analytical grade sugars or cellulose as substrates for catalysis. Real biomass can include various energy crops, agricultural residues and waste streams, with significant scope for differentiation. Previous studies have utilised a range of starting feedstocks including: rice and wheat straw, cherry and eucalyptus woods, grasses such as giant reed as well as waste food streams, such as orange peel, domestic waste and cow manure [1–7]. Ideally, a biorefinery could utilise any lignocellulosic feedstock with minimal adaption however, the compositional variations can have a significant impact on catalytic yields, hence should be considered carefully at planning stage. It is not possible to investigate a process with every available feedstock, thus the selection of representative feedstocks for biomass catalysis must be chosen carefully to maximise relevancy. Therefore, it was deemed necessary to study the integration of catalysis and anaerobic digestion on biomass materials most suitable for UK biorefineries.

4.2 Biomass Selection Criteria

Given the incredible diversity of lignocellulosic biomass feed sources globally, UK based feedstocks were screened. This also facilitates the ease of sample collection. After which, the following criteria was used to consider biomass feedstocks:

- Supply availability of over 100,00 tons per annum in the UK;
- High C6 and C5 sugar content, as these are the primary conversion substrate of catalytic processes;
- Minimal competition with food production to alleviate social implications;
- High homogeneity and composition;
- No indication of catalyst poisons or inhibitors;
- Relatively low cost.

4.3 Survey of materials

One of the more comprehensive reviews of lignocellulosic availability in the UK was conducted by NNFCC in 2014 [8]. The report looked specifically at straw, crop residues, forestry residues, paper waste, municipal waste and SRC willow, as well as miscanthus, and estimated that the UK's annual production is positioned at 15.6 million tons of the biomass materials, obtained through current land use practises. In 2018, the UK Government estimated a potential 27 million oven-dry tonnes of lignocellulosic biomass can be sustainably produced in-house for energy and chemical production [9]. The NNFCC noted that there is a variation is supply between various sources with energy crops and crop residues, due to seasonal production that will limit yearlong availability, which contrasts with the yearlong availability of forestry residues and paper. The report does not elaborate further on the yearlong supply issues however,

a stable supply/availability could be achieved via appropriate storage, globalised biomass transport or the development of co-catalysis of several feedstocks [10].

The findings of the NNFCC report therefore identify perennial energy crops, forestry, agricultural residues and waste products as the main materials to focus on as a starting point for biomass valorisation. The organic fraction of municipal solid waste has been hypothesised as a biorefinery feedstock, due to its low cost, large volume and high sugar contents [11]. Though this feedstock was ruled out for the time being, due its high variability in composition that makes acquiring representative samples difficult [12]. This was also the case for most consumer-derived waste materials.

The UK is also a large producer of cereal crops such as barley, oats and wheat, where the straw branches are often considered an agricultural waste product. The high cellulose content of wheat and barley straws makes them ideal candidate feedstocks for biorefineries, hence have been characterised in detail for biorefinery applications [13]. Though it should be pointed out that the use of oat straw for energy or commodity chemicals production is not advisable, due its unique properties for animal bedding, feed and insulation that render it more valuable in its native form. Additionally, rapeseed straw is an often underutilised lignocellulosic straw, the presence of soluble cyanide groups would make both catalysis and anaerobic digestion difficult [14] and was consequently also ruled out of this study.

Forestry residues from managed woodland (such as wood chip and bark) represent an interesting feedstock from a compositional perspective (e.g. high cellulose content and minimal impurities) but also its characterisation as a waste material. However, forestry residues have been estimated to cost 200-500% more than agricultural

residues [15], due to its alternative use as a combustion fuel and should be used sparingly as a result. To reduce costs, it is possible to focus on woods with short growth periods of 3-5 years such as willow and poplar, which have both been promoted as low cost energy crop [16]. The high homogeneity and cellulose content of woods make them ideal feedstocks for biorefineries, with willow and poplar wood chosen to be investigated further in this research.

Perennial energy crops such as, rye grass, willow and *Miscanthus x Giganteus* do not need to be replanted each year and regrow after annual harvesting. Perennial crops greatly reduce or eliminate the need of tillage which reduces topsoil loss and production costs as well as improving local water sources. Most perennial energy crops utilise the more efficient C4 carbon fixation mechanism during photosynthesis that allows for higher yields compared with wheat straw, even on marginal land [17,18]. *Miscanthus x Giganteus* is a hybrid C4 grass with excellent yields of nearly 15 tons per hectare in the UK requiring minimal nitrogen fertiliser, due to bacteria nodules in the root system. Due, to the low fertiliser requirements and suitability for marginal grasslands, *Miscanthus x Giganteus* is considered the most promising energy crop in the UK, though its composition can vary between species. *Miscanthus x Giganteus* alongside hemp , which can also be grown on marginal land, have been found to improve soil fertility if used as part of a crop rotation system [19–21] . Although the hemp is an excellent yielding C4 perennial crop, fibre structure of the stem may make it resistant to catalysis the husk. Perennial energy crops have been proposed as part of the UK's integrated land use strategy to meet net-zero targets [22]. Current studies estimate that if Grades 1, 2 and 3 agricultural lands are excluded there is between 0.7-2.2 million hectares of land suitable for Miscanthus[23].

Short rotation coppice (SRC) for energy consists of fast growing woody material such as willow or longer growing poplar are suitable for high incline fields (>15˚). As such McDermott *et al.* proposed that there was 0.7-2.8 million hectares of land suitable for SRC production in the UK that is unsuitable for the traditional crops[24]. SRC production has been shown to improve biodiversity, increase soil carbon and water retention, with 10,000 hectares already planted in Scotland[25]. The high cellulose contents of woody materials such as SRC would enable higher levulinic acid yields and lower separation costs. Interestingly high yielding SRC willow has expected similar costs of £60/ton as *Miscanthus x Giganteus* compared with slightly higher cost poplar wood[24].

4.4 Biomass Samples Collected

From survey of lignocellulosic biomass in the UK, it was decided to focus on agricultural residues and energy crops. Several samples were obtained, and include:

- Barley Straw
- Wheat Straw
- Hemp Husk
- 3 varieties of *Miscanthus x Giganteus*
- Poplar Wood
- Short Rotation Coppice (SRC) Willow

All samples were received as in-kind contribution to this research from UK growers, except for SRC willow which was obtained via a forestry consultant.

4.5 Extractives Analysis

Prior to sugar analysis, all samples must be treated with water and ethanol solvent extraction to remove impurities [26]. The impurities can include soluble sugars, but primarily consist of proteins, inorganic material and soluble lignin [27]. The biomass extracts can affect catalysis due to significant amounts of short chain soluble lignin monomers that can interact with homogenous catalysts [28]. Though as a whole the extractives are usually inert proteins and cytoplasm. Table 4.1, shows that a substantial amount of the biomass is solvent extractable with over 14% of the willow extractable, and *Miscanthu*s x G*iganteus* 1 with the lowest exhaustible extractives at 6.87. The willow sample had not been fully seasoned resulting in the highest extractives yield of 14% and under normal circumstances would be expected to be similar to Poplar. The effect of harvesting time can have a significant effect on moisture

content and composition of lignocellulose [29], however this has not been fully explored with regards to biomass catalysis.

Table 4.1: Comparison of extractives, moisture and ash contents of several feedstocks

	Water Extractives (wt% dry basis)	Ethanol Extractives (wt% dry basis)	Exhaustive Extractives (wt% dry basis)	Moisture (wt%)	Ash (wt% dry basis)
Barley Straw	5.10±0.17	4.46±0.53	8.26±0.14	4.04±0.19	3.12±0.11
Wheat Straw	11.05±0.36	6.71±0.29	12.86±0.73	3.24±0.08	7.06±0.01
Hemp Husk	4.53±0.18	4.09±0.03	6.87±0.11	4.79±0.07	1.90±0.0.05
Miscanthus x Giganteus (1)	7.38±0.26	5.67±0.32	10.65±0.22	4.23±0.26	2.87±0.03
Miscanthus x Giganteus (2)	6.21±0.04	6.25±0.36	8.62±0.14	4.55±0.06	2.41±0.03
Miscanthus x Giganteus (3)	3.10±0.44	3.76±1.02	5.32±0.77	4.62±0.11	1.82±0.0.4
Poplar Wood	4.18±0.01	5.48±0.78	5.53±0.59	5.25±0.16	0.16±0.0.16
SRC Willow	13.83±0.18	8.46±0.16	18.26±0.14	9.78±0.29	0.28±0.0.8

Wheat straw exhibited a substantial amount of ash, in fact 7.06% of the dry matter remain after 6 hours at 550˚C, which indicates the wheat straw has significant quantities of inorganic material that cannot be used catalytically or biologically. Analysis by Dodson *et al.* found that wheat straw in UK primarily consisted of 40-70% SiO_2 [30], which is mostly inert and will not affect the catalysis process. However, it was noted that free chlorine could constitute up to 9% of the ash constituents, which could significantly poison heterogeneous catalysts. The rest of the herbaceous biomass present a varied ash content from 1.82-3.12%, while for the two varieties of wood this value fell below 0.3%, which is comparable to values found in the literature [31–33]. The inorganic ash content will most likely not affect the catalysis significantly however, it reduces the amount of volatile material available for conversion, reducing absolute dry weight yields.

4.6 Elemental Analysis of Biomass

The elemental characterisation of the samples is presented in Table 4.2, alongside the derived C/N ratios. It can be seen that all samples had similar elemental composition with minimal difference between the herbaceous biomass samples. A high carbon content is generally a good indicator for pyrolytic bio-oil yields however, while it has not been directly correlated to catalysis products, it is used by scientist as indicative of high sugar contents [34].

Table 4.2: Elemental composition of the samples on mass basis adjusted for ash

	Carbon	Hydrogen	Nitrogen	Sulphur	Oxygen	C/N
Barley Straw	47.57±0.09	5.99±0.02	0.51±0.01	0.26±0.06	42.56±0.17	93
Wheat Straw	45.98±0.12	5.65±0.06	0.42±0.02	0.24±0.01	40.65±0.14	109
Hemp Husk	47.57±0.09	5.97±0.01	0.34±0.01	1.45±0.59	40.7±1.07	146
Miscanthus x Giganteus (1)	48.07±0.02	6.04±0.04	0.53±0.02	0.10±0.01	42.39±0.03	91
Miscanthus x Giganteus (2)	48.01±0.01	6.16±0.01	0.48±0.02	0.06±0.01	42.88±0.01	100
Miscanthus x Giganteus (3)	48.67±0.03	6.03±0.04	0.33±0.01	0.13±0.03	43.03±0.01	147
Poplar Wood	51.18±0.02	6.28±0.01	0.11±0.03	0.06±0.01	42.22±0.03	465
SRC Willow	49.02±0.05	6.23±0.06	0.78±0.05	0.12±0.01	43.57±0.04	73

The sulphur content of the hemp husk was 1.45%, which is very high relative the < 0.3% of all the other samples and may cause issues with both catalysis and anaerobic digestion [35,36]. The sulphur is often found as part of amino acids, such as methionine and cysteine, with cysteine containing an easily oxidisable thiol group [37]. A study by Malomo *et al.* [38] also reported the presence of sulphur as part of the disulphide protein bonding in hemp husk, which could potentially deactivate heterogeneous catalysts. For these reasons, the presence of a large quantity of sulphides makes hemp a less suitable feedstock for catalysis or subsequent Anaerobic Digestion (AD).

The C/N ratio is an often used to determine suitability for anaerobic digestion, as it nitrogen deficiency or excess can easily affect the microbial community, with the optimum value varying between 15 and 30. The C/N ratios listed in Table 4.2 ranged between 73 and 465, which is significantly above the recommended anaerobic digestion conditions, indicating co-digestion is recommended for stable and maximised yields of biogas. To benefit the discussion in this regard, it should be pointed out that catalytic pre-treatments enable a greater suitability for AD, as the post-catalysis solid residue will be depleted in carbon as a consequence of sugar catalysis. This typically results in a lower C/N ratio in the post catalysis residue, although such decrease will not be sufficient for using the residues feedstock in mono-digestion. Therefore, it will be necessary for the solid residues to be used as an additive or co-substrate during anaerobic digestion with nitrogen rich materials.

4.7 Structural Sugars

The amount and type of structural sugars in lignocellulosic biomass is a crucial variable when assessing the suitability for biorefining as the catalytic process primarily uses sugars are the primary building reactants.

Table 4.3: Structural sugars of the biomass samples as determined by NREL method

	C6 Sugars				C5 Sugars			
	Glucose	Mannose	Galactose	Rhamnose	Xylose	Arab-inose	Total C6	Total C5
Barley Straw	40.5 ±0.78	0.28 ±0.02	0.53 ±0.01	0.11 ±0.01	20.38 ±0.28	2.19 ±0.01	41.44 ±0.81	22.58 ±0.3
Wheat Straw	36.84 ±0.76	0.19 ±0.02	0.5 ±0.01	0.11 ±0.01	18.44 ±0.33	2.13 ±0.01	37.66 ±0.79	20.58 ±0.34
Hemp Husk	37.28 ±0.22	1.35 ±0.02	0.53 ±0.01	0.46 ±0.01	15.76 ±0.45	0.25 ±0.06	39.65 ±0.24	16.02 ±0.38
Miscanthus x Giganteus (1)	38.8 ±0.64	0.20 ±0.01	0.48 ±0.01	0.05 ±0.08	20.23 ±0.32	1.77 ±0.01	39.55 ±0.73	22.02 ±0.34
Miscanthus x Giganteus (2)	41.11 ±0.82	0.19 ±0.01	0.46 ±0.01	0.1 ±0.01	20.37 ±0.43	1.66 ±0.07	41.87 ±0.8	22.05 ±0.51
Miscanthus x Giganteus (3)	38.00 ±1.42	0.26 ±0.02	0.47 ±0.01	0.1 ±0.01	22.31 ±0.74	1.76 ±0.01	38.86 ±1.42	24.08 ±0.73
Poplar Wood	41.96 ±1.77	11.46 ±0.43	1.77 ±0.08	0.18 ±0.01	5.84 ±0.34	1.37 ±0.05	55.39 ±2.3	7.22 ±0.41
SRC Willow	36.0.2 ±1.33	2.47 ±0.12	2.51 ±0.04	0.04 ±0.01	10.87 ±0.40	2.41 ±0.51	41.04 ±1.8	13.28 ±0.91

Table 4.3 shows the structural sugars of the biomass samples investigated. All of the samples analysed contain significant amounts of glucose (> 36%), which indicates that the selection of the biomass samples was appropriate. Poplar wood presented by far the highest content of C6 sugars, primarily due to its high mannose content (resulting in total C6 sugars of 54%), along with the smallest concentration of C5 sugars. *Miscanthus x Giganteus* (2) and barley straw contained approximately 41% C6 sugars and an important amount of C5 sugars (> 20%) compared with poplar wood. A higher C5 sugar content is functional to the conversion pathway as it would enable the dual production of furfural in addition to levulinic acid, although furfural degradation would increase solid residue yields from humin formation The hemp husk sample exhibits

noticeable amounts of galactose and rhamnose, which are stereoisomers of glucose. Isomerization between sugars can be catalysed under most acidic or basic conditions, with a slight decrease in expected levulinic acid yields [39] . As a whole, the structural sugars characterisation indicated that all biomass samples were suitable for catalysis.

4.8 Crystallinity Index

The CI of lignocellulosic material, a measurement of the relative recalcitrance to hydrolysis dependant on the ratio of amorphous to crystalline cellulose, was calculated for the investigated feedstocks and shown in Figure 4.1.

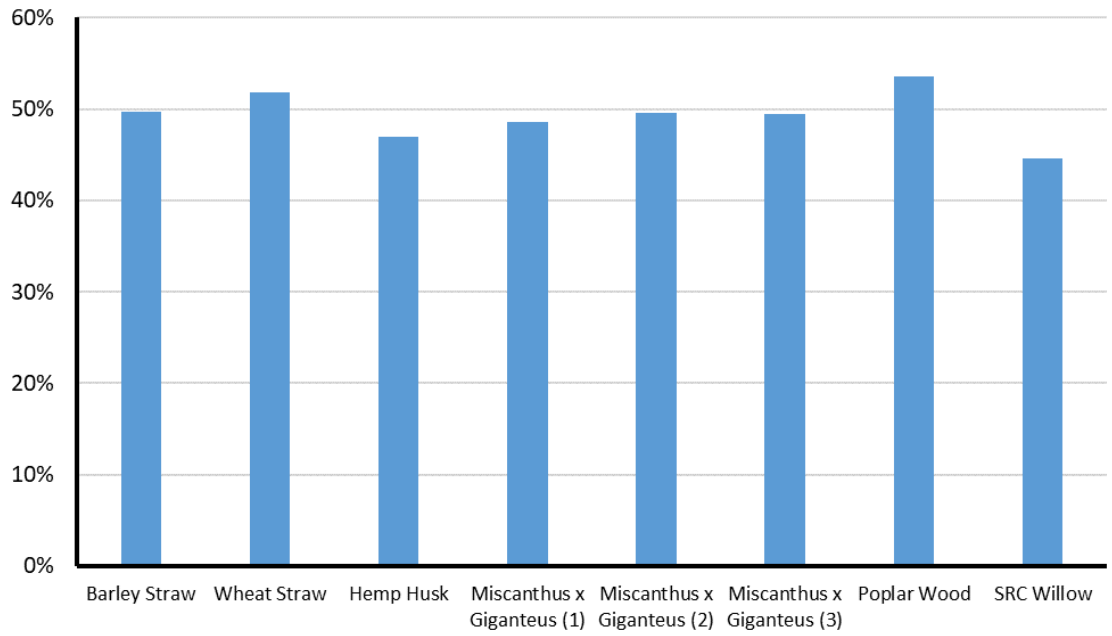

Figure 4.1: CI of the biomass samples using XRD

The lignocellulosic samples ranged between 44%-53%, which is comparable with other works [40,41]. Poplar wood exhibited the highest CI of 53.52%, followed by wheat straw at 51.84% andc barley straw at 49.64%. An increase in CI is indicative of slower cellulose hydrolysis, with the 44.57% CI of willow indicating an easily hydrolysable cellulose fraction. However, none of the feedstocks exceed a value of 60%, which has

been associate with highly recalcitrant cellulose [42]. The similar crystallinity across all samples may be partially be due to the effects of size reduction on reducing CI [40]. However, the measurement of uneven powders of raw biomass can introduce XRD shadows and was not investigated, though the CI does indicate that all prepared samples have a balanced mix of crystalline and amorphous cellulose that is suitable for further conversion.

4.9 Conclusions

Through the careful review of available lignocellulosic biomass available in the UK, the characterisation of eight lignocellulosic feedstocks was successfully conducted. The sample lignocellulose materials were chosen through a carefully considered criteria which found some of the most sustainably appropriate feedstocks. The characterisation of all eight feedstocks included the evaluation of structure and composition, while all eight samples could be considered suitable for biomass catalysis due to their high cellulose contents. Poplar wood was considered to be the most promising feedstock for catalytic conversion, primarily due to the abundant C6 sugar content exceeding 56 wt.% which would inherently increase absolute levulinic acid yields and possibly reduce by-product yields. While *Miscanthus x Giganteus* and barley straw showed promise as alternative feedstocks due to combined high C6 and C5 sugar contents that could possibly enable the duel production of levulinic acid and furfural. The results from this Chapter enabled the most appropriate choice of feedstocks for catalysis in later chapters and the compositional analysis is also referred to.

4.10 References

1. Bozym, M., Florczak, I., Zdanowska, P., Wojdalski, J. & Klimkiewicz, M. An analysis of metal concentrations in food wastes for biogas production. Renew. Energy 77, 467–472 (2015).
2. Glińska, K., Lerigoleur, C., Giralt, J., Torrens, E. & Bengoa, C. Valorization of cellulose recovered from wwtp sludge to added value levulinic acid with a brønsted acidic ionic liquid. Catalysts 10, 1–16 (2020).
3. Galletti, A. M. R., Antonetti, C., De Luise, V., Licursi, D. & Di Nasso, N. N. O. Levulinic acid production from waste biomass. BioResources 7, 1824–1834 (2012).
4. Kłosowski, G., Mikulski, D. & Menka, A. Microwave-Assisted One-Step Conversion of Wood Wastes into Levulinic Acid. Catalysts 9, 753 (2019).
5. Dussan, K., Girisuta, B., Haverty, D., Leahy, J. J. & Hayes, M. H. B. Kinetics of levulinic acid and furfural production from Miscanthus×giganteus. Bioresour. Technol. 149, 216–224 (2013).
6. Di Fidio, N., Fulignati, S., De Bari, I., Antonetti, C. & Raspolli Galletti, A. M. Optimisation of glucose and levulinic acid production from the cellulose fraction of giant reed (Arundo donax L.) performed in the presence of ferric chloride under microwave heating. Bioresour. Technol. 313, 123650 (2020).
7. Su, J, Shen, F., Qiu, M., Qi, X. High-yield production of levulinic acid from pretreated cow dung in dilute acid aqueous solution. Molecules 22, (2017).
8. Maio, D. Di, Turley, D. & Hopwood, L. Lignocellulosic feedstock in the UK November 2014. NNFCC (2014).
9. Committee on Climate Change. Biomass in a low-carbon economy. 161 (2018).

10. Lamers, P. & Falls, I. Strategic supply system design – a holistic evaluation of operational and production cost for a biorefinery supply chain. Biofuels, Bioproducts and Biorefining 6, 648–660 (2015). doi:10.1002/bbb

11. Matsakas, L., Gao, Q., Jansson, S., Rova, U. & Christakopoulos, P. Green conversion of municipal solid wastes into fuels and chemicals. Electron. J. Biotechnol. 26, 69–83 (2017).

12. Alibardi, L. & Cossu, R. Composition variability of the organic fraction of municipal solid waste and effects on hydrogen and methane production potentials. Waste Manag. 36, 147–155 (2015).

13. Plazonić, I., Barbarić-Mikočević, Ž. & Antonović, A. Chemical Composition of Straw as an Alternative Material to Wood Raw Material in Fibre Isolation Drvna Industrija. 67, 119–125 (2016).

14. Hu, Q., Hua, W., Yin, Y., Zhang, X., Liu, L., Shi, J., Zhao, Y., Qin, L., Chen, C., Wang, H. Rapeseed research and production in China. Crop J. 5, 127–135 (2016).

15. Daioglou, V., Stehfest, E., Wicke, B., Faaij, A. & van Vuuren, D. P. Projections of the availability and cost of residues from agriculture and forestry. GCB Bioenergy 8, 456–470 (2016).

16. Taylor, P., Keoleian, G. A., Volk, T. A. & Keoleian, G. A. Renewable Energy from Willow Biomass Crops : Life Cycle Energy , Environmental and Economic Performance Renewable Energy from Willow Biomass Crops : Life Cycle Energy , Environmental and Economic Performance. 37–41 (2007). doi:10.1080/07352680500316334

17. van der Weijde, T., Kamei, C. L. A. Torres, A. F., Vermerris, W., Dolstra, O., Visser, R. G. F., Trindade, L. M. & Breeding, P. The potential of C4 grasses for cellulosic biofuel production. Frontiers in Plant Science 4, 1–18 (2013).

18. Mantziaris, S., Iliopoulos, C., Theodorakopoulou, I. & Petropoulou, E. Perennial energy crops vs . durum wheat in low input lands : Economic analysis of a Greek case study. Renew. Sustain. Energy Rev. 80, 789–800 (2017).

19. Finnan, J. & Styles, D. Hemp : A more sustainable annual energy crop for climate and energy policy. Energy Policy 58, 152–162 (2013).

20. Mamirova, A., Pidlisnyuk, V., Amirbekov, A., Ševců, A. & Nurzhanova, A. Phytoremediation potential of Miscanthus sinensis And. in organochlorine pesticides contaminated soil amended by Tween 20 and Activated carbon. Environ. Sci. Pollut. Res. 28, 16092–16106 (2021).

21. Andrejić, G., Šinžar-Sekulić, J., Prica, M., Dželetović, Ž. & Rakić, T. Phytoremediation potential and physiological response of Miscanthus × giganteus cultivated on fertilized and non-fertilized flotation tailings. Environ. Sci. Pollut. Res. 26, 34658–34669 (2019).

22. Newbery, David; Echenique Marcial; Goddard, John; Heathwaite, Louise;Morris, Joe;Schultz, Wendy; Swanwick, Carys; Tewdwr-Jones, M. Foresight Land Use Futures Project: Making the most of land in the 21st century. Gov. Off. Sci. 46 (2010).

23. Konadu, D. D., Mourão, Z. S., Allwood, J. M., Richards, K. S., Kpoec, G., McMahon, R., Fenner, R. Land use implications of future energy system trajectories-The case of the UK 2050 Carbon Plan. Energy Policy 86, 328–337 (2015).

24. Ayott, M. & McDermott, F. Domestics Energy Crops; Potential and Constraints Review. NNFCC 12–21 (2012).

25. Martin, G., Ingvorsen, L., Willocks, J., Wiltshire, J., Bates, J., Jenkins, B., Priestley, T., McKay, H., Croxton, C. Evidence Review: Perennial Energy Crops and their Potential in Scotland. ClimateXChange 1–68 (2020).

26. Thammasouk, K., Tandjo, D. & Penner, M. H. Influence of Extractives on the Analysis of Herbaceous Biomass. Journal of Agricultural and Food Chemistry 45, 437-443 (1997). doi:10.1021/jf960401r

27. Sluiter, A. et al. Determination of Extractives in Biomass Laboratory Analytical Procedure (LAP) Issue Date : 7 / 17 / 2005 Determination of Extractives in Biomass Laboratory Analytical Procedure (LAP). (2008).

28. Xiu-juan, G. U. O., Shu-rong, W., Kai-ge, W., Qian, L. I. U. & Zhong-yang, L. U. O. Influence of extractives on mechanism of biomass pyrolysis. J. Fuel Chem. Technol. 38, 42–46 (2010).

29. Marinho-Soriano, E., Fonseca, P. C., Carneiro, M. A. A. & Moreira, W. S. C. Seasonal variation in the chemical composition of two tropical seaweeds. Bioresour. Technol. 97, 2402–2406 (2006).

30. Dodson, J. R. Wheat straw ash and its use as a silica source. (2011).

31. Baxter, X. C., Darvell, L.I., Jones, J.M., Barraclough, T., Yates, N.E., Shield, I. Study of Miscanthus x giganteus ash composition – Variation with agronomy and assessment method. Fuel 95, 50–62 (2012).

32. Garcia, A. G. M. HEMP: A COMPOSITION REVIEW PLUS. (2017).

33. Mann, J. D. & Mann, J. D. Comparison of Yield , Calorific Value and Ash Content in Woody and Herbaceous Biomass used for Bioenergy Production in Southern Ontario (2012).

34. Lin, F., Waters, C. L., mallinson, R. G., Lobban, L. L., Bartley, L. E. Relationships between biomass composition and liquid products formed via pyrolysis. Frontiers in Energy Research 3, 45 (2015).

35. Nasri, N. S., Jones, J. M., Dupont, V. A. & Williams, A. A comparative study of sulfur poisoning and regeneration of precious-meted catalysts. Energy and Fuels 12, 1130–1134 (1998).

36. Koster, I. W., Rinzema, A., de Vegt, A. L. & Lettinga, G. Sulfide inhibition of the methanogenic activity of granular sludge at various pH-levels. Water Res. 20, 1561–1567 (1986).

37. Tang, C. H., Ten, Z., Wang, X. S., Yang, X. Q. Physicochemical and Functional Properties of Hemp (Cannabis sativa L .) Protein Isolate. Journal of Agricultural and Food Chemistry 54, 8945–8950 (2006).

38. Structure-function properties of hemp seed proteins and protein-derived peptides. Malomo, S. A. (2015).

39. Delidovich, I. & Palkovits, R. Catalytic Isomerization of Biomass-Derived Aldoses: A Review. ChemSusChem 9, 547–561 (2016).

40. Rongpipi, S., Ye, D., Gomez, E. D. & Gomez, E. W. Progress and opportunities in the characterization of cellulose – an important regulator of cell wall growth and mechanics. Front. Plant Sci. 9, 1–28 (2019).

41. Park, S., Baker, J. O., Himmel, M. E., Parilla, P. A. & Johnson, D. K. Cellulose crystallinity index: measurement techniques and their impact on interpreting cellulase performance. Biotechnol. Biofuels 3, 10 (2010).

42. Zoghlami, A. & Paës, G. Lignocellulosic Biomass: Understanding Recalcitrance and Predicting Hydrolysis. Front. Chem. 7, (2019).

Chapter 5: Solid Residue and by-product yields from the acid hydrolysis of poplar wood

Published in: Chemical Papers 2020, 74: 1647-1661

DOI: 10.1007/s11696-019-01013-3

Graphical Abstract

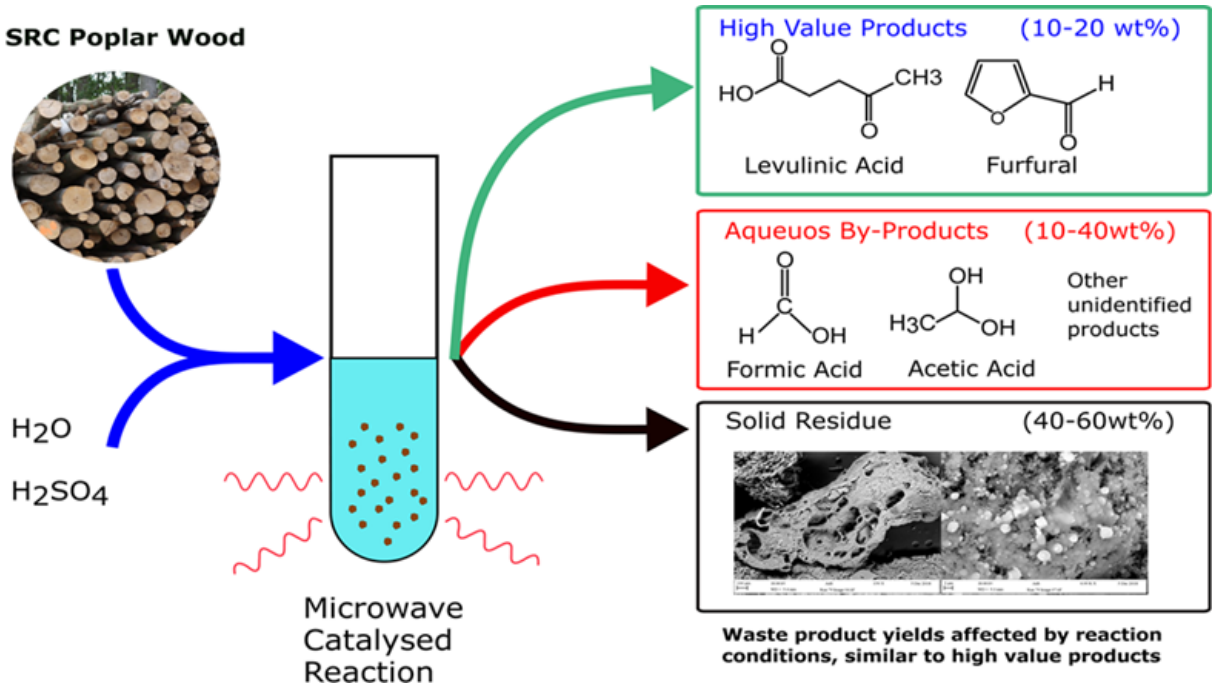

Abstract

This chapter investigates the yields of high value products, solid residues and aqueous by-products from the microwave assisted acid hydrolysis of poplar wood with sulphuric acid. The aim of this chapter is to investigate the effect of process conditions on aqueous by-products such as; furfural, formic acid, acetic acid and solid residues with regards to levulinic acid production optimisation via Response Surface Methodology (RSM). In this work, a maximum theoretical levulinic acid yield of 62.1% (21.0 wt.%) was predicted using RSM which corresponded with a solid residue yield of 59.2 wt.%. The solid residue yields from the acid hydrolysis of poplar wood yields were found to increase significantly with increasing reaction time and temperature. Under all reaction conditions the solid residue yield exceeded the levulinic acid, justifying the need for alternative disposal methods. Selected solid resi-dues were further characterised for potential applications using FTIR, combustion elemental analysis and XRF. The overall results show that poplar wood has great potential to produce renewable chemicals, but also highlights by-products must be considered during optimization, with consideration for future application.

5.1. Introduction

Acid catalysts such as HCl and H_2SO_4 can partially decompose the lignocellulose into individual sugars before conversion into a range of platform chemicals; specifically, levulinic acid and furfural from cellulose and hemicellulose respectively[1–6]. Both levulinic acid and furfural have been recognised among the top 30 platform chemicals by the United States Department of Energy [7]. However, as discussed in Chapter 4, lignocellulosic biomass is inherently heterogeneous and contains non-sugar based fractions that can react under the catalytic fractions to form by-products alongside humin degradation products. Among the most abundant by-products are solid residue, formic acid and acetic acid. The development of biorefineries will require the minimisation and valorisation of all by-products, but the effects of reaction conditions on by-product yields is not well understood.

Acid catalysis of lignocellulosic biomass with mineral acids such as sulphuric acid and hydrochloric acid are reported to reach levulinic acid and furfural theoretical yields between 50-80% [8–10]. Solid residue by-products are typically composed of hydrolysis resistant material, primarily acid-insoluble lignin and also contain condensation products from FF and reactive intermediaries (e.g. 5-HMF), known as catalytically derived humins [11]. Humins are polymeric carbonaceous degradation products formed during the acid catalysed dehydration of sugars, intermediaries and platform chemicals [12,13]. The formation of recalcitrant furan rich humins have been found to account for 10-50% of carbon losses during acid hydrolysis and reducing both levulinic acid and furfural yields [14,15].

Solid residue yields from acid catalysis of *Miscanthus* spp. and bamboo have been reported between 33-40 wt.%[16,17]. Zandvoort et al. modelled humin yields from sugars, using Response Surface Methodology (RSM), finding yields up to 36 wt.%[12]. Several applications for solid residues have been investigated in recent years including as fuel, building material and as feedstock for pyrolysis, bio oil yields of 10-20% [18–20]. However, further characterisation is required at different reaction conditions to better evaluate different applications and the effects of process parameters.

In this chapter Response Surface Methodology was utilised to model the effects of the process variables; temperature, Sulphuric acid concentration and reaction time (T, C_{H2SO4} and t) on the yields of solid and aqueous by-products, during the microwave-assisted acid hydrolysis of poplar wood with sulphuric acid. The effects of process conditions on individual product yields are discussed with the consideration of future biorefinery development. Selected solid residues are further characterised using FTIR, combustion elemental analysis and XRF, with discussion regarding future applications.

5.2. Extended Methodology

5.2.1. Sample Preparation and Characterisation

Poplar wood sawdust was acquired from a local Short-Rotation-Coppice (SRC), dried at 105 °C for 24 hours and reduced to fine powder (≤ 1 mm) with a Restsch ZM500 ball mill. The obtained compositions (on an oven-dry basis wt.%) from Poplar Sawdust was 2.16% ± 0.05 ash, 4.18% ± 0.01 water extractives, 25.05% ± 0.66 Klason lignin, 41.97% ± 0.77 cellulose (glucan), 11.47% ± 0.43 mannose, 7.22% ± 0.41 hemicelluloses.

5.2.2. Acid Hydrolysis

An Anton Parr Monowave 300 microwave reactor was used as the bench scale microwave reactor for the acid hydrolysis. The acid hydrolysis of poplar wood and solid residue separation was conducted according to the procedure depicted in Figure 5.1. In each experiment 0.15 g of polar wood was mixed with 6 ml of sulphuric acid solution (0.1-2.0 M) to achieve a biomass loading ratio of 5 wt.%. The catalysis operating parameters of Temperature, time and Sulphuric Acid concentration were the primary operating variables and are described in detail in section 5.2.3. Following the completion of the desired reaction time solid residue was separated and the hydrolysate was analysed using HPLC with an RID detector.

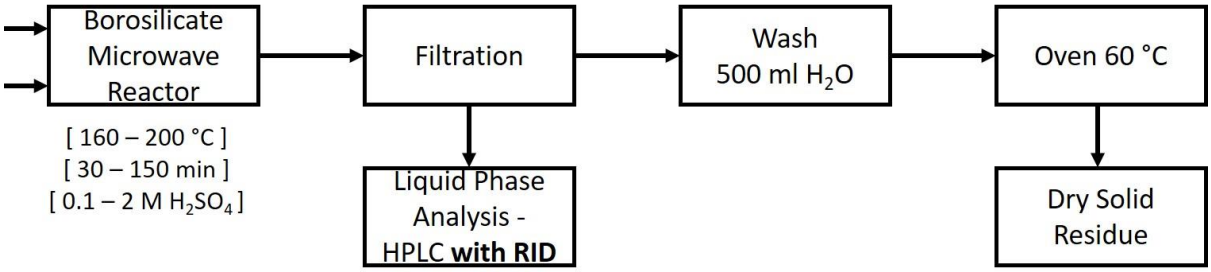

Figure 5.1: Microwave hydrolysis process and solid residue separation

5.2.3. Statistics and Experimental design

The formation of levulinic acid can be adequately explained using kinetic models however, such kinetic models have not yet been developed for the by-product formation (this is outside the scope of this work). RSM was used in this study to allow the evaluation of process parameters on product yields without detailed understanding of the underlying process using a limited data set. Previous studies have successfully utilised RSM for modelling levulinic acid yields and humins [6,12]. Further rationale for using RSM is provided in Chapter 3, Section 3.7.

The RSM model was built using 17 experimental data points as per a three level Box-Behnken design, as shown in Table 5.1. The central point was replicated 5 times (as dictated by the method) in order to estimate the model variance and the non-central points were replicated in triplicate to reduce experimental error. The run order was randomised and the full experimental design, including order randomisation, is shown in Appendix A - Table 1.

Table 5.1: Levels of the acid hydrolysis process variables

	Unit	Variable Levels		
		low	medium	high
Temperature	°C	160	180	200
Time	min	30	90	150
H_2SO Concentration	M	0.1	1.05	2.0

5.3. Results and discussion:

5.3.1. Green chemical and solid product yields

The complete dataset of all product yields used for the development of the RSMs are shown in Table 5.2. The response surfaces included in the following subsections were generated from statistically significant models for estimating the platform chemical yields with a reduced data set. The yields of each building block will be referred to in the hereafter subsections for focussed discussion.

5.3.2. Levulinic Acid Yields

The poplar wood was subjected to acid hydrolysis with sulphuric acid according to the Box-Behnken experimental design shown in Table 5.1 and all the results of all measured compounds are shown in Table 5.2. The highest observed theoretical levulinic acid was 59.5% for poplar wood at 180 ˚C, 150 min and 2 M sulphuric acid (Run 1) that corresponds to a levulinic acid yield of 20.1 wt.% of the initial biomass. The yields are in line with those from other lignocellulosic feedstocks such as wheat straw, pine chips and miscanthus that have been reported between 50-70 % [6,21]. While the theoretical yield is more appropriate for discussing the catalysis process effect on the maximum stoichiometric yields achievable, the absolute weight yield evaluates the economic implications of both the technology and feedstocks, therefore both solid and theoretical yields will be discussed. The high C6 sugar content of the feedstock has resulted in levulinic acid yields exceeding 20 wt.%, which justifies the choice of polar wood as feedstock. However, the maximum yields were found at unusually long reaction times for microwave technology (150 mins), which could be attributed to the recalcitrance of woody biomass and moderate reaction temperature (180 °C). This result indicates the advantages of microwave-assisted heating are less pronounced when using recalcitrant biomass types.

Table 5.2: Experimental Results of sulphuric acid hydrolysis of poplar sawdust

Run	Temperature / ˚C	Reaction Time /min	Sulphuric Acid Concentration / M	Theoretical Yield*		Yield g/ 100g of reactant*						Net Formic Acid Yield *(g/g)	Cumulative
				Levulinic Acid	Furfural	Glucose	Levulinic Acid	Furfural	Formic Acid	Acetic Acid	Solid Residue		
13	160	30	1.05	4.9%	22.5%	7.70	1.66	1.86	1.04	2.20	51.57	0.38	66.02
15	160	90	0.1	3.2%	40.0%	10.23	1.10	3.31	2.01	2.35	62.96	1.58	81.96
5	160	90	2.00	31.8%	44.3%	14.79	10.75	3.66	6.43	2.27	48.41	2.16	86.31
10	160	150	1.05	23.0%	29.2%	15.45	7.77	2.41	4.08	2.53	51.71	1.00	83.95
7	180	30	0.1	7.8%	10.3%	6.04	2.64	0.85	10.32	2.34	69.53	9.27	91.72
6	180	30	2	27.8%	11.5%	10.70	9.40	0.95	7.84	2.06	44.26	4.11	75.22
2	180	90	1.05	55.0%	11.5%	9.52	17.60	0.95	10.35	2.56	38.75	3.37	79.74
3	180	90	1.05	52.7%	15.7%	8.78	17.84	1.30	10.18	2.52	38.47	3.10	79.08
4	180	90	1.05	51.0%	17.1%	9.21	16.56	1.41	10.21	2.43	45.61	3.64	80.43
8	180	90	1.05	49.0%	17.1%	9.20	16.56	1.41	9.58	2.28	42.60	3.01	81.63
16	180	90	1.05	47.5%	16.9%	8.99	16.09	1.40	10.21	3.05	41.25	0.83	71. 65
11	180	150	0.1	9.1%	34.8%	10.48	3.08	2.87	2.48	2.37	59.07	1.26	80.36
1	180	150	2	59.5%	0.4%	0.17	20.14	0.03	10.60	3.12	59.48	2.61	93.54
17	200	30	1.05	25.9%	1.9%	20.34	8.78	0.15	6.12	1.82	40.06	2.64	77.27
9	200	90	0.1	21.8%	46.8%	18.53	7.36	3.87	5.79	2.88	50.68	2.87	89.11
14	200	90	2	49.6%	0.2%	0.60	16.78	0.02	5.71	1.66	46.12	-0.94	70.88
12	200	150	1.05	43.9%	0.2%	0.52	14.85	0.02	0.95	2.64	48.40	-4.94	67.38

* The runs were conducted in triplicate and values averaged except for the central point of 180 ˚C, 90 min and 1.05 M H_2SO_4

The conversion of polar wood to levulinic acid was optimised using RSM and was modelled using analysis of variance (ANOVA) to produce a quadratic model, shown in *Equation 5.1*. The proposed model was statistically significant with an adj. R^2 of 98% and a lack of fit of 0.44, the full ANOVA table is shown in Appendix A- Table 2.The highest predicted theoretical levulinic acid yield was of 62.1% or 21.0 wt.%, at 188 °C, 126 min and 1.93M sulphuric acid, which is higher than other works with untreated poplar wood, i.e. 52 % with HCl [2] and 49 % with H_2SO_4 [14]. The results of this study further highlight the potential of poplar wood as feedstock for levulinic acid production in a biorefinery context.

$$Y_{LA} = -3.77 + 0.0398\,T + 0.00223\,t + 0.102\,C_{H2SO4} + 0.000452\,t * C_{H2SO4} - 0.00106\,T^2 - 0.0000123\,t^2 - 0.0409\,{C_{H2SO4}}^2 \qquad \textit{Equation 5.1}$$

The 3D-contour graphs in Figure 5.2 shows the performance of levulinic acid yield, according to *Equation 5.1*, in relation to the three process variables. The sulphuric acid concentration had the highest impact on the levulinic acid yield, according to 5.2b and 5.2c. Low concentrations of H_2SO_4 (0.1 M) appear not to be sufficient to fully catalyse either the cellulose degradation or further conversion to levulinic acid, as shown by the high concentrations of glucose and solid residue, as shown in Runs 9, 11 and 15. There was a slight decrease in levulinic acid yields with at higher acid concentrations in correlation with acid catalysed humin formation, as shown in Figures 5.2b and 5.2c. Similarly, a decrease of levulinic acid yield can be observed at higher temperatures and longer times, indicating levulinic acid degradation is occurring. It can therefore be concluded that interdependence of the three process variables shows that the highest levulinic acid yield can only be determined by co-optimization.

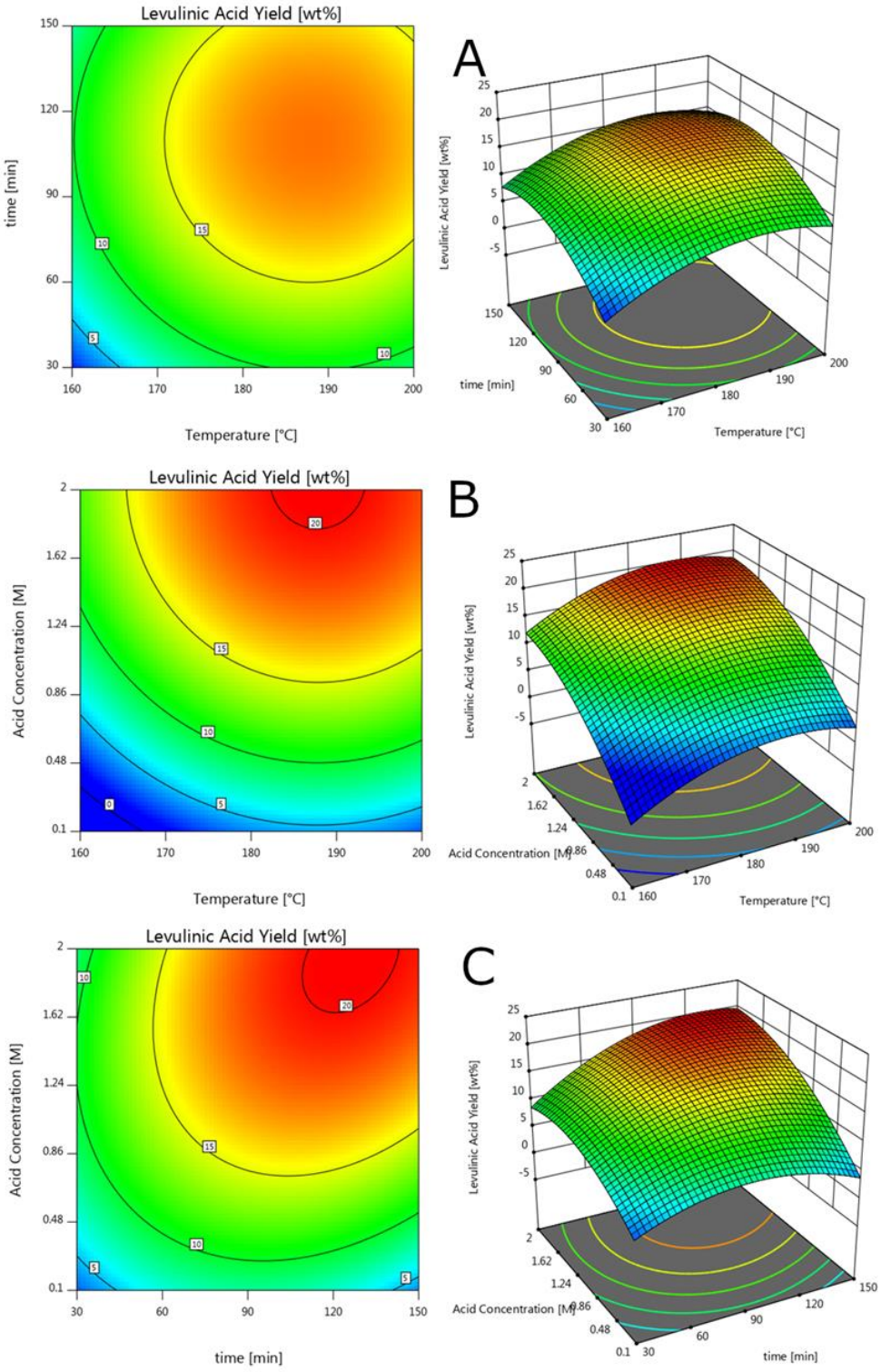

Figure 5.2: 3D response surface plots and 2D contour plots of levulinic acid yield (wt.%) whist (A) varying temperature and time; (B) varying sulphuric acid concentration and temperature; (C) varying time and sulphuric acid concentration

5.3.3. Furfural Yields

Fufural yields were modelled using a modified ANOVA model, with an adj R^2 of 95.8% (Appendix A- Table 3) and the RSM plots are shown in Figure 5.3. The overall furfural yields were lower than expected and decreased significantly with increasing temperature and sulphuric acid concentration, as seen in Figure 5.3b. The speed at which the furfural degraded was unexpected with the optimum furfural conditions, according to *Equation 5.2*, being 160 °C, 71 min and 2 M H_2SO_4 which results in theoretical furfural and levulinic acid yield of 15.1% and 26.3% respectively. The highest furfural yield had a correspondingly low levulinic acid yield, which suggests that the hemi-cellulose solubilisation and subsequent transformation to furfural is significantly faster than cellulose to levulinic acid [22]. Furfural can degrade under the same conditions that is formed and can degrade into a multitude of products including formic acid and solid residues [23]. The difference in reaction rates makes co-optimization of the two products using a single stage process difficult and the production of levulinic acid should be prioritised due to its higher potential yield.

$$Y_{FF} = +0.5204 - 0.00596\,T + 0.000598\,t + 0.0858\;C_{H2SO4} - 0.000554\,T * C_{H2SO4} - 0.000129\,t * C_{H2SO4} - 0.0000169\,T^2 - 2.391\text{x}\,10^{-3}t^2 + 0.00823\,{C_{H2SO4}}^2$$

Equation 5.2

There was a small increase in furfural yields with reaction time, peaking at approximately 90 min, following which a sharp decrease in furfural yield was observed. It should be noted that the rapid decrease in furfural yields corresponds to a significant increase in solids yield, as shown in Figure 5.5. Furfural decomposition and polymerisation towards humins has been reported under acidic conditions [24,25].

Moreover, Runge and Zhang proposed that the degradation of furfural caused the formation of tar-like humin structures, inhibiting cellulose hydrolysis[14]. Therefore, the solid residue yields can be partially attributed to the furfural degradation and the conversion of furfural to solid residue could be an interesting optimisation feature in future works, if solid residues can be valorised and low furfural concentrations do not warrant separation cost.

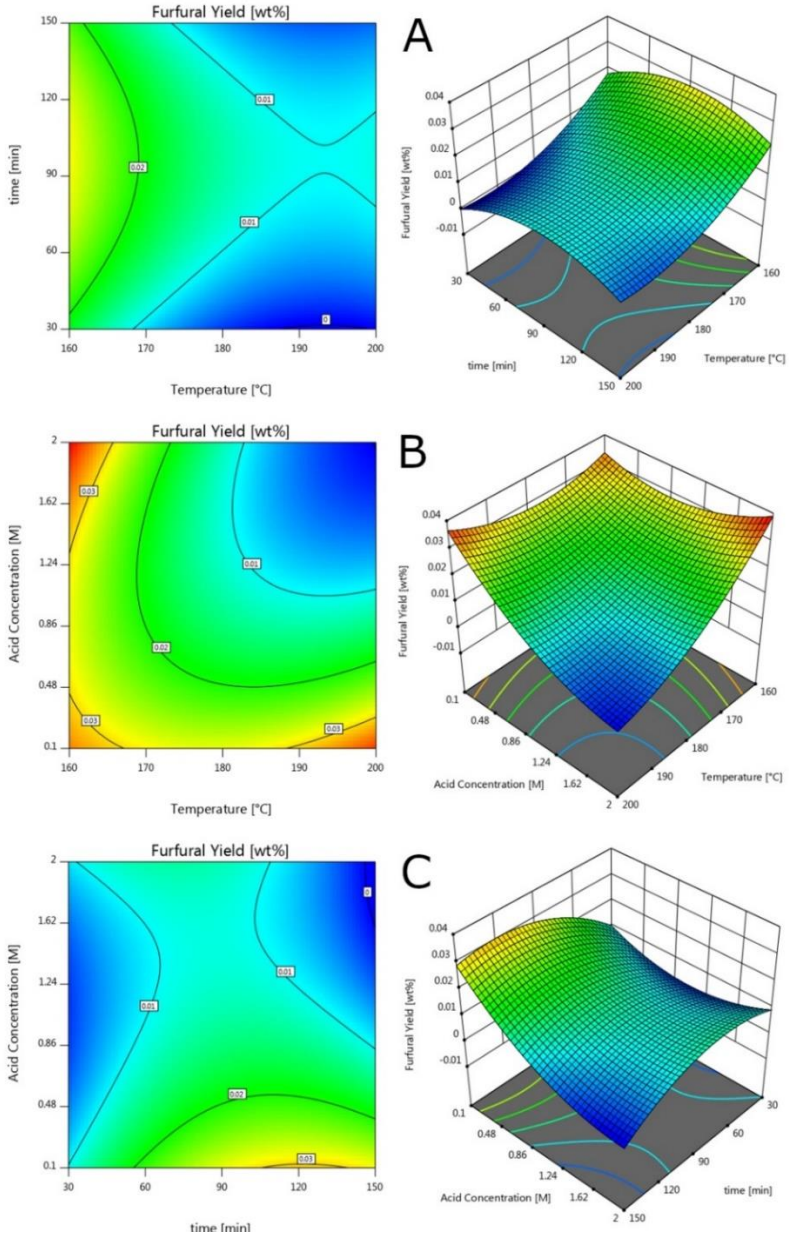

Figure 5.3: 3D response surface plots and 2D contour plots of furfural yield (wt.%) whist (A) varying temperature and time; (B) varying sulphuric acid concentration and temperature; (C) varying time and sulphuric acid concentration

5.3.4. Net Formic Acid

Formic acid was expected to primarily come as a stoichiometric by-product of levulinic acid formation [1]. However, the formic-to-levulinic acid ratio was never stoichiometric in this study and a discrepancy has also been reported in other works, which have attributed it to the degradation of sugars among other side reactions[26,27]. An understanding of the side reactions could be calculated by excluding the formic acid produced from levulinic acid. Though it should be noted that the formic acid from decomposed levulinic acid is not accounted for in this model and will over-estimate the net formic acid formation at higher conditions. The RSM model developed, shows that net formic can modelled to a high level of significance, represented by an adjusted R^2 of 90.64% and a lack of fit test of 0.896 (Appendix A – Table 4).

The highest observed net formic acid yield of +9.4 wt.% was recorded at 180 °C, 30 min and 0.1M H_2SO_4, which indicates that an initially large 9.4 wt.% of the poplar wood was converted to formic acid, possibly from the fast hydrolysis of hemi-cellulose and degradation of sugars. Formic acid formed in this manner should remain constant at higher temperatures and reaction times. It was therefore unexpected to observe an overall trend of decreasing formic acid with higher reaction time and temperature. The overall trends and negative net yields of formic acid of -0.9 wt.% and -4.9 wt.% were recorded at (200 ˚C, 90 min, 2M) and (180 ˚C, 150 min and 1.05M), indicate that formic acid is consumed in a side reaction. Formic acid has been found to be stable under similar conditions with monomeric sugars, suggesting such consumption is linked to the lignocellulose feedstock [26,28]. Lignin has been observed to decrease formic acid yields during acid hydrolysis [29] and could be attributed to the formylation of lignin under

microwave heating [30]. It is possible that consumption of formic acid is linked with the solid residue formation, however this aspect was not further investigated.

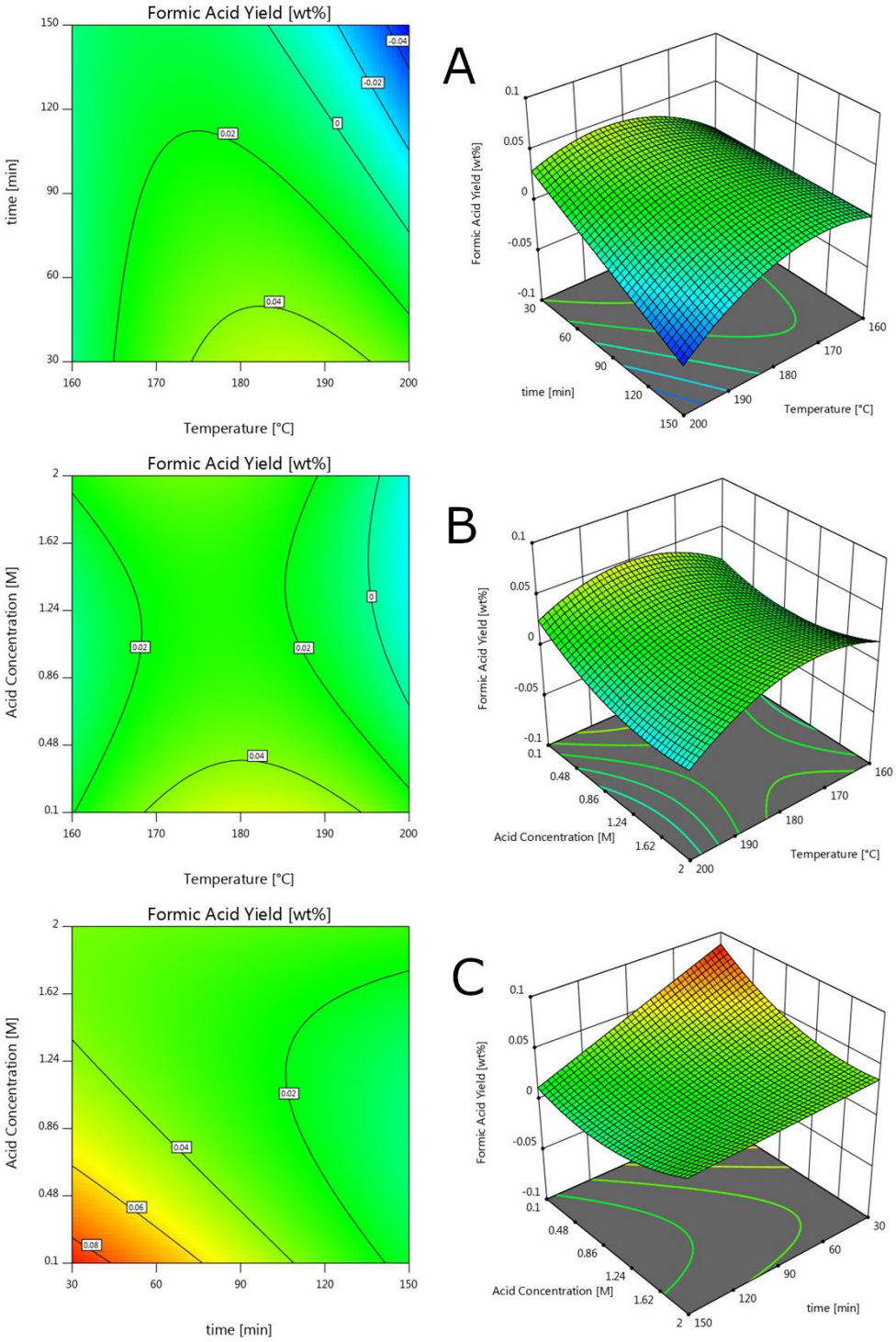

Figure 5.4: 3D response surface plots and 2D contour plots of net formic acid yield (wt.%) whilst (A) varying temperature and time; (B) varying sulphuric acid concentration and temperature; (C) varying time and sulphuric acid concentration

5.3.5. Acetic Acid Yields

Attempts were made at modelling the formation of acetic acid using ANOVA with no success in identifying a correlation of significance. The acetic acid appears to be relatively constant in the range of 2.43 wt.% ± 0.30 wt.% across most conditions. The highest and the lowest yields were 3.12% (180 ˚C,150 min, 2M) and 1.66% (200 ˚C, 90 min 2M) respectively. These outliers may suggest minor reactions are occurring. The consistent yield across all parameters, indicates the acetic acid was mostly present in the unreacted biomass and is easily solubilised [31]. This seems to indicate that acetic acid yields are not significantly affected by the reaction parameters but are rather inherent to feedstock composition.

5.3.6. Solid Residue Yields

The post-reaction solid residues were expected to contain the products of several distinct reactions including cellulose hydrolysis and humin formation. Though kinetic models would offer greater insight into optimization and reactor design, they require detailed reaction models that simply do not exist for all solids formation mechanisms. Despite this, it was possible to achieve a highly significant model (adj R^2 of 93.61%), with lack of fit being insignificant (p=0.94), as shown in the Appendix A – Table 5. The RSM model is, therefore, shown to be an appropriate tool for modelling the solid yields under catalytic conditions without the need of detailed of models as shown by the high R^2.

The lowest observed solids yield was 40.0 wt.% at 200 ºC, 30 min and 1.05M H_2SO_4 (Run 17), which corresponded with observed theoretical levulinic acid yield of 25.9%.

The low levulinic acid yield was associated with glucose yields of 20.1 wt.%, indicating substantial cellulose hydrolysis without sufficient time for the conversion of glucose into levulinic acid. The low solids yield was still in excess of the lignin content of poplar wood (25 wt.%) and can be further minimised, by using *Equation 5.3*, to 36.6 wt.% (theoretical levulinic acid yield of 52.3 wt.%) at the conditions of 200 ˚C, 64 min and 1.31M H_2SO_4. These low solids yields can be attributed to the hydrolysis of the cellulose and hemicellulose, after which solid residue yield will be affected by addition of condensed materials. In fact, from Figure 5.5a, it can be seen that high temperature and short reaction time appear to facilitate sufficient biomass solubilisation without causing significant solids formation. The second lowest observed solids yield of 41.3 wt.%[2] and 50.6% theoretical levulinic acid yield at 180 ˚C, 90 min and 1.05M H_2SO_4 shows that the process parameters can be optimised to increase levulinic acid yields with minimal effects on the solid residue yields. There was also a decrease in the solids yield between the highest actual and predicted levulinic acid yields (20.1 wt.% and 20.9 wt.%), which corresponded with solids yields of 59.2% and 52.1% respectively. The decrease in solids yield with levulinic acid optimisation is most likely caused by the reduction of parallel humin formation reactions, which shows a possible synergy between levulinic acid maximisation alongside solids minimisation.

$$Y_{solids} = 1.682 - 0.0475\,T - 0.00715\,t - 0.639\,C_{H2SO4} + 0.0000171\,T*t + 0.00131\,T*C_{H2SO4} - 0.00113\,t*C_{H2SO4} - 0.0000176\,t^2 + 0.116{C_{H2SO4}}^2 \qquad \textit{Equation 5.3}$$

[*] The conditions of 180 ˚C, 90 min and 1.05M $H2SO_{-4}$ were recorded 5 times in table 5.2 as part of the RSM methodology to estimate variance and stated values represent the average value

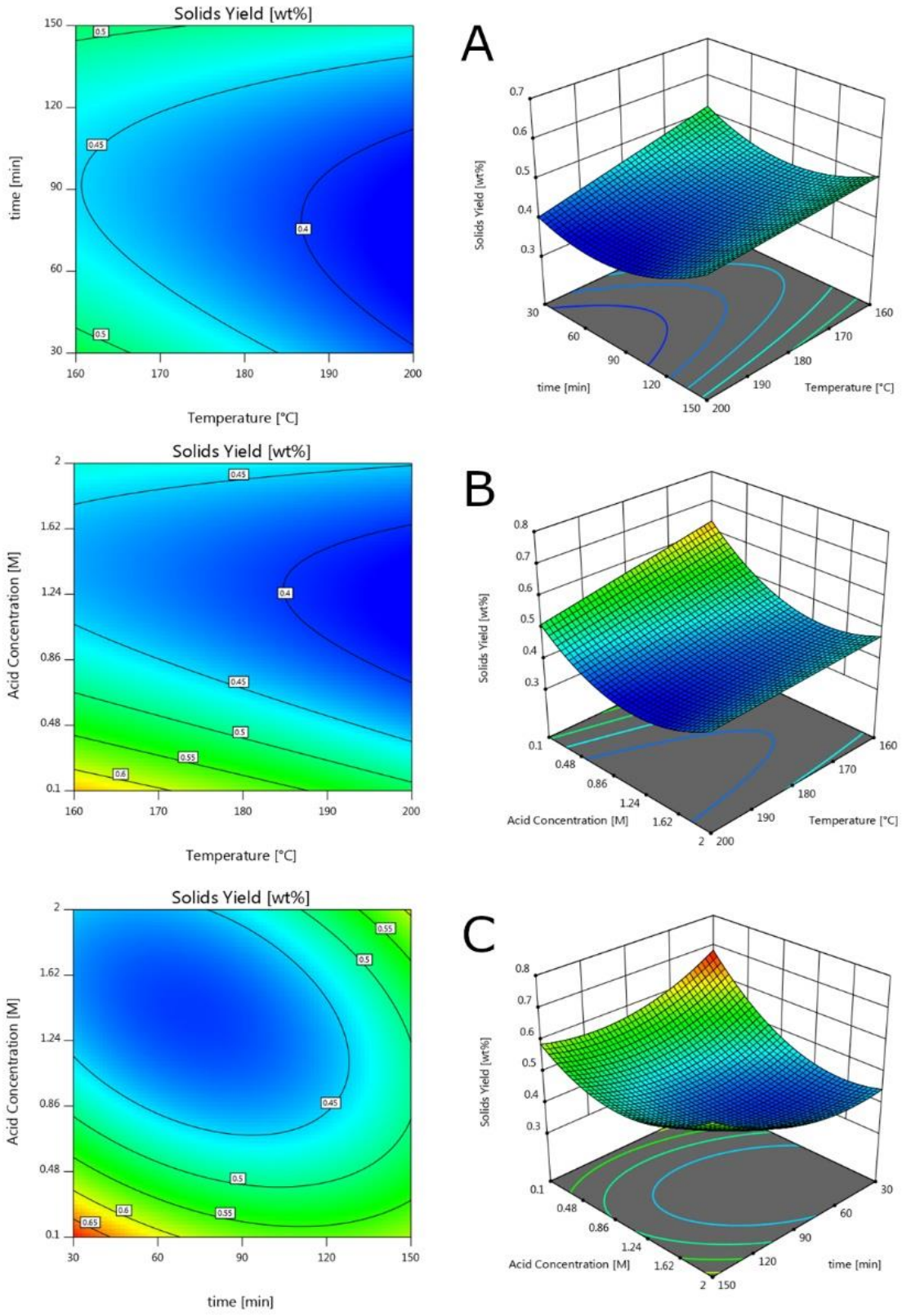

Figure 5.5: 3D response surface plots and 2D contour plots of solid residue yield (wt.%) whilst (A) varying temperature and time; (B) varying sulphuric acid concentration and temperature; (C) varying time and sulphuric acid concentration

The acid concentration had a significant effect on the solid yields, as shown in Figure 5.5b and 5.5c, by regulating both the solubilisation of the biomass as well as the formation of solid residues, which implies that the solids formation from lignocellulosic biomass is primarily acid catalysed. The moderate effect of temperature on the solids yield, as shown in Figure 4a and 4b, suggests that the formation of solids is reactant limited, meaning that solids could be minimised by utilising high temperature reactors in conjunction with low residence time. The solid residue yields significantly increased from 38.5wt.% to 57.5 wt.% between, 90 and 150 mins at 180 ˚C. This 20 wt.% increase in solids yield over 60 min indicates a large solids forming reaction process or system. The reduction in levulinic acid, formic acid and furfural over that time does not fully explain the increase in solids weight. This can only be partially attributed to the acid catalysed formation of humins by cross-polymerisation of 5-HMF and dehydration by-products [13,32,33]. The cross-polymerisation of sugars and intermediaries can be further catalysed by phenolic compounds similar to lignin [34], but would not fully explain the dramatic increase in yield after 90 min. Acid soluble lignin is a significant fraction of biomass that was not measured in this study. However, previous studies have reported condensation of acid soluble lignin with reactive intermediaries and sugars [25,35]. In order to fully understand the process of solid residue formation from lignocellulosic material, analysis and measurement of all aqueous by-products would be required.

Furthermore, a notable excess of gas formation at higher temperatures (200˚C) was observed, that could not be explained by gas expansion alone. Although the amount of gas formed could not be measured accurately, the formation of gas would potentially indicate hydrothermal carbonization (HTC) is taking place [36]. HTC has been reported

under sub-critical conditions for cellulose and lignin at 180-200˚C [37]. There are similarities between the catalytic formation of humins and biomass, with regards to polymerisation mechanisms and especially the role of 5-HMF[12,38]. Studies by Guiotoku *et al.* [39] hydrothermal carbonization of pine sawdust at 200 ˚C with citric acid found similar increases with reaction time (35%-45% increase between 60 and 240 min). Guiotoku attributed the increase in solids to the reaction of volatile compounds with lignin and observed deposition with SEM. This potentially could resemble catalytic humin growth and further study in this area is needed to elucidate some of the more complex reactions in both processes.

Under all reaction conditions, the solid residue yield exceeded that of levulinic acid despite the solids typically being considered a waste product. The solid residues should, therefore, be considered a distinct by-product that warrants further analysis. It would be desirable to either minimise solid residue yields or modify the characteristic properties of the solids for commercial applications, as the disposal of the solid residue would be of significant cost for future biorefineries.

5.3.7 Residues Characterisation and Potential Applications

The solid residues corresponding to the lowest solids yield (200 ºC, 30 min and 1.05 M H_2SO_4, Run 17) and highest levulinic acid yield (180 ºC, 150 min and 2 M H_2SO_4 , Run 1) were chosen for further characterisation alongside untreated poplar wood for comparison. The solid residue yields were quantified at 40 wt.% and 59 wt.% respectively. The solid residue elemental composition, identified by CHNSO and XRF analyses using the methods described in Chapter 3, is reported in Table 5.3, which

suggest similar chemical compositions despite differing reaction conditions. The decreases in H/C and O/C are indicative dehydration reactions, which are associated with the polysaccharide hydrolysis and humin formation [19,32]. The elemental composition of the solid residue indicates that the atomic ratios of H/C and O/C are similar to hydrochars [40].

Table 5.3: Elemental composition of solid residues and poplar wood on a dry basis

	Raw Poplar Wood	Lowest Solids Yield	Highest Levulinic Acid Yield
Solid Residue Yield (wt.%)	-	40.06	59.48
C (wt.%)	51.18	60.37	62.12
H (wt.%)	6.28	5.37	5.33
N (wt.%)	0.11	0.08	0.16
S (wt.%)	0.06	0.07	0.12
O (wt.%)*	42.22	32.46	30.84
Ash (wt.%)	2.16	1.64	1.45
$HHV_{predicted}$ (MJ / kg)	24.6	27.8	27.6
H/C	1.47	1.07	1.03
O/C	0.62	0.40	0.37
C/N	465	755	388
Mg (mg/kg)	224	20.8	9.3
Al (mg/kg)	71	28.1	29.9
Si (mg/kg)	52.9	41.2	41.6
P (mg/kg)	18.1	4.3	1.4
Cl (mg/kg)	11.3	16.8	13.6
K (mg/kg)	258	45.6	4.3
Ca(mg/kg)	525	20.7	10.9
Fe (mg/kg)	6.4	2.5	3.4
Cu (mg/kg)	2.2	0.6	0.5
Zn (mg/kg)	5.4	2.6	1.0

A significant increase in the carbon content from 51 wt.% to 60-62 wt.% occurred during the acid catalysis, with the solid residue forming carbon rich chars. This is further evidenced by the minimal difference between the calculated HHV of the two samples (28.2 and 28.0 $MJkg^{-1}$) in Table 5.3, which indicates potential the use of the solid residue as a fuel source. Therefore, the acid hydrolysis acts as an energy

densification process in the form of solid residue (when compared with HHV of commercially available poplar wood as fuel), in addition to the production of high value chemicals generated by this biorefining technique. Similar algae hydro-char, from the fast catalysis of red seaweed with sulphuric acid, found experimental higher heating values of 19–25 MJ kg^{-1} [20]. However, an increase in sulphur content, due to sulphuric acid catalyst, from 0.06 wt.% to 0.07-0.12 wt.% can also be observed. This would require post-combustion flue gas treatment and must be accounted for in a biorefinery scenario, where solid residue is used for combustion.

Trace elements analysis via XRF shows a decrease in concentrations of Mg, Al, Si, P, K, Ca, Fe, Cu and Zn due to leaching of these elements, as shown in Table 5.3. It is well known that metals have increased mobility at low pH and the catalysis process has caused acid extraction of the biomass [41], which may affect subsequent aqueous processes. The overall decrease in nutrients required for biological growth of microorganisms or soil amendment should also be noted, including a significant increase in the C/N ratio. The untreated poplar wood was inherently low in nutrients and, as result, the solid residue would perform poorly as fertiliser. However, there may be opportunities in the use of the solid residue as a hydrochar for stimulating microbial proliferation in anaerobic digestion systems or for carbon sequestration purposes. The use solid residue in hydrochar applications would require further investigation but could potentially be used as a soil amendment for energy crops, as a way to create a closed loop production method.

The structural changes in the solid residue between the two settings can be visually seen in Figure 5.6. The residue at the lowest solids yield, Figure 5.6a, has a similar

morphology to unreacted biomass, implying incomplete hydrolysis of the polysaccharide matrix. A honeycomb structure appears to have formed at the highest levulinic acid setting, Figure 5.6b, with significant spherical humin formation covering most of the residues external surface. Carbonaceous spheres are also present on Figure 5.6a, possibly linked with the fast degradation of furfural. The carbonaceous spheres resemble those reported in other works, [28,39] investigating humin growth from acid hydrolysis of lignocelluloses, confirming earlier discussions. Consequently, the increase in solid yields can be attributed to humin formation and can could be controlled to modify the solid residue properties in the future.

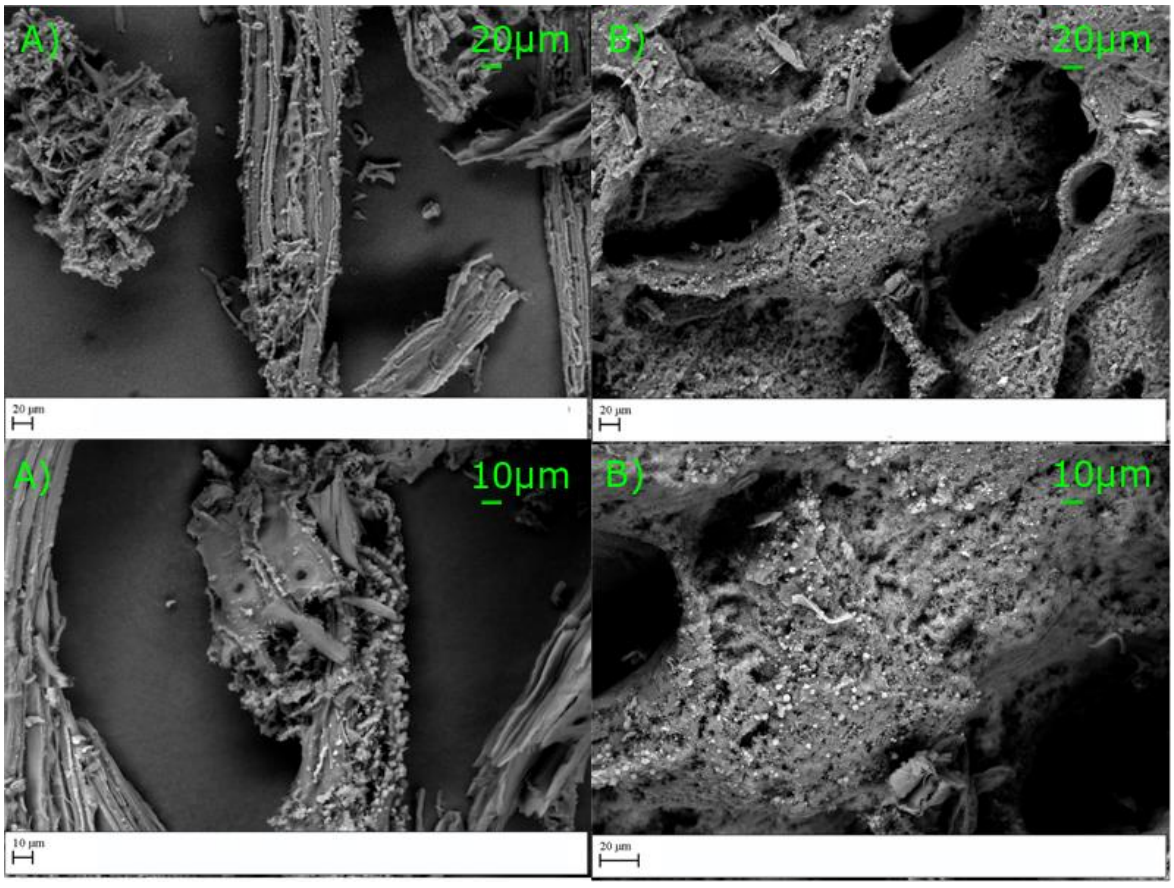

Figure 5.6: SEM images of solid residues produced from different reaction conditions: lowest Solids yield (A) and highest Levulinic acid yield (B)

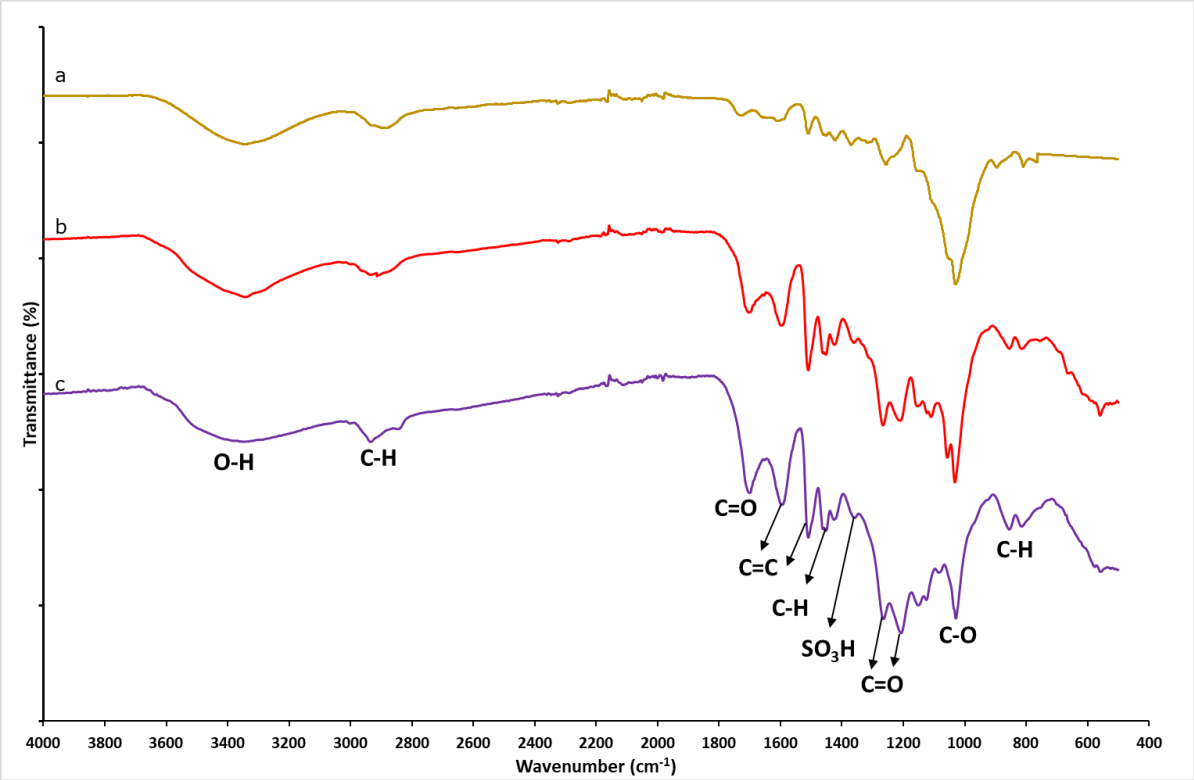

Figure 5.7: FTIR spectra of poplar wood (a), lowest solid residue (b), Highest levulinic acid yield (c).

The FTIR spectra of the solid residues and poplar wood are reported in Figure 5.7 and show the structural changes occurred during the acid hydrolytic process. The peaks at 3600-3000 cm^{-1}, 3000-2800 cm^{-1} and 1032 cm^{-1} are associated with O-H stretching, C-H bending and C-O stretching respectively from cellulose and hemicellulose. The gradual decrease in these three peaks indicates the partial degradation of the polysaccharide structures, with residual cellulose persisting at the longer reaction times. Other peaks can be attributed to a variety of functional groups such as: at 1700 cm^{-1} to C=O stretching, at 1595 and 1510 cm^{-1} to aromatic C=C stretching, finally at 1450 cm^{-1} to C-H bending. Moreover, the peaks at 1260 and 1210 are attributed to C-O stretching, while peaks between 950-750 cm^{-1} are normally associated with aromatic

C-H bending. Interestingly, the peak around 1360 cm^{-1} can be linked to SO_3H indicating sulfonation of the residue, which is in agreement with the elemental analysis findings. The functional groups present in the residue resemble lignin, hydochars and humins [13,15,42]. However, the increase in adsorption spectra with regards to time is atypical for hydrothermal carbonisation and can be attributed to humin formation. This is also demonstrated by the increase in C=C stretching at 1595 and 1510 cm^{-1}, which indicates further aromatisation and furan formation earlier associated with humins. The formation of stable aromatic structures with greater biogeochemical recalcitrance can potentially be used as a hydrochar for carbon sequestration [43].

5.4. Conclusions

This data from this chapter shows that the levulinic acid yields from the sulphuric acid catalysed conversion of poplar wood can be optimized through RSM methods, leading to yields of up to 21.0 wt.%. The levulinic acid yield correspond with a 61.2 mol.% which is near equivalent to current best standards. However, the solids yield varied significantly from 38-63 wt.% and under all conditions the solid residue yield exceeded that of levulinic acid, validating the necessity of solid residue valorisation. The solid residue was characterised and found to have potential use as a fuel or as hydrochar. The surface area was highly functionalised with a high surface O/C ratio due to catalytic humin deposition. The solid residue from sulphuric acid homogenous catalysis was investigated in Chapter 7 for the application of solid residue as an anaerobic digestion hydrochar-esque supplement.

The solid residue yields could be minimised by low reaction times and moderate acid conditions; however further work is needed to understand the reaction mechanisms involved with the formation of solid residue from the acid hydrolysis of lignocellulosic materials. Results indicate the hemicellulose and furfural conversion rates were excessively rapid and do not allow co-optimization of alongside levulinic acid yield in a single-stage reactor. It should also be noted that formic acid was greatly affected by variation of reaction conditions as well as important side reactions that appear to affect the yields of other products. This work constitutes a useful starting point for further studies aiming to understand how side reaction mechanisms are affected by reaction variables, as this is critical for developing cost-effective lignocellulosic biorefineries of the future.

5.5 References

1. Shen, J. & Wyman, C. E. Hydrochloric Acid-Catalyzed Levulinic Acid Formation from Cellulose: Data and Kinetic Model to Maximize Yields. AIChE J. 58, 236–246 (2012).

2. Galletti, A. M. R., Antonetti, C., De Luise, V., Licursi, D. & Di Nasso, N. N. O. Levulinic acid production from waste biomass. BioResources 7, 1824–1834 (2012).

3. Dussan, K., Girisuta, B., Haverty, D., Leahy, J. J. & Hayes, M. H. B. Kinetics of levulinic acid and furfural production from Miscanthus×giganteus. Bioresour. Technol. 149, 216–224 (2013).

4. Yu, I. K. M. & Tsang, D. C. W. Conversion of biomass to hydroxymethylfurfural: A review of catalytic systems and underlying mechanisms. Bioresour. Technol. 238, 716–732 (2017).

5. Chen, S. S., Wang, L., Yu, I. K. M., Tsang, D. C. W., Hunt, A. J., Jerome, F., Zhang, S., Ok, Y. S., Poon, C. S., Valorization of lignocellulosic fibres of paper waste into levulinic acid using solid and aqueous BrØnsted acid. Bioresour. Technol. 247, 387–394 (2018).

6. Kłosowski, G., Mikulski, D. & Menka, A. Microwave-Assisted One-Step Conversion of Wood Wastes into Levulinic Acid. Catalysts 9, 753 (2019).

7. Moriarty, K., Milbrant, A., Warner, E., Lewis, J., Schwab, A. 2016 Bioenergy Industry Status Report 2016 Bioenergy Industry Status Report. NREL Reports (2018).

8. Chen, S. S., Maneerung, T., Tsang, D. C. W., Ok, Y. S. & Wang, C. H. Valorization of biomass to hydroxymethylfurfural, levulinic acid, and fatty acid methyl ester by heterogeneous catalysts. Chem. Eng. J. 328, 246–273 (2017).

9. Su, J., Shen, F., Qiu, Qi, X. High-yield production of levulinic acid from pretreated cow dung in dilute acid aqueous solution. Molecules 22, (2017).

10. Kang, S., Pan, J., Gu, G., Wang, C., Wang, Z., Tan, J., Liu, G. Sequential production of levulinic acid and porous carbon material from cellulose. Materials. 11, 1–15 (2018).

11. Lopes, E. S., Leal-Silva, J .F., Rivera, E. C., Gomes, A. P., Lopes, M. S., Filho, R., Tovar, L. P. Challenges to Levulinic Acid and Humins Valuation in the Sugarcane Bagasse Biorefinery Concept. Bioenergy Res. (2020). doi:10.1007/s12155-020-10124-9

12. van Zandvoort, I., Wang, Y., Rasrendra, C. B., van Eck, E. R. H., Bruijincx, P. C. A., Heeres, H. J., Weckhusen, B. M. Formation , Molecular Structure , and Morphology of Humins in Biomass Conversion : Influence of Feedstock and Processing Conditions. Chem. Sus. Chem. 6 1745–1758 (2013).

13. Patil, S. K. R. R., Heltzel, J. & Lund, C. R. F. F. Comparison of structural features of humins formed catalytically from glucose, fructose, and 5-hydroxymethylfurfuraldehyde. Energy and Fuels 26, 5281–5293 (2012).

14. Runge, T. & Zhang, C. Two-Stage Acid-Catalyzed Conversion of Carbohydrates into Levulinic Acid. Ind. Eng. Chem. Res. 51, 3265–3270 (2012).

15. Tsilomelekis, G., Orella, M. J., Lin, Z., Cheng, Z., Zheng, W., Nikolakis, V., Vlachos, D. Molecular structure, morphology and growth mechanisms and rates

of 5-hydroxymethyl furfural (HMF) derived humins. Green Chem. 18, 1983–1993 (2016).

16. Melligan, F., Dussan, K., Auccaise, R., Novonty, E. H., Leahy, J. J., Hayes, M. H. B., Kwapinski, W. Characterisation of the products from pyrolysis of residues after acid hydrolysis of Miscanthus. Bioresour. Technol. 108, 258–263 (2012).

17. Sweygers, N., Dewil, R. & Appels, L. Production of Levulinic Acid and Furfural by Microwave-Assisted Hydrolysis from Model Compounds : Effect of Temperature , Acid Concentration and Reaction Time. Waste and Biomass Valorization 9, 343–355 (2018).

18. Mija, A., Waal, J. C. Van Der, Pin, J., Guigo, N. & Jong, E. De. Humins as promising material for producing sustainable carbohydrate-derived building materials. Constr. Build. Mater. 139, 594–601 (2017).

19. Agarwal, S., Es, D. Van & Jan, H. Catalytic pyrolysis of recalcitrant , insoluble humin byproducts from C6 sugar biorefineries. J. Anal. Appl. Pyrolysis 123, 134–143 (2017).

20. Cao, L., Yu, I. K. M., Cho, D. W., wang, D., Tsang, D. W., Zhang, S., Ding, S., Wang, L., Ok, Y. S. Microwave-assisted low-temperature hydrothermal treatment of red seaweed (Gracilaria lemaneiformis) for production of levulinic acid and algae hydrochar. Bioresour. Technol. 273, 251–258 (2019).

21. Kang, S., Fu, J. & Zhang, G. From lignocellulosic biomass to levulinic acid: A review on acid-catalyzed hydrolysis. Renew. Sustain. Energy Rev. 94, 340–362 (2018).

22. Hendriks, A. T. W. M. & Zeeman, G. Bioresource Technology Pretreatments to

enhance the digestibility of lignocellulosic biomass. 100, 10–18 (2009).

23. Danon, B., Aa, L. Van Der & Jong, W. De. Furfural degradation in a dilute acidic and saline solution in the presence of glucose. Carbohydr. Res. 375, 145–152 (2013).

24. Sairanen, E., Karinen, R. & Lehtonen, J. Comparison of Solid Acid-Catalyzed and Autocatalyzed C5 and C6 Sugar Dehydration Reactions with Water as a Solvent. Catalysis Letters 14, 839–1850 (2014)

25. Dussan, K., Girisuta, B., Lopes, M., Leahy, J. J. & Hayes, M. H. B. Effects of Soluble Lignin on the Formic Acid-Catalyzed Formation of Furfural: A Case Study for the Upgrading of Hemicellulose. ChemSusChem 9, 492–504 (2016).

26. Flannelly, T., Lopes, M., Kupiainen, L., Dooley, S. & Leahy, J. J. Non-stoichiometric formation of formic and levulinic acids from the hydrolysis of biomass derived hexose carbohydrates. RSC Adv. 6, 5797–5804 (2016).

27. Swift, T. D., Baiga, C., Choudhray, V., Peklaris, G., Nikolakis, V., Vlachos, D. G. Kinetics of homogeneous Brønsted acid catalyzed fructose dehydration and 5-hydroxymethyl furfural rehydration: A combined experimental and computational study. ACS Catal. 4, 259–267 (2014).

28. Qi, Y., Song, B. & Qi, Y. The roles of formic acid and levulinic acid on the formation and growth of carbonaceous spheres by hydrothermal carbonization. RSC Adv. 6, 102428–102435 (2016).

29. Yoon, S. Y., Han, S. H. & Shin, S. J. The effect of hemicelluloses and lignin on acid hydrolysis of cellulose. Energy 77, 19–24 (2014).

30. Wang, Q., Guan, S. & Shen, D. Experimental and kinetic study on lignin

depolymerization in water/formic acid system. Int. J. Mol. Sci. 18, (2017).

31. Gong, S. H., Im, H. S., Um, M., Lee, H. W. & Lee, J. W. Enhancement of waste biomass fuel properties by sequential leaching and wet torrefaction. Fuel 239, 693–700 (2019).

32. van Zandvoort, I., Koers, E. J., Weingarth, M., Bruijnincx, P. C. A., Baldus, M., Weckhuysen, B. M. Structural characterization of 13C-enriched humins and alkali-treated 13C humins by 2D solid-state NMR. Green Chem. 17, 4383–4392 (2015).

33. Patil, S. K. R. & Lund, C. R. F. Formation and Growth of Humins via Aldol Addition and Condensation during Acid-Catalyzed Conversion of 5-Hydroxymethylfurfural. 4745–4755 (2011). doi:10.1021/ef2010157

34. Ryu, J., Jin, D. & Ahn, D. J. Hydrothermal preparation of carbon microspheres from mono-saccharides and phenolic compounds. Carbon N. Y. 48, 1990–1998 (2010).

35. Matsushita, Y., Kakehi, A., Miyawaki, S. & Yasuda, S. Formation and chemical structures of acid-soluble lignin II: Reaction of aromatic nuclei model compounds with xylan in the presence of a counterpart for condensation, and behavior of lignin model compounds with guaiacyl and syringyl nuclei in 72% sulfuric. J. Wood Sci. 50, 136–141 (2004).

36. Nizamuddin, S., Baloch, H. A., Siddiqui, M. T. H., Mubarak, N. M., Tunio, M. M., Bhutto, A. W., Jatoi, A. S., Griffin, G. J., Srinivasan, M. An overview of microwave hydrothermal carbonization and microwave pyrolysis of biomass. Rev. Environ. Sci. Bio/Technology 17, 813–837 (2018).

37. Heidari, M., Dutta, A., Acharya, B. & Mahmud, S. A review of the current knowledge and challenges of hydrothermal carbonization for biomass conversion. J. Energy Inst. (2018). doi:10.1016/j.joei.2018.12.003

38. Lei, Y. & Tian, R. Morphology evolution , formation mechanism and adsorption properties of hydrochars prepared by hydrothermal carbonization of corn stalk RSC Advances, 107829–107835 (2016). doi:10.1039/c6ra21607b

39. Guiotoku, M., Rambo, C. R., Hansel, F. A., Magalhães, W. L. E. & Hotza, D. Microwave-assisted hydrothermal carbonization of lignocellulosic materials. Mater. Lett. 63, 2707–2709 (2009).

40. Kambo, H. S. & Dutta, A. A comparative review of biochar and hydrochar in terms of production , physico-chemical properties and applications. Renew. Sustain. Energy Rev. 45, 359–378 (2015).

41. Kröppl, M. & Lanzerstorfer, C. Acidic extraction and precipitation of heavy metals from biomass incinerator cyclone fly ash. E3S Web Conf. 1, 10–13 (2013).

42. Jaruwat, D., Udomsap, P., Chollacoop, N., Fuji, M. & Eiad-Ua, A. Effects of hydrothermal temperature and time of hydrochar from Cattail leaves. AIP Conf. Proc. 2010, (2018).

43. Singh, B., Fang, Y. & Johnston, C. T. A fourier-transform infrared study of biochar aging in soils. Soil Sci. Soc. Am. J. 80, 613–622 (2016).

Chapter 6: Synergistic catalytic effect of Sulphated Zirconia – HCl system for levulinic acid and solid residue production

Published in: Energies 2021, 14(6): p1582

DOI: 10.3390/en14061582

Graphical Abstract

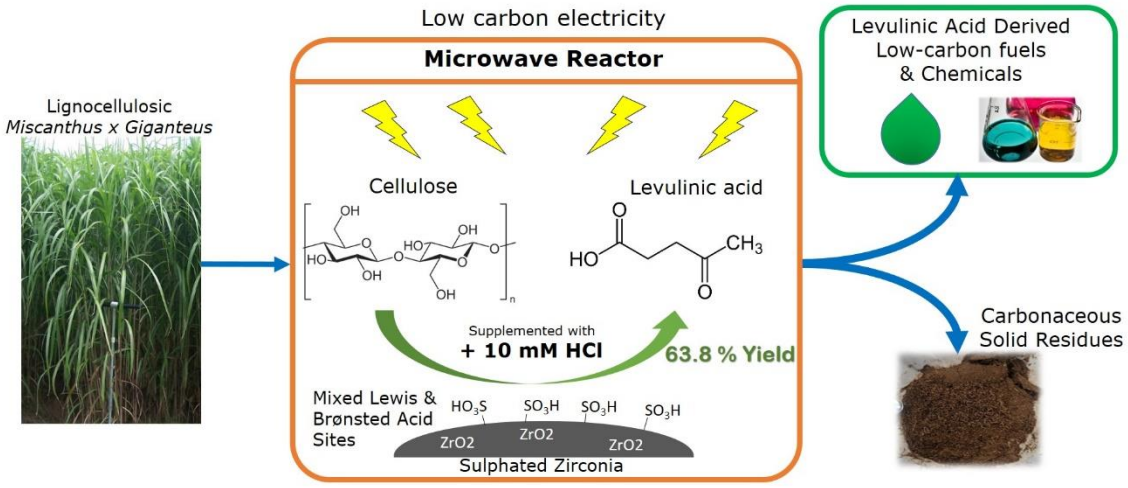

Abstract

This chapter investigates the synergistic conversion of *Miscanthus x Giganteus* with sulphated zirconia and dilute hydrochloric acid. The sulphated zirconia was prepared using H_2SO_4 impregnation and characterized using XRD, EDX, SEM and nitrogen adsorption-desorption measurements. The microwave assisted reaction was evaluated at various temperatures, reaction times and catalysts-to-biomass ratios, with and without the presence of trace HCl in the solution medium, for the conversion of *Miscanthus x Giganteus* to levulinic acid. The highest levulinic acid yield of 63.8% was achieved at 160 ˚C, 80 mins, 2:1 CBR with 10 mM HCl. The catalyst recyclability was investigated with and without calcination, finding that significant humins deposition on the catalysts surface likely caused catalyst deactivation. The post-reaction Solid Residue (SR) was also characterized using SEM, EDX, XRD, elemental composition and nitrogen ad-sorption-desorption measurements. SR produced with heterogeneous catalysts were contained significant amounts of unreacted cellulose and did not exhibit noticeable surface functionalisation. This resulted in SR that was markedly different to equivalent homogenous catalyst derived residue. Findings indicate that this residue could potentially be used as a soil amendment or as fuel source. The synergistic conversion of real lignocellulosic biomass with sulphated zirconia and trace hydrochloric acid showed remarkable promise and should be investigated further.

6.1. Introduction

Heterogeneous solid acid catalysts have been proposed by several studies [1–8] as replacements for H_2SO_4 and HCl mineral acids for the production of levulinic acid (LA). Solid acid catalysts can significantly reduce equipment corrosion, lower environmental impact and offer a more cost-effective catalyst recovery method. The acidic properties of some metal oxides can be further increased by sulphate doping in order to increase the number of Brønsted and Lewis acid sites [9]. Additionally, widely used industrial solid acids such as sulphated zirconia (SZR) catalyse the formation of LA from lignocellulose at significantly lower concentrations than mineral acids [10,11]. SZR displays both Lewis and Brønsted acidy, which is required for glucose isomerization to fructose, and subsequent dehydration to 5-HMF respectively. SZR has been reported to convert both simple and complex carbohydrates into 5-HMF at high rates (30-62% and 98% yield respectively [12,13]).

However, the conversion of solid lignocellulosic biomass with heterogeneous catalysts has resulted in significantly lower LA yield compared with monosaccharide sugars, primarily caused by limited ‘solid-solid’ interaction. Recent studies have shown that efficiency of solid catalysts can be promoted through addition of chloride salts or dilute HCl, reducing the solid-solid interaction bottleneck [1,14,15] As the efficient conversion of mono-saccharides towards LA with ZrO2 has been previously reported, the synergism with trace HCl could potentially increase LA yields when using real lignocellulosic biomass. Whilst the solid residue (SR) formation mechanism with homogenous catalysts have been greatly explored however there has been no confirmation if the SRs are similar. Specifically, the SR from heterogeneous catalysis of biomass has been under characterised and unexplored with regards to both composition and yields.

To address this gap in knowledge, this study investigated the use of sulphated zirconium dioxide as heterogeneous catalyst for the production of LA from a lignocellulosic energy crop, *Miscanthus x Giganteus. Miscanthus x Giganteus* was chosen as exemplar lignocellulosic feedstock, due to its high hexose content, low fertiliser requirements and widespread growing capacity; that makes it among the most promising energy crops in the UK [16]. This study also included the investigation of the addition of dilute 10 mM HCl, the optimisation of the reaction conditions for maximised yield of desired product (LA) and the quantification of SR by-product. The latter was also characterised for their potential applications.

6.2. Extended Methodology

6.2.1. Materials and Catalyst Characterisation

The Sulphated Zirconium Dioxide (SZR) catalyst was prepared using commercial $Zr(OH)_4$ (Sigma Aldrich 97%), which was suspended in a 0.5M solution of H_2SO_4 under vigorous stir-ring for 1 hour. *Miscanthus x Giganteus* (3) was dried at 105 °C for 24 hours and reduced to fine powder (≤ 1 mm) with a Restsch ZM500 ball mill. The obtained compositions (on an oven-dry basis wt.%) were 1.82% ±0.02 ash, 5.33% ±0.28 total extractives, 17.95% ±0.14 Klason lignin, 38.86% ±0.42 cellulose (glucan), and 24.08% ±0.73 hemicelluloses.

6.2.2. Acid Hydrolysis

A CEM MARS 5 microwave reactor was used as the bench scale reactor for the acid hydrolysis. The acid hydrolysis of poplar wood and SR separation was conducted according to the procedure depicted in Figure 6.1. In each experiment 0.25 g of *Miscanthus x Giganteus* was mixed with 10 ml of either grade 2 deionised water or 10 mM HCl acid solution (depending on experimental objectives) to achieve a biomass loading ratio of 5 wt.%. The catalysis operating parameters of Temperature, time and catalyst-to-biomass ratio (CBR) were the primary operating variables, in addition to the presence of 10 mM HCl. Following the completion of the desired reaction time SR was separated and the hydrolysate was analysed using HPLC with a UV detector (λ =266 nm).

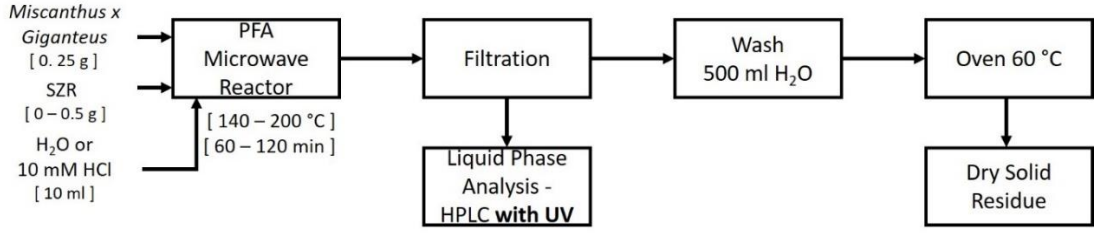

Figure 6.1: Microwave hydrolysis process and SR separation

6.2.3. Catalyst Separation and Regeneration

The dried post-reaction solids were separated by size using 68 µm and 125 µm mesh screens with a sieve shaker, before storing in airtight containers for further use. With the <68 µm and >125 µm fractions corresponding with the recycled catalyst and SR respectively. The weight of each fraction was recorded and adjusted for solids lost during the screening process due to solids transfer. Recycled catalyst was either dried at 105 °C (uncalcined) and calcined catalyst was prepared using a muffle furnace at 450 °C for 6 hours.

6.2.4. Statistics and Experimental design

The effects of the reaction parameters; Temperature (˚C), Time (minutes) and CBR on the levulinic acid yield were investigated using Response Surface Methodology (RSM). The experimental order was designed using a three level Box-Behnken experimental design with a randomised run order, each set of conditions was repeated in triplicate, except the central point was replicated 5 times (as dictated by the method) and individually reported. The levels of the 3 variables in this RSM is shown in Table 6.1, and the full run order is shown in Appendix B – Table 1.

Table 6.1: Levels of the acid hydrolysis process variables

	Unit	Variable Levels		
		low	medium	high
Temperature	°C	160	170	180
Time	min	30	60	90
CBR	-	0.0	1.0	2.0

6.2.5 ICP Analysis

Inductively coupled plasma optical emission spectrometry (ICP-OES) was used to measure the dissolved Zr(IV) in the post reaction solution using a ICS5000, Thermo Scientific, USA. The rate of leaching was evaluated at the optimum reaction conditions (160 ˚C, 80 mins and 2:1 CBR) with and without biomass. In order to stabilise the soluble ions and prevent precipitation, 1 ml of 67 wt.% nitric acid was added to 9 ml of liquor using a volumetric flask.

6.3. Results and discussion:

6.3.1. Effects of process variables on LA production

The SZR catalyst was investigated for the conversion of biomass to LA with only deionised water at first, then with 10 mM HC as the reaction medium. Process variables ranged between 140 – 200 °C for 60 – 120 minutes, as shown in Figure 6.2. The highest LA yield was 32% at 160 °C for 1 hour in deionised water only, which was less than literature LA yields with a similar sulphated catalyst for the conversion of microcrystalline cellulose [17]. This study detected negligible yields of key intermediates of LA production, such as 5-HMF, which was previously reported as the bottleneck by Kassaye et al. with similar sulphated zirconium [17]. Other zirconium based catalysts with zirconia and zirconium phosphate reported LA yields of 53.9% and 52.9% respectively from micro-crystalline cellulose with deionised the water [12,13]. The LA yields achieved in this study indicate the heterogeneity and physical complexity of real lignocellulose substrates reduces solid-solid interaction compared with pure microcrystalline cellulose, and can be regarded as the primary cause of the decrease in LA when using real biomass.

The addition of trace HCl drastically increased the LA yields under nearly all conditions, achieving a 61.5% LA yield at 160 °C for 1 hour with a CBR of 2:1. This yield is comparable with the commercialised Biofine process, which achieved a 67% LA yield using H_2SO_4 catalysts with similar Miscanthus x Giganteus [18]. The increase in LA yields could be attributed to the increased efficiency of SZR due to the acidic medium and/or a direct effect of trace HCl on biomass conversion towards oligosaccharides. The use of 10 mM HCl in the absence of SZR exhibited low LA yields

(below 5% under all conditions), showing that trace HCl had minimal direct effect other than synergism with the sulphated zirconium

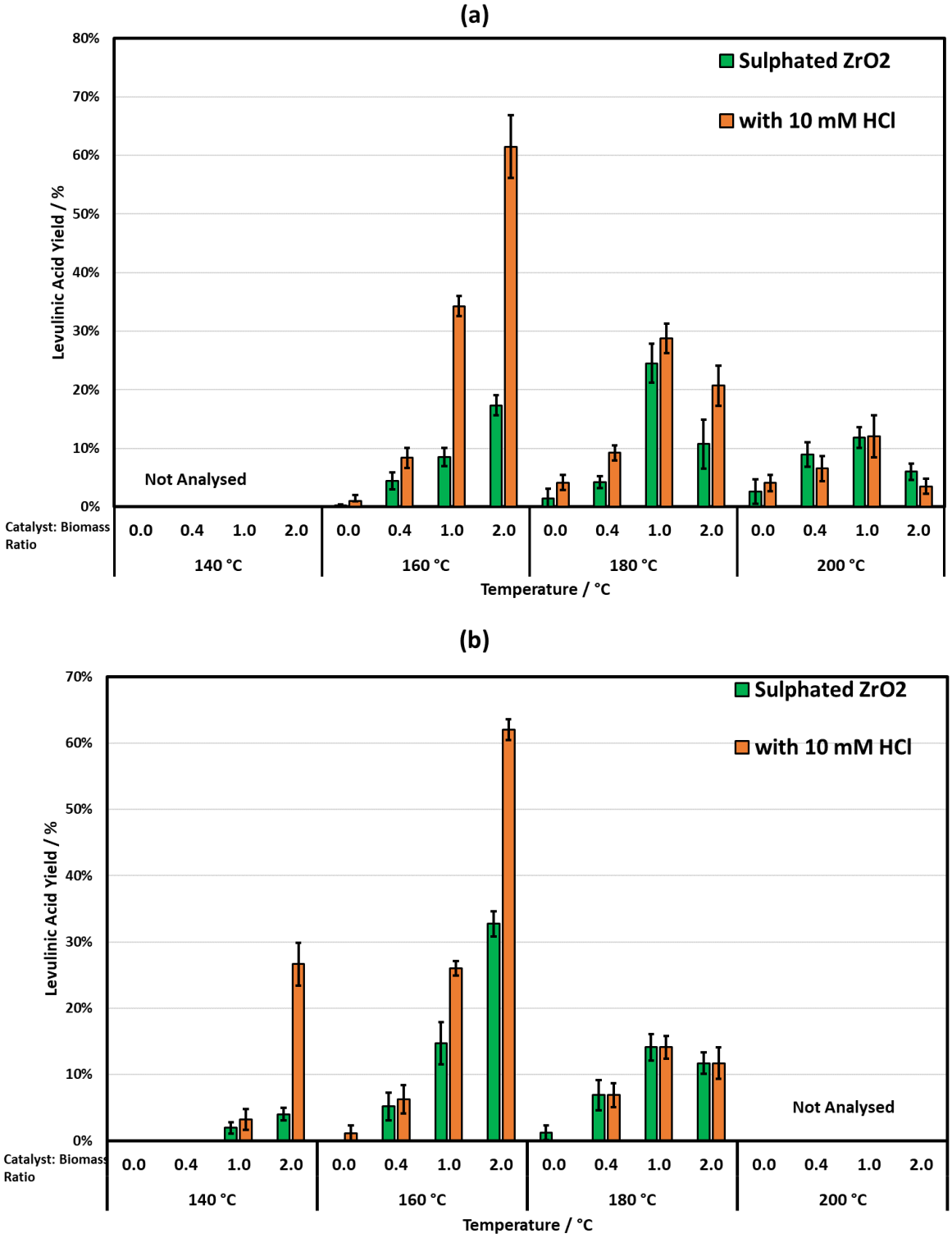

Figure 6.2: LA yield from SZR catalysis of Miscanthus x Giganteus in 10 ml of water or 10 mM HCl with varying CBR for; (a) 60 mins; (b) 120 mins

Oligosaccharides and monosaccharides were not measured in this study although, it may be possible that the trace HCl at such low quantities is acting as a simultaneous pre-treatment alongside the SZR catalysis [15]. The LA yields increased significantly with increasing CBR up to 2:1, below 160 °C. This clearly suggests that the SZR is the primary catalyst compared to the dilute hydrochloric acid, and higher catalyst ratios could yield further benefits. However, a CBR beyond 2:1 was not investigated, due to slurry issues with such high solids loading in the reactor configuration.

A noticeable reduction of LA yields occurs with increasing CBR from 1 to 2 at temperatures exceeding 180 °C. This suggests that at higher temperatures SZR could be catalysing the degradation of LA or high temperature humin formation is partially deactivating the catalyst. Most promisingly, the effect of dilute HCl at 140 °C showed a remarkable increase from 3.0% to 26.6%, despite the low temperature conversion of cellulose being notoriously difficult. This improvement may be indicative of the potential heterogeneous catalyst synergy with aqueous ions for low temperature biomass catalysis and should be explored further.

6.3.2 RSM Optimization

The reaction parameters (time, temperature and CBR) were further optimised via RSM modelling of the system for maximised LA production. The optimisation of the HCl-SZR ratio, with regards to Lewis - Brønsted acid ratio optimisation, was not considered in study as the focus was the investigation of SZR. The levulinic acid yields were modelled using a modified ANOVA, resulting in an adj-R^2 = 87.40% (Appendix B – Table 2) according to *Equation 6.1* and shown in Figure 6.3. Using *Equation 6.1*, the highest predicted LA yield was predicted at approximately 160 °C for 80 mins, which upon validation was found to result in a 63.8% LA yield. The levulinic acid yields followed similar patterns with regards to reaction time and temperature as that of H_2SO_4 in Chapter 5. However, at higher CBR there was minimal decrease in levulinic acid yields, suggesting that catalyst was not directly degrading to levulinic acid or that the system was catalyst limited. As the optimised reactions conditions resulted in the highest product yields, these conditions were chosen for the investigation of catalyst recyclability and SR characteristics.

$$Y_{LA} = -47.27 + 0.500\,T + 0.118\,t + 2.960CBR - 0.0006T * t - 0.016\,t * CBR - 0.00132\,T^2 - 0.00014\,t^2 \qquad \textit{Equation 6.1}$$

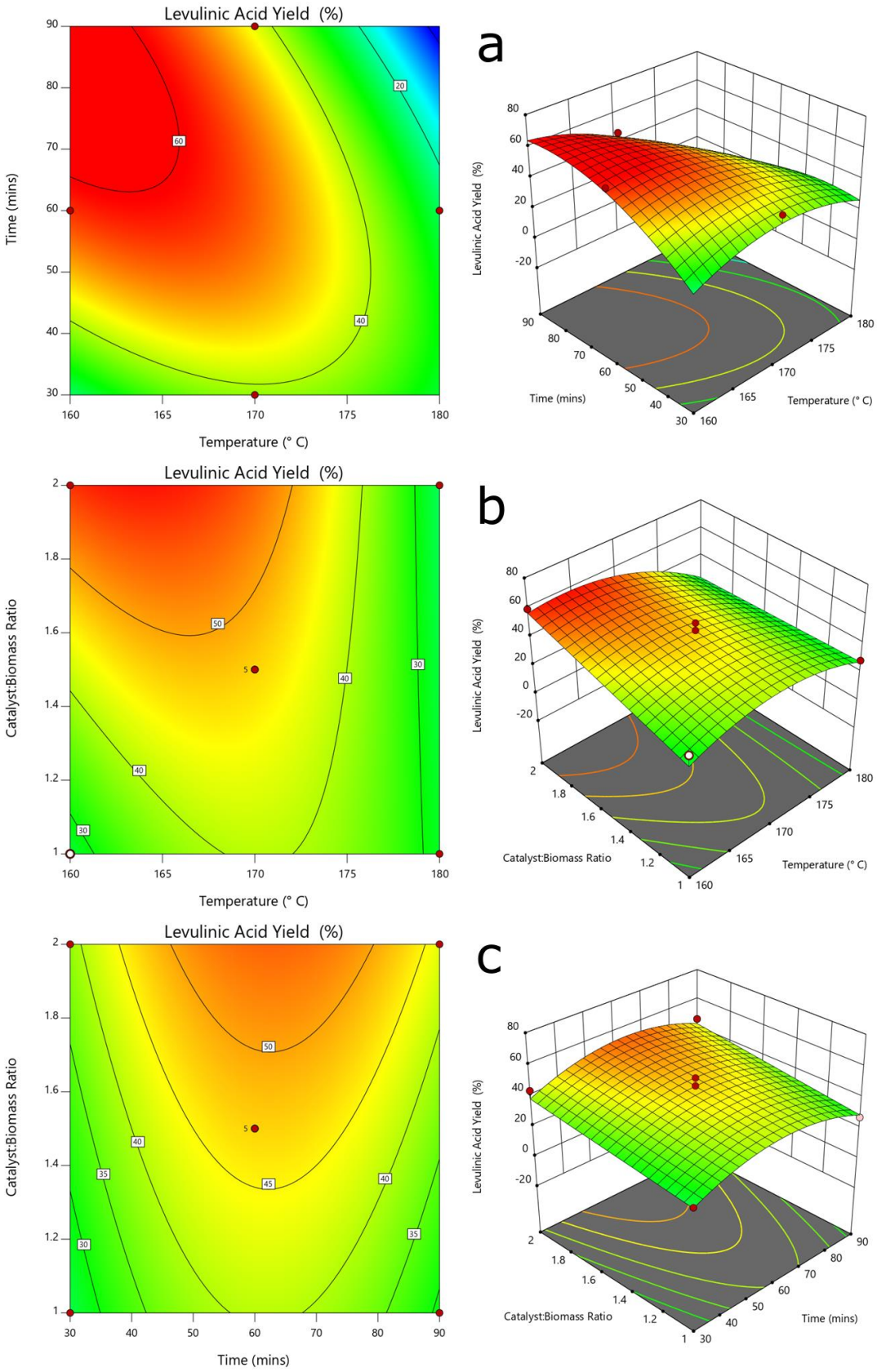

Figure 6.3: 3D response surface plots and 2D contour plots of levulinic acid yield (mol.%) whist (A) varying time and temperature; (B) varying CBR and temperature; (C) varying CBR and time.

6.3.3 Catalyst Characterisation and Recyclability

The sulphation of zirconium dioxide resulted in the surface modification shown in Figure 6.4a and 6.4b. The XRD pattern (Figure 2c) shows the presence of tetragonal phase of zirconium dioxide, given by the reflections at 31°, 50° and 60° two theta, which closely corresponds with those previously reported in literature [19]. The surface composition was analysed using EDX (Figure 2d) and revealed a high degree of sulphation was achieved with a surface sulphur content at 4.0 % wt., which is directly responsible for the required acidity during the reaction. This suggests a significant increase of the surface acidity compared to uncoated ZrO_2. The BET surface area, shown in Table 6.2, was measured at 72 m^2/g with a significant external surface area of 53 m^2/g and presence of mesopores (Appendix B - Figures 1 & 2) available for cellulose hydrolysis. The NH3-TPD acidity of unreacted SZR was measured to be 0.47 mmol/g, which aligns with values in other works with sulphated zirconias[12,20].

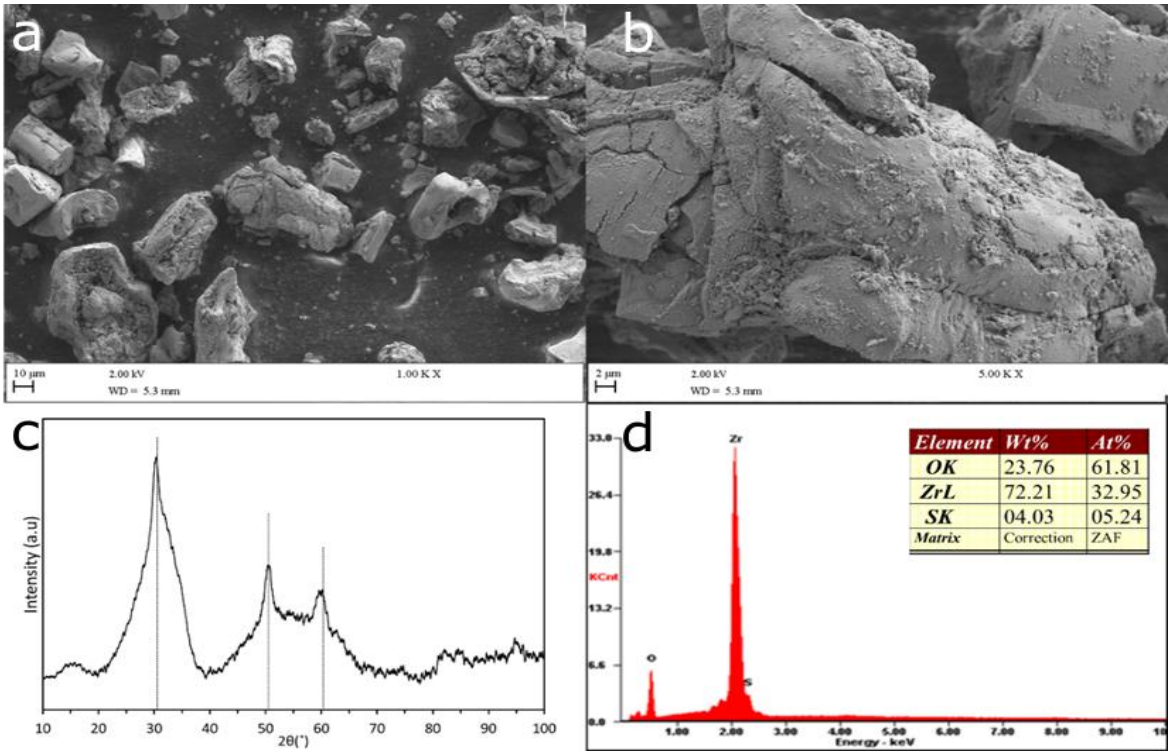

Figure 6.4: (a & b) SEM images of SZR catalyst; (c) XRD pattern of SZR; (d) EDX of SZR

Table 6.2: BET surface area (SBET), total pore volume (VTOTAL), micropore volume (VMICRO), external surface area (SEXT) and average pore size (D) (calculated from the BET surface area and the total pore volume assuming cylindrical pores ($D = 4V_{TOTAL}/S_{BET}$)) of Raw SZR and SR.

Sample	S_{BET} ($m^2\ g^{-1}$)	V_{TOTAL} ($cm^3\ g^{-1}$)	V_{MICRO} ($cm^3\ g^{-1}$)	S_{EXT} ($m^2\ g^{-1}$)	D (nm)
Raw SZR	72	0.10	0.009	53	5.6
SR formed under optimum conditions	23	0.11	0.005	13	19.9

The catalyst recyclability is of utmost importance to lower the running costs of catalytic biorefineries. The solid acid catalyst was mechanically separated from the SR through a 68 µm sieve, which resulted in a 63% catalyst recovery and ~12% volatile solids catalyst contamination. The volatile solids were measured after each recycle and the weight of catalyst was adjusted to maintain a 2:1 CBR on a non-volatile solid basis. The effects of calcination at 450 °C on catalyst reusability was investigated to understand both the possible catalyst deactivation mechanisms and to evaluate possible non-calcined catalyst recovery processes, as shown in Figure 6.5.

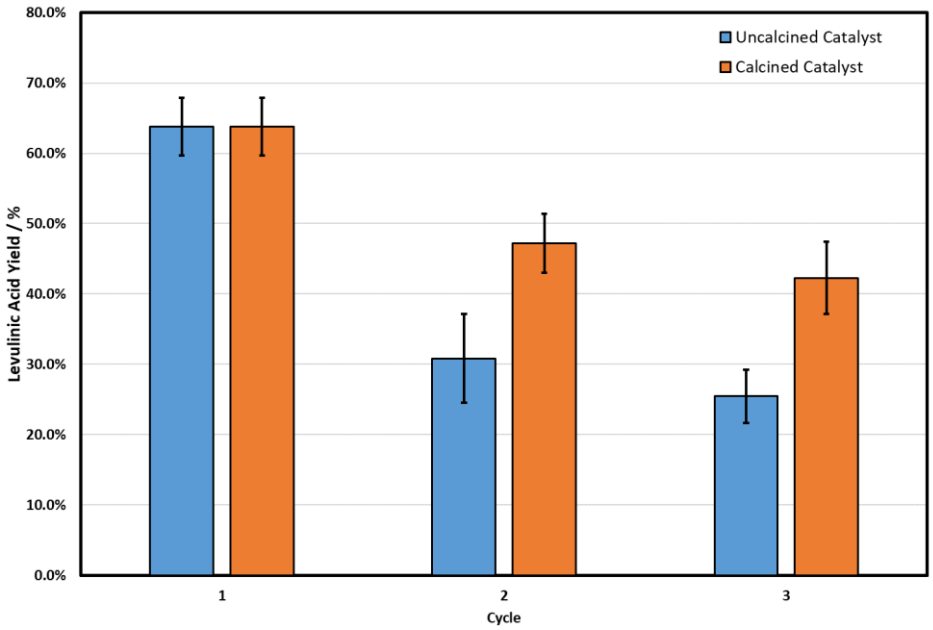

Figure 6.5: Reusability of the SZR catalyst using uncalcined and calcined at 450 °C catalyst with 0.25 g of *Miscanthus x Giganteus* in 10 ml of 10 mM HCl at 160 °C at 80 mins with a 2:1 catalyst top biomass ratio.

The reuse of SZR over 3 consecutive cycles with and without calcination (uncalcinated) resulted in a drop in levulinic acid yields from *Miscanthus x Giganteus*. The non-calcined SZR experienced a significant drop in LA yields to 25.5% at the third cycle compared with a 42.3% yield with calcined catalyst. The EDX analysis of the recycled catalysts (Figure 6.6a) shows that uncalcined catalyst surface has a higher surface carbon content (28.6 wt.%) compared to calcined catalyst (20.4 wt.%).

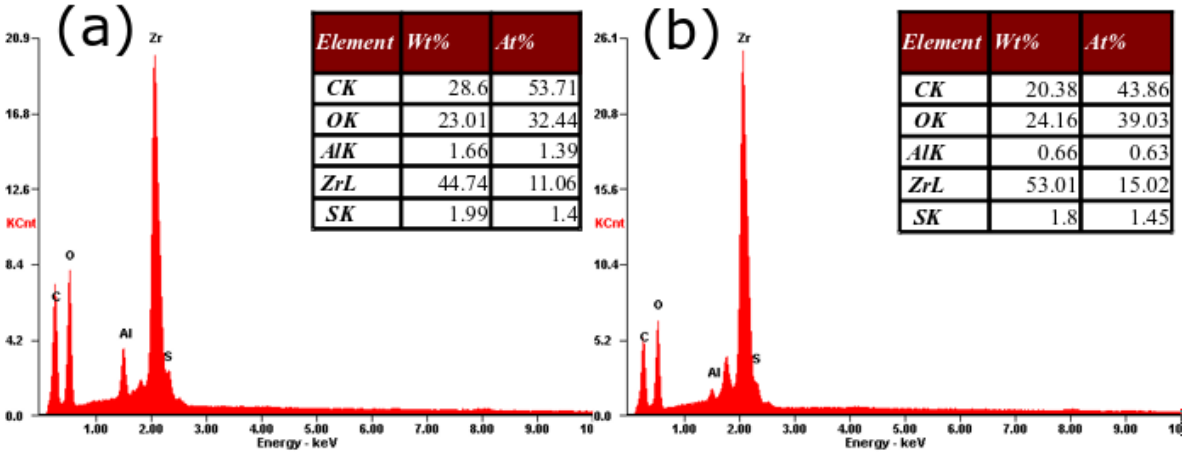

Element	Wt%	At%
CK	28.6	53.71
OK	23.01	32.44
AlK	1.66	1.39
ZrL	44.74	11.06
SK	1.99	1.4

Element	Wt%	At%
CK	20.38	43.86
OK	24.16	39.03
AlK	0.66	0.63
ZrL	53.01	15.02
SK	1.8	1.45

Figure 6.6: EDX pattern of; (a), uncalcined catalyst and (b), calcined catalyst after 3 catalysis cycles with *Miscanthus x Giganteus at* 180 °C for 80 minutes with a 2:1 catlyst:biomass ratio in 10 mM HCl

The increase of surface carbon suggests the adsorption of carbon compounds, humin formation or other carbonaceous residues forming on the catalyst surface are. Such higher carbon could be indicative of the transfer of humin formation from the SR, as seen with homogenous catalysts in Chapter 5, towards forming near the acid sites of the catalysts which caused the reduction in LA yields with multiple recycles. Calcination of the recycled catalysts at 450 °C partially alleviated this issue but did not completely reduce the surface carbon. Higher calcination temperature may reduce the surface carbon content further, however others studies have found that synthetic humins are thermally robust at higher temperatures with only a 66 wt.% decomposition at 1000 °C [21]. Therefore, thermal calcination of SZR may not be sufficient to reduce

humin poisoning without catalytic tar reduction. In addition, a decrease in surface sulphur content (1.73-1.95%) was observed compared to 4.3 wt.% in the unreacted catalyst, which indicates possible desulphation of the catalyst by the trace HCl, poisoning of the sulphate groups by humin formation or leaching.

The amount of Zr leaching caused by the presence of HCl was determined via ICP analyses to be <0.1%, as shown in Table 6.3. Such minimal Zr leaching following exposure to microwave irradiation is comparable to other works using zirconium in deionised water[12]. The inclusion of biomass during the heating cycle reduced the amount of soluble Zr, which either indicates that humin formation reduced Zr leaching or that the SR absorbed Zr. However, due to SZR contamination in the SR, it was not possible to verify SR absorption.

Table 6.3: Catalyst recyclability based on post-reaction Zr(IV) leaching

Sample	Zr concentration (mg/L)	Leaching Rate (wt.%)
Optimum Conditions without Biomass	60.5	0.121%
Optimum Conditions	2.4	0.005%

The deactivation of solid acid catalysts by humin formation can be controlled by the residence time of the reactor, which can be partially achieved using continuous reactors [22]. Porous solid acid ZSM-5 has recently been found to be an effective pyrolysis catalyst for synthetic humins at 550 °C [23], as well as a potential catalyst for levulinic acid [3] . Han *et al.* [24] suggested that solid acid catalysts can catalyse the degradation of lignin-like residues but, a porous catalyst structure is required to prevent repolymerisation of intermediaries towards tar formation. Moreover, as the minimisation of the humin formation is challenging and as not yet been achieved, future work in this area should focus on developing solid catalysts capable of

degrading humins during calcination or pyrolysis, in order to enhance the catalyst reusability.

The SZR was ineffective at converting real lignocellulosic biomass in water only media however, the addition of the dilute HCl has proven sufficient to potentially debottleneck the recalcitrance of cellulose to hydrolysis and increase levulinic acid yields. The formation of humins and other chars on the catalysts surface remains a significant issue that seems intrinsic to the reaction, this needs to be tackled by future research in catalysis for biorefining applications.

6.3.4 SR Yields

Similarly, to the LA optimisation described in section 6.3.2, the SR yields from the biomass catalysis of *Miscanthus x Giganteus* were modelled using RSM and optimised following a minimising objective function. The statistical model had a adj. R^2 of 96.5% (full ANOVA table shown in Appendix B – Table 3) and the RSM 3D surface and contour plots are shown in Figure 6.7 according to *Equation 6.2*. The overall model shows that temperature had the largest effect on SR yield (F = 1392) during the acid catalysis process followed by time (F=99). The CBR had minimal effect on the SR yield (F=6) which indicates that SZR catalyst was not catalysing the cellulose hydrolysis process. The effects of temperature and time on SR yield suggests that hydrothermal hydrolysis of the cellulose, with the SZR catalysing short-chain polysaccharides or monosaccharides towards levulinic acid.

$$Y_{SR} = 16.577 - 0.156\,T - 0.0202\,t - 1.309CBR + 0.0001T * t + 0.0075T * CBR + 0.00009\,t * CBR + 0.0004\,T^2 - 0.00014\,t^2 \qquad \textit{Equation 6.2}$$

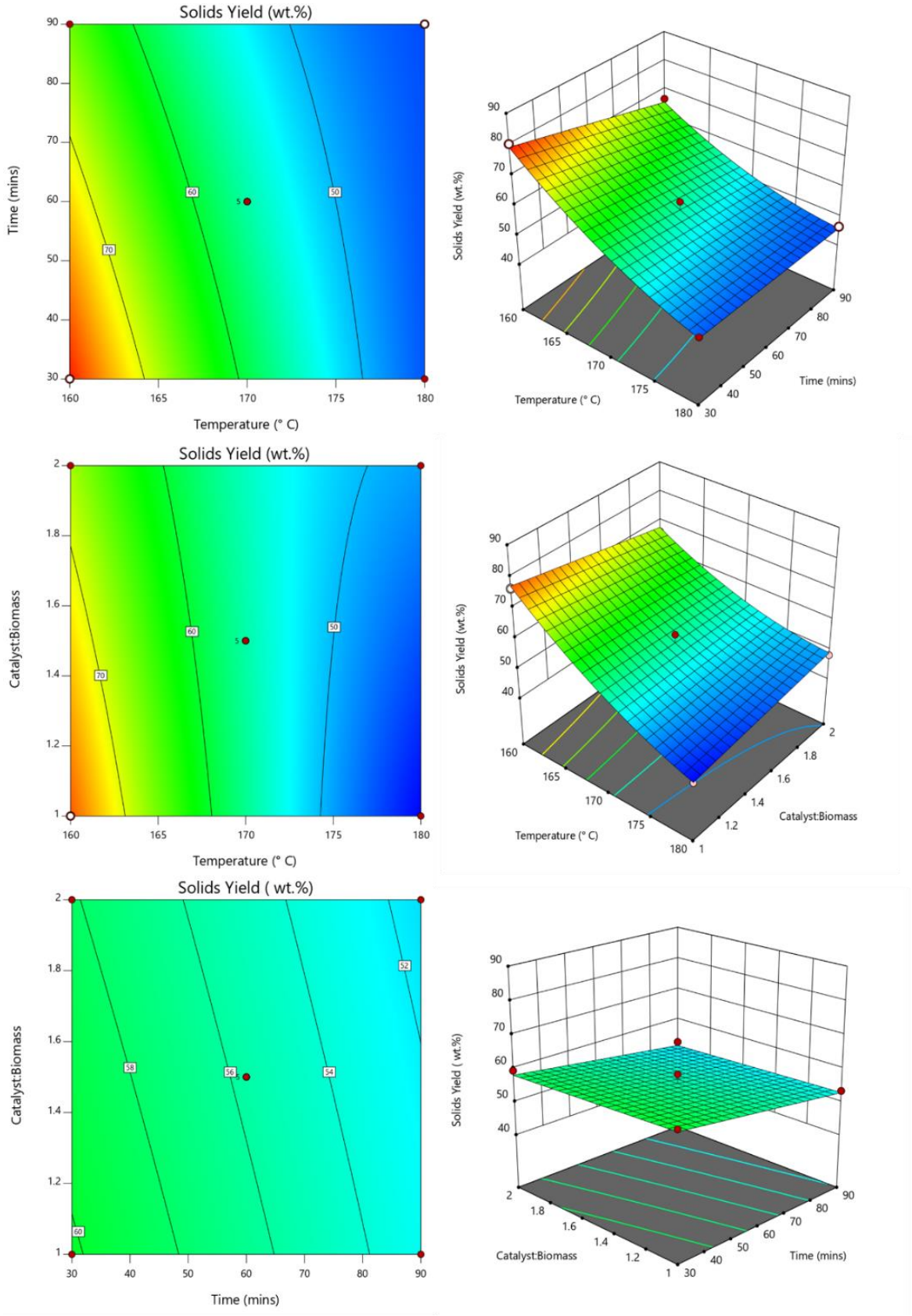

Figure 6.7: 3D response surface plots and 2D contour plots of SR yield (wt%) whist (A) varying time and temperature; (B) varying CBR and temperature; (C) varying CBR and time.

The addition of 10 mM HCl reduced the pH of the catalysis reactants under all conditions (<2 pH) and the addition of increasing SZR loads did not result in a further drop in reactor pH, as shown in Table 6.4. As cellulose hydrolysis is primarily driven by Brønsted acidity, the synergy between HCl and SZR maybe mainly caused by lower reactor pH. Although, Potvin *et al.* found similar improvements in levulinic acid yield from cellulose with neutral NaCl (25.wt%) and attributed the improvement to the effect of the Cl^- anion on cellulose hydrolysis and stabilising intermediate compounds. The exact effect of the dilute HCl on the process cannot be determined in this study it is possible to suggest that the dilute acid improved cellulose hydrolysis towards allowing the further conversion towards levulinic acid through the SZR.

Table 6.4: Effect of catalyst loading on pH with and without 10 mM HCl

Catalyst Loading / wt.%	Distilled Water	10 mM HCl
	pH	pH
0.0%	6.07	1.92
1.0%	3.29	1.92
2.0%	2.85	1.92
2.5%	2.65	1.92
5.0%	2.40	1.92

It should be noted that higher temperatures and longer time in the reaction resulted in a minimal increase in SR yields. This significantly differs to prior work with homogenous catalysts, suggesting that there was no significant humin or by-product formation, as seen with homogenous catalysts in Chapter 5. The most likely cause is due to the low reaction temperature of 180 ˚C and lower overall acidity of the heterogeneous catalyst compared with mineral acids. Although, the SR yield was calculated before catalyst separation and includes humin deposited on the catalyst surface. The lower solid by-product yields with heterogeneous catalysts is a previously unreported advantage compared with homogenous catalysts, but this will have an effect on SR characteristics.

6.3.5 SR Characterisation

The SR weights after each trial were determined assuming no catalyst leaching. The catalyst and SR were separated by sieving and correspond to <68 μm and >125 μm respectively. The >125 μm contained approximately 26% ZrO_2, as identified using XRF and shown in Table 6.5, indicating significant catalyst contamination despite the high SR separation yield, 79 wt.%. However, on industrial scale the catalyst – SR separation can be carried out using more efficient methods such as froth flotation, therefore as the >125 μm fraction is predominately SR, it utilised to evaluate the SR properties as described in Chapter 3, sections 3.6.2-3

Table 6.5: Material characterisation of separated SR produced during the optimum conditions of 160 °C for 80 mins with a 2:1 CBR

	Value
Estimated SR Sep. Yield / wt.%	79.0%
ZrO2 content / wt.%	26.4%
Ash / %	36.3%
ZrO2 adjusted Ash / wt.%	9.9%
C / wt.%	36.8%
H / wt.%	4.3%
O / wt.%	20.2%
Bulk C/N	134.00
Bulk H/C	1.40
Bulk O/C	0.42
Surface O/C	0.41
HHV* / MJ kg^{-1}	16.2

* $HHV_{predicted}$ = 0.3491(C)+1.1783(H) + 0.1005(N) − 0.1034(O) − 0.0015(A), where C, H, S, O, A represent the weight percentages of carbon, hydrogen, sulphur, oxygen and ash of the sample, respectively[25]

Throughout the work higher catalyst ratios resulted in lower SR yields. This was especially significant when dilute HCl was added to the reaction medium. At the validated optimum point identified by the RSM model (160°C, 80 minutes, 2:1 CBR with 10 mM dilute HCl), the SR yield was about 58-62 wt.%. The compositional properties of the residues at the optimum point are reported in Table 6.5. The initially high ash content (36.3%) can be attributed to the catalyst contamination, although the ZrO_2-adjusted ash content is still considerably high (9.9%), as exceeding previously

reported values in other similarly attained residues. This may indicate that the mild acidic conditions do not extract acid soluble elements during the process unlike concentrated sulphuric acid, resulting in a higher ash content in the residue. However, the high C/N ratio limits the application of the residue as a soil fertiliser, despite the increase in trace mineral elements. After the catalysis process the H/C and O/C ratios decreased compared with the raw feedstock, shown in Figure 6.8. The relative decrease in both H/C and O/C strongly indicate that the feedstock primarily underwent hydrolysis as expected with an acid hydrolysis process. However, the surface O/C shown in Table 6.5 (measured by EDX) was similar to that of the bulk properties which indicates a lack of surface functionalisation apparent with hydrochars and humins [26,27]. Ren *et al.* [28] found a direct correlation between oxygen containing surface groups on hydrochar and improved electron transfer. Therefore, the resulting SR elemental composition had similar bulk properties to hydrochars produced under non-acidic conditions but lacked the similar surface functionalisation [29].

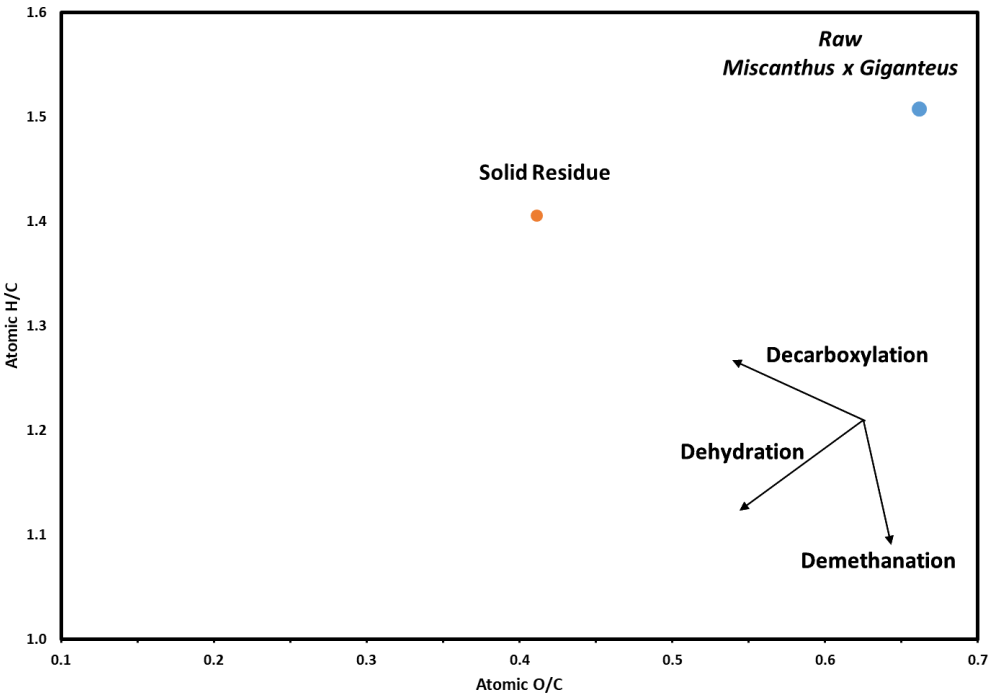

Figure 6.8: Van Krevelen diagram of raw *Miscanthus x Gigante*us and SR produced under the optimum conditions of 10 mM HCl with a 2:1 CBR at 180 °C for 80 mins

The SR produced during the catalysis with and without the addition of 10 mM HCl was analysed using X-Ray Diffraction (XRD) and compared with raw biomass as shown in Figure 6.9. The relative crystallinity of the raw biomass, SR from SZR in water medium and 10 mM HCl catalysis were 77.8%, 88.3% and 93.5% respectively. This strongly suggests that the SZR favourably removes amorphous cellulose, which is in agreement with the effects of other solid acid catalysts in literature [30]. However, the crystallinity index is a relative ratio that cannot determine the absolute effect on both cellulose fractions.

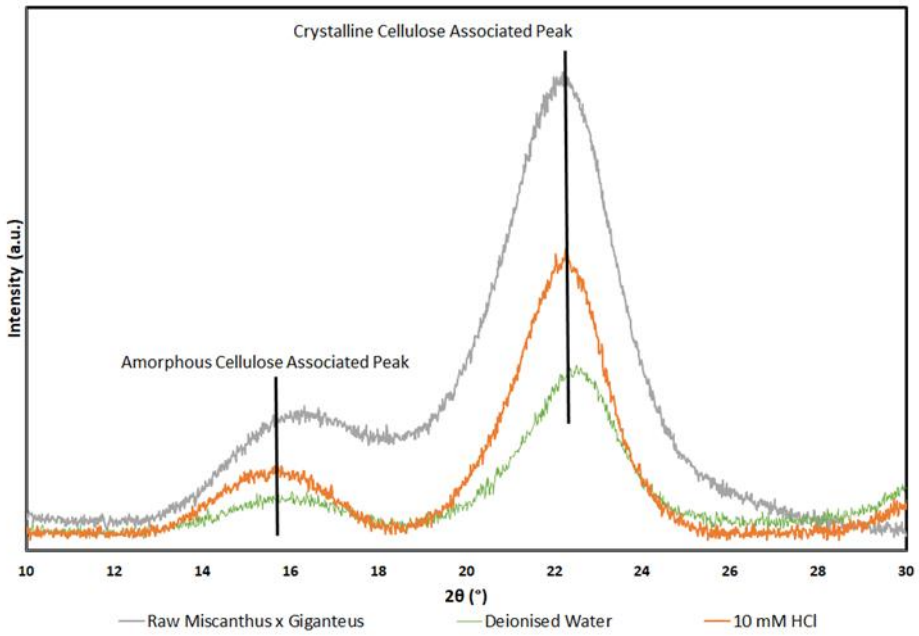

Figure 6.9: XRD pattern of Raw *Miscanthus x Giganteus* and SR produced in deionised water and 10 mM HCl with a 2:1 CBR at 180 °C for 60 mins

In order to understand the effect of humins formation between homogenous versus heterogeneous catalysts, the SR from the optimum conditions was compared to homogenous catalysts conditions investigated in Chapter 5 using SEM as shown in Figure 6.10. It can be clearly seen how the carbonaceous spheres (humins) do not form when the reaction runs at the optimum conditions identified by the RSM model. The use of heterogeneous acid catalyst is mainly responsible for this phenomenon.

As the biomass does not have any active acidic sites, it is not possible for the initialisation of humin formation via DHH aldol condensation. Therefore, the formation and humin growth by aldol polymerization primarily occurs on the heterogeneous catalyst surface area. Also, as the solid reaction progresses across, the solid catalyst's active sites become deactivated, preventing further initialisation of the humin formation mechanism.

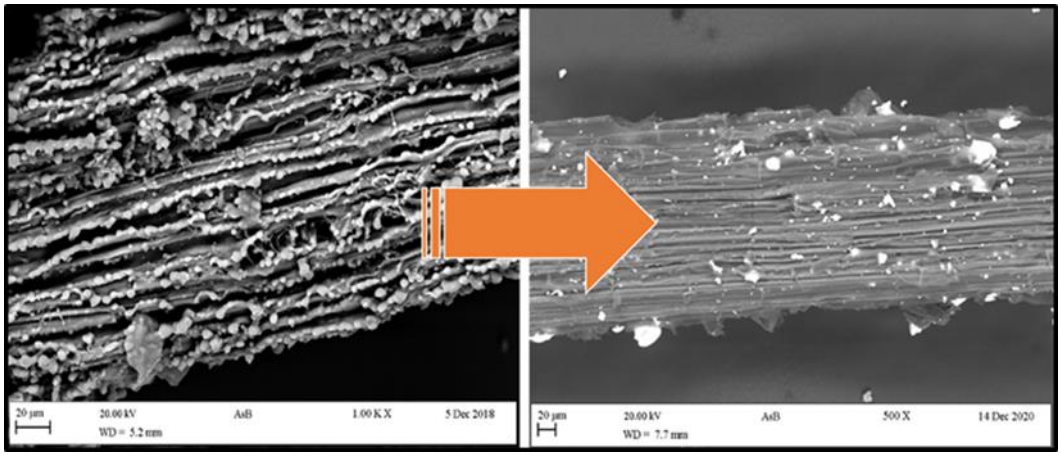

Figure 6.10: Humins deposition on SR between Biofine-like (on the left) and optimum RSM (on the right) conditions.

It was evident from all of the RSM combinations tested (non-optimum) that there was no significant increase in residues yields at extreme conditions, indicating minimal solid by-product forming reaction, where humin deposition appears to shift from residue towards catalyst. The lack of structural change from the XRD analysis and lack of obvious humin solid by-product suggests that the SR produced with SZR, are more akin to degraded biomass than the chars. This is confirmed by the previously mentioned bulk and surface O/C ratios that indicate a lack of surface functionalisation which is characteristic of hydrochars. As such it might be suggested that SR from heterogeneous catalysis is inherently different from the equivalent homogenous catalysis processes.

6.3.6 SR Possible Applications

The use of heterogeneous catalysts in a biorefinery will require novel catalyst separation to recover and recycle the catalyst, which would leave a possibly contaminated SR by-product fraction in need of valorisation. Previous studies have looked at harnessing the char-like properties of SR from LA production as a solid fuel or feedstock for pyrolysis. The Higher Heating Value (HHV) was estimated to be 16.2 MJ kg^{-1}(as shown in Table 6.5), which allows for a possible use as a solid fuel. The higher ash content will significantly reduce the combustion performance. Also the SR's HHV value identified in this study are 20-45% lower than the raw feedstock, other hydrochars and synthetic humins, 22 MJ kg^{-1}, 20-29 MJ $kg^{-1}$and 21-24 MJ kg^{-1} respectively [29,31]. The low HHV of the SR can be attributed to the high ash content and lack of carbonisation or humin formation. A more appropriate application could therefore be as a soil amendment to increase soil carbon content and fertility. As previously mentioned, the increased ash, and thus mineral content of the SR, could possibly increase soil buffering capacity as well as providing a supply of available of nutrients to promote soil microbial growth. The modest surface area of 23 m^2 g^{-1} with presence of larger pores (Table 6.5 and Appendix B - Figures 1 & 2) could additionally boost microbial growth, while the presence of un-reacted cellulose would provide an energy source for rapid microbial colonisation without the requirement of an extra food source for soil microorganisms. However, the applicability of the SR as a soil amendment will require further field investigation, due to the complex nature of soil amendments. Though, the SR from heterogeneous catalysis appears to be primarily be composed of unreacted biomass while also potentially containing metal contamination. This combination does not have easily comparative literature

materials, making commercialisation difficult and could have stark economical applications without extensive further research.

The separation of heterogeneous catalyst and SR post reaction must also be considered. SR separation is technically possible but will add major costs. As the catalyst calcination (or other regenerative method) will be required for catalyst recycling, it may be simpler and more cost effective to use the SR as calcination fuel, unless a higher-value application for the unreacted-biomass-like material can be proven.

6.4 Comparison Between Homogenous and Heterogeneous SR

The homogenous and heterogeneous SR evaluated in Chapters 5 & 6 respectively displayed significant differences in organic SR generated by the microwave-assisted catalytic reaction. The use of H_2SO_4 and synergistic SZR-HCl catalysts achieved similar levulinic acid yields of 62.3% and 63.8% respectively. However, the SR formed with H_2SO_4 catalyst exhibited higher carbon content, lower H/C and O/C contents, as well as lower ash content compared with SZR-derived residue. These changes were also evident in the morphological and surface properties of the residues, with the heterogeneous catalyst-derived residue being closer to unreacted biomass. The differences can be fundamentally attributed to lack of acid sites on the heterogeneous catalyst near the SR, due to solid-solid interaction limitations. The acidity of the solid catalyst is a requirement for the formation of humins and for further dehydration of inert biomass fractions, which is lacking on the SZR-derived SR. At the same time, it

should be noted that the trace HCl addition to the reaction (10 mM) appeared to be insufficient to catalyse the formation of humins in significant quantities on the SR. The overall change in catalytic properties of SR when using two different catalysts types (homogeneous versus heterogeneous) indicates that each post-reaction SR should be considered distinct, as it will exhibit different attributes.

These attributes and properties will certainly affect the pathways to valorisation of the SR from each process. The char-like residue from the H_2SO_4 catalysis of poplar wood presented a highly functionalised surface area similar to that of hydrochar and humins. The functionalised surface could be used in similar high-value applications to that of hydrochar such as catalyst support material or as carbon based electrodes[15,32], while there is no apparent high-value application for depolymerised biomass formed during the SZR-HCl catalysis. As such the combustion of SR from hetergonous catalysis must be considered the best current application, with future high value upscaling focusing on biorefinery SR from homogenous catalysis.

6.5 Conclusions

The results from this chapter indicate that microwave-assisted conversion of lignocellulosic biomass to levulinic acid using sulphated zirconia and trace hydrochloric acid is a promising method for valorising this biomass to platform chemicals. The performed lab-scale experiments showed an optimum yield of about 63% wt. can be achieved at 160°C, 80 minutes, 2:1 CBR with 10 mM dilute HCl. The synergistic performance of the sulphated zirconia and hydrochloric acid significantly improved levulinic acid yields compared with that of each individual catalyst. The results indicate that the trace HCl debottlenecked the cellulose hydrolysis stage in particular, with minimal effect on subsequent sub-reactions. This approach could be applied to a range of heterogeneous catalysts to improve product yields with real lignocellulosic biomass. Further work is required to optimize the trace HCl to heterogeneous catalyst ratio, with special regards to Lewis-Brønsted acid ratio, which may facilitate important progress in the area of heterogeneous catalysis of real biomass. The SR was primarily composed of unreacted biomass and did not undergo any major transformation, suggesting that heterogeneous catalysis of biomass results in a significantly different residue to that of homogenous catalysts. Consequently, the range of possible commercial applications will differ depend on the catalyst type used to generate the residue. The development of the SZR catalysts in conjunction with synergistic approach with a dilute mineral acid could enable the debottlenecking of cellulose hydrolysis with a range of heterogeneous catalysts for the production of high value chemicals from biomass. This expansion of viable heterogeneous catalysts could significantly reduce catalysts separation costs and improve overall yields

facilitating the production of low-cost green chemicals, thus should be investigated in greater detail.

6.6 References

1. Van De Vyver, S., Thomas, J., Geboers, J., Keyzer, S., Smet, M., Dehean, W., Jacobs, P. A., Sels, B. F. Catalytic production of levulinic acid from cellulose and other biomass-derived carbohydrates with sulfonated hyperbranched poly(arylene oxindole)s. Energy Environ. Sci. 4, 3601–3610 (2011).

2. Weingarten, R., Conner, W. C. & Huber, G. W. Production of levulinic acid from cellulose by hydrothermal decomposition combined with aqueous phase dehydration with a solid acid catalyst. Energy Environ. Sci. 5, 7559–7574 (2012).

3. Pratama, A. P., Rahayu, D. U. C. & Krisnandi, Y. K. Levulinic acid production from delignified rice husk waste over manganese catalysts: Heterogeneous versus homogeneous. Catalysts 10, (2020).

4. Acharjee, T. C. & Lee, Y. Y. Production of levulinic acid from glucose by dual solid-acid catalysts. Environ. Prog. Sustain. Energy 37, 471–480 (2018).

5. Liu, Y., Lin, L., Sui, X., Zhuang, J. & Pang, C. Conversion of Glucose to Levulinic Acid Catalyzed by ZSM-5 Loading. Appl. Mech. Mater. 291, 249–252 (2013).

6. Kang, S. & Yu, J. Maintenance of a Highly Active Solid Acid Catalyst in Sugar Beet Molasses for Levulinic Acid Production. Sugar Tech 20, 182–193 (2018).

7. Ding, D., Wang, J., Xi, J., Liu, X., Lu, G., Wang, Y. High-yield production of levulinic acid from cellulose and its upgrading to γ-valerolactone. Green Chem. 16, 3846–3853 (2014).

8. Signoretto, M., Taghavi, S., Ghedini, E. & Menegazzo, F. Catalytic Production of Levulinic Acid (LA) from Actual Biomass. Molecules 24, 1–20 (2019).

9. Osatiashtiani, A. et al. Hydrothermally Stable, Conformal, Sulfated Zirconia Monolayer Catalysts for Glucose Conversion to 5-HMF. ACS Catal. 5, 4345–4352 (2015).

10. Antonetti, C., Licursi, D., Fulignati, S., Valentini, G., Galletti, A. M. R. New Frontiers in the Catalytic Synthesis of Levulinic Acid : From Sugars to Raw and Waste Biomass as Starting Feedstock. 1–29 (2016). doi:10.3390/catal6120196

11. Lappalainen, K., Volger, N., Kärkkäinen, J., Dong, Y., Rusanen, A., Ruotsalainen, A., Wäli, P., Markkola, A., Lassi, U. Microwave-assisted conversion of novel biomass materials into levulinic acid. Biomass Convers. Biorefinery 8, 965–970 (2018).

12. Joshi, S. S., Zodge, A. D., Pandare, K. V. & Kulkarni, B. D. Efficient conversion of cellulose to levulinic acid by hydrothermal treatment using zirconium dioxide as a recyclable solid acid catalyst. Ind. Eng. Chem. Res. 53, 18796–18805 (2014).

13. Qi, X., Watanabe, M., Aida, T. M. & Smith, R. L. Sulfated zirconia as a solid acid catalyst for the dehydration of fructose to 5-hydroxymethylfurfural. Catal. Commun. 10, 1771–1775 (2009).

14. Pyo, S. H., Glaser, S. J., Rehnberg, N. & Hatti-Kaul, R. Clean Production of Levulinic Acid from Fructose and Glucose in Salt Water by Heterogeneous Catalytic Dehydration. ACS Omega 5, 14275–14282 (2020).

15. Kobayashi, H., Kaiki, H., Shrotri, A., Techikawara, K. & Fukuoka, A. Hydrolysis of woody biomass by a biomass-derived reusable heterogeneous catalyst. Chem. Sci. 7, 692–696 (2016).

16. McCalmont, J. P., Hastings, A., McNamara, N., Richter, G., Robson, P., Donnison, I., Clifton-Brown, J. Environmental costs and benefits of growing Miscanthus for bioenergy in the UK. GCB Bioenergy 9, 489–507 (2017).

17. Kassaye, S., Pagar, C., Pant, K. K., Jain, S. & Gupta, R. Depolymerization of microcrystalline cellulose to value added chemicals using sulfate ion promoted zirconia catalyst. Bioresour. Technol. 220, 394–400 (2016).

18. Dussan, K., Girisuta, B., Haverty, D., Leahy, J. J. & Hayes, M. H. B. Kinetics of levulinic acid and furfural production from Miscanthus×giganteus. Bioresour. Technol. 149, 216–224 (2013).

19. Muthu, H., SathyaSelvabala, V., Varathachary, T. K., Selvaraj, D. K., Nandagopal, J., Subramanian, S. Synthesis of biodiesel from neem oil using sulfated zirconia via tranesterification. Brazilian J. Chem. Eng. 27, 601–608 (2010).

20. Yuan, H., Dong, Z., He, J., Wang, Y. & Zhang, H. Surface characterization of sulfated zirconia and its catalytic activity for epoxidation reaction of castor oil. Chem. Eng. Commun. 206, 1618–1627 (2019).

21. Agarwal, S., Es, D. Van & Jan, H. Journal of Analytical and Applied Pyrolysis Catalytic pyrolysis of recalcitrant , insoluble humin byproducts from C6 sugar biorefineries. J. Anal. Appl. Pyrolysis 123, 134–143 (2017).

22. Pyo, S. H., Sayed, M. & Hatti-Kaul, R. Batch and Continuous Flow Production of 5-Hydroxymethylfurfural from a High Concentration of Fructose Using an Acidic Ion Exchange Catalyst. Org. Process Res. Dev. 23, 952–960 (2019).

23. Abdilla-Santes, R. M., Agarwal, S., Xi, X., Deus, P. J., Heeres, H. Valorization of humin type byproducts from pyrolytic sugar conversions to biobased chemicals. J. Anal. Appl. Pyrolysis 152, (2020).

24. Han, T., Ding, S., Yang, W. & Jönsson, P. Catalytic pyrolysis of lignin using low-cost materials with different acidities and textural properties as catalysts. Chem. Eng. J. 373, 846–856 (2019).

25. Channiwala, S. A. & Parikh, P. P. A unified correlation for estimating HHV of solid, liquid and gaseous fuels. Fuel 81, 1051–1063 (2002).

26. van Zandvoort, I., Wang, Y., Rasrendra, C. B., van Eck, E. R. H., Bruijincx, P. C. A., Heeres, H. J., Weckhusen, B. M. Formation, Molecular Structure , and Morphology of Humins in Biomass Conversion : Influence of Feedstock and Processing Conditions. ChemSusChem 6, 1745–1758 (2013). doi:10.1002/cssc.201300332

27. He, J., Ren, S., Zhang, S. & Luo, G. Modification of hydrochar increased the capacity to promote anaerobic digestion. Bioresour. Technol. 341, 125856 (2021).

28. Ren, S., Usman, M., Tsang, D. C. W., O'thong, S., Angelidaki, I., Zhu, X., Zhang, S., Luo, G. Hydrochar-Facilitated Anaerobic Digestion: Evidence for Direct Interspecies Electron Transfer Mediated through Surface Oxygen-Containing Functional Groups. Environ. Sci. Technol. 54, 5755–5766 (2020).

29. Kambo, H. S. & Dutta, A. A comparative review of biochar and hydrochar in terms of production , physico-chemical properties and applications. Renew. Sustain. Energy Rev. 45, 359–378 (2015).

30. Di Fidio, N., Galetti, A. M. R., Fulignati, S., Licursi, D., Liuzzi, F., de Barri, I., Antonetti, C. Multi-step exploitation of raw arundo donax L. For the selective synthesis of second-generation sugars by chemical and biological route. Catalysts 10, (2020).

31. Agarwal, S., Es, D. Van, Jan, H., van Es, D. & Heeres, H. J. Catalytic pyrolysis of recalcitrant, insoluble humin byproducts from C6 sugar biorefineries. J. Anal. Appl. Pyrolysis 123, 134–143 (2017).

32. Randviir, E. P., Kanou, O., Liauw, C., Miller, G. J., Andrews, H., Smith, G. The physicochemical investigation of hydrothermally reduced textile waste and application within carbon-based electrodes. RSC Adv. 9, 11239–11252 (2019).

Chapter 7: Effect of Hydrochar from Acid Hydrolysis on Anaerobic Digestion of Chicken Manure

Under Review in: Journal for Environmental Chemical Engineering

7.01 Graphical Abstract

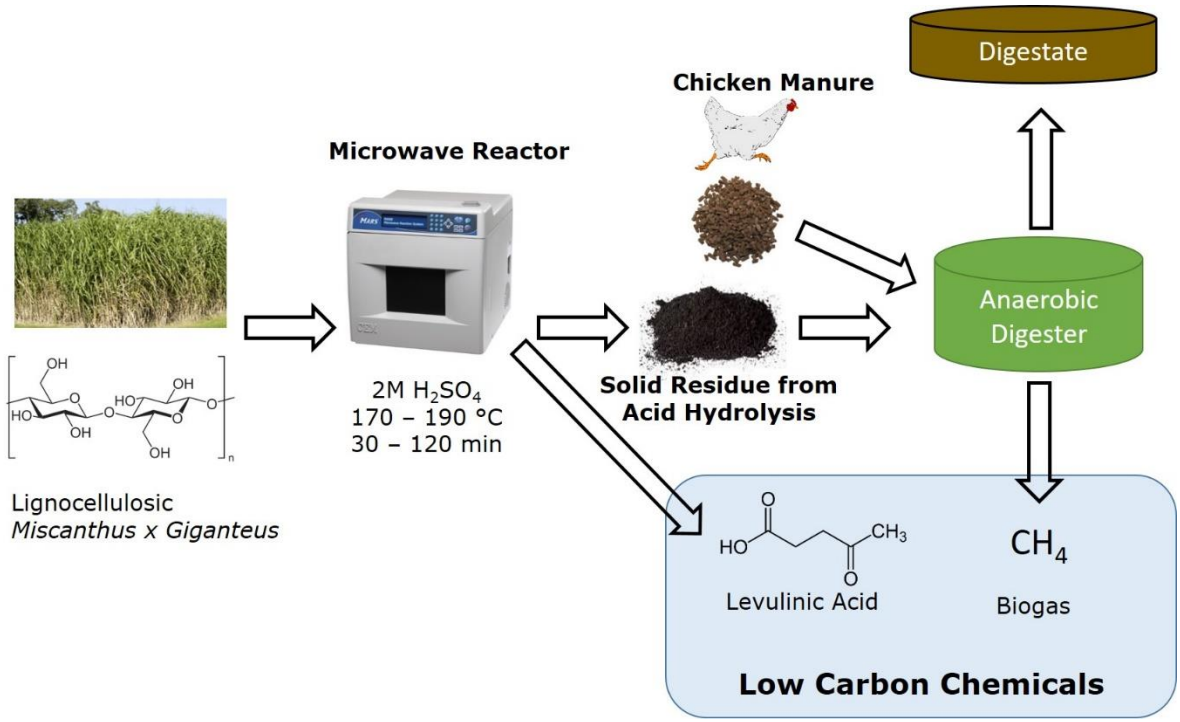

7.02 Abstract

This chapter investigated, solid residues from the production of biofuel precursor levulinic acid generated via microwave-assisted acid hydrolysis of *Miscanthus x Giganteus* and subsequent supplementation of anaerobic reactors digesting Chicken Manure. Five solid residues were produced under various acid catalysis conditions and characterised in depth with regards to surface and bulk properties using TGA, FTIR, EDX, CHNO, SEM. This included detailed discussion on the degree of humin formation and carbonisation. The addition of these solid residues to anaerobic digesters increased the methane yields by up to 14.1%, depending on the additive concentration levels, 2-10 g/L. A mild ammonium related inhibition was observed during the fermentation trials, which was mitigated by the solid residue (SR) additive, with an experimental optimum found at 6 g/L for the maximisation of methane yields. The effects of acid catalysis conditions on the SR properties and methane yields from chicken manure were evaluated. All investigated solids residue exhibited ammonium adsorption and improved microbial diversity during digestion. These results suggest that, the integration of anaerobic digestion downstream of second generation biorefineries is a promising green waste disposal method for solid by-products from thermo-catalytic processes.

7.1 Introduction

The supplementation of anaerobic digesters with carbonaceous materials, including hydrochars and biochars to increase methane yields by inhibitor adsorption and support for microbial growth, has become a burgeoning field of research [1–4]. Anaerobic digestion (AD) is a widely used low-cost disposal process for organic matter as well as a source renewable energy in the form of biogas. AD inhibition has been reported when high concentrations of inhibitors such as ammonia, fatty acids, furans, heavy metals and organic compounds, disrupt and destabilise the complex microbial community [5]. Inhibitory compounds can directly or indirectly destabilise AD and reduce methane yields. Chars have been reported to reduce aqueous concentrations of ammonia and metals ions, with notably improved methane yields [6]. This is especially applicable to the degradation of nitrogen-rich animal manures, which have been highlighted by serval authors as a growing environmental concern[7–9].

In particular, the addition of biochar and hydrochar have both been observed to improve methane yields from manures by +17% to +500% from the digestion of nitrogen rich feedstock's [10]. Another benefit of char addition is it can act as a form of carbon sequestration [11]. However, the energy consumption and subsequent costs of carbonaceous material production has been so far a limiting factor [12] . As solid residues (SR) from acid hydrolysis is an inherent waste stream of lignocellulosic biorefineries, it could potentially be utilised as a large-scale low-cost supplement in AD digesters. In line with the potential of this application, it is important to elucidate the effects of acid hydrolysis SR as additive in AD systems, since they have not been covered in great detail by the literature.

The aim of this chapter is to investigate the addition of residual solids from acid hydrolysis on the anaerobic digestion of Chicken Manure (CM). Several SRs were co-produced alongside levulinic acid (LA), using homogenous sulphuric acid as the catalyst and different acid hydrolysis reaction conditions of Miscanthus x Giganteus feedstock, in microwave heated reactors. Increasing SR concentrations were added in batch AD reactors for the digestion of ammonia-rich CM. The effects of SR loadings on methane yields were experimentally modelled and determined using the modified Gompertz equation, in conjunction with readings of detected ammonium concentrations. The effects of the different acid hydrolysis reaction conditions on the SR structural and compositional properties have also been examined and discussed. Microbiome analysis of each AD reactor was also conducted to understand the effects of SR on AD microbial cell count, diversity and composition.

7.2 Extended Methodology

7.2.1 Inoculum Seed and Substrate

The inoculum used in the experiments was collected from a mesophilic (31 ± 1 °C) from an industrial brewery anaerobic digester in two stages seven months apart, hereafter referred to as Trial 1 and 2, respectively.

Each inoculum's composition used in these trials is reported in Table 7.1, which includes characterisation results of the CM substrate. CM was collected, dried and stored in a desiccator until use in AD trials to maintain consistency.

Table 7.1: Characteristics of Inoculum and Chicken Manure (CM)

	CM	**Inoculum Trial 1**	**Inoculum Trial 2**
TS (%, wt.%)	87.7 ± 0.3	7.6 ± 0.8	9.0 ± 0.1
VS (%, wt.%)	64.7 ± 0.2	5.5 ± 0.6	7.0 ± 0.1
VS (%)	73.7 ± 0.4	72.1 ± 0.5	78.2 ± 1.1
pH	N/A	7.78	7.00
Ammonia (g/L)	N/A	1.10	0.94
C (%, dw. basis)	34.7	32.1	38.0
H (%, dw. basis)	5.2	4.7	5.9
N (%, dw. basis)	7.7	7.2	8.1
S (%, dw. basis)	0.8	0.9	0.8
O (%,dw. basis)	23.8	27.1	25.3

7.2.2 SR Preparation and Characterisation

A CEM MARS 5 microwave reactor was used as the bench scale microwave reactor for the acid hydrolysis. The acid hydrolysis of poplar wood and SR separation was conducted according to the procedure depicted in Figure 7.1. In each experiment 0.5 g of *Miscanthus x Giganteus* was mixed with 10 ml 2M H_2SO_4 solution to achieve a biomass loading ratio of 5 wt.%. Following the completion of the desired reaction time, the SR was separated and the hydrolysate was analysed using HPLC with an RID detector.

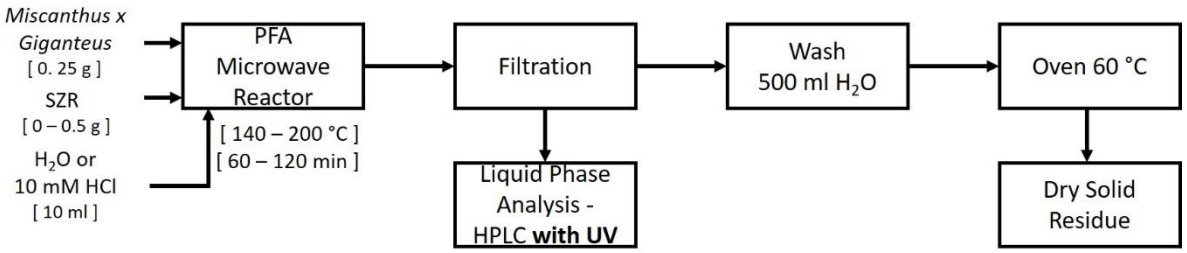

Figure 7.1: Microwave hydrolysis process and SR separation

The reaction conditions were chosen to produce a diverse range of SR properties with consideration to high achieving levulinic acid yields, as shown in Table 7.2. The highest levulinic acid yield (16.7 wt.%) and the lowest solids yield of 30.8 wt.% was achieved at 180 ˚C for 60 mins (SR3). The reaction conditions were chosen as to produce a variety of SR properties around the optimum point while maintaining high levulinic acid yields, in excess of 45%. SRs were stored in airtight containers and placed in a desiccator before further characterisation and prior to supplementation to AD reactors.

Table 7.2: Reaction conditions for SR production and associated levulinic acid yields

	Reaction Conditions		Product Yields		
Sample I.D.	Time (mins)	Temperature (˚C)	Levulinic Acid Yield % (Theoretical)	Levulinic Acid Yield (wt.%)	SR Yield (wt.%)
SR 1	30	180	48.6	12.6	34.4
SR 2	30	190	56.4	14.6	34.2
SR 3	60	180	64.5	16.7	30.8
SR 4	120	170	47.1	12.2	42.9
SR 5	120	180	59.1	15.3	32.1

The SRs were characterised according to the methods presented in Section 3.6. In addition, the pH and Electrical Conductivity (EC) of the SR in deionised water was determined at 25 °C, at a solid-to-water ratio of 1:20. Fixed Carbon was determined as the remaining solids after heating for 7 min at 900 ˚C, excluding ash content

according to CEN/TS 15148:2005. Thermal Gravimetric Analysis (TGA) was conducted using a TA Instrument SDT Q50 at 10 ˚C /min to 900 ˚C in a nitrogen atmosphere.

7.2.3 Anaerobic digestion experimental design and set up

The total volatile solids (VS) of CM and inoculum was set at 8 wt.% with a C/N ratio of 7.1. The SR was not included in the total VS calculations, due to the slow microbial degradation of chars according to Gronwald *et al.* [13]. The summary of the experimental design is shown in Table 7.3, which had the objective to determine the optimum SR concentration and the effect of acid hydrolysis operating conditions on SR addition to the AD of nitrogen rich feedstock (CM). The loading values of added SR have been selected based on work by Xu *et al.* , and correspond to a SR addition of 2.5 – 11.0% of TS. Since SR3 corresponded with the best acid hydrolysis conditions with regards to levulinic acid production, it was thus selected for the appraisal of the optimum SR concentration in the AD reactors in Trial 1. Trial 2 aimed instead at the investigation of different SR types, and used the experimentally determined optimum concentration of 6 g/L, identified in Trial 1.

Table 7.3: Summary of batch anaerobic digestion of SR and CM

	Reaction Conditions	Biochar Type	SR Concentration (g /L)
Trial 1- Effects of Solid Concentration	Control	None	None
	C1	SR 3	2
	C2	SR 3	4
	C3	SR 3	6
	C4	SR 3	8
	C5	SR 3	10
Trial 2- Effects of Different SR	Control	None	None
	D1	SR 1	6
	D2	SR 2	6

D3	SR 3	6
D4	SR 4	6
D5	SR 5	6

7.3 Results and Discussion

7.3.1 SR Characterisation for AD Suitability

Figure 7.2 shows the thermogravimetric (TGA) and differential thermogravimetric (DTG) analysis of the five SRs from the acid hydrolysis process. The initial mass loss can be primarily associated to the loss of residual water, while the peaks between 200-300 °C on the DTG plot represent the degradation of sugars. In particular, the broad peaks in this region for SR1 and SR4 indicate incomplete hydrolysis of the cellulose, due to the milder reaction conditions of 180 °C for 30mins and 170 °C for 120 mins respectively. This is especially evident from the low surface area value of 9 m^2/g of SR4, suggesting some cellulose structures remained intact, due to the low reaction temperature of 170 °C, Table 7.5. While the 400- 500 °C peaks on all 5 SRs show the presence of lignin in the residues which has been reported by multiple authors [14,15].

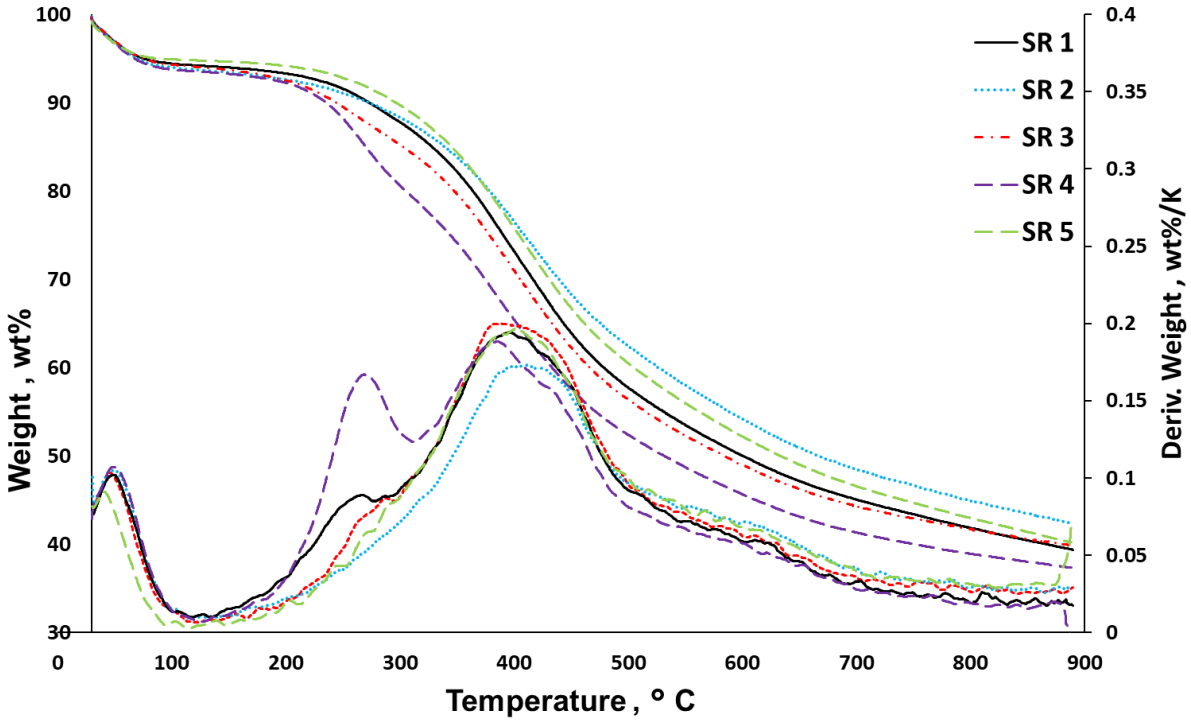

Figure 7.2: TGA and DTG curves of SR samples

The incomplete hydrolysis of SR4 can be further observed in the van Krevelen plot, Figure 7.3, which also shows the primary SR underwent dehydration reactions, as also reported by Zandvoort *et al.*[16]. Incomplete hydrolysis present in SR4 will result in intermediate biomass-hydrochar properties that can be used as control to compare the effect of the relative effect of surface properties. SR 1, 2 and 3 exhibit higher surface area of 17-21 m^2/g indicating degradation of the cellulose matrix, leaving the unreacted lignin. SR5 (180 °C, 120 mins) has a surface area of 35 m^2/g, which is significantly higher than SRs produced in shorter time periods. This represents an opposite trend associated with HTC, which has noted a decrease in hydrochar surface area [17,18]. The increase in surface most likely attributable the formation of humins on the surface particle, which is partially confirmed by the predominant dehydration of the SRs with increasing reaction time and temperature.

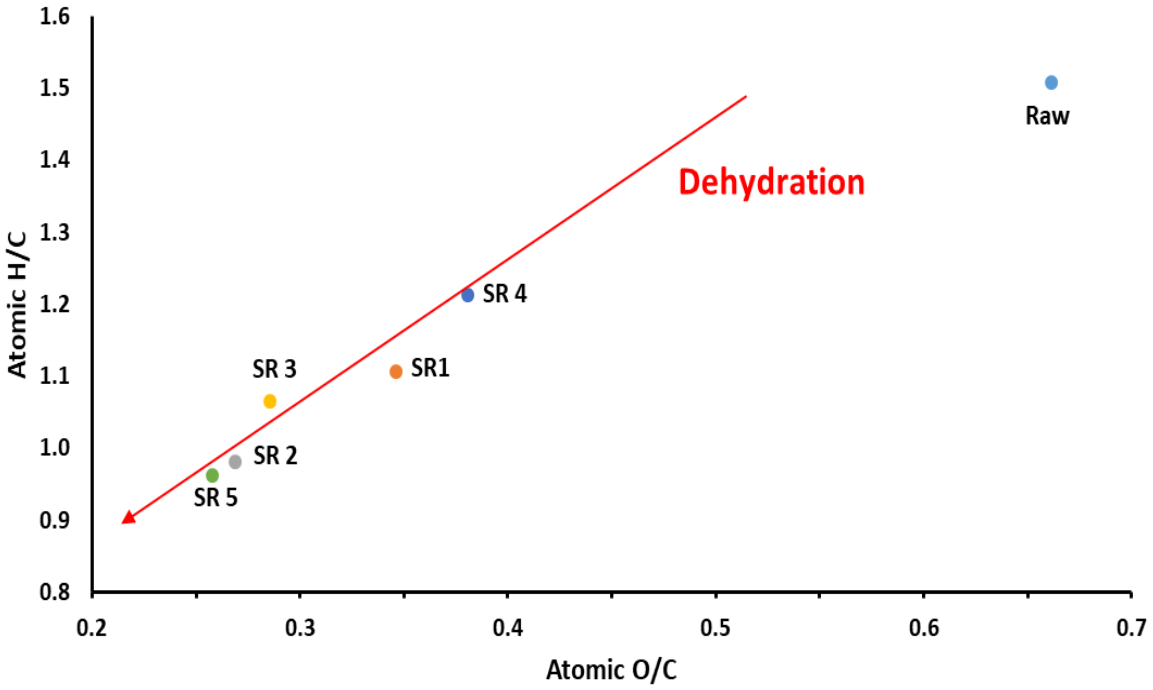

Figure 7.3: Van Krevelen plot of the untreated miscanthus and the prepared solid residues

These are then further confirmed by the SEM images presented in Figure 7.4, showing significant carbon spheres growth on the surface of the material, which would be responsible for increased surface areas. The carbon spheres were similar to those found on the surface of the SR discussed in Chapter 5 and, again, can be attributed to the formation of humins [19,20]. All SRs except for SR4 exhibited morphological humin formation in carbon sphere coverage, with SR5 having the most widespread humin formation. Under all conditions the underlying cellulose microfibrils were observable to varying degrees. This reaffirms that the residues contain unreacted lignocellulosic structures that form the bulk structure upon the partial humin surface modification occurs.

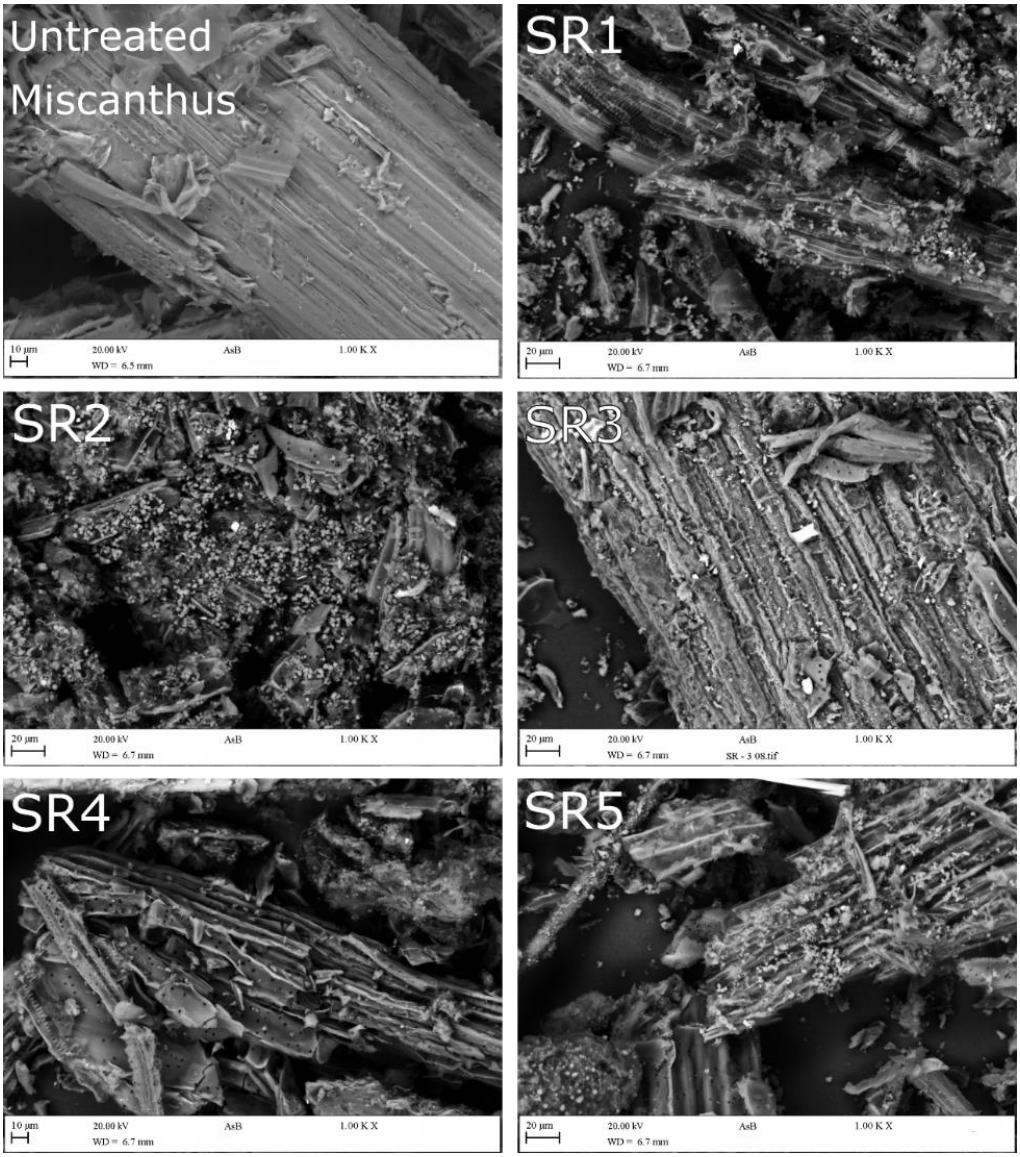

Figure 7.4: SEM images of the untreated miscanthus and the prepared solid residues

The elemental surface composition of carbonaceous spheres was estimated using EDX (presented in Table 7.4), which shows that surface O/C ratio varied between 0.41 - 0.54. The surface O/C differed with the bulk O/C ratio determined by combustion analysis (0.26-0.38), indicating that the outer surface area is rich in oxygenated functional groups. The surface functional groups were not characterised in detail however, it can be inferred that the increased O/C will increase the SR hydrophilicity and cationic exchange capacity compared with the biomass residue [21,22]. This may suggest that SR 3 & 5 have increased ammonium cation adsorption capacity, which

is further discussed in section 7.3.4. The decreases in surface trace element composition, due to acid leaching, further suggest that pre-existing exchange sites have been made vacant for further increases in cation exchange capacity. SR2 exhibited a lower O/C ratio and high fixed carbon content, possibly due to the higher degree of aromatisation caused by the higher reaction temperature. This suggests that lower temperatures and long reaction times are required to maintain the humic surface structures and prevent hydrothermal carbonisation.

Table 7.4: EDX composition of the untreated miscanthus and the prepared solid residues on an atomic basis

Element	Miscanthus	SR 1	SR 2	SR 3	SR 4	SR 5
C (%)	49.54	62.66	62.02	58.47	64.64	56.26
O (%)	47.58	33.99	33.36	39.29	32.67	40.59
Na (%)	0.35	0.28	0.09	0.12	0.33	0.21
Si (%)	1	2.33	3.92	0.97	1.14	2.34
S (%)	0.24	0.74	0.6	0.63	1.22	0.43
Al (%)	0.25	N.D	N.D	0.51	N.D	0.18
P (%)	0.15	N.D	N.D	N.D	N.D	N.D
Cl (%)	0.13	N.D	N.D	N.D	N.D	N.D
K (%)	0.37	N.D	N.D	N.D	N.D	N.D
Ca (%)	0.4	N.D	N.D	N.D	N.D	N.D

N.D. = Not Detected

The FTIR spectroscopy of the five SRs, shown in Figure 7.5, further indicates a high degree of surface oxygenation. All SRs exhibited associated to C=O stretching peaks at peaks at 1700 cm^{-1} and C-O peaks at 1260 and 1210 cm^{-1}. The presence of humin compounds was evident with pronounced peaks at 1510 & 1595 cm^{-1}, associated with furanic C=C bonds. The C=C peak shifted to ~1580 cm^{-1}, which indicates the presence of polycyclic furanic compounds, mostly due to hydrothermal carbonisation. Polycyclic surface properties have been previously found to enhibit hydrophobic properties [21], which promote biofilm formation and stimulate microbial activity. There were still peaks at 3600-3000 cm^{-1}, 3000-2800 cm^{-1} and 1032 cm^{-1} that are associated with O-H

stretching, C-H bending and C-O stretching respectively, from unreacted cellulose and hemicellulose. The small peaks at 1360 cm^{-1} are linked to SO_3H, due to sulfonation of the surface area from the acid catalyst.

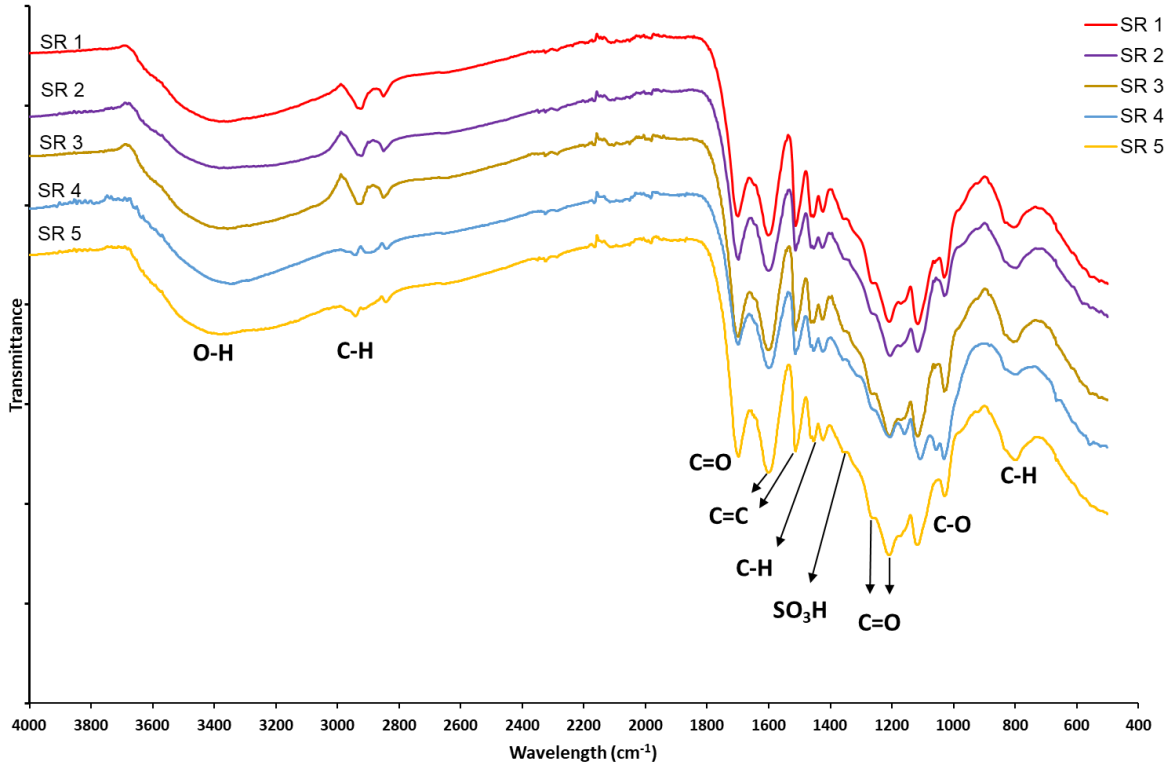

Figure 7.5: FTIR spectra of SRs 1-5

Conductive carbon materials have been proposed to promote direct interspecies electron transfer in methanogens [23], however Cruz Viggi *et al.* suggested that bulk electrical conductivity (EC) is one of many indicators of char electron transfer capacity. SR5 exhibited a remarkable EC of 11.7 mS in water, as shown in Table 7.5, compared with SRs 1-4, This may be attributed to the reaction conditions of 180 °C and 120 minutes facilitated the formation of graphitic and crystalline structure of humin derived carbon spheres on SR5 causing the increased EC [17].

Table 7.5: Characteristion of untreated miscanthus and five different solid residues

Biomass Type	Miscanthus	SR 1	SR 2	SR 3	SR 4	SR 5
Ash (wt%)	2.9	2.19	2.64	2.63	2.08	1.85

Volatile Matter (wt%)	84.7	68.2	53.6	64.2	72.5	65.2
Fixed Carbon (wt%)	9.6	26.4	40.4	28.3	22.2	29.6
pH	3.56	2.79	2.54	2.5	2.43	2.32
EC (mS)	5.48	1.71	3.36	3.14	4.28	11.68
BET (m2 / g)	/	17	21	19	9	35
Bulk Atomic O/C	0.66	0.35	0.27	0.29	0.38	0.26
Surface Atomic O/C	0.72	0.41	0.40	0.50	0.38	0.54

Enhanced interspecies electron transfer can be observed as increase in biogas quality, due to the promotion of more efficient conversion of organic acids to methane relative to CO_2 [24]. However, it should be noted that SRs 1-4 exhibited lower electrical conductivity than that of the untreated *Miscanthus* feedstock. This is could be caused by the significant reduction of metal ions identified by XRF (Appendix C – Table 1), due to acid leaching and it is further evidenced by their lower ash contents (range of 1.85-2.64 wt.%), in contrast with other hydrochars, which generally exhibit higher ash contents than the starting feedstocks [25]. Previous studies have proposed that hydrochars increase the bioavailability of trace elements, which have been partially attributed to promotion of methanogen enzymatic activity and, consequently, increased CH_4 yields. Due to the low trace element composition of the SR compared with the initial feedstock, it can be hypothesised that the SR will not increase nutrient bioavailability as previously reported with hydrochars [26]. Therefore, it can be assumed that the potential benefits of SR additives in this study would be confined to biofilm promoted microbial diversity and adsorption of cation inhibitors.

7.3.2 Effects of SR addition on methane production (Trial 1)

The acid hydrolysis parameters (shown in Table 7.2) were investigated with a focus on levulinic acid production and the highest yield of 17.1 wt.% (64.5% theoretical) was achieved for operating conditions leading to SR3 type residue. Therefore, SR3 (hereafter simply referred to as SR) was selected as additive to study in greater detail the effect of supplementing AD reactors (methane yields were measured daily for 14 days) for digestion of problematic feedstock (CM). This was achieved investigating increasing additive levels (2 -10 g/L) that were loaded at the start of the digestion period (batch mode digestion). The cumulative methane yields over the 14 days are shown in Figure 7.6, alongside the predicted methane yields according to the Gompertz model.

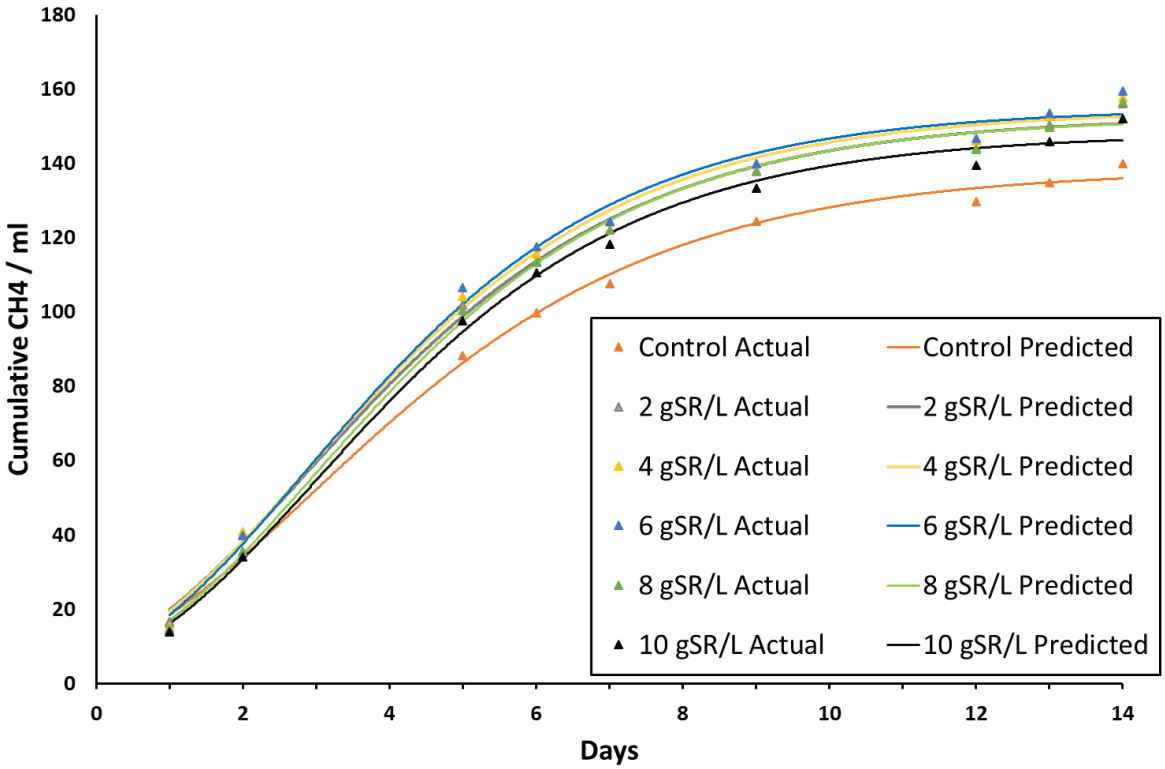

Figure 7.6: Cumulative methane yield of different SR addition and predicted yields

The Gompertz model was statistically significant, and the calculated Gompertz model parameters are shown in Table 7.6. The SR addition did not stop the anaerobic digestion of CM and all reactors normally produced methane-containing biogas. The CM control yielded 136 ml CH_4/gVS was compared with a stoichiometric CH_4 potential of 459 ml/gVS and resulted in a biodegradability index of 30%. The addition of 2 gSR/L significantly increased the cumulative methane yield (+12% CH_4) with respect to the CM control, strongly demonstrating a beneficial effect to AD, with a further minor improvement (+14.1% CH_4) at 6 g/L. Tripling the SR concentration did not lead to a significant increase in CH_4 production, suggesting the additive's organic component (volatile solids) is not being degraded in the reactors however, results indicate it is promoting microbial growth and/or adsorbing inhibitors. Furthermore, the small change in methane yields (~2%) between 2-6 gSR/L indicates that overall the AD system is not undergoing significant stress and SR addition could potentially be more beneficial to destabilised (or closer to inhibiting thresholds) environments.

Table 7.6: Summary of Kinetic data for the AD of CM with different SR concentrations

Condition	Cumulative CH_4 Yield / ml	Modified Gompertz parameter			Statistics	
	F	A_{Max}	R^{Max}	λ	R^2	*p*
Control	140	138.4	18.44	0.1696	0.9960	0.9976
2 g/L	156	152.7	21.7	0.256	0.9946	0.9966
4 g/L	158	154.4	22.51	0.3189	0.9937	0.9942
6 g/L	160	154.8	23.22	0.3974	0.9917	0.9939
8 g/L	157	152.4	22.32	0.4615	0.9949	0.9960
10 g/L	152	148	21.81	0.492	0.9945	0.9963

F is the measured cumulative methane production, mL/g VS added, A_{max} is the predicted cumulative methane production, mL/g VS added day, R_{Max} is the maximum methane production rate, mL/ g VS day, and λ is the duration of the lag phase

A noticeable decrease in CH_4 yields occurred at higher SR loads (8 and 10 gSR/L), despite remaining significantly above the CM control. At higher concentrations, chars have been reported to inhibit microbial communities [27]. We estimate this to be

associated with the SR's acidic properties to a very minor extent as well as the presence of chemical inhibitors on the SR surface that were formed during the acid hydrolysis process, such as organic compounds or sulphates. Although the high sulphur content of the inoculum used in this study would suggest microbial acclimation to sulphate groups, sulphur inhibition cannot be discarded based solely on the bio-methane potential (BMP). Future work should investigate the cause of the inhibitory effect and the long-term effects in AD systems fed in continuous mode, with the opportunity to adapt acid hydrolysis variables to target minimised long term inhibition. It is worth pointing out that for all BMP conditions, SR addition resulted in higher methane yield than the CM control, which emphasises its positive effects on biogas production.

The Gompertz model has successfully been used to model BMP experiments from a range of substrates [8,28]. The models' regression values in this study were all greater than 0.99 for all experimental conditions, indicating an outstanding fit of the predictive model. SR additive increased the maximum methane production (A_{max}) achievable by 6.9 – 11.8% and the maximum methane production rate (R_{Max}) by 18.3-25.9 %, both compared with performance of control reactor. This suggests that SR not only increases the absolute methane yields from CM over the digestion period, but it also increases the maximum methane production rate achievable. The Gompertz model parameters demonstrates that higher SR concentrations also prolonged the lag phase compared with the CM control, from 0.17 days to 0.49 days. This shows that the SR slowed the microbial activity, however a lag time <1 day indicates a high initial microbial activity and overall microbial acclimation to the system conditions. The increase in lag time for 8-10 gSR/L implies a mild inhibition is taking place and that the

microbial community reacted negatively to those SR levels. This can be further seen with a decrease in A_{max} from 17.15 to 16.46 ml CH_4/ gVS day between 6 g/L and 8 g/L, suggesting that inhibition is caused by the hydrochar itself and not from long term imbalances in the complex system. Although the overall increase in methane yields negates this inhibition and would only be of concern at significantly higher SR concentrations.

7.3.3 Effect of different SRs on Anaerobic Digestion

Four of the five SRs investigated in this study resulted in higher methane yields from the anaerobic digestion of CM with 6 g/L SR concentration, as presented in Figure 7.7. The highest cumulative methane yield was observed with the addition of SR3 followed by SR5, SR4 and SR1, as shown in Table 7.7 alongside the Gompertz model parameters. SR3 improved the cumulative methane yield relative to the un-supplemented (control) digester(by + 3.1%), which was less than 14.1% observed in Trial 1. Both trials utilised the same conditions though there were significant changes in the inoculum digester source in terms of initial composition and microbial diversity, as shown in section 7.3.5. This change was most evident in the rise of the biodegradability index between Trial 1 and 2, from 30% to 35%. This suggests that the addition of SR has less beneficial effect on AD systems with higher biodegradability. It may be relevant in future to assess hydrochar addition to anaerobic digestion relative to the overall systems to accurately gauge the effects.

Table 7.7: Summary of kinetic data for the AD of CM with different SR concentration

Condition	Cumulative CH_4 Yield		Modified Gompertz parameter			Statistics	
	F	Change due to SR	A_{Max}	R^{Max}	λ	R^2	*p*
Control	163.5	0.0%	162	19.1	-0.40	0.9958	0.9962

SR 1	165.5	1.2%	166	18.2	-0.43	0.9932	0.9953
SR 2	157.4	-3.7%	156	18.1	-0.41	0.9949	0.9963
SR 3	168.4	3.1%	168	19.3	-0.35	0.9937	0.9966
SR 4	165.9	1.5%	164	19.4	-0.43	0.9917	0.9935
SR 5	166.6	1.9%	166	18.8	-0.49	0.9970	0.9972

F is the measured cumulative methane production, mL/g VS added, A_{max} is the predicted cumulative methane production, mL/g VS added day, R_{Max} is the maximum methane production rate, mL/ g VS day, and λ is the duration of the lag phase

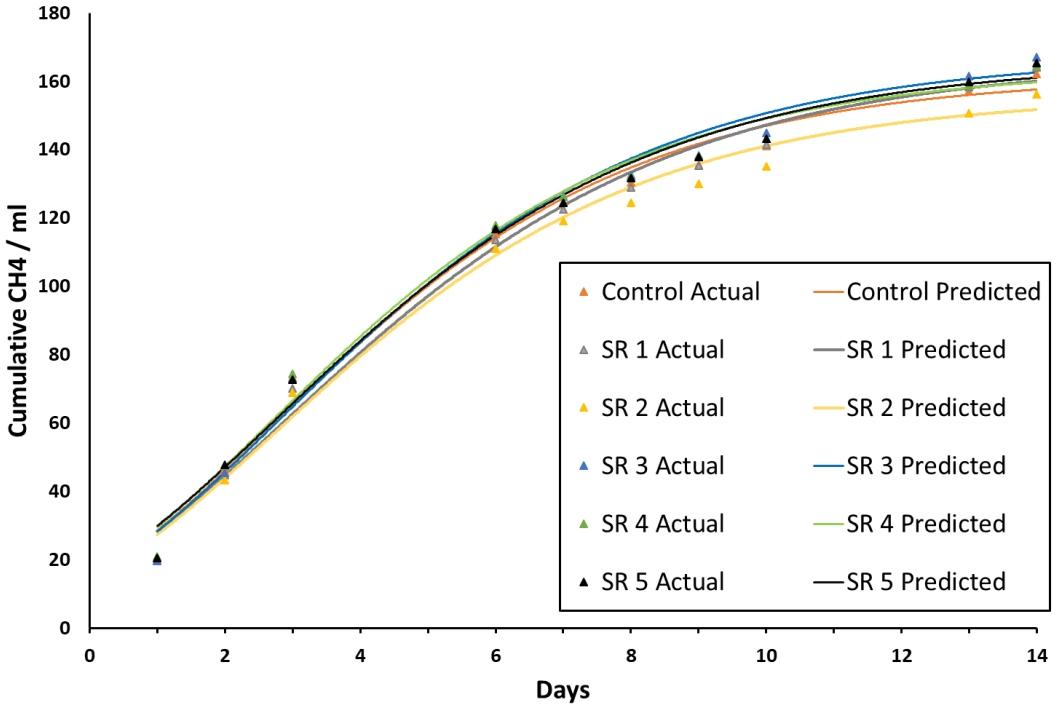

Figure 7.7: Cumulative methane yield of SRs formed under different reaction conditions

The SR3 was produced as the solid product from the 2M H_2SO_4 catalysis of *Miscanthus x Giganteus* under 180 °C for 30 minutes, which not only corresponded with the highest levulinic acid yield (17.1 wt.%) but also to the best methane yield improvement (3.1%). This natural synergy may suggest that more extreme catalysis conditions produce AD inhibitors such as humins. This inhibition was observed from SR2 (190 °C 30 minutes), the highest reaction temperature, which was the only SR type leading to a negative effect on the methane yields. SR2 was noted as being highly carbonaceous with the highest fixed carbon content, lowest bulk O/C ratio and high aromaticity indicated by the FTIR analysis.

Higher reaction temperatures may be the direct cause of this toxicity and not the humins directly, as SR5 had the most observed humin formation, which did not impede the AD process. Due to the similarity in methane yields between the different SRs it is difficult to assess directly each material property, however it can be concluded that a wide variety of SRs can be used as an AD supplement.

7.3.4 Ammonium Content

The addition of even a small amount of the SR significantly decreased the ammonium contents of the reactors at the end of the digestion period, as shown in Table 7.8. In Trial 1, the un-supplemented control reactor with CM had an ammonium content exceeding 3 g/L, which strongly indicates ammonium inhibition associated with the digestion of nitrogen rich CM. The addition of SR decreased the ammonium concentration under all conditions, indicating partial adsorbance of the ammonium. In Trial 1, increasing the SR concentration from 2 g/L to 8 g/L had negligible effect on the ammonium content indicating that SR adsorbed the excess ammonium without disturbing the ammonia/ammonium buffered state. Trial 2, which investigates the different SR types, had a far lower ammonium concentration (2.3 g/L) in the control reactor, which was attributed to changes in the inoculum composition, although the addition of SR did result in decreasing ammonium concentrations detected.

Table 7.8: Ammonium content and pH of reactors after 14 days of digestion

Trial 1			Trial 2		
Condition	Ammonium g/L	pH	Condition	Ammonium g/L	pH
Control	3.0 ± 0.2	7.62	Control	2.3 ± 0.1	8.00
2 g/L	2.3 ± 0.3	7.57	SR 1	2.0 ± 0.0	7.77
4 g/L	2.0 ± 0.1	7.56	SR 2	1.9 ± 0.1	7.69
6 g/L	2.4 ± 0.2	7.57	SR 3	2.1 ± 0.1	7.76
8 g/L	2.2 ± 0.1	7.58	SR 4	2.1 ± 0.1	7.74

10 g/L	1.9 ± 0.3	7.56	SR 5	2.1 ± 0.0	7.83

The addition of SR2 caused the lowest observed ammonium concentration (1.9 g/L), which can be attributed to the higher degree of aromaticity from hydrothermal carbonisation. However, the effect of all 5 SRs on the ammonium concentration were broadly similar, with values in the range of 1.9-2.1 g/L suggesting similar equilibrium conditions. It is not clear if the decrease ammonium concentration was the only direct effect of the increased methane yields associated with the SR addition, although this shows a possible mechanism of action. It should also be noted that the addition of SR under all conditions caused a drop in the final pH of the reactors caused by mild acidity introduced via the SR addition. Which was destabilising for the digestion in this trial, however larger and more impactful pH drops cannot be excluded on an equivalent commercial scale operation based on this concept.

7.3.5 Effect of Hydrochars on Microbial Composition

7.3.5.1 Effect of Loading Dose (Trial 1)

The effect of the varying addition of SR3 to the AD of CM was investigated for the correlation between methane yield and microbial community composition. The presence of hydrochars significantly altered the abundance of microbial cells ($F_{4,5}$=10.5, p=0.006), as shown in Table 7.9. The increase in of hydrochar loading resulted in a statistically significant increase in microbial cell count ($F_{4,5}$=7.32, p=0.025)

Table 7.9: Quantitative PCR analysis for the hydrochar conditions for Trial 1

Condition	Cells	Diversity			
	Cells per ml	Observed	Chao1	Shannon	Simpson
Control	1.46E+11	134.5	149	3.97	0.9449

SR3 2g/L	2.13E+11	267	1958	5.19	0.9919
SR3 4g/L	1.84E+11	273	313	5.22	0.9919
SR3 6g/L	1.16E+11	247.5	1636	5.16	0.9918
SR3 8g/L	2.87E+11	278.5	403	5.09	0.9891
SR3 10g/L	2.92E+11	269.5	339	5.14	0.9899

The addition of hydrochar increased the microbial diversity of the AD systems according to three different alphas diversity indices Chao1, Shannon and Simpson. Increased microbial diversity has been associated with increased reactor stability and higher methane yields[29]. Similar increases in microbial diversity have been found with the addition of hydrochar by different authors [30–32]. Although the addition of more than 2g/L had minimal effect on microbial diversity indicating that the effect of SR was not linear. It should also be noted that at 8-10 g/L, no significant decrease in microbial diversity was detected, despite the decrease in methane yields. This suggests that the SR related inhibition was 'metabolic' related and not due to microbes' death.

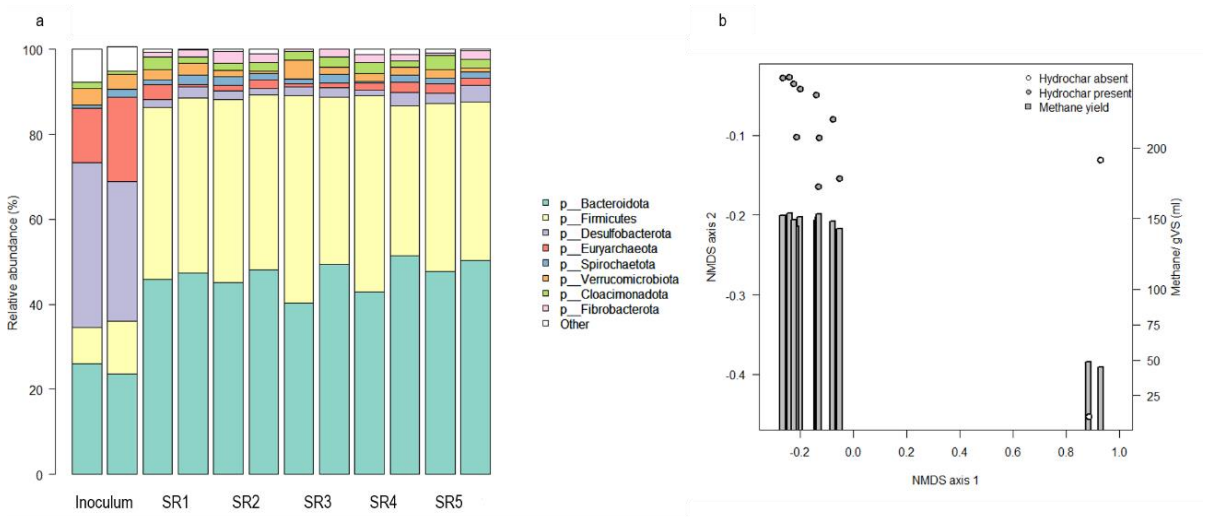

Figure 7.8: a) genus level changes in microbial composition correlated with increased methane yield. b) NMDS dissimilarity analysis of SR supplemented AD reactors (circles), and correlation with methane yield (bars).

Analysis also indicated that the microbial diversity at the domain level was dominated by bacteria in all the samples (97.5±0.7%). Organisms belonging to domain bacteria were significantly more abundant on the hydrochar samples than the inoculum ($F_{5,6}$ =

11, p = 0.005). This result meant that there was a lower abundance of archaea in the hydrochar samples (2.5±0.7%). Microbial communities were dominated by phyla Bacteroidetes (43.2 ± 1.1%) and Firmicutes (38.5 ± 2.1%), as shown in Figure 7.8a. Differences in microbial composition were visualised on NMDS ordination space and the presence of hydrochars significantly (PERMANOVA $F_{1,11}$=37.14, p=0.016, R^2=0.79) altered the composition of the communities and this change was strongly correlated (R^2=0.99, t_{10}=22.825, p<0.001) with an increase in methane yield (Figure 4b).

7.3.5.2 Effect of Different Hydrochars (Trial 2)

Samples treated with different substrates (SR1 to SR5) ranged between $2.51x10^{11}$ to $6.09x10^{11}$ cells mL^{-1} ($3.86x10^{11} \pm 1.3 \times 10^{11}$ cells mL^{-1}), as shown in Table 7.10. Similar to Trial 1, the addition of hydrochars ($F_{4,5}$=8.37, p=0.010) altered the total abundance of microorganisms. Further differences ($F_{4,5}$=6.31, p=0.030) were observed between the different hydrochars used. Most notably, SR3 displayed the lowest microbial cell count relative to the other SRs in Trial 2, despite having the highest methane yields. While SR2, which had a negative effect on the methane yields, displayed the highest microbial cell count. This indicates that the effect of SR is not directly linked to microbial abundance and suggests that the SRs properties have differing effects on the complex microbial communities.

Table 7.10: Quantitative PCR analysis for the hydrochar conditions for Trial 2

Condition	Cells	Diversity			
	Cells per ml	Observed	Chao1	Shannon	Simpson
Control	5.08E+11	170	184	4.53	0.9797
SR 1	5.23E+11	313.5	356	5.42	0.9934
SR 2	6.02E+11	259	1682	5.15	0.9915

SR 3	1.93E+11	236	1730	5.11	0.9915
SR 4	2.84E+11	275.5	360	5.26	0.9923
SR 5	3.15E+11	261.5	339	5.23	0.9924

The alpha diversity (observed, Chao1, Simpson and Shannon indices) showed more variation than observed in Trial 1, which was due to the 7-month gap between trials. The increased microbial diversity between trials could therefore be the cause of higher methane yields between trials [33]. This is consistent with Usman *et al*. who suggested that microbial diversity was primarily linked with ammonium concentration, which was also lower in Trial 2 [34].

No change in the dominant microorganisms was observed between Trial 1 and , where organisms affiliated to Bacteroidetes (40.9 $\pm$ 1.55%) and Firmicutes (39.1 $\pm$ 2%) were the most prevalent. Organisms affiliated to phyla Bacteroidetes and Firmicutes have been reported as the main microbial components in similar anaerobic digestion processes, and the main bacteria impacting methane yield [31,35]. Regarding archaeal organisms, phylum Euryarchaeota includes hydrogenotrophic, acetate/H_2/formate oxidizing, methanogenic, hydrocarbon utilizing groups (order/genus), and its presence has frequently been detected on refinery waste environments [36]. The cumulative yield of methane detected on this project corroborates that the syntrophic interaction between bacterial and archaeal organisms (established by acidogenesis and methanogenesis) occurs within the AD system [33].

Additionally, the production of methane may be occurring through other processes such as direct interspecies electron transfer [34,37]. The results above show that the relative abundance of Archaea (Euryarchaeota) decreased in the presence of the hydrochar substrates (SR3 2 to 10 g/L and SR1 to SR5) compared to inoculum control.

However, the high methane yields may indicate that the lower relative abundances did not result in the lower absolute concentrations of methanogens archaea [32]. In addition, results suggest that the archaeal community is becoming more specialized towards using the substrate to produce methane, a phenomenon observed in similar anaerobic digestion processes [38]. Another possible explanation for the decrease of the methanogens is the stability of the AD system, since it has been reported that archaeal methanogens are more often observed in extreme conditions, due to their higher robustness [39]. Interestingly, SR2 which negatively impacted the 14-day methane yields compared with the control reactor had minimal differences in microbial composition compared with the other SRs. This shows that the SR2 still exhibited microbial promotion properties. Indicating that the microbial inhibitors formed during the high temperature catalysis (190 °C) were likely metabolic inhibitors, which corresponds with the abnormally high microbial cell count.

Our results show that whilst the presence of hydrochar has a significant effect on microbial composition (PERMANOVA $F_{1,9}$=70.02, p=0.010, R^2=0.88). However, once the presence of any hydrochar is accounted for during AD, there is no statistical correlation between the microbial composition and either the amount of hydrochar loaded ($F_{1,9}$=0.38, p=0.597, R^2=0.01) or methane yield (R^2=0.11, t_8=0.31, p=0.767). Therefore, the addition of a small quantity of SR formed under any conditions was sufficient to induce microbial change towards a more diverse equilibrium condition. The microbial promotion activity of solid residues could be caused by either the functionalised microporous structures, supporting microbial growth or due to the associated reduction in ammonium concentrations.

7.4 Conclusions

The overall results from the trials presented in this chapter show that the SR from the acid catalysed production of levulinic acid from lignocellulosic biomass, can be beneficially used as an anaerobic digestion supplement. The SR produced at the optimum levulinic acid conditions resulted in a 14% increase in methane yields compared with the control reactor with an optimised concentration of 6g/L. The optimum SR was produced under the catalysis conditions of 180 °C for 60 minutes, which corresponded with the optimum levulinic acid synthesis yields, suggesting possible natural synergy between levulinic acid and AD optimisation. Furthermore, the residues were shown to decrease ammonium concentration across all conditions by up to 33%.

Microbial diversity analysis proved community's richness significantly increased with the addition of small quantities of SR formed under any of the examined set of catalytical conditions, showing the inherent microbial growth's promotion effects of the SR. The solid residues showed some metabolic inhibition of the microbial community that mostly negated by more efficient microbial conversion pathways. These results show that the application of waste SR from biorefineries could potentially be used as a low-cost char substance for the improvement of a large variety of difficult AD feedstocks.

7.5 References

1. Cruz Viggi, C., Simonetti, S., Palma, E., Pagliaccia, P., Braguglia, C., Faz, S., Baronti, S., Navrarra, M., Pettiti, I., Koch, C., Harnish, F., Aulenta, F. Enhancing methane production from food waste fermentate using biochar: The added value of electrochemical testing in pre-selecting the most effective type of biochar. Biotechnol. Biofuels 10, 1–13 (2017).
2. Xu, J., Mustafa, A. M., Lin, H., Choe, U. Y. & Sheng, K. Effect of hydrochar on anaerobic digestion of dead pig carcass after hydrothermal pretreatment. Waste Manag. 78, 849–856 (2018).
3. Jin, H., Sun, E., Xu, Y., Guo, R., Zheng, M., Huang, H., Zhang, S. Hydrochar derived from anaerobic solid digestates of swine manure and rice straw: A potential recyclable material. BioResources 13, 1019–1034 (2018).
4. Masoumi, S., Borugadda, V. B., Nanda, S. & Dalai, A. K. Hydrochar: A review on its production technologies and applications. Catalysts 11, (2021).
5. Chen, J. L., Ortiz, R., Steele, T. W. J. J. & Stuckey, D. C. Toxicants inhibiting anaerobic digestion: A review. Biotechnol. Adv. 32, 1523–1534 (2014).
6. Hurst, G., Peeters, M. & Tedesco, S. Integration of Catalytic Biofuel Production and Anaerobic Digestion for Biogas Production. Energy and Sustainable Futures, Springer Proceedings in Energy, 16 (2021). doi:10.1007/978-3-030-63916-7_16
7. Petersen, S. O., Blanchard, M., Chadwick, D., Prad, A. D., Eduoard, N., Mosquera, J., Sommer, S. G. Manure management for greenhouse gas mitigation. Animal 7, 266–282 (2013).
8. Kafle, G. K. & Chen, L. Comparison on batch anaerobic digestion of five different

livestock manures and prediction of biochemical methane potential (BMP) using different statistical models. Waste Manag. 48, 492–502 (2016).

9. Ngumah, C., Ogbulie, J., Orji, J. & Amadi, E. Potential of Organic Waste for Biogas and Biofertilizer Production in Nigeria. Environ. Res. Eng. Manag. 63, 60–66 (2013).
10. Qiu, L., Deng, Y. F., Wang, F., Davaritouchaee, M. & Yao, Y. Q. A review on biochar-mediated anaerobic digestion with enhanced methane recovery. Renew. Sustain. Energy Rev. 115, 109373 (2019).
11. Majumder, S., Neogi, S., Dutta, T., Powel, M. A. & Banik, P. The impact of biochar on soil carbon sequestration: Meta-analytical approach to evaluating environmental and economic advantages. J. Environ. Manage. 250, 109466 (2019).
12. Kumar, M., Dutta, S., You, S., Luo, G., Zhang, S., Show, P. L., Sawarkar, A. D., Singh, L., Tsang, D. C. W. A critical review on biochar for enhancing biogas production from anaerobic digestion of food waste and sludge. J. Clean. Prod. 305, 127143 (2021).
13. Gronwald, M., Vos, C., Helfrich, M. & Don, A. Stability of pyrochar and hydrochar in agricultural soil - a new field incubation method. Geoderma 284, 85–92 (2016).
14. Melligan, F., Dussan, K., Auccaise, R., Novonty, E. H., Leahy, J. J., Hayes, M. H. B., Kwapinski, W. Characterisation of the products from pyrolysis of residues after acid hydrolysis of Miscanthus. Bioresour. Technol. 108, 258–263 (2012).
15. Sweygers, N., Somers, M. H. & Appels, L. Optimization of hydrothermal conversion of bamboo (Phyllostachys aureosulcata) to levulinic acid via response surface methodology. J. Environ. Manage. 219, 95–102 (2018).

16. van Zandvoort, I., Wang, Y., Rasrendra, C. B., van Eck, E. R. H., Bruijincx, P. C. A., Heeres, H. J., Weckhusen, B. M. Formation, molecular structure, and morphology of humins in biomass conversion: Influence of feedstock and processing conditions. ChemSusChem 6, 1745–1758 (2013).

17. Hoffmann, V., Jung, D., Zimmermann, J., Correa, C., Elluech, A., Halouani, K., Kruse, A. Conductive carbon materials from the hydrothermal carbonization of vineyard residues for the application in electrochemical double-layer capacitors (EDLCs) and direct carbon fuel cells (DCFCs). Materials (Basel). 12, (2019).

18. Cai, J., Li, B., Chen, C., Wang, J., Zhao, M., Zhang, K. Hydrothermal carbonization of tobacco stalk for fuel application. Bioresour. Technol. 220, 305–311 (2016).

19. van Zandvoort, I., Koers, E. J., Weingarth, M., Bruijnincx, P. C. A., Baldus, M., Weckhuysen, B. M. Structural characterization of 13C-enriched humins and alkali-treated 13C humins by 2D solid-state NMR. Green Chem. 17, 4383–4392 (2015).

20. Patil, S. K. R. R., Heltzel, J. & Lund, C. R. F. F. Comparison of structural features of humins formed catalytically from glucose, fructose, and 5-hydroxymethylfurfuraldehyde. Energy and Fuels 26, 5281–5293 (2012).

21. Masís-Meléndez, F., Segura-Chavarría, D., García-González, C. A., Quesada-Kimsey, J. & Villagra-Mendoza, K. Variability of physical and chemical properties of TLUD stove derived biochars. Appl. Sci. 10, 1–20 (2020).

22. Dieguez-Alonso, A., Funke, A., Anca-Couce, A., Rombola, A. G., Ojeda, G., Bachmann, J., Behrendt, F. Towards biochar and hydrochar engineering-influence of process conditions on surface physical and chemical properties, thermal stability, nutrient availability, toxicity and wettability. Energies 11,

(2018).

23. Guo, W., Li, Y., Zhao, K., Jiang, H., Zhou, H. Performance and Microbial Community Analysis of Anaerobic Digestion of Vinegar Residue with Adding of Acetylene Black or Hydrochar. Waste and Biomass Valorization, 0123456789 (2019). doi:10.1007/s12649-019-00664-3
24. Masebinu, S. O., Akinlabi, E. T., Muzenda, E. & Aboyade, A. O. A review of biochar properties and their roles in mitigating challenges with anaerobic digestion. Renew. Sustain. Energy Rev. 103, 291–307 (2019).
25. Wang, T., Zhai, Y., Zhu, Y., Li, C. & Zeng, G. A review of the hydrothermal carbonization of biomass waste for hydrochar formation: Process conditions, fundamentals, and physicochemical properties. Renew. Sustain. Energy Rev. 90, 223–247 (2018).
26. Ambaye, T. G., Rene, E. R., Nizami, A. S., Dupont, C., Vaccari, M., van Hullebusch, E. D. Beneficial role of biochar addition on the anaerobic digestion of food waste: A systematic and critical review of the operational parameters and mechanisms. J. Environ. Manage. 290, 112537 (2021).
27. Dudek, M., Świechowski, K., Manczarski, P., Koziel, J. A. & Białowiec, A. The effect of biochar addition on the biogas production kinetics from the anaerobic digestion of brewers' spent grain. Energies 12, 1–22 (2019).
28. Pan, J., Ma, J., Liu, X., Zhai, L., Ouyang, X., Liu, H. Effects of different types of biochar on the anaerobic digestion of chicken manure. Bioresour. Technol. 275, 258–265 (2019).
29. Ramirez, I., Volcke, E. I. P., Rajinikanth, R. & Steyer, J. P. Modeling microbial diversity in anaerobic digestion through an extended ADM1 model. Water Res. 43, 2787–2800 (2009).

30. Wu, B., Yang, Q., Yao, F., Chen, S., He, L., Hou, K., Pi, Z., Yin, H., Fu, J., Wang, D., Li, X. Evaluating the effect of biochar on mesophilic anaerobic digestion of waste activated sludge and microbial diversity. Bioresour. Technol. 294, (2019).

31. Usman, M., Shi, Z., Ren, S., ngo, H. N., Luo, G., Zhang, S. Hydrochar promoted anaerobic digestion of hydrothermal liquefaction wastewater: Focusing on the organic degradation and microbial community. Chem. Eng. J. 399, 125766 (2020).

32. He, J., Ren, S., Zhang, S. & Luo, G. Modification of hydrochar increased the capacity to promote anaerobic digestion. Bioresour. Technol. 341, 125856 (2021).

33. Bareither, C. A., Wolfe, G. L., McMahon, K. D. & Benson, C. H. Microbial diversity and dynamics during methane production from municipal solid waste. Waste Manag. 33, 1982–1992 (2013).

34. Usman, M., Hao, S., Chen, H., Ren, S., Tsang, D. C. W., O-Thing, S., Luo, G., Zhang, S. Molecular and microbial insights towards understanding the anaerobic digestion of the wastewater from hydrothermal liquefaction of sewage sludge facilitated by granular activated carbon (GAC). Environ. Int. 133, 105257 (2019).

35. Krakat, N., Schmidt, S. & Scherer, P. Potential impact of process parameters upon the bacterial diversity in the mesophilic anaerobic digestion of beet silage. Bioresour. Technol. 102, 5692–5701 (2011).

36. Sarkar, J., Kazy, S. K., Gupta, A., Dutta, A., Mohaptra, B., Roy, A., Bera, P., Mitra, A., Sar, P. Biostimulation of indigenous microbial community for bioremediation of petroleum refinery sludge. Front. Microbiol. 7, 1–20 (2016).

37. Hemme, C. L. et al. Metagenomic insights into evolution of a heavy metal-

contaminated groundwater microbial community. ISME J. 4, 660–672 (2010).

38. Vasconcelos, E. A. F., Santaella, S. T., Viana, M. B., dos Santos, A. B., Pinheiro, G. C., Leitao, R. C. Composition and ecology of bacterial and archaeal communities in anaerobic reactor fed with residual glycerol. Anaerobe 59, 145–153 (2019).

39. Pasalari, H., Gholami, M., Rezaee, A., Esrafili, A. & Farzadkia, M. Perspectives on microbial community in anaerobic digestion with emphasis on environmental parameters: A systematic review. Chemosphere 270, (2021).

Chapter 8: Conclusions and Recommendations

8.1 Introduction

The aim of this thesis was to investigate the integration of AD into catalytic lignocellulosic biorefineries through the utilisation of the post-catalysis solid residue waste. A survey of lignocellulosic biomass available in the UK was conducted and seven different cellulose-rich feedstocks were characterised in detail for the preparation of representative solid residues. The effects of catalysis process parameters on solid residue yields and properties was investigated from poplar biomass with sulphuric acid catalysts, in conjunction with levulinic acid and aqueous by-product yields. Equivalent levulinic acid yields to that of sulphuric acid were achieved with synergistic heterogeneous catalysts and the solid residue yields and material properties were characterised. Comparison of solid residue properties from levulinic acid production obtained with homogenous and heterogeneous catalysts, revealed significant differences in morphology and composition. Similarly, several different solid residues resulted from sulphuric acid catalysis of *Miscanthus x Giganteus* under different reaction conditions, which were characterised in detail. The addition of solid residue to AD of CM (used as exemplar ammonium rich digestion feedstock) improved methane yields by up to +14%, through the adsorption of ammonium inhibitors and resulted increased microbial diversity. This chapter highlights how the research objectives have been achieved as well as the strengths and limitations of this work with regards to the novelty of the findings, including recommendations for future work.

8.2 Summary of Research

A literature review of solid residues from acid catalysis presented in **Chapter 2** found possible connections between the catalytically-derived humins and hydrochar. By-product humin residues from the production of levulinic using sugars has been investigated in depth by multiple authors and resulted in detailed characterisation and reaction's mechanism understanding. These material properties have previously not been compared to more commonly used hydrochars and the review of literature found similarities in formation mechanism. Further studies of the hydrochar formation revealed possible carbonisation and condensation of extractives, namely acid soluble lignin condensation, which has previously not been explored. Solid residues from the acid catalysis of lignocellulosic biomass, therefore, exhibit material properties similar to both those of humins and hydrochar. Based on current knowledge several hydrochar applications are considered not economically feasible, due to the energy requirements of hydrochar production, and specifically AD supplementation, despite offering unique answers to pressing environmental issues.

In **Chapter 4,** the first objective was achieved by the characterisation of several varieties of biomass to identify suitable materials for catalysis. Considerations were made using the UK integrated energy policy framework to select representative locally available feedstocks in the UK for full characterisation. Analysis was conducted to identify high yielding energy crops with low fertiliser requirements as well as agricultural residues. Selected lignocellulosic biomass samples were chosen for full quantitative compositional characterisation, using international standards, to identify

the individual monomeric sugar contents as well as inert and condensable compounds. The feedstocks varied between 37-55 wt.% in cellulose content, with poplar wood having the highest cellulose content and lowest extractive fraction.

In **Chapter 5,** the second objective to Study the effects of operating parameters on the by-product yields was achieved in conjunction with high value products yields and solid residue properties. Cellulose-rich poplar wood was chosen as the first representative feedstock and was converted to levulinic acid yield using sulphuric acid catalyst under a microwave heating regime. The levulinic acid, solid residue, furfural and net formic acid yields were modelled using mathematical RSM techniques to produce statistically significant models. Using the RSM models a maximum levulinic acid of 62 mol.% (21.0 wt.%) was achieved at 188 °C, 126 min with 1.93M sulphuric acid, which was equivalent to other works. The maximum levulinic acid yield corresponded to a solids residue yield 52.1 wt.% and showed the importance of solid waste on the overall mass balance.

The optimisation of levulinic acid used a minimising objective function, which targeted reduced solids yield formation that inherently resulted in reduced by-product formation. In conjunction with the solid residue RSM model, there were indications of natural synergy between the maximisation of products and solid residue minimisation across the investigated process parameters. In addition, the net formic acid and acetic yields were modelled, the results showed that acetic was inert through the reaction process. While the net formic acid suggested that the initial poplar wood hydrolysis yielded significant formic acid by-products but was later consumed as the reaction progressed.

The solid residue from the sulphuric acid catalysis was characterised using FTIR, EDX, SEM, XRF and CHNO compositional analysis. The characterisation indicated a high degree of surface functionalisation, with differences between the surface O/C ratio bulk O/C ratio. The surface functionalisation with O-H, C=O and COOH groups indicated catalytically-derived humins formed on the particle surface area. This was confirmed by the presence of carbon spheres on the surface area, visually appraised via SEM imaging. Upon consideration of these material properties, similarities between the solid residue and hydrochar were identified and discussed in depth. The residues exhibited similar surface properties to hydrochar with less carbonised bulk properties. In addition, the acid catalysed process resulted in reduced ash and elemental composition compared with the starting biomass. Proposed applications for the solid residue were discussed based on hydrochar similarities, including use as combustion material and as a sorbent material.

In **Chapter 6**, the third objective of solid residue characterisation with different catalysts was achieved by the evaluation of the solid residue by-product from the production of levulinic acid with heterogeneous catalyst. Synergetic catalysis was investigated using sulphated zirconia and dilute hydrochloric acid to increase levulinic acid yields from *Miscanthus x Giganteus*. The addition of dilute 10 mM HCl was found to increase levulinic acid yields under all conditions with sulphated zirconia, as opposed to deionised water only. The effect of the dilute acid was proposed to lead to catalyst promotion or increased cellulose depolymerisation but could not be experimentally determined. The levulinic acid yields with 10 mM HCl and sulphated zirconia were optimised using RSM to achieve a maximum levulinic acid yield 63.8% at 160 ˚C, 80 mins, 2:1 catalyst-to-biomass ratio. The levulinic acid yields were

comparable with literature, however hinted to the possibility of increasing heterogeneous catalysts yield using simple aqueous modifiers.

The catalyst recyclability was investigated with and without calcination, finding that significant humins deposition on the catalysts surface likely caused or contributed to catalyst deactivation. After 3 cycles the levulinic acid yields decreased from 63.8% to 42.3% for calcined catalyst and 25.5% for uncalcined catalyst. The corrosive effect of dilute hydrochloric acid on the zirconium-based catalysts was assessed using ICP analysis to be <0.02wt%, indicating that the homogenous modifier did not affect catalyst recyclability. This strongly suggested that the predominant catalyst deactivation mechanism was caused by humin formation on the catalyst surface area.

The solid residue separated from the heterogeneous catalyst was characterised using SEM, EDX, XRD and CHNO analysis. The solid residue differed in several aspects to the residues produced in Chapter 5. Most notably, the lack of carbon spheres on the residue surface resulted in a lower surface O/C ratio and indicated the lack of humic materials in the solid residue matrix. This was confirmed through analysis of spent catalyst, which showed that humin formation was predominately occurring on the catalyst surface area. The XRD analysis revealed the solid residue contained significant quantities of unreacted crystalline cellulose. The overall solid residue composition was similar to that of unreacted biomass, with minimal surface functionalisation due to the formation of humin materials on the catalyst surface rather than the carbonaceous solid residue.

In **Chapter 7**, solid residue was produced from the acid catalysis of *Miscanthus x Giganteus* with sulphuric acid catalysts formed under five different process parameters ranging from 170-190 °C for 30-120 minutes. The solid residues were characterised with XRD, XRF, SEM, EDX, CHNO, FTIR, and BET analysis. The different reaction conditions resulted in varying surface and bulk properties in agreement with work from earlier chapters. The solid residues were subsequently investigated for the supplementation of AD of nitrogen-rich chicken manure. Using the solid residue formed under the optimum levulinic acid conditions (180 °C for 60 minutes), the AD process resulted in an increase in methane yields of +14% over a standard 14-day digestion. The solid residue concentration was varied between 0-10 g/L, with the optimum concentrations found at 6 g/L and a positive correlation between ammonium absorption and microbial diversity. At 8-10 g/L, there were signs of microbial inhibition (quantified as reduction in methane yields), however no significant change microbial diversity or cell count was detected. This suggested that the solid residue included metabolic inhibitors, which was further confirmed by the decreased methane yields obtained when adding residues formed at the highest temperature parameter of 190 °C, e.g. SR2.

All five of different solid residues produced under various conditions had an effect on the methane yields, ammonium composition and microbial composition during AD. The results indicated that the solid residue under the optimum levulinic acid conditions corresponded to the highest improvement in methane yields. Therefore, the optimisation of levulinic acid yields and solid residue properties for AD may be complementary.

8.3 Contribution to Knowledge

The outcomes of this thesis are of benefit to the fields of lignocellulosic biorefineries, acid catalysis, hydrochar formation and anaerobic digestion. This work was the first study to utilise solid residue from lignocellulose catalysis as an anaerobic digestion supplement and, thus, combining the fields of biomass catalysis, hydrochar production and anaerobic digestion under the concept of biorefinery integration. The positive research findings have the potential to offer a unique and alternative low carbon waste disposal and valorisation method for lignocellulosic biorefineries. Through the course of this work, several additional novel findings arose that greatly add to existing literature. This section outlines the contribution to knowledge of the PhD and how it will benefit individual fields of research.

The evaluation and modelling of process parameters on solid residue waste was the first detailed investigation of solid residue yields and was disseminated through a peer-reviewed journal article. The simultaneous investigation of the levulinic acid and solid residue yields revealed apparent synergy between levulinic acid optimisation and solid residue minimisation which potentially could act as a long-term heuristic approach. Also, the evaluation of the net formic acid yields found a previously unreported formic acid consuming process during acid hydrolysis that warrants further investigation. The synergetic catalysis was the first reported example of this phenomena for the production of levulinic acid from lignocellulosic biomass. The synergetic catalysis with sulphated zirconia and dilute hydrochloric acid was disseminated through a peer-review article publication. The addition of dilute mineral acids could be applied to a wide range of solid catalysts to improve levulinic acid yields and facilitate the use of a broader range of solid catalysts. The analysis of the solid residues with homogenous

and heterogeneous catalysts explicitly demonstrated the differences in residue properties, which would require different valorisation pathways. Furthermore, results presented in this thesis show the similarities between the humin-rich solid residue and hydrochar in both surface and bulk properties. The remarkable similarity was critically examined and further works should utilise this thesis as a reference for the cross-application of the two materials.

Most of all this thesis contributed to the fields of AD and biorefinery waste disposal by demonstrating the potential of solid residue as an AD supplement. The solid residue was quantitatively linked to increase of methane yields, microbial diversity and decrease of ammonium concentrations during AD. These results are under peer-review and are the first ever demonstration of this concept. The implications of this research will spark further interest in using solid residue as low-cost AD supplement.

8.4 Limitations of the Research

The research findings presented in this thesis are limited to the materials investigated, hence not universally applicable to all lignocelluloses. This thesis utilised two energy crops as starting materials alongside two different catalysts, which was sufficient to achieve the project objectives. However, it cannot be implied that solid residues from other feedstocks will have similar properties, more specifically from agricultural wastes, which can contain more varied extractive compounds. As such, it is possible that other unknown solid residue formation mechanisms could affect products properties and yields with other feedstocks than those investigated in this thesis. Similarly, this research only investigated microwave assisted acid catalysis and solid residue properties may differ with conventional-thermal heating systems. Also, the investigation of the synergistic catalysis did not include the quantification of soluble sugar compounds. Consequently, it was not possible to evaluate the effects of the dilute acid on cellulose hydrolysis or catalyst promotion. Furthermore, the separation of solid residue from spent catalysts was difficult on a lab-scale and limited the evaluation of the corresponding solid residues.

The limitations of this work was most apparent during the anaerobic digestion stage, as the control conditions only exhibited mild ammonium inhibition. Investigation of the solid residue supplementation under more stressed microbial environments could result in greater increases in methane yields, as opposed to the non-supplemented control. Also, the low ammonium-inhibition resulted in similar methane yields across the five different solid residues investigated. As such, the evaluation of the different catalysis conditions on anaerobic digestion was limited. The comparison of different

solid residue properties would be better facilitated by investigating a more toxic anaerobic digestion control.

8.5 Recommendations for Future Research

In relevance with regards to the limitations of the project which were presented in the previous section, suggestions for future research include the following points:

i. Since the study utilised a limited number of feedstocks, further dedicated research is required to evaluate any potential interferences between biomass extractives and the solid residue formation during acid catalysis.

ii. Given the importance of solid residue to the overall biomass catalysis process shown in this research, it should be recommended that all future catalytic research with biomass include the quantification of solid residue in order to enable a better comparison of different catalysts with regards to by-product yields.

iii. Future work should also investigate the fate of formic acid during acid hydrolysis to determine if it is contributing to the solid residue yields or, more generally, to understand the role of formic acid in the overall reaction process.

iv. Detailed investigation into the underlying mechanisms between the dilute acid and solid catalysts found as part of this research, would enable the utilisation or a larger variety of bottlenecked heteronomous catalysts.

v. The supplementation of anaerobic digestion with solid residues from acid catalysis should be studied in greater detail. More specifically, digestion with other nitrogen rich feedstocks and/or under higher ammonium concentrations than 2 g/Las higher ammonium concentrations in the control reactor may result in more significant increases in methane yields, which would significantly improve the integration of the two processes.

vi. In addition, a life cycle assessment of the integration of anaerobic digestion and acid catalysis is recommended, as it could elucidate the overall performance of the digestion of residues as compared with combustion, and suggest areas for further improvement.

8.6 Concluding Remarks

This PhD thesis describes the first steps towards the valorisation of solid residue from acid catalysis of lignocellulosic biomass. The experimental data and modelling results have been used to explore solid residue yields, properties and potential applications. The findings of this research highlights the importance of solid residue variability and its morphological and biochemical similarities to materials obtained via other known thermochemical routes, such as hydrochar. Exploring and investigating the solid residue applications from catalytic processes could enable the further development of low carbon production of high value chemicals through lignocellulosic biorefineries.